Tissue Engineering Group
School of Pharmacy, University of Nottingham

NOVEL POROUS SCAFFOLDS FOR TISSUE ENGINEERING CARTILAGE

Jennifer M. Unsworth, B.Sc.

Thesis submitted to the University of Nottingham for the degree of Doctor of Philosophy, September 2004

Abstract

Damage to cartilage, caused either by disease or injury, affects a large number of people worldwide, severely reducing the patient's quality of life and generating a huge burden on healthcare systems. The limited success of treatment options such as tissue grafts has been the driving force behind much research into tissue engineering strategies for cartilage repair. One of the challenges associated with tissue engineering cartilage is that of generating constructs of clinically relevant sizes since the formation of a crust of tissue at the scaffold periphery restricts the supply of nutrients to the growing tissue. The hypothesis of this thesis was that a tissue engineering system incorporating scaffolds containing both random and anisotropic porosity and a novel flow perfusion bioreactor system would facilitate *in vitro* tissue formation by enhancing the supply of nutrients to the growing construct. This hypothesis was examined using cartilage as a model tissue. It was shown that scaffolds combining both random and anisotropic porosity (sparse knit scaffolds) had improved flow properties compared to scaffolds containing random porosity alone (needled felt scaffolds). Following studies to characterise the scaffolds and to determine the appropriate conditions for seeding cells into the scaffolds, cartilage formation within the different scaffolds was assessed over a four week culture period. It was found that the flow perfusion system was not as favourable for *in vitro* cartilage formation as either the commercially available Rotary Cell Culture System™ (RCCS™) or static culture. One of the sparse knit scaffolds (sparse knit 4) and the needled felt were further compared for cartilage formation over an eight week culture period, using static and RCCS™ culture. With respect to collagen and glycosaminoglycan (GAG) production, cartilage constructs generated from the two scaffold systems were similar. Following static culture it was found that more viable cells were present at the centre of sparse knit 4 scaffolds than needled felt scaffolds. It was therefore concluded that scaffolds combining random and anisotropic porosity were advantageous for culturing tissues in environments where nutrient supply was reliant on diffusion alone.

Publications

The work presented in this thesis has given rise to the following publications and presentations.

Publication in peer reviewed journal

Unsworth JM, Rose FRAJ, Wright, E, Scotchford, CA, Shakesheff, KM. Seeding cells into needled felt scaffolds for tissue engineering applications. *Journal of Biomedical Materials Research*, 66(A), 425-431 (2003).

Oral presentations

Unsworth JM, Grant DM, Rose FRAJ, Silva MC, Cyster LA, Howdle SM, Scotchford CA and Shakesheff KM. Novel porous scaffolds for cartilage and bone tissue engineering. Presented at Tissue Engineering: Prospects, Challenges and Opportunities for Exploitation meeting, Leeds (UK), February 2004.

Unsworth JM, Rose FRAJ, Howdle SM, Grant DM, Smith M, Farrar D, Scotchford CA and Shakesheff KM. Cartilage tissue engineering in scaffolds with random and anisotropic porosity. Presented at Yorkshire Tissue Engineering meeting, York (UK), December 2003.

Unsworth JM, Rose FRAJ, Cyster L, Silva MC, Grant DM, Scotchford CA, Howdle SM and Shakesheff KM. Porous tissue engineering novel technology scaffolds. Presented at Smith & Nephew Student Research Day, York (UK), September 2002.

Poster presentations

Unsworth JM, Rose FRAJ, Scotchford CA and Shakesheff KM. Comparison of the Rotary Cell Culture System™ and Static Culture for Cartilage Tissue Engineering in Novel Scaffolds with Random and Anisotropic Porosity. Presented at Smith & Nephew Student Research Day, York (UK), September 2003.
This poster was awarded the "best poster" prize.

Unsworth JM, Rose FRAJ, Harrison M, Lee-Webb J, Scotchford CA, Shakesheff KM. Bioreactor culture of chondrocytes in scaffolds for tissue engineering articular cartilage. Presented at 3rd International Smith and Nephew Symposium on Tissue Engineering, Georgia Institute of Technology, Atlanta (USA), October 2002.

Unsworth JM, Rose FRAJ, Scotchford CA and Shakesheff KM. Tissue engineering articular cartilage. Presented at Smith & Nephew Student Research Day, York (UK), September 2001.

Acknowledgements

I would like to take this opportunity to thank my supervisors Professor Kevin Shakesheff and Dr Colin Scotchford for the guidance, inspiration and support they offered throughout my PhD studies. I would like to extend my gratitude to Dr Felicity Rose for her continual enthusiasm and for being such a great mentor.

My thanks also go to everyone I had the opportunity to work with during this project: Professor Steve Howdle, Professor David Grant, Dr Lesley Cyster and Miss Marta Silva (University of Nottingham) and Mr David Farrar, Dr Frederic Turquier, Mr Matthew Harrison, Mr Julian Lee-Webb, Dr Emma Wright and Mr Mark Smith (Smith & Nephew). The knowledge that these people have shared with me has been invaluable. I would also like to acknowledge the funding that this Foresight LINK project received from EPSRC, DTI, University of Nottingham, Smith & Nephew, Molecular Profiles, Uniquema and Plasma Biotal Limited.

It is essential that I also thank Marta, Liz, Tri and Paddy for all their help isolating and culturing chondrocytes. I would like to acknowledge Mrs Christine Grainger-Boultby (School of Pharmacy) for her assistance with the scanning electron microscopy and Dr Susan Anderson and Mr Ian Ward (School of Biomedical Sciences) for carrying out the confocal microscopy on my behalf. I would like to extend my thanks to Mr Peter Broomhall (Broomhall's Butchers Ltd, Dursley) and Mr Chris Barren (G. Wood and Sons Abattoir, Clipstone) for supplying the ovine and bovine joints used in this work.

I would like to thank my friends in Nottingham for making my PhD days so enjoyable, especially Fliss, Sarah, Marta, Kathryn, Katrina, Fog, Martin, Hugh and Owen. A big thank you must also go to my "other" friends who also saw me through my PhD days, especially Tamsin, Helena, Alli, Lisa, Ellie and Alice.

I must also thank my colleagues at Smith & Nephew, in particular Dr Andrew Harrison, who I cannot thank enough his encouragement and support whilst I was writing this thesis, and Saira, Liz and Jon of the NIS “dream team” for making me feel so welcome in York.

Special thanks also go to my family for all their support, especially Mum & Dad for always encouraging me to pursue my dreams and for their financial assistance throughout my education. Finally, I would like to thank Craig for the inspiration he offered throughout my PhD, for always being there for me and for everything he did to make life as normal as possible while I was working and writing this thesis!

Table of Contents

List of Figures

Chapter 1

Chapter 2

Chapter 3

Chapter 4

Chapter 5

List of Tables

Chapter 1

Chapter 3

Chapter 5

Abbreviations

%	per cent
π	pi (3.14217)
±	plus or minus
°C	degrees Celcius
μg	microgram
μL	microlitre
μm	micrometer
<	less than
ACI	Autologous chondrocyte implantation
ANOVA	one-way analysis of variance
A-T	adenosine-thymidine
BACs	Bovine articular chondrocytes
bFGF	Basic fibroblast growth factor
BMP-2	Bone morphogenetic protein-2
BMPs	Bone morphogenetic proteins
chloramine T	N-chloro-p-toluenesulfonamide sodium salt
cm	centimetre
cm^3	cubic centimetre
CO_2	carbon dioxide
CPM	Continuous passive motion
DABCO	1,4 diazobicyclo-2-2-2-octane
DMEM	Dulbecco's modified Eagle's medium
DMMB	1, 9-dimethylmethylene blue
DMSO	dimethylsulphoxide
DNA	deoxyribonucleic acid
DPBS	Dulbecco's phosphate buffered saline
DPX	distyrene plasticiser xylene mountant
ECACC	European Collection of Cell Cultures
ECM	Extracellular matrix

EDTA	ethylenediaminetetraaceitic acid
F	flow rate
FCS	Foetal calf serum
FDA	Food and Drug Administration
g cm^{-3}	grams per cubic centimetre
g	force due to gravity (9.81Pa)
g	gram
GAG	Glycosaminoglycan
h	height
HBSS	Hank's balanced salt solution
HCl	hydrochloric acid
HEPES	4-(2-hydroxyethyl)-1-piperazineethanesulfonic acid
HMDS	hexamethyldisilaxane
HOS TE85	Human osteosarcoma cell line TE85
IMS	industrial methylated spirits
L	litre
M	molar
mg/mL	milligram per millilitre
mL	millilitre
mL/min	millilitres per minute
mm	millimetre
mM	millimolar
MSCs	Mesenchymal stem cells
NASA	National Aeronautics Space Administration
N-CAM	Neuronal cell adhesion molecule
NEAA	non essential amino acids
NF	needled felt
nm	nanometre
OMCs	Ovine meniscal fibrochondrocytes
P	pressure of air
P	probability
Pa	Pascals

PBS	phosphate buffered saline
PCL	poly caprolactone
p-DAB	p-dimethylaminobenzaldehyde
PEGT/PBT	poly ethyleneglycol terephthalate / poly butylene terephthalate
PET	poly ethyleneterephthalate
PGA	poly glycolic acid
pH	measure of acidity/alkalinity
PLA	poly lactic acid
PLGA	poly lactic-co-glycolic acid
PTFE	poly tetrafluoroethylene
r	radius
R	resistance to flow
RCCS™	Rotary Cell Culture System™
REDOX	reduction-oxidation
RGD	arginine-glycine-aspartine
rpm	revolutions per minute
SEM	scanning electron microscopy or standard error of the mean
SK	sparse knit
SSC	saline sodium citrate
TGF-β	Transforming growth factor-beta
V	volume
v/v	volume/volume
w/v	weight/volume

Chapter 1
Introduction

1.1 General introduction

Musculoskeletal conditions, such as arthritis, affect 15% of people in the United Kingdom; severely reducing the patient's quality of life and costing in excess of £5 billion per year (Arthritis Research Campaign 2002). In 1999 it was estimated that the worldwide market for cartilage repair was $1 billion (LGC Biomaterials State of the Art Report 2002). With an increasingly ageing population it is anticipated that the number of people affected and the resulting burden on healthcare systems will increase dramatically over the years to come (Buckwalter and Mankin 1998a, Bentley and Minas 2000 and Peretti *et al* 2000). Treatment options currently available include the use of tissue grafts and prosthetic joints; however these methods are limited by the poor availability of suitable donor tissue and the risk of infection and implant failure associated with total joint replacements (Langer and Vacanti 1993). These limitations are the driving force behind much research into cell-based methods for effectively treating diseased or damaged cartilage (Cima and Langer 1993). Tissue engineering has been defined as "an interdisciplinary field that applies the principles of engineering and the life sciences toward the development of biological substitutes that restore, maintain, or improve tissue function" (Langer and Vacanti 1993). Tissue engineering strategies generally involve the following stages: (1) identification and isolation of a suitable source of cells; (2) manufacture of a device to either carry or encapsulate the cells; (3) uniform seeding of cells onto or into the device and appropriate culture; and (4) *in* vivo implantation of the engineered construct (Figure 1.1; Langer 2000). Cartilage tissue engineering studies to date have addressed the use of different cell types, scaffolds and culture systems.

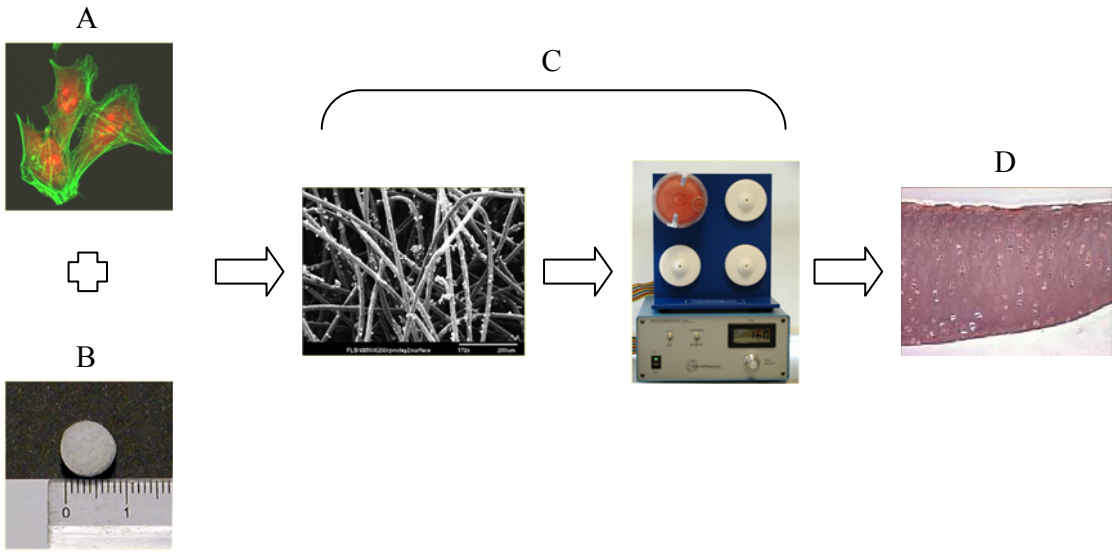

Figure 1.1 Schematic representation of a tissue engineering strategy: (A) isolation of an appropriate cell population; (B) fabrication of a scaffold; (C) seeding of cells into scaffold and *in vitro* culture of cell-scaffold construct; and (D) implantation of tissue engineered device.

One of the major challenges of tissue engineering is the formation of a "shell" of tissue at the periphery of the device, which limits the supply of nutrients to the centre of the growing tissue causing cell and tissue death. This thesis investigates the use of scaffolds with novel architectures and a new flow-through bioreactor to facilitate the formation of tissues *in vitro*. Cartilage was selected as an example tissue on which to perform the studies since the phenomenon of capsule formation at the periphery of scaffolds has been reported in previous cartilage tissue engineering studies (Freed *et al* 1999). The aim of this chapter is to describe cartilage - its composition, structure and function; cartilage damage and repair; and tissue engineering as a potential method for repairing cartilage defects. A detailed explanation of the aims of this thesis is given at the end of this chapter.

1.2 Cartilage

Cartilage has three key functions within the body. Firstly, it acts as a template for the growth and development of long bones. Cartilage forms a large part of the foetal skeleton and has an important role in endochondral ossification. In addition, cartilage is present at the articulating surfaces of bones, where it provides a low-friction surface. It also acts as a supporting framework in some organs within the body, for example in the trachea where it prevents airway collapse. There are three types of cartilage: elastic cartilage, fibrocartilage and hyaline cartilage. Cartilage differs with respect to biochemical composition, structure and location within the body (Serafini-Fracassini and Smith 1974). Elastic cartilage, which is found within the external ear and larynx, contains elastin, which comprises approximately 20% of the dry tissue weight (Serafini-Fracassini and Smith 1974 and Temenoff and Mikos 2000a). Fibrocartilage contains lower glycosaminoglycan (GAG) levels than other types of cartilage, possesses highly organised collagen fibres and is found at the ends of ligaments and tendons (Serafini-Fracassini and Smith 1974 and Temenoff and Mikos 2000a).

Menisci, which are present within the knee joint, are formed from fibrocartilage. Hyaline cartilage contains increased quantities of GAGs compared to the other cartilage types (Serafini-Fracassini and Smith 1974). Articular cartilage, which is present at the articulating surfaces of bones within synovial joints, is formed from hyaline cartilage (Mankin 1974).

1.3 Articular cartilage and meniscal fibrocartilage

The location of articular cartilage and the menisci within the knee joint are shown in Figure 1.2. Articular cartilage forms a durable layer 0.5 to 7.0 mm thick at the surface reducing friction between the bones and distributing loads across the entire joint surface (Carver and Heath 1999). The meniscus is a fibrocartilaginous tissue which consists of two semilunar wedge-shaped sections. The two sections lie between the tibia and fibia in the knee joint (Sweigart and Athanasiou 2001). Menisci within the knee are responsible for shock absorption, lubrication and stability (Mow *et al* 1990 and Sweigart *et al* 2003).

1.3.1 Composition of articular cartilage and meniscal fibrocartilage

The exact biochemical composition of both articular cartilage and meniscal fibrocartilage varies with species, age and location within the tissue (Serafini-Fracassini and Smith 1974 and McDevitt and Webber 1990). In general terms, both tissues are composed of cells within an extracellular matrix (ECM) composed of fibrillar components, for example collagen, proteoglycans, non-collagenous proteins and water (Figures 1.3 and 1.4, Alberts *et al* 2002). Articular cartilage is considered to be one of the simplest tissues within the body since it possesses a single cell type, the chondrocyte; it is aneural and has no vascular or lymphatic supply (Buckwalter and Mankin 1997a).

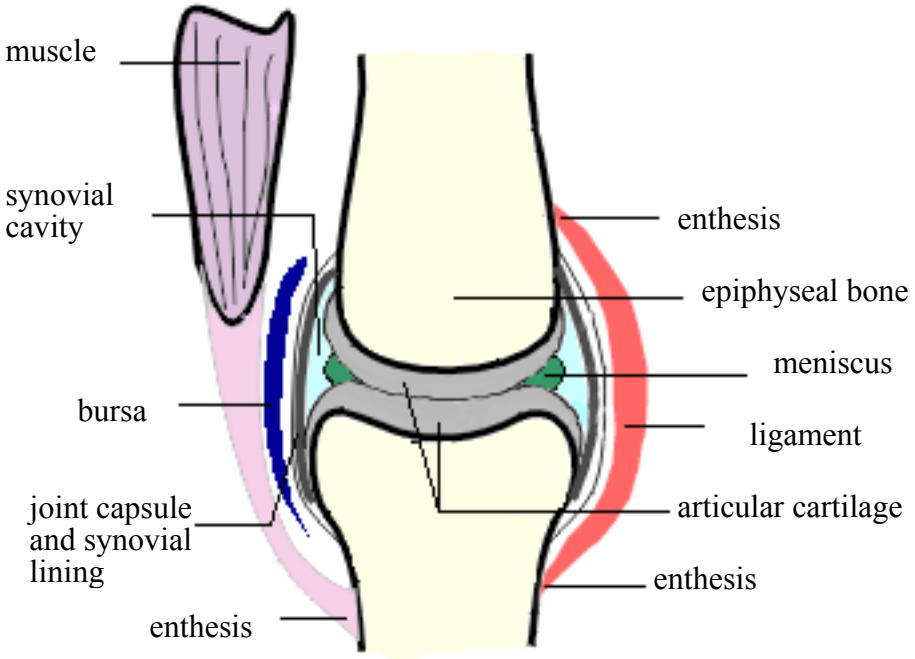

Figure 1.2 The location of articular cartilage within a knee joint (adapted from Drury and Shipley 1998).

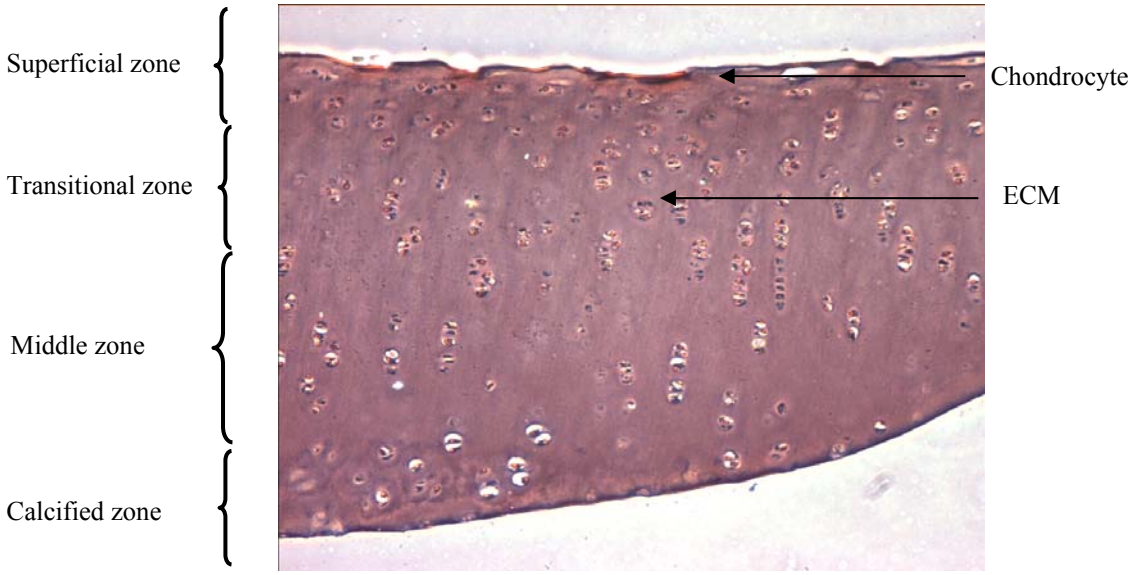

Figure 1.3 The organisation of chondrocytes and ECM within articular cartilage. The ECM is composed of collagen, proteoglycan, water and other proteins.

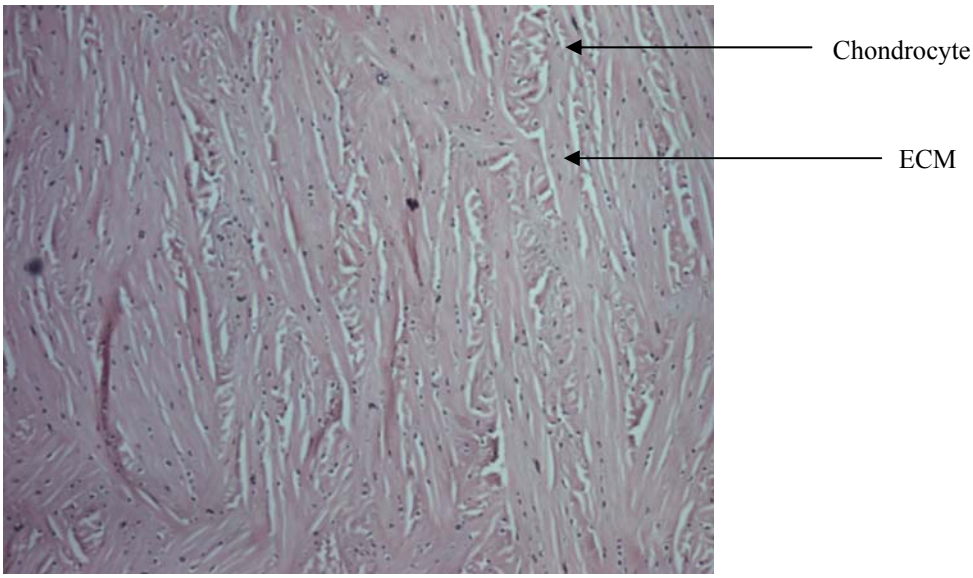

Figure 1.4 The organisation of cells and ECM within meniscal fibrocartilage. The ECM is composed of collagen, proteoglycan, water and other proteins.

Meniscal fibrocartilage, in contrast, contains a region of vascularisation (the red zone at the periphery) and an avascular region (the inner white zone) (Sweigart *et al* 2003). The proportion of meniscal tissue that is vascularised decreases with age (Sweigart and Athanasiou 2001).

1.3.1.a Cells

Chondrocytes form a very small proportion of articular cartilage, typically around 1% of the dry tissue weight (Buckwalter and Mankin 1997a). The cells within meniscal fibrocartilage are called fibrochondrocytes as they are generally considered to be a cross between chondrocytes and fibroblasts (Sweigart *et al* 2003). Both chondrocytes and fibrochondrocytes are responsible for synthesis of the cartilage ECM macromolecules, the assembly and organisation of these macromolecules into an ordered framework and the continual replacement of degraded matrix components (Buckwalter and Mankin 1997a). In both tissues, the cells are rounded and contained within lacunae (Sweigart *et al* 2003). One of the key differences between chondrocytes and fibrochondrocytes is that the predominant collagen secreted by fibrochondrocytes is type I, whereas that of chondrocytes is type II (Benjamin and Ralphs 2004).

1.3.1.b Proteoglycans

Proteoglycans consist of a core protein to which one or more GAG chains are attached (Buckwalter and Mankin. 1997a). GAGs are unbranched polysaccharide chains which contain repeating disaccharide units where one of the sugars within the repeating unit is an amino sugar, for example N-acetylglucosamine, and the second is usually a uronic acid, for example glucuronic acid (Alberts *et al* 2002). Since each of the disaccharides contains at least one negatively charged carboxylate or sulphate group, GAGs contain long chains of negative charge which attract cations and repel anions (Buckwalter and Mankin 1997a).

There are four groups of GAGs: i) hyaluronan, ii) chondroitin sulphate and dermatan sulphate, iii) keratan sulphate and iv) heparan sulphate, the first three groups of which are present in articular cartilage (Buckwalter and Mankin 1997a). The two most abundant GAGs within meniscal cartilage are chondroitin sulphate and dermatan sulphate, which between them account for approximately 80% of the total GAG content (Almarza and Athanasiou 2004). Proteoglycans comprise between 15 and 30% of the dry weight of articular cartilage (Freed *et al* 1998). Within both cartilage types, two classes of proteoglycan are present: large aggregating proteoglycan monomers, for example aggrecan, and small proteoglycans, such as decorin, biglycan and fibromodulin (Buckwalter and Mankin 1997a and Nakano *et al* 1997). Aggrecan consists of chains of chondroitin and keratan sulphate bound to core proteins. Individual aggrecan monomers interact with hyaluronan, as shown in Figure 1.5, to form high molecular weight aggregates. These interactions are stabilised by link protein, which binds to both the hyaluronan and a specific binding site at the N-terminus of the aggrecan (Hardingham 1979). The GAG/proteoglycan aggregates form gels which occupy a large volume relative to their mass. These hydrophilic gels draw in considerable quantities of water that confer high compressive strength properties to the tissue (Bryant and Anseth 2001). The smaller non-aggregating proteoglycans are involved in binding macromolecules, for example decorin and fibromodulin bind with type II collagen and therefore it is postulated that they may play a role in organising and stabilising the collagen meshwork (Hedbom and Heinegard 1993 and Hasler *et al* 1999). The smaller proteoglycans are also able to bind transforming growth factor-β (TGF-β), a cytokine known to stimulate cartilage matrix synthesis (Buckwalter and Mankin 1997a).

1.3.1.c Fibrillar components

In articular cartilage, GAGs and proteoglycans are contained within and associated with a fibrous network of collagen, which accounts for 50-60% of the dry tissue weight (LeBaron and Athanasiou 2000). The predominant collagen of articular cartilage is type II (Heath and Magari 1996). Type II collagen forms rope-like fibrils which aggregate into larger cable-like bundles or fibres (Alberts *et al* 2002).

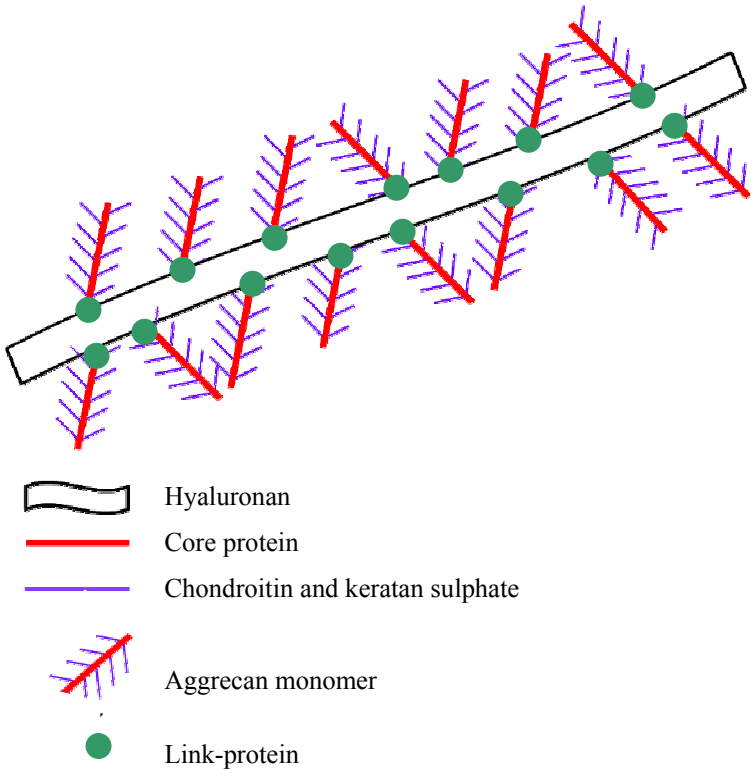

Figure 1.5 The association of aggrecan molecules with hyaluronan.

Articular cartilage also contains other members of the collagen family such as type XI, a fibrillar collagen involved in the establishment of a fibre network; type IX collagen, a fibril-associated collagen thought to aid linkage of the collagen fibrils to the rest of the ECM, type VI, which is found in the matrix immediately surrounding chondrocytes and is believed to help attachment of the cells to the ECM; and type X, which is involved in chondrocyte hypertrophy (Loeser 1993). The collagen network provides articular cartilage with tensile strength (Alberts *et al* 2002). In contrast to articular cartilage, meniscal fibrocartilage contains small quantities of elastin (0.6% dry weight). The majority of the fibrillar component of meniscal tissue is collagen (Sweigart and Athanasiou 2001). The predominant collagen of meniscal fibrocartilage is type I, with types II, III, V and VI also present. These collagens account for between 60 and 70% of the dry tissue weight. Within the menisci, the orientation of collagen fibres varies with location, for example collagen fibres within the deep zone are circumferentially orientated (Petersen and Tillmann 1998).

1.3.1.d Non-collagenous proteins and glycoproteins

In addition to proteoglycans and collagens, both articular cartilage and meniscal fibrocartilage contain non-collagenous proteins and glycoproteins. Some of these molecules are thought to be involved in the organisation and maintenance of the ECM structure (Buckwalter and Mankin 1997a). Anchorin CII, for example, is a collagen binding protein found at the surface of chondrocytes that is believed to help anchor chondrocytes to collagen fibrils (Von der Mark *et al* 1986). Another example is fibronectin, a protein that has been idenitifed in many other tissues. It has been shown that chondrocytes attach to fibronectin and that the binding is mediated by integrins (Sommarin *et al* 1989 and Loeser 1993). Whilst the exact role of fibronectin in cartilage is not fully understood, it is postulated that it may be involved in matrix organisation or cell-matrix interactions (Hayashi *et al* 1996). Three adhesion glycoproteins have been identified within meniscal fibrocartilage all of which have been found to contain the arginine-glycine-aspartine (RGD) peptide sequence: type VI collagen, fibronectin and thrombospondin (McDevitt and Webber 1990).

1.3.1.e Tissue fluid

Tissue fluid contains gases, small proteins, metabolites and a large number of cations (Buckwalter and Mankin 1997a). Interactions between the negative charge of the large aggregating proteoglycans and the cations within the tissue fluid help retain water within the tissue and contribute to the mechanical properties of both cartilage types (Buckwalter and Mankin 1997a).

1.3.2 Structure of articular cartilage and meniscal fibrocartilage

Both articular cartilage and meniscal fibrocartilage are highly organised structures. Throughout the tissues differences in cell morphology, metabolic activity and matrix composition have been observed (Buckwalter and Mankin 1997a). Articular cartilage can be divided into regions according to the distance of matrix from the cells: the pericellular, territorial and interterritorial compartments (Newman 1998). In general, the pericellular and territorial regions are thought to facilitate attachment of chondrocytes to the ECM and to protect them during loading of the tissue (Buckwalter and Mankin 1997a). The mechanical properties of articular cartilage are due to the interterritorial matrix which may be divided into four zones according to distance from the articular surface: the superficial, transitional, middle and calcified zones (Figure 1.3, Buckwalter and Mankin 1997a). The knee meniscus can be divided into three zones, in which cell morphology and collagen fibre orientation differs: the superficial, middle and deep zones (Figure 1.6). In addition, the tissue can be divided according to vascularisation into the inner third (avascular white zone), middle third (partially vascularised red-white zone) and the outer third (vascularised red zone) (Figure 1.6).

1.3.2.a Regions of the articular cartilage matrix

The pericellular region occurs where the membranes of cells appear to be attached to the ECM (Temenoff and Mikos 2000a). The matrix in this region contains a high concentration of proteoglycans. Anchorin CII and type VI collagen are present in this region of articular cartilage, supporting the hypothesis that this matrix region is involved in attachment of chondrocytes to the ECM (Buckwalter and Mankin 1997a).

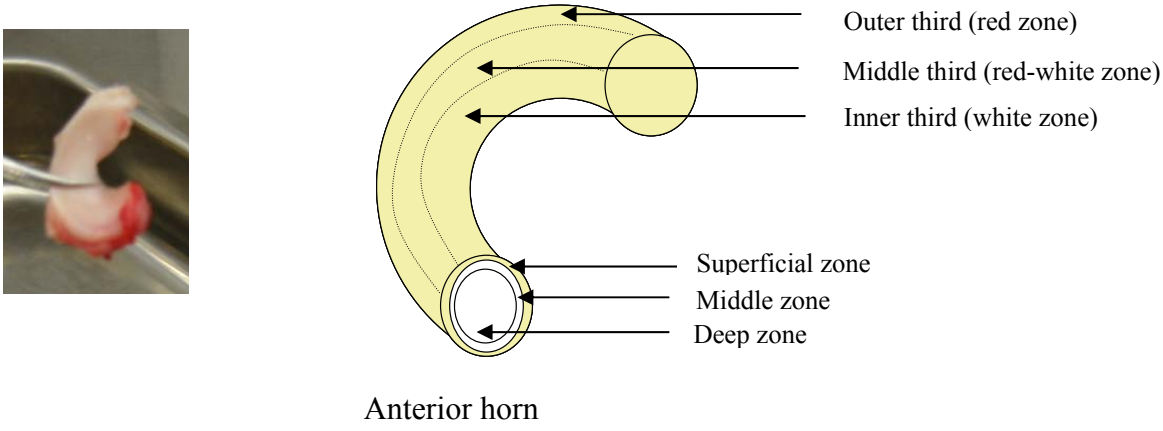

Figure 1.6 A schematic representation of the structural organisation of the knee meniscus.

The pericellular matrix of each chondrocyte is contained within envelopes of territorial matrix known as lacunae (Temenoff and Mikos 2000a). It is believed that these collagenous envelopes protect the cells from mechanical forces experienced within the tissue (Buckwalter and Mankin 1997a). The interterritorial region comprises the majority of the ECM and is considered to be responsible for the mechanical properties of articular cartilage (Temenoff and Mikos 2000a). Within each of the different zones of articular cartilage, the collagen fibres of the interterritorial matrix regions are orientated differently. For example, whilst the collagen fibres within the superficial zone are arranged parallel to the articular surface, those within the middle zone lie perpendicular to the articular surface (Buckwalter and Mankin 1997a).

1.3.2.b Zones of articular cartilage

The superficial zone is organised into two layers, a layer of elongated chondrocytes and a sheet of collagen fibres arranged parallel to the articulating surface of the joint (Temenoff and Mikos 2000a). The dense arrangement of collagen fibres in this region of the tissue provides it with its low friction surface and high tensile strength (Guilak and Mow 2000). It has been shown that the surface of articular cartilage plays an important role in the development of the diarthrodial joint (Ward *et* al 1999) and that many growth factors and their receptors are expressed at the articular surface (Archer *et al* 1994 and Hayes *et al* 2001). It has been reported that a population of progenitor cells, which are probably involved in cartilage development via appositional growth, reside within the superficial zone of cartilage (Douthwaite *et al* 2004). The transitional zone of articular cartilage is so-called because the composition of the matrix is transitional between that of the superficial and middle zones (Buckwalter and Mankin 1997a). Chondrocytes within the transitional zone are rounded and contained within a matrix containing a higher proportion of proteoglycans and lower concentration of collagens than the superficial zone (Temenoff and Mikos 2000a). Within the middle zone, spheroidal chondrocytes are found within lacunae and organised in columns perpendicular to the articulating surface (LeBaron and Athanasiou 2000).

The matrix within the middle zone contains the highest concentration of proteoglycans and the largest diameter collagen fibrils (Buckwalter and Mankin 1997a). The calcified zone forms a thin transitional layer between the cartilage and the subchondral bone (Buckwalter and Mankin 1997a). The chondrocytes within the calcified ECM occupy a smaller volume than cells within the middle region and in some cases are completely embedded in a calcified matrix (Temenoff and Mikos 2000a).

1.3.2.c Zones of meniscal fibrocartilage

The superficial zone faces the femur and is the thinnest of the zones. *In situ*, cells within the superficial zone are oval and fusiform and collagen fibres are arranged in a random mesh. The middle zone is embedded between the superficial and deep zones. The majority of collagen fibres within the middle zone are randomly orientated, although at the anterior and posterior sections, the fibres are orientated into a radial configuration. The deep zone accounts for the largest portion of the meniscus and contains a population of cells with a rounded morphology. The collagen fibres in this region of the tissue are arranged circumferentially (Almarza and Athanasiou 2004).

1.4 Articular cartilage formation *in vivo*

Cartilage is initially formed by undifferentiated mesenchymal stem cells (MSCs) (Buckwalter and Mankin 1997a). Clustering of these cells by cell condensation is necessary for chondrogenic differentiation (Tavella *et al* 1997). It has been proposed that cell condensation is a two-stage process. In the first step, cells aggregate via integrin-fibronectin interactions. Cell adhesion molecules, such as neuronal cell adhesion molecule (N-CAM) and N-cadherin, strengthen cell-cell interactions in the second stage (Tavella *et al* 1997). Once cells are differentiated, secretion of ECM proteins occurs (Buckwalter and Mankin 1997a). During phases of cartilage formation and growth, a high density of metabolically active cells are present within the tissue (Buckwalter and Mankin 1997a).

Cartilage development may occur in one of two different ways: interstitial growth, where chondrocytes grow and divide and lay down additional matrix within the existing tissue; or appositional growth, where new surface layers of matrix are added to pre-existing matrix by cells in the perichondrium (Alberts *et al* 2002). Studies have shown that the superficial zone of articular cartilage is responsible for appositional tissue growth and that this region of the tissue contains a population of progenitor cells (Hayes *et al* 2001 and Douthwaite *et al* 2004).

1.5 Articular cartilage damage

Although articular cartilage is able to withstand high levels of mechanical stress and continually renew its ECM, during normal aging processes the ability of chondrocytes to synthesise some proteoglycans and respond to stimuli that aid its continual remodelling decrease (Buckwalter and Mankin 1997a). The limited ability of mature chondrocytes to maintain the integrity of the tissue increases its vulnerability to injury and disease, and can lead to the natural degeneration of cartilage (Buckwalter and Mankin 1997a). Disease may cause degeneration of articular cartilage either directly or indirectly. Primary osteoarthritis (Kreklau *et al* 1999), osteochondrosis dissecans (Hunziker 1999a) and tumours (Schaefer *et al* 2000) can all directly impair articular cartilage. There are, in addition, a large group of conditions that can cause changes in cartilage that stimulate the onset of secondary osteoarthritis and consequently degeneration of the cartilage (Buckwalter and Mankin 1997b).

Two types of defect can be seen in articular cartilage: intrinsic injuries, which are confined to the cartilage (Wakitani *et al* 1994), and extrinsic injuries, in which the subchondral bone is penetrated (Mankin 1974). Degeneration of articular cartilage leads to chronic pain and, in severe cases, loss of the joint's function and consequently total joint replacement is necessary (Brittberg *et al* 1994, Shortkroff *et al* 1996 and Gugala and Gogolewski 2000).

The poor quality of life for patients and the substantial cost to health services has stimulated a great deal of research into methods of repairing articular cartilage injuries (Buckwalter and Mankin 1998a, Bentley and Minas 2000 and Peretti *et al* 2000).

1.6 Cartilage repair *in vivo*

The classical response of most tissues to injury requires two components: specific cells types which are involved removing necrotic material and synthesis of new tissue and a vascular supply by which cells and bioactive molecules, such as growth factors, may reach the site of damage (Newman 1998). Several factors influence the healing response of articular cartilage including the size of the defect and the age of the organism. It has been shown in animal models that there is a proportional relationship between increasing defect size and decreasing ability to heal, with defects less than 3 mm in diameter able to heal completely without intervention (Convery *et al* 1972). It is widely accepted that chondrocytes from skeletally immature animals have a greater capacity for proliferation and proteoglycan synthesis (Kreder *et al* 1994) which correlates with the observation that improved healing is observed in younger patients (Newman 1998). In addition, whether the defect is confined to cartilaginous tissue (intrinsic defect) or whether it penetrates the subchondral bone (extrinsic defect) influences its ability to heal.

1.6.1 Healing of intrinsic defects

Since articular cartilage is avascular, classical tissue repair processes are rarely observed in intrinsic defects (Newman 1998). Initial increases in mitotic activity and matrix synthesis have been detected in chondrocytes close to defect sites, although no significant healing was observed (Campbell 1969). The containment of chondrocytes within a meshwork of collagens and proteoglycans is thought to prevent their migration from regions of healthy tissue to the injury site (Newman 1998). It has been proposed that the articular cartilage matrix contains natural inhibitors of vascular and macrophage invasion (Mankin 1982).

Whilst intrinsic defects rarely heal, they are relatively stable and progression to osteoarthritis is uncommon (Mankin 1982).

1.6.2 Healing of extrinsic defects

The penetration of the subchondral bone in extrinsic defects allows access to vascular tissue and so a more classical healing response may be observed (Convery *et al* 1972). It has been reported that fibrin clot formation is seen within extrinsic defects (Shapiro *et al* 1993). Such clots allow entrapment of cells from blood and MSCs from within the bone marrow (Shapiro *et al* 1993). Metaplasia of the repair tissue allows formation of a hyaline-like chondroid tissue (Shapiro *et al* 1993).

Although initial repair tissue is hyaline-like with rounded chondrocytes and substantial amounts of type II collagen, the amount of type I collagen within the tissue may increase with time and in less than 3 months degenerative changes in the cartilage composition may be evident (Furukawa *et al* 1980 and Shapiro *et al* 1993). Between 6 and 12 months post-injury it is not uncommon for the tissue to resemble fibrocartilage rather than hyaline cartilage (Shapiro *et al* 1993).

1.7 Clinical attempts to repair cartilage

A summary of different strategies for treating articular cartilage defects is presented in Table 1.1. In general, these methods involve one or more of the following: (i) surgical intervention; (ii) a space-filling device e.g. a tissue graft; or (iii) a treatment or component to stimulate a healing response and chondrogenesis e.g. penetration of the subchondral bone to allow infiltration of inflammatory and progenitor cells into the defect site (O'Driscoll 1998). Something that all current treatment options have in common is the variability in their success – functional repair can be achieved in some joints in some patients, but no one treatment allows complete healing of all defects in all patients (Lohmander 2003).

Strategy	Method	Reference(s)
Surgery/Arthroscopy	Chondral shaving	Buckwalter and Lohmander 1994
	Abrasion arthroplasty	Johnson 1986 & Altman *et al* 1992
	Subchondral drilling	Pridie 1959
	Osteotomy	Byers 1974
Physical stimulation of chondrogenesis	Continuous passive motion	Salter *et al* 1980
Tissue grafts	Perichondral graft(autograft/allograft)	Skoog *et al* 1972
	Periosteal graft (autograft/allograft)	Rubak *et al* 1982
	Cartilage graft (autograft/allograft)	Schatten *et al* 1958
	Mosaicplasty	Hangody *et al* 1998
	Osteochondral graft (autograft/allograft)	Herndon and Chase 1952
Cellular transplantation	Autologous chondrocyte transplantation	Chesterman and Smith 1968, Bentley and Greer 1971 & Brittberg *et al* 1994
	Mesenchymal stem cells	Wakitani *et al* 1994

Strategy	Method	Reference
Pharmacologic modulation	Corticosteroids	Olah and Kostenszky 1976
	Hyaluronan	Smith and Ghosh 1987
	Bioactives Bone morphogenetic protein-2 (BMP-2)	Sato and Urist 1984
	TGF- β	van Beuningen *et al* 1993-1994
	Basic fibroblast growth factor (bFGF)	Cuevas *et al* 1988
Biomaterials	Space filling device	Wyre and Downes 2000
	Matrix for delivery of cells/bioactives/both	Martin *et al* 2001

Table 1.1 Methods used in articular cartilage repair.

1.7.1 Surgical intervention

A variety of surgical procedures have been used in the treatment of articular cartilage defects. These include chondral shaving, abrasion arthroplasty, subchondral drilling and osteotomy. It has been reported that chondral shaving of degenerated and partial thickness defects has provided symptomatic relief as a consequence of removing the source of irritation from within the joint (Buckwalter and Lohmander 1994). This procedure does not, however, stimulate chondrogenesis or repair of the injury site since there is no penetration of the subchondral bone (Chen *et al* 1999). Abrasion arthroplasty involves scraping a few millimetres of the subchondral cortex and so allows penetration of cells from the vasculature and bone into the defect site (Friedman *et al* 1984). The repair tissue resulting from the procedure has been reported to be highly variable, ranging from fibrous to hyaline-like cartilage (Buckwalter and Lohmander 1994). It has been proposed that subchondral drilling, where multiple holes are drilled through the cartilage into the subchondral bone, produces more favourable results than both chondral shaving and abrasion arthoplasty (Chen *et al* 1999). In animal studies, however, similar variability in repair tissue has been observed following use of this technique as for abrasion arthroscopy (Mitchell and Shepard 1976).

Osteotomies involve mechanical realignment of the joint in order to redistribute loads within the joint away from the diseased or damaged articular cartilage (Buckwalter and Lohmander 1994). This method is generally reserved for patients who are considered too young for total joint replacement (Newman 1998). In addition there is some evidence to suggest that changes in loading result in stimulation of repair in the diseased tissue (Buckwalter and Mankin 1997b). Total joint replacements are often used in patients with arthritis when other treatment options have been unsuccessful and severe degeneration of the joint has occurred (Moran and Tourret 2001). Prosthetic joints have a limited lifetime since they often loosen within the joint, creating bone loss and pain (Moran and Tourret 2001). For this reason the use of total joint replacements is often restricted to the elderly (Moran and Tourret 2001).

1.7.2 Physical stimulation of chondrogenesis

Several studies have reported the detrimental effect of immobilisation and the benefits of intermittent motion on synovial joints (Mooney and Ferguson 1966, Woo *et al* 1975 and Salter *et al* 1984). It was reported by van Kampen and van de Stadt that in *in vivo* models, immobilisation of joints led to degenerative changes, for example loss of proteoglycan (van Kampen and van de Stadt 1987). Continuous passive motion (CPM) is a method used whereby the joint is continuously moved within a mechanical splint. It is often used after surgery in order to prevent stiffness and increase the range of movement within the joint. Whilst repair tissue resembling hyaline cartilage has been observed within defects treated with CPM, complete healing was not seen within joints where the defect was either greater than 3 mm in diameter or confined to the articular cartilage surface (Salter *et al* 1984). These observations imply that CPM does not initiate or stimulate cartilage healing, although it does have beneficial effects once repair has been initiated (Chen *et al* 1999).

1.7.3 Pharmacologic modulation

A variety of pharmacologic agents have been used in the treatment of cartilage defects including growth factors, hyaluronan and corticosteroids. These treatments have been applied as a means to increase the number of chondrocytes within the defect and their secretion of matrix components (Temenoff and Mikos 2000a). The agents may be administered either systemically or locally (O'Driscoll 1998). There is conflicting evidence as to whether corticosteroids enhance cartilage-healing or if they induce arthropathy (Behrens *et al* 1976, Salter *et al* 1967). Hyaluronan is used as a "viscosupplement" since it is has been shown in arthritis models that it binds to and penetrates into damaged articular cartilage, giving the cartilage a coating which is potentially both a lubricant and protectant (Iwata 1993). Growth factors such as TGF-β and bone morphogenetic proteins (BMPs) have been shown to have chondrogenic effects *in vitro* (Elford *et al* 1992).

Whilst intra-articular injections of TGF-β have been shown to increase proteoglycan synthesis, the formation of osteophytes, consistent with osteoarthritis, have also been observed (van Beuningen *et al* 1993-1994). More recent attempts to utilise the therapeutic effects of growth factors has concentrated on the use of carrier devices which can release the active factors into the defect site in a controlled manner (Elisseeff *et al* 2001).

1.7.4 Tissue grafts

Tissue grafting involves removal of suitable tissue from a donor site and transplanting it into the defect site. The graft tissue may be obtained from the patient (autograft) or from a donor (allograft). Each of these types of graft has advantages and disadvantages (O'Driscoll 1998). Whilst autografts do not carry the risk of an immune response associated with use of tissue from a donor, the amount of autologous cartilage available for transplantation is limited. In addition the removal of healthy tissue introduces a second defect within the joint (Temenoff and Mikos 2000a). Perichondral, periosteal, chondral and osteochondral grafts have all been used in the treatment or articular cartilage defects (Buckwalter and Mankin1997b).

1.7.4.a Perichondral grafts

Skoog and colleagues first reported the use of perichondral grafts for joint resurfacing (Skoog *et al* 1972). The perichondrium is a membrane of fibrous connective tissue that surrounds cartilage, except at the articulating surface. It has been reported to contain MSCs which are capable of proliferation and chondrogenic differentiation. Perichondral grafts have been used to repair articular cartilage defects in human and animal models. The repair tissue observed within these studies has varied from fibrocartilage to hyaline-like neocartilage (Chen *et al* 1999). The use of rib perichondrium in full thickness defects has led to hyaline-like cartilage formation within 8 weeks, although following 8-12 months of normal joint function degeneration of the repair tissue has been reported (Amiel *et al* 1985, Homminga *et al* 1989 and Homminga *et al* 1990).

1.7.4.b Periosteal grafts

The perisoteum is present at the outermost surface of bones and is also a fibrous connective tissue believed to contain a population of MSCs (Chen *et al* 1999). As a cartilage graft material, perisoteal tissue has generally shown more promise than perichondral tissue (Chen *et al* 1999). The use of periosteal grafts offers the advantage that it is present in larger quantities. It has been shown that perisoteum can be securely fitted into defects of a range of sizes and shapes (O'Driscoll 1998). Differentiation of periosteal grafts into hyaline-like cartilage has been observed in both lapine and equine models (Rubak *et al* 1982 and Vachon *et al* 1989). Adhesives such as fibrin and cyanoacrylate have been used to secure periosteal grafts within defect sites with variable success (Sullins *et al* 1985, Vachon et al 1989 and Tsai *et al* 1992). Clinical data for the use of periosteal grafts in combination with adhesives and postoperative physical stimulation, such as continuous passive motion in younger patients, shows promise for this therapy (Buckwalter *et al* 1993 and Buckwalter and Lohmander 1994).

1.7.4.c Cartilage grafts

Small plugs of cartilage from low-weight-bearing regions of joints may be used for transplantation. Articular cartilage autografts have been harvested from the patella, femoral condyle and proximal fibula (O'Driscoll 1998). The use of articular cartilage grafts has shown mixed results in patients. In one study, 70% of patients reported improved symptoms, while in others immune responses were observed following implantation of fresh allografts (Wirth and Rudert 1996 and Goldberg and Caplan 1999). Other concerns associated with the use of cartilage grafts include the effect of harvesting on tissue morbidity in the donor site and the ability of cartilage from a less weight-bearing region to withstand the forces experienced at the joint surface (Temenoff and Mikos 2000a and Hunziker 1999b). It has recently been reported that cartilage resected with blunt instruments contained a band of dead cells at the edge of the injury site, whilst cartilage resected using sharp scalpels contained a limited number of dead cells and matrix regeneration was observed.

This has implications in the use of cartilage grafts since the authors propose that the use of sharp, precise instruments is necessary to facilitate integration of tissue at the defect site (Redman *et al* 2004).

1.7.4.d Osteochondral grafts

Osteochondral grafts offer the advantage that in addition to providing a fully formed articular cartilage matrix they can restore the subchondral bone in extrinsic defects (Czitrom *et al* 1990). A study carried out by Outerbridge and colleagues reported successful treatment of patients using osteochondral grafts up to six years after the procedure was performed (Outerbridge *et al* 1995). Mosaicplasty is a technique which involves the removal of plugs of osteochondral tissue from a relatively non-weight-bearing region of the knee and transplanting them into an articular defect (O'Driscoll 1998). The success of osteochondral grafts depends on the cause of the cartilage damage, for example studies have shown that osteochondral allografts provide effective treatment of localised post-traumatic defects but they perform unpredictably in patients with osteoarthritis (Buckwalter and Mankin 1998a).

1.7.5 Cellular transplantation

An alternative to filling the defect site with tissue is to use cells with the ability to form a new cartilage matrix (Temenoff and Mikos 2000a). The aim of cellular transplantation methods is to take a small biopsy of cells with chondrogenic potential, expand the number of cells *in vitro* and then return them to the defect site to restore the tissue mass (Temenoff and Mikos 2000a). The cells may be mature differentiated chondrocytes or osteochondral progenitor cells, such as MSCs (Buckwalter and Mankin 1997b, Caplan *et al* 1997). MSCs may prove advantageous for the treatment of full-thickness defects where both bone and cartilage healing are required (O'Driscoll 1998). In a study comparing MSCs and articular chondrocytes for the treatment of defects in rabbit knees, similar healing was observed in both treatment groups (Wakitani *et al* 1994). Whilst the repair tissue exhibited good mechanical properties, the repair tissue failed to integrate with the host tissue (Wakitani *et al* 1994).

The implantation of chondrocytes into cartilage defects has been studied for many years (Chesterman and Smith 1968). One of the challenges associated with filling a defect site with cells in suspension is how to retain the cells within the site for long enough to allow the formation of a cartilaginous matrix (Aston and Bentley 1986). In the case of autologous chondrocyte implantation (ACI) this problem has been overcome by suturing a flap of periosteal tissue over the defect site (Temenoff and Mikos 2000a). Clinical studies have shown promising results, with good repair tissue maintained in a large number of patients up to ten years after the treatment (Gillogly *et al* 1998). Whilst ACI is a well-established method for treating joint surface defects, it may not be appropriate for the treatment of all cartilage defects. Although excellent repair has been observed in defects within the femoral condyle, only limited healing was observed in patellar defects (Brittberg *et al* 1994 and Brittberg 1999). A further disadvantage of ACI is the requirement for a periosteal flap and the morbidity that occurs at the donor site. An alternative method for retaining cells within the defect site is to use a porous scaffold (Temenoff and Mikos 2000a). Tissue engineering has evolved as a method for regenerating tissues both *in vitro* and *in vivo* based on the idea of seeding cells into a highly porous scaffold that facilitates cell attachment and tissue formation (Langer and Vacanti 1993).

1.8 Tissue engineering cartilage

The ultimate aim of cartilage tissue engineering is the *in vitro* generation of cartilaginous constructs for implantation. These constructs should be able to develop further upon implantation into the patient so that functional cartilage with the required anisotropic biochemical composition and mechanical properties is able to fully integrate with the host cartilage and bone (Vunjak-Novakovic 2003). Figure 1.1 shows a schematic representation of an approach commonly employed in cartilage tissue engineering. In this strategy, a biopsy of cells would be obtained from the patient and expanded by *in vitro* culture. The cells would then be seeded into a scaffold structure which would support cell attachment, extracellular matrix secretion and tissue formation.

It has been proposed that the tissue may either be grown entirely *in vitro* and implanted into the defect as hyaline cartilage or that the developing tissue within the scaffold structure may be implanted and allowed to form cartilage *in vivo* (Hutmacher 2000). Tissue engineering methods offer solutions to problems encountered with transplantation of tissue grafts, namely the shortage of suitable tissue to provide an autograft and the risk of immune responses to the foreign tissue used in an allograft (Freed and Vunjak-Novakovic 1998, Sittinger *et al* 1996). The type of cells, the scaffold material and design and the culture conditions employed can all be varied in order to optimise the properties of the cartilage formed. Table 1.2 presents a summary of some cartilage tissue engineering studies from the last twelve years. It is clear from this table that a variety of cell sources, scaffold types and culture systems have been used in cartilage engineering studies. The cells used in these studies have varied not only with respect to the animal from which the tissue was obtained, but also with respect to the type of cartilage or tissue that the cells were isolated from. For example articular, meniscal and nasal cartilage have all been used as a source of chondrocytes for articular cartilage engineering studies (Kafienah *et al* 2002 and Huckle *et al* 2003). The scaffolds used in tissue engineering studies have been fabricated from both synthetic (for example PGA) and natural (for example collagen and hyaluronan) materials (Freed *et al* 1993 and Nehrer *et al* 1998). In addition the scaffolds used have been hydrogels, fibrous meshes and porous matrices (Buschmann *et al* 1992 and Freed *et al* 1993). Both *in vivo* and *in vitro* environments have been employed to allow cartilage regeneration. Examples of *in vivo* systems include the subcutaneous implantation of cell-scaffold constructs into immuno-compromised mice and implantation of constructs directly into cartilage defects (Puelacher *et al* 1994 and Vacanti *et al* 1994). *In vitro* culture systems used have varied from static tissue culture plates to more complex bioreactor systems (Buschmann *et al* 1992 and Dunkelman *et al* 1995). The length of time for which the cell-scaffold constructs were cultured in these studies varied from 1 week to 7 months (Freed and Vunjak-Novakovic 1995 and Freed *et al* 1997).

Cell source	Scaffold type(s)	Culture system(s)	Culture time	Reference
Bovine articular cartilage	Agarose gel	Static culture	10 weeks	Buschmann *et al* 1992
Bovine articular cartilage	Non-woven PGA mesh Porous PLA matrix	Static culture	6 weeks	Freed *et al* 1993
Bovine articular cartilage	Non-woven PGA mesh	Mixed dish Static culture	8 weeks	Freed *et al* 1994a
Bovine articular cartilage	Non-woven PGA mesh	Spinner flask Static culture (75 cm^2 tissue culture flask)	6 weeks	Freed *et al* 1994c
Bovine articular cartilage	Non-woven PGA mesh	*In vivo* (subcutaneously implanted into nude mice)	12 weeks	Puelacher *et al* 1994
Lapine articular cartilage	Non-woven PGA mesh	*In vivo* (within cartilage defects in rabbits)	7 weeks	Vacanti *et al* 1994
Lapine articular cartilage	Non-woven PGA mesh	Perfused cartridge	4 weeks	Dunkelman *et al* 1995
Bovine articular cartilage	Non-woven PGA mesh	Rotating wall bioreactor Spinner flask	1 week	Freed and Vunjak-Novakovic 1995
Bovine articular cartilage	Non-woven PGA mesh	Rotating wall bioreactor	7 months	Freed *et al* 1997

Bovine articular cartilage	Non-woven PGA mesh Porous collagen matrix	Closed-loop recirculation system Static culture (Petri dishes)	35 days	Grande *et al* 1997
Embryonic chick bone marrow	Non-woven PGA mesh	Mixed dish	4 weeks	Martin *et al* 1998
Canine articular cartilage	Type I collagen – GAG sponge Type II collagen – GAG sponge	*In vivo* (Superficial cartilage defects in adult dogs)	15 weeks	Nehrer *et al* 1998
Bovine articular cartilage	Non-woven PGA mesh	Mixed agarose-coated petri dish	6 weeks	Martin *et al* 1999
Bovine meniscal cartilage	Type I collagen – GAG sponge Type II collagen – GAG sponge	Not stated by author	3 weeks	Mueller *et al* 1999
Bovine articular cartilage	Non-woven PGA mesh	Static culture (static spinner flask) Spinner flask Rotating wall bioreactor	6 weeks	Vunjak-Novakovic *et al* 1999
Bovine articular cartilage	Cell - fibrinogen suspension in PLGA fleece	Flow perfusion followed by *in vivo* (subcutaneous implantation in athymic nude mice)	*In vitro* 8 days followed by *In vivo* 12 weeks	Duda *et al* 2000

Canine cartilage	articular	Type I collagen – GAG copolymer matrix Type II collagen – GAG copolymer matrix	Static culture (24-well plates)	14 days	Lee *et al* 2000
Bovine cartilage	articular	Cells encapsulated in alginate within demineralised trabecular bovine bone matrix Cells encapsulated in alginate within non-woven PLGA matrix	*In vivo* (subcutaneously implanted into athymic mice)	8 weeks	Marijnissen *et al* 2000
Lapine cartilage	articular	Ethisorb 210 (polydioxanone/polyglactin) fleece PLLA fleece	Static (96-well plate)	4 weeks	Rudert *et al* 2000
Human bone marrow		PLA cube PLA-alginate cube	Static (12 mm culture plate)	21 days	Caterson *et al* 2001

Bovine cartilage	articular	Non-woven PGA mesh	Static culture (Petri dish) Mixed Petri dish Static spinner flask Mixed spinner flask Rotating wall bioreactor	4 weeks	Gooch *et al* 2001
Human cartilage	articular	non (pellet cultures)	Mixed conical tubes	2 weeks	Jakob *et al* 2001
Bovine cartilage	articular	Non-woven PGA mesh	Mixed 6-well plates	7 weeks	Kellner *et al* 2001
Rat cartilage	articular	Alginate sponge Alginate-hyaluronan sponge Cells encapusalated in alginate	Static (24-well plate)	40 days	Miralles *et al* 2001
Foetal bovine epiphysis		Diphenylphosphorylazide cross-linked collagen sponge	Static culture (24-well plate)	1 month	Roche *et al* 2001
Bovine cartilage	articular	PLGA sponge Collagen sponge PLGA-collagen sponge	*In vivo* (subcutaneous implantation in athymic mice)	8 weeks	Sato *et al* 2001

Bovine cartilage	articular	Cross-linked type I collagen-chondroitin sulphate matrix	Static culture (96-well plates)	14 days	van Susante *et al* 2001
Human cartilage	articular	Hyaluronan benzyl ester non-woven mesh	Static culture	60 days	Grigolo *et al* 2002
Bovine cartilage	articular	Non-woven PGA mesh	Orbital shaker (75 rpm)	40 days	Kafienah *et al* 2002
Bovine cartilage Human cartilage	nasal articular		Orbital shaker (75 rpm) followed by *in vivo* (subcutaneous implantation in athymic mice)	*in vitro* 40 days followed by *in vivo* 6 weeks	
Human cartilage	nasal				
Human cartilage	auricular	Alginate beads	Static culture (24 well plates, 10 beads per well)	21 days	Mandl *et al* 2002
Porcine cartilage	articular	Gelatin-chondroitin-hyaluronan tri-copolymer porous matrix	Static culture (Petri dishes) Spinner flasks	5 weeks	Chang *et al* 2003
Bovine cartilage	articular	Polyurethane porous matrix PLA porous matrix	Static culture (12-well plates)	42 days	Grad *et al* 2003

Ovine mensical cartilage Human articular cartilage	Non-woven PGA mesh PCL porous foam PLGA porous foam Polyethylene glycol dimethacrylate hydrogel	Static culture (Petri dishes)	4 weeks	Huckle *et al* 2003
Bovine articular cartilage	Alginate beads	Static culture (24-well plates)	14 days	Masuda *et al* 2003
Bovine articular cartilage (full thickness) Bovine articular cartilage (mid and deep zone) Bovine articular cartilage (deep zone)	Porous calcium polyphosphate	Static culture	8 weeks	Waldman *et al* 2003

Bovine articular cartilage	Poly($_L$-lactic acid-ε caprolactone) porous scaffold	Static culture (10cm dishes) followed by *in vivo* (subcutaneous implantation in athymic mice)	*In vitro* 1 week followed by *in vivo* 40 weeks	Isogai *et al* 2004
Human ear cartilage Human nasal cartilage Human rib cartilage	non (pellet culture)	Pellet culture (on orbital shaker at 30rpm)	2 weeks	Tay *et al* 2004
Bovine articular cartilage	Macroporous alginate hydrogel	*In vivo* (subcutaneous implantation in immunocomprimised mice)	24 weeks	Thornton *et al* 2004
Bovine articular cartilage	Poly (ethylene glycol) – terephthalate / poly (butylene terephthalate) co-polymer (PEGT/PBT) compression moulded sponge PEGT/PBT fibrous scaffold	Spinner flask followed by *in vivo* (subcutaneous implantation in nude mice)	*In vitro* 14 days followed by *In vivo* 28 days	Malda *et al* 2005

Table 1.2 Summary of cartilage tissue engineering studies.

1.8.1 Cells

Cells used in tissue engineering must be biosynthetically active and have nutrients, metabolites and other regulatory molecules readily available (Jackson and Simon 1999). The donor age and differentiation state have all varied in the cells used in cartilage tissue engineering studies to date (Buckwalter and Mankin 1997b, Huckle *et al* 2003 and Vunjak-Novakovic 2003). Mature, differentiated chondrocytes are advantageous for cartilage regeneration as they are the native cell population within cartilage and synthesise the appropriate ECM components (Grande *et al* 1999 and Freed *et al* 1999). Different chondrocyte populations are present in the different types of cartilage, for example articular chondrocytes are found in articular cartilage and fibrochondrocytes in meniscal cartilage. Articular chondrocytes are therefore the most obvious choice of cell for articular cartilage tissue engineering. Whilst articular chondrocytes can easily be isolated, obtaining an appropriate number of cells with the capacity to regenerate cartilage is one of the challenges facing tissue engineers (Huckle *et al* 2003). It is possible to expand cell populations using *in vitro* cell culture techniques; although it has been observed that in monolayer culture articular chondrocytes dedifferentiate, become fibroblastic in appearance and secrete a fibrous matrix. It has been documented that culturing the cells within a 3-dimensional environment such as a porous scaffold can help them retain their chondrocytic phenotype (Freed and Vunjak-Novakovic 1998). A population of progenitor cells have recently been isolated from the superficial zone of articular cartilage (Douthwaite *et al* 2004). These cells have been shown to form cartilage in pellet cultures, when implanted into wounded explant cultures and when injected *in ovo* (Thomson *et al* 2004). In addition it has been shown that these cells retain their ability to produce articular cartilage following several population doublings (Bishop 2003). The use of chondrocytes from other cartilage types for engineering articular cartilage has also been studied (Huckle *et al* 2003). Huckle and colleagues reported that fibrochondrocytes isolated from whole ovine menisci produced a cartilaginous matrix following 2 week dynamic culture and that the cells contained within the matrix were rounded, although there was some controversy as to whether the cartilage formed was more like articular or meniscal cartilage (Huckle *et al* 2003).

Kafienah and co-workers have published data showing that chondrocytes from nasal cartilage can be used to engineer articular cartilage following *in vitro* expansion (Kafienah *et al* 2002). The regenerative capacity of cells also varies with respect to animal age (Webber *et al* 1986). Other cell types that have been used in cartilage tissue engineering studies include stem cells isolated from a variety of tissues, such as muscle (Deasy *et al* 2002) and adipose (Erikson *et al* 2001); MSCs (Caplan *et al* 1997 and Pittenger *et al* 1999); and even adult dermal fibroblasts (Nicoll *et al* 1998). Despite these cells having greater proliferative capacities than adult articular chondrocytes they do not have the intrinsic ability to differentiate into chondrocytes unless given specific stimuli (Huckle *et al* 2003).

1.8.2 Scaffolds

A wide range of scaffolds have been used in cartilage tissue engineering studies. These scaffolds may be categorised with respect to the types of material used (natural or synthetic, degradable or non-degradable), the geometry of the scaffold (gels, fibrous meshes or porous sponges) and their structure (total porosity, pore size, connectivity and distribution; Vunjak-Novakovic 2003). It is crucial that a tissue engineering scaffold is fabricated from a material that is biocompatible, allowing attachment of cells, ECM secretion and tissue formation without the induction of an inflammatory or toxic response (Freed *et al* 1994a, Sawtell *et al* 1995, Chapekar 2000, Middleton and Tipton 2000, Temenoff and Mikos 2000b and Agrawal and Ray 2001). In order for cells to be able to infiltrate the structure uniformly, it should contain a large number of interconnected pores (Chapekar 2000, Freed *et al* 1994a and Kuo and Ma 2001). The size of the pores is important to the infiltration and attachment of the cells, for chondrocytes an optimum pore size of between 100 and 200 μm has been suggested (Agrawal and Ray 2001 and Freyman *et al* 2001). The scaffold must also be permeable, to allow diffusion of nutrients into the matrix and the removal of metabolic and degradation by-products from it (LeBaron and Athanasiou 2000). Finally, it is important that the scaffold has mechanical properties that allow it to withstand implantation and the loads experienced *in vivo* (Chapekar 2000, Agrawal and Ray 2001, Kuo and Ma 2001 and Freyman *et al* 2001).

The material used should be easily processed into the required structure and shape and be able to withstand sterilisation processes (Freed and Vunjak-Novakovic 1998, Middleton and Tipton 2000, Freed *et al* 1994a, Temenoff and Mikos 2000a and Ishaug-Riley *et al* 1999).

1.8.2.a Scaffold material

1.8.2.a.i Natural materials

Many natural materials have been used because of their similarity with cartilage ECM components, for example hyaluronan (Brun *et al* 1999, Lindenhayen *et al* 1999 and Allemann *et al* 2001) and collagen (Fujisato *et al* 1996, Uchio *et al* 2000 and Allemann *et al* 2001). Other natural materials used in cartilage tissue engineering studies include agarose (Saris *et al* 2000), alginate (Fragonas *et al* 2000) and chitosan (Suh and Matthew 2000). Natural polymers are advantageous in tissue engineering applications as they can undergo cell-specific interactions (Grande *et al* 1997 and Chen *et al* 2002). The use of natural materials, however, is limited by the large variation between batches, the lack of large supplies for commercial use and as they are often derived from non-human tissue they carry the risk of transferring pathogens (Marler *et al* 1998 and Temenoff and Mikos 2000b).

1.8.2.a.ii Synthetic materials

Synthetic polymers are often used in preference to natural materials as it is possible to mass-produce polymers with custom-designed properties. Poly(lactic acid) (PLA), poly(glycolic acid) (PGA) and co-polymers of PLA and PGA (PLGA) are commonly used in tissue engineering studies as they have Food and Drug Administration (FDA) approval for use within the human body. Other synthetic polymers that have been used in tissue engineering applications include poly(ethyleneterephalate) (PET) (Ishaug-Riley *et al* 1999 and Li *et al* 2001), poly(caprolactone) (PCL) (Middleton and Tipton 2000) and poly(tetrafluoroethylene) (PTFE) (Neher *et al* 1998, Freed et *al* 1999 and Wyre and Downes 2000). Ideally a scaffold that is to be implanted into the human body should be biodegradable (Freed and Vunjak-Novakovic 1998, Hunziker 1999a and Ishaug-Riley *et al* 1999) and the degradation products should be non-toxic (Freed *et al* 1994a and Agrawal and Ray 2001).

The degradation profiles of synthetic polymers can be controlled to match the rate at which the tissue develops, hence ensuring the structural integrity of the construct is maintained throughout tissue regeneration (Woodfield *et al* 2002). In addition, it is possible to incorporate biologically active species such as growth factors into synthetic scaffolds in order to encourage specific cell responses, for example differentiation (Whitaker *et al* 2001).

1.8.2.b Scaffold design

Both injectable and preformed scaffolds have been used in tissue engineering studies (Lu *et al* 2001). Injectable scaffold materials can be combined with cells *in vitro*, injected into the defect and polymerised *in situ* (Lu *et al* 2001 and Hou *et al* 2004). From a clinical perspective, injectable scaffolds are an attractive option since they minimise patient discomfort, scar formation and risk of infection (Hou *et al* 2004). Injectable scaffolds also offer the advantage that they may be implanted using minimally invasive surgery techniques into defects of various shapes and sizes, although on implantation they may lack the mechanical stability of porous and fibrous scaffolds (Lu *et al* 2001). Preformed scaffolds, for example porous foams, may be implanted into defects either alone as a space filling device; in combination with cells and/or growth factors; or with tissue that has formed within the scaffold during a period of *in vitro* culture (Temenoff and Mikos 2000a and Lu *et al* 2001). Pores can be introduced into polymer scaffolds using particulate leaching, emulsion freeze drying or supercritical fluid technology (Hutmacher 2000). Since the use of high temperatures and organic solvents are not necessary in supercritical fluid scaffold processing, it is possible to incorporate biological factors into the scaffold during processing that encourage favourable cell responses (Watson *et al* 2002 and Yang *et al* 2003). Non-woven fibrous scaffolds can be fabricated from a variety of polymers, both natural, for example hyaluronan and synthetic, for example PLA. Manufacture of fibrous scaffolds involves extrusion of the polymer into fibres, the fibres are then crimped and cut and then needle punched into a non woven mesh from which scaffolds may be cut (Vunjak-Novakovic *et al* 1999). Sittinger and colleagues have proposed that non woven fibrous scaffolds may be preferable to porous scaffolds for *in vitro* tissue formation (Sittinger *et al* 1996).

Non woven fibrous scaffolds have previously been shown to support *in vitro* cartilage regeneration (Freed and Vunjak-Novakovic 1993, Puelacher *et al* 1994 and Aigner *et al* 1998).

1.8.3 Culture environment

Different methods of culturing cells within scaffolds *in vitro* have been used including static petri-dishes, dynamic spinner flasks, flow perfusion systems and rotating wall bioreactors (Figure 1.7; Temenoff and Mikos 2000a and Vunjak-Novakovic *et al* 1999).

1.8.3.a Static culture

Constructs grown in static culture tend to remain small, with the majority of ECM formation at the edges of the scaffold. Any tissue formed tends to be fibrous and poorly organised (LeBaron and Athanasiou 2000, Marler *et al* 1998, Vunjak-Novakovic *et al* 1999 and Freed and Vunjak-Novakovic 1997).

1.8.3.b Dynamic culture

Dynamic systems allow improved mixing and therefore enhanced mass transfer rates for gases, nutrients, metabolites and growth factors (Temenoff and Mikos 2000a and Freed and Vunjak-Novakovic 1998). Using dynamic culture systems, such as the spinner flask, flow perfusion systems or the rotating wall bioreactor, cells have been uniformly seeded throughout scaffolds (Marler *et al* 1998) which is thought to encourage ECM formation throughout the entire structure (Temenoff and Mikos 2000a). In addition to improving cell seeding, dynamic culture systems have been shown to improve cartilage regeneration (Vunjak-Novakovic *et al* 1999 and Temenoff and Mikos 2000a). Customised culture systems have also been developed by various researchers, which allow investigation of specific mechanical stimuli (for example dynamic compression) on *in vitro* cartilage formation (Chowdhury *et al* 2003).

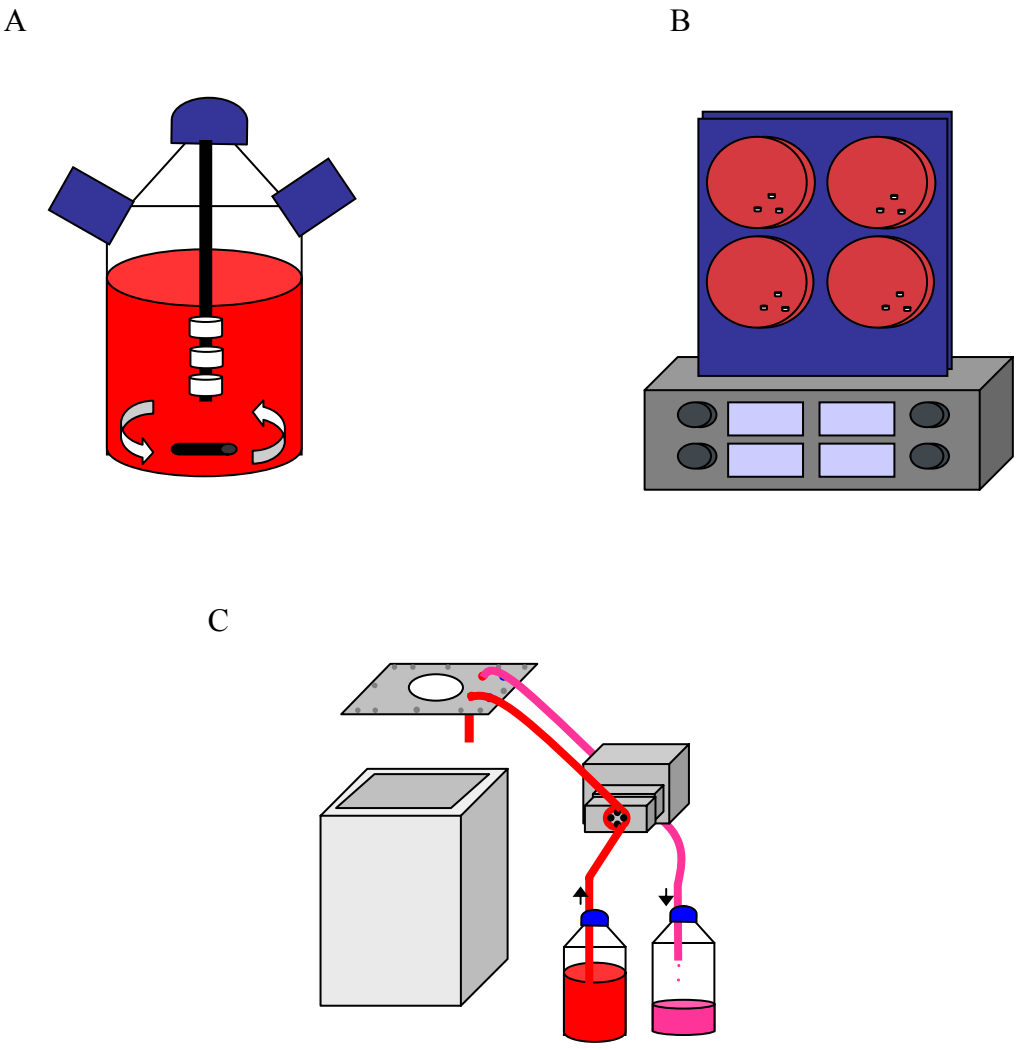

Figure 1.7 Dynamic culture systems: (A) spinner flask, (B) rotating wall bioreactor and (C) flow perfusion system.

1.8.3.b.i Spinner flask culture systems

Spinner flasks are a relatively simple culture system. A diagrammatic representation of a spinner flask is given in Figure 1.7 A. A needle, to which scaffolds may be attached, is suspended from the flask's stopper and the medium may be mixed within the flask by a magnetic stirrer. Spinner flasks may be used for seeding cells into scaffolds as well as for culture of cell-scaffold constructs. Freed and colleagues have reported that cartilage constructs cultured within spinner flasks were larger than those grown statically (Freed and Vunjak-Novakovic 1997).

1.8.3.b.ii Stimulated microgravity bioreactor systems

Rotating wall bioreactors, for example the Rotary Cell Culture System (RCCS™) originally designed by the National Aeronautics Space Administration (NASA), simulate the effects of microgravity and thereby limit the mechanical mixing that occurs within the culture system (Temenoff and Mikos 2000a). A schematic representation of a rotating wall bioreactor is shown in Figure 1.7 B. Scaffolds may be maintained within a constant state of free-fall by adjusting the speed at which the bioreactor rotates to that at which the centrifugal force within the system balances the forces of gravity and fluid drag (Freed and Vunjak-Novakovic 1997). Gaseous exchange occurs within the bioreactor through a semi-permeable membrane. Small movements of the scaffolds relative to the culture medium generate gentle mixing within the system (Freed and Vunjak-Novakovic 1997). Freed and co-workers have reported that cartilage with a composition similar to that of hyaline cartilage has been generated using rotating wall bioreactors (Freed and Vunjak-Novakovic 1997 and Freed *et al* 1998).

1.8.3.b.iii Flow perfusion culture systems

Flow perfusion systems typically consist of a chamber, within which the scaffolds are maintained, which is connected to a peristaltic pump used to control the exchange of fresh and waste medium between a reservoir and the cell culture chamber (Figure 1.7 C, Temenoff and Mikos 2000a).

Two groups have reported good matrix formation by chondrocytes cultured in perfusion systems (Sittinger *et al* 1996 and Vunjak-Novakovic *et al* 1999), although a more recent study by Mizuno and colleagues showed little cartilage formation by articular chondrocytes in a flow perfusion system (Mizuno *et al* 2001) indicating that there is some controversy as to the benefit of using flow perfusion systems in cartilage tissue engineering studies.

1.9 Thesis aims

Tissue engineering methods are being developed to allow the repair or replacement of diseased or damaged tissues. A strategy often employed in tissue engineering is to take a biopsy of the required tissue, isolate the cells and seed them into scaffolds. The cell-seeded scaffolds are cultured within an appropriate culture system to allow tissue regeneration. One of the limitations of current cartilage tissue engineering methods is the formation of a capsule of tissue around the periphery of the scaffold. This capsule impedes the flow of nutrients from the culture medium to the centre of the tissue, resulting in necrosis of the construct centre. The work within this thesis aims to address this limitation by incorporating innovative scaffold architectures and a novel flow-through bioreactor system into the tissue engineering strategy outlined above.

1.9.1 General aims

The principal aim of this thesis was to investigate a novel system for tissue engineering based on new scaffold and bioreactor designs. In order to assess this system two hypotheses were addressed. The first hypothesis was that scaffolds with both random and anisotropic porosity would be beneficial for engineering tissue of a clinically relevant size. The scientific basis for this hypothesis was that the presence of wider aligned pores within the random porous network would improve the supply of nutrients to the centre of the construct and prevent the formation of a necrotic core. Within this thesis, four scaffold types were assessed for cartilage tissue engineering (Figure 1.8).

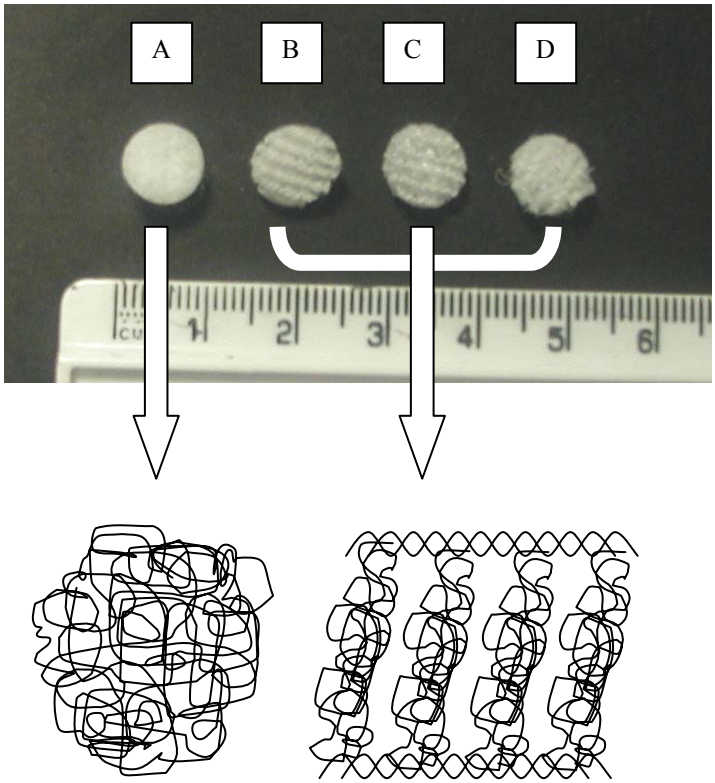

Figure 1.8 The different scaffolds used in this thesis and schematic representations of the fibre arrangements within the scaffolds: (A) needled felt, (B) sparse knit 3, (C) sparse knit 4 and (D) sparse knit 5.

Scaffolds containing random and anisotropic porosity of three different designs (sparse knit (SK) scaffolds 3, 4 and 5) were compared to scaffolds with random porosity alone (needled felt, NF). The second hypothesis was that a flow-through bioreactor system would be advantageous for tissue engineering. It was proposed that the flow of medium within the novel bioreactor system would provide an enhanced supply of nutrients to the growing constructs. The work presented in this thesis compares the flow-through system with static culture and a bioreactor that simulates microgravity (RCCS™) for *in vitro* culture of cartilage.

1.9.2 Experimental objectives

The experimental objectives of this thesis and the chapters within which they will be considered are presented in Figure 1.9. In Chapter 3, the different scaffolds are described with respect to fibre arrangement, density and resistance to flow. In addition, the optimum conditions for obtaining a high-density of evenly distributed cells throughout the scaffolds were determined for three different cell types: a human osteosarcoma cell line (HOS TE85), bovine articular chondrocytes (BACs) and ovine meniscal fibrochondrocytes (OMCs). SK and NF scaffolds were assessed for *in vitro* engineering cartilage using OMCs in Chapter 3. In the work presented in Chapter 4, each of the different scaffold types were cultured in static 6-well plates, the RCCS™ and a novel flow perfusion bioreactor for four weeks. The two best performing scaffolds and culture systems from Chapter 4 were further assessed for *in vitro* cartilage regeneration in the work presented in Chapter 5. OMCs were cultured in both scaffold types and culture environments for 8 weeks. The biochemical composition and histological appearance of native ovine articular and meniscal cartilage were determined and used as a comparison for the engineered tissue.

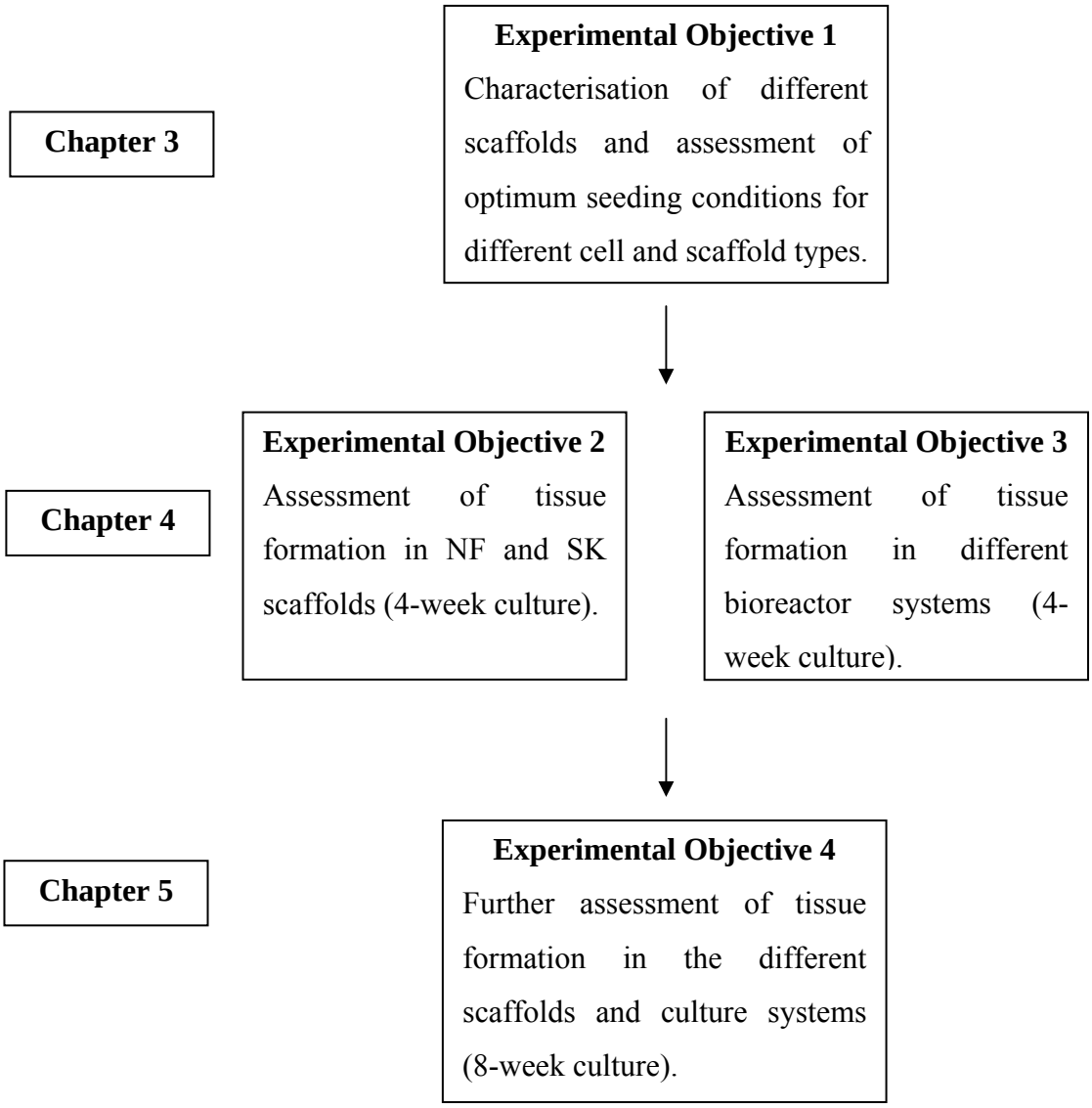

Figure 1.9 The organisation of the experimental aims within chapters of this thesis.

Chapter 2

General Materials and Methods

2.1 Materials

A list of materials and suppliers is given in Appendix 1.

2.2 Methods

2.2.1 Scaffold manufacture

Scaffolds used in this work were fabricated from polyethylene terephthalate (PET). The structure of PET is shown in Figure 2.1.

2.2.1.a Manufacture of needled felt scaffolds

Smith & Nephew (York, UK) supplied needled felt scaffolds. The needled felt (NF) material was woven from PET fibres 15 μm in diameter using the methods shown in Figure 2.2. Sheets of the PET NF material were cut into discs 9 mm in diameter and 4 mm thick. Figure 2.3 A shows a digital image of an NF scaffold. A schematic representation of the fibre arrangement within NF scaffolds is shown in Figure 2.4 A.

2.2.1.b Manufacture of sparse knit scaffolds

Sparse knit scaffolds were manufactured using the Raschel Warp Knitting process at Culzean Fabrics (Kilmarnock, Scotland) on behalf of Smith & Nephew. Sparse knit scaffolds contained PET fibres of two diameters, 15 and 100 μm. Three different sparse knit (SK) scaffold materials were produced (SK 3, 4 and 5). Sheets of the SK materials were cut into discs 9 mm in diameter and 4 mm thick. Figures 2.3 B, C & D show digital images of the SK scaffolds. A schematic representation of the fibre arrangement within SK scaffolds is shown in Figure 2.4 B.

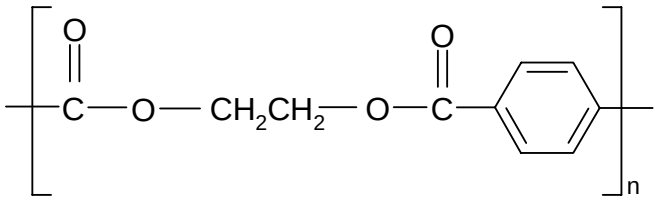

Figure 2.1 The structure of polyethylene terephthalate (PET).

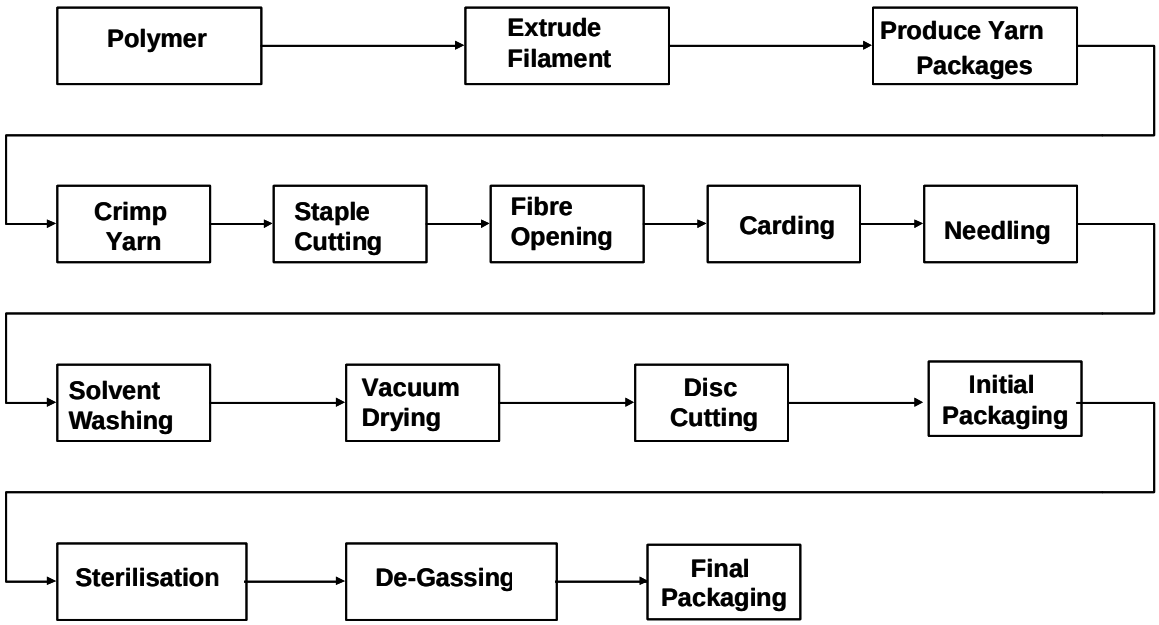

Figure 2.2 The stages in needled felt material manufacture.

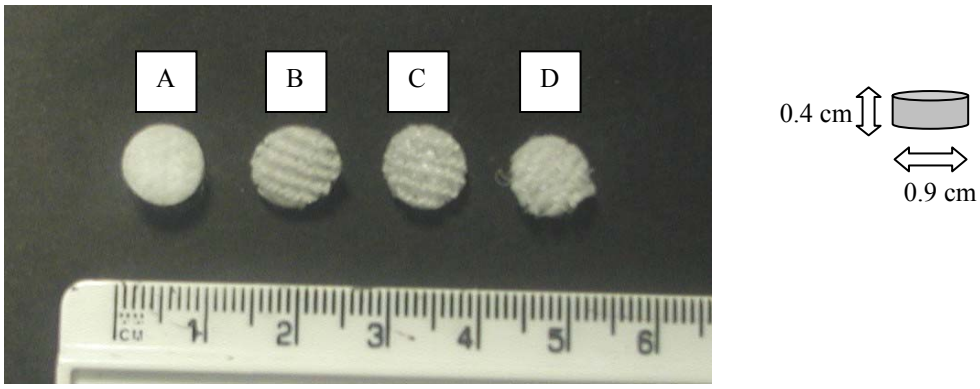

Figure 2.3 Digital image of (A) a needled felt scaffold, (B) a sparse knit 3 scaffold, (C) a sparse knit 4 scaffold and (D) a sparse knit 5 scaffold.

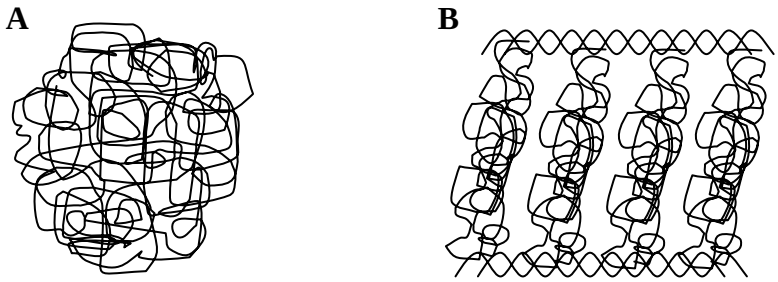

Figure 2.4 Schematic representations of the fibre arrangement in (A) a needled felt scaffold and (B) a sparse knit scaffold.

2.2.2 Isolation of cartilage

2.2.2.a Isolation of bovine articular cartilage

Bovine lower limbs were supplied by G. Wood and Sons Abattoir (Clipstone, Nottinghamshire, UK). Bovine articular cartilage was isolated from the metacarpalphalangeal joint of 30 month old cows using a method originally described by Archer and colleagues (Archer *et al* 1990). Figure 2.5 shows the stages involved in the isolation procedure. The joint was opened under aseptic conditions and washed with Gentamicin phosphate buffered saline (PBS) solution (Appendix 2.1.2). The cartilage was removed from the upper articulating surface of the joint using a scalpel blade and washed in Gentamicin PBS solution.

2.2.2.b Isolation of ovine meniscal cartilage

Ovine meniscal cartilage was isolated from the stifle joint of 4 month old sheep (obtained from Broomhall Butchers Ltd, Dursley, Gloucestershire) using a method previously described by Collier and Ghosh (Collier and Ghosh 1995). Figure 2.6 shows the stages involved in the isolation procedure. The joint was opened under aseptic conditions and washed with Gentamicin PBS solution. The menisci were removed from the joint using a scalpel blade and washed in Gentamicin PBS solution.

2.2.2.c Isolation of ovine articular cartilage

Ovine articular cartilage was isolated from the stifle joint of 4-month old sheep using a method similar to that described in Section 2.2.2.a (Archer *et al* 1990). The joint was opened under aseptic conditions and washed with Gentamicin PBS solution. The cartilage was removed from the upper articulating surface of the joint and washed in Gentamicin PBS solution.

2.2.3 Isolation of chondrocytes

2.2.3.a Isolation of bovine articular chondrocytes (BACs)

Bovine articular cartilage was isolated as described in Section 2.2.2.a. Cartilage pieces were washed in Gentamicin PBS solution and diced finely.

Stage 1 Incisions were made across the surface of the metacarpalphalangeal joint.	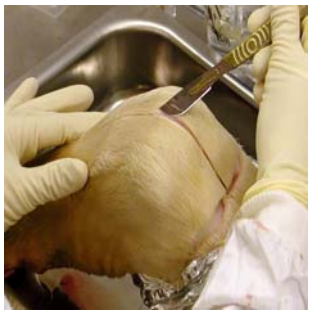
Stage 2 The skin was cut away from the joint.	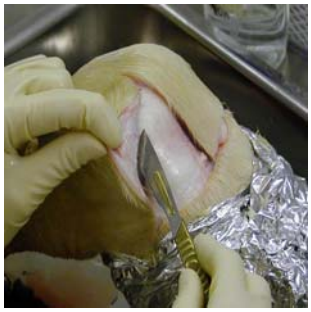
Stage 3 The ligaments at the centre of the joint were cut in order to fully expose the joint.	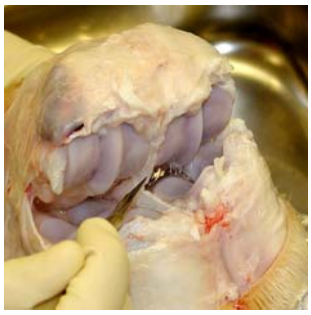
Stage 4 Cartilage was removed from the upper articulating surface of the joint.	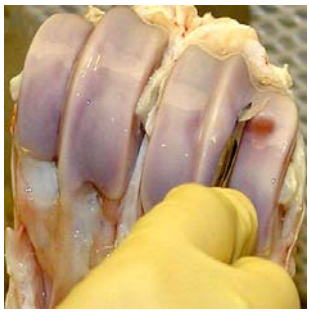

Figure 2.5 The stages involved in the isolation of bovine articular cartilage.

Stage 1 An incision was made across the upper surface of the stifle joint.	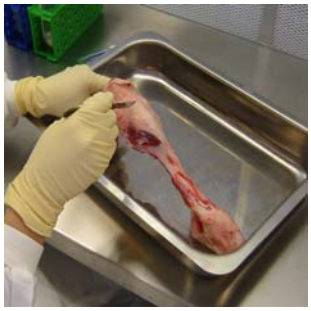
Stage 2 The skin was cut away from the joint.	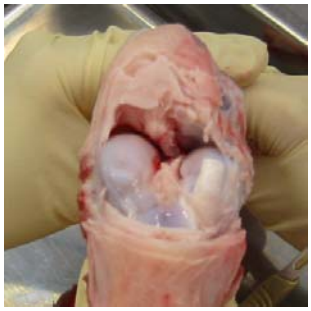
Stage 3 The ligaments at the centre of the joint were cut in order to fully expose the joint.	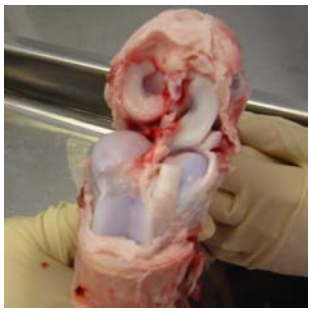
Stage 4 The menisci were removed from the joint.	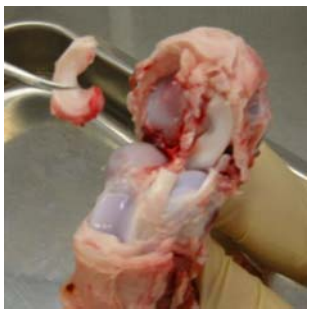

Figure 2.6 The stages involved in the isolation of ovine meniscal cartilage.

Chondrocytes were obtained by enzymatic digestion, with agitation in pronase digestion medium (Appendix 2.2.2) for 1 hour and collagenase digestion medium (Appendix 2.2.3) for 3 hours in a humidified incubator (37ºC, 5% CO_2). The resulting cell suspension was passed through a 70 μm cell strainer (BD Falcon, Fahrenheit Laboratory Supplies, Rotherham, South Yorkshire, UK) to remove any debris and washed by centrifugation (1200 rpm, 259 *x g*; Sigma SciQuip 3K15, Scientific Laboratory Supplies, Nottingham, UK) in chondrocyte medium (Appendix 2.3.1). Cell viability and number were determined using a haemocytometer and trypan blue exclusion.

2.2.3.b Isolation of ovine meniscal fibrochondrocytes (OMCs)

Ovine meniscal cartilage was isolated as described in Section 2.2.2.b. Meniscal tissue was washed in Gentamicin PBS solution and diced finely. Fibrochondrocytes were obtained by enzymatic digestion, with agitation in pronase digestion medium for 2 hours and collagenase digestion medium for 20 hours in a humidified incubator (37ºC, 5% CO_2). Debris was removed from the cell suspension by filtration through a 70 μm cell strainer. The cells were washed by centrifugation (1200 rpm, 259 *x g*) in chondrocyte medium and their number and viability determined using a haemocytometer and trypan blue exclusion.

2.2.3.c Isolation of ovine articular chondrocytes (OACs)

Ovine articular cartilage was isolated as described in Section 2.2.2.c. Cartilage pieces were washed in PBS and diced finely. Chondrocytes were obtained by enzymatic digestion, with agitation in pronase digestion medium for 1 hour and collagenase digestion medium for 3 hours in a humidified incubator (37ºC, 5% CO_2). The resulting cell suspension was passed through a 70 μm cell strainer to remove any debris and washed by centrifugation (1200 rpm, 259 *x g*) in chondrocyte medium. Cell viability and number were determined using a haemocytometer and trypan blue exclusion.

2.2.4 Cell culture

2.2.4.a Culture of BACs

BACs were isolated as described in Section 2.2.3.a. Primary BACs with viability greater than 95% were used in each experiment (i.e. cells were not expanded *in vitro*).

2.2.4.b Culture of OMCs

OMCs were isolated as described in Section 2.2.3.b. Cells with viability greater than 95% were cultured in Nunc™ tissue culture flasks with a surface area of 175 cm^2. When cells were 80-90% confluent, a cell suspension was obtained by enzymatic digestion with trypsin ethylenediaminetetraceitic acid (EDTA) in PBS (Appendix 2.3.2). Cells were split 1 in 2 and cultured to a maximum of passage 4 for tissue formation studies and to a maximum of passage 10 for seeding studies.

2.2.4.c Cryopreservation of OMCs

Long term storage of OMCs was achieved by cryopreservation. Cells were suspended in freezing medium (Appendix 2.3.3) and stored at -80°C overnight before being transferred to liquid nitrogen.

2.2.4.d Culture of OACs

OACs were isolated as described in Section 2.2.3.c. Primary OACs with viability greater than 95% were used in each experiment (i.e. cells were not expanded *in vitro*).

2.2.4.e Culture of Human Osteosarcoma (HOS) TE85 cells

HOS TE85 cells obtained from the European Collection of Cell Cultures (ECACC; Wiltshire, UK) were cultured in Nunc™ tissue culture flasks with a surface area of 75 cm^2 in HOS TE85 medium (Appendix 2.3.4) until 80-90% confluent. When confluent, a cell suspension was obtained by enzymatic digestion with trypsin/EDTA in PBS. Cells were used between passage 81 and 95.

2.2.4.f Cryopreservation of HOS TE85 cells

Long term storage of HOS TE85 cells was achieved by cryopreservation as described in Section 2.2.4.c.

2.2.5 Culture of cell seeded scaffolds

2.2.5.a Preparation of scaffolds

Scaffolds were autoclaved at 120°C for 20 minutes, transferred to the appropriate cell culture medium and allowed to soak for at least 12 hours.

2.2.5.b Seeding cells into scaffolds

A cell suspension was obtained by enzymatic digestion with trypsin EDTA in PBS. The cells were washed by centrifugation (1200 rpm, 259 *x g*) and diluted to a concentration of 4 x 10^6 cells per mL in the appropriate culture medium. Scaffolds were arranged in separate wells of 24-well non-tissue culture treated plates (BD Falcon, Fahrenheit Laboratory Supplies, Rotherham, South Yorkshire, UK). The cell suspension was pipetted through each scaffold ten times (1 mL per scaffold) in order to encourage cell attachment and the plate transferred immediately to an orbital shaker (IKA® Schüttler MTS4, Sigma-Aldrich, Poole, Dorset, UK) in a humidified incubator (37ºC, 5% CO_2) and agitated for 18 hours.

2.2.5.c Static culture

Seeded scaffolds were transferred to 6-well non-tissue culture treated plates (BD Falcon). One scaffold was placed in each well containing 10 mL medium. Three times per week, 5 mL of medium was removed and replaced with fresh culture medium. Cell seeded scaffolds were cultured for 4 or 8 weeks in a humidified incubator (37ºC, 5% CO_2).

2.2.5.d Rotary cell culture system™ (RCCS™) culture

Seeded scaffolds were placed in RCCS™ vessels (Cellon SA, Luxembourg). Each vessel contained 5 scaffolds and 50 mL culture medium. Culture medium was replenished at a rate of 50% (25 mL) every three days.

Vessels were cultured for 4 or 8 weeks in a humidified incubator (37ºC, 5% CO_2). The speed at which the vessels rotated was increased throughout the culture period to maintain cell-seeded scaffolds within a "microgravity-like" environment.

2.2.5.e Flow perfusion culture

This bioreactor system was designed and custom-built at Smith & Nephew Research Centre (York, UK). Figure 2.7 shows the arrangement of the Smith & Nephew flow perfusion bioreactor. Seeded scaffolds were transferred to 12 individual ports within the bioreactor, which contained 600 mL culture medium that was replenished at a rate of 0.15 mL per minute. Flow through the scaffolds was achieved by a separate peristaltic pump, which transferred liquid from one side of the bioreactor to the other at a rate of 342 mL per minute (equivalent to approximately 1 mL per minute through each scaffold). Bioreactor culture experiments were carried out for 4 weeks in a humidified incubator (37ºC, 5% CO_2).

2.2.6 Biochemical analyses

2.2.6.a Preparation of samples

2.2.6.a.i Preparation of ovine meniscal cartilage samples

Ovine meniscal cartilage was isolated as described in Section 2.2.2.b, weighed (wet weight) and lyophilised. Lyophilised cartilage samples were re-weighed (dry weight) and stored at -20°C until required for analysis.

2.2.6.a.ii Preparation of ovine articular cartilage samples

Ovine articular cartilage was isolated as described in Section 2.2.2.c. Cartilage samples were prepared as described in Section 2.2.6.a.i.

2.2.6.a.iii Preparation of cell-seeded scaffolds

Scaffolds were seeded with cells and cultured as described in Sections 2.2.6.b-2.2.6.e. Scaffolds were removed from culture, washed three times in PBS, lyophilised, weighed and stored at -20°C until required for analysis.

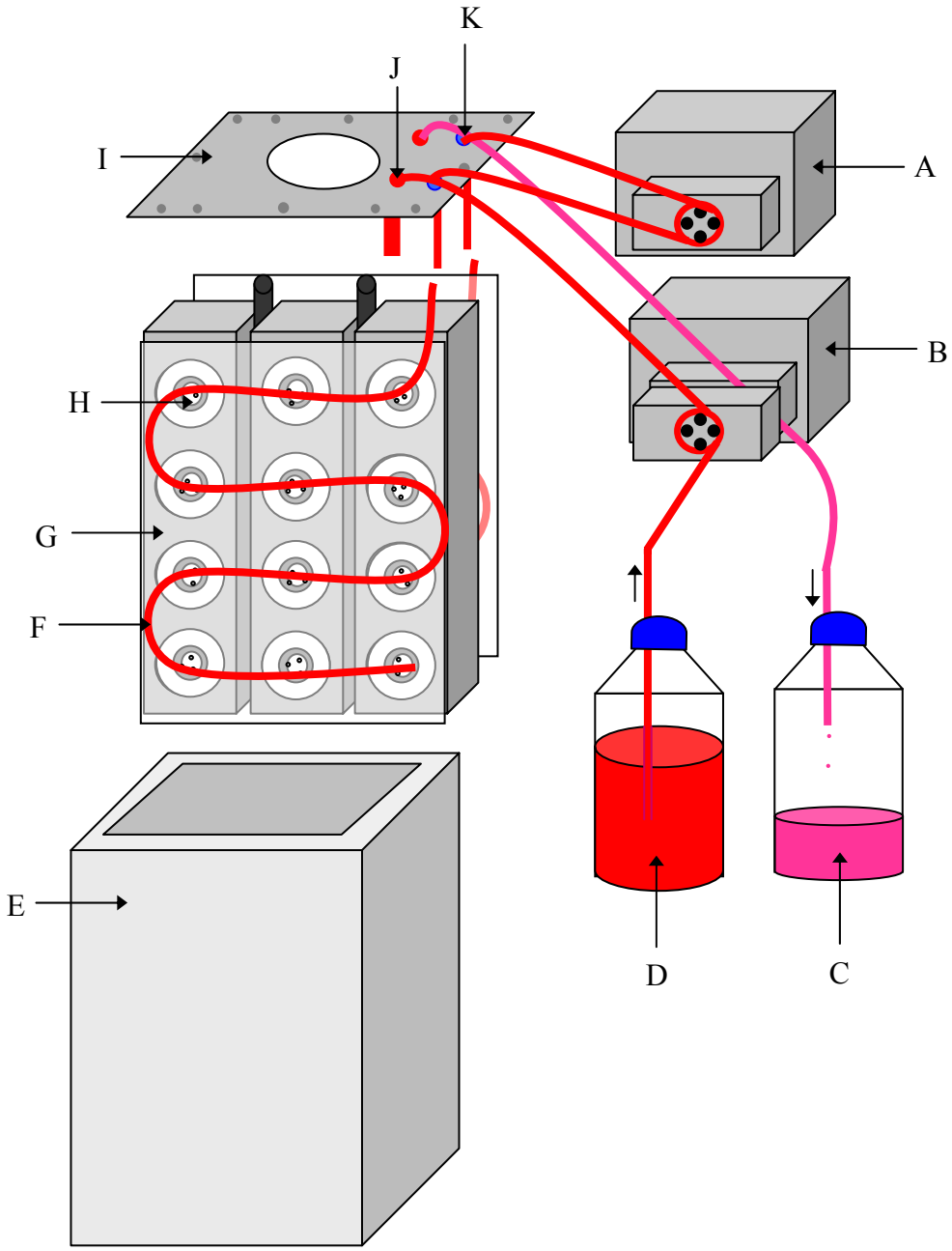

Figure 2.7 The Smith & Nephew flow perfusion bioreactor.
Peristaltic pump (A) controls the flow of medium through the system. Peristaltic pump (B) controls the removal of waste medium (C) and supply of fresh medium (D). The culture system is contained within a tank (E). Tubing (F) and perspex sheets (G) direct medium flow through the scaffolds, which are held within individual ports (H). The bioreactor lid (I) contains two sets of ports, one for attachment to pump B (J) and the other for attachment to the pump A (K).

2.2.6.a.iv Preparation of standard cell pellets

Cells were cultured as described in Section 2.2.4 and washed by centrifugation (1200 rpm, 259 *x g*). The cell suspension was diluted to a concentration of 8 x 10^6 cells per mL in the appropriate culture medium. Pellets of 8 x 10^6 cells were obtained by centrifugation of a 1 mL aliquot and removal of the supernatant. Cell pellets were lyophilised and stored at -20°C until required for analysis.

2.2.6.b Papain digestion

Papain, a proteolytic enzyme, was used to solubilise tissue samples. This allowed dissociation of deoxyribonucleic acids (DNA) from nucleoproteins (Kim *et al* 1988) and sulphated glycosaminoglycans (GAGs) from other glycoproteins (Farndale *et al* 1986). Samples were prepared for papain digestion as described in Section 2.2.6.a. Samples were incubated with 1 mL papain solution (Appendix 2.4.1) overnight in a water bath at 60°C. Papain solution without tissue or cells was also incubated at 60°C overnight to be used as a diluent in biochemical assays (heat-treated papain solution). Papain digests were allowed to cool to room temperature prior to use in biochemical assays.

2.2.6.c Hoechst 33258 assay for quantification of DNA

Hoechst 33258 is a bisbenzimidazole dye (2-[2-(-4-hydroxyphenyl)-6-benzimidazole]-6-(-1-methyl-4-piperazyl)-benzimidazole trihydrochloride), which intercalates in adenosine-thymidine (A-T) regions of DNA producing fluorescence (Cesarone *et al* 1979). Measurements of fluorescence intensity were used to assess cell number within cartilage samples and cell seeded scaffolds.

2.2.6.c.i Preparation of standard solutions for assay calibration

To produce a calibration curve of cell number versus fluorescence, cell pellets (Section 2.2.6.a.iv) were papain digested as described in Section 2.2.6.b and serially diluted with heat-treated papain to give standard solutions with the following cell concentrations: 0, 3.13 x 10^4, 6.25 x 10^4, 1.25 x 10^5, 2.5 x 10^5, 5 x 10^5, 1 x 10^6, 2 x 10^6, 4 x 10^6 and 8 x 10^6 cells/mL. For each assay a calibration curve was generated for the appropriate cell type.

2.2.6.c.ii Assessment of cell number in cartilage samples

Papain digested cartilage samples were diluted 1:10 with heat-treated papain solution. Aliquots of each cartilage sample, calibration standard and heat-treated papain solution (75 μL) were placed in triplicate in a 24-well assay plate. Hoechst buffer (1 mL; Appendix 2.4.2) and Hoechst 33258 working solution (1.5 mL; Appendix 2.4.3) were added to each well. Plates were incubated in darkness for 5 minutes, gently agitated and the fluorescence at excitation wavelength 355 nm and emission wavelength 460 nm measured using a fluorescence plate reader (MFX Microtiter Plate Fluorimeter, Dynex Technologies (UK) Ltd, West Sussex, UK). The cell number was expressed as the number of cells per gram of dry tissue, which was determined by normalising the number of cells within the sample with respect to the lyophilised cartilage weight.

2.2.6.c.iii Assessment of cell number in cell-seeded scaffolds

Analysis of the number of cells within cell-seeded scaffolds was carried out as described in Section 2.2.6.c.ii, with the exception that cell-seeded scaffold digests were not diluted 1:10 with heat-treated papain solution. As a control, scaffolds without cells were analysed as described above.

2.2.6.d Alamar blue ™assay for assessment of cell viability

The Alamar blue™ assay is based on the detection of metabolic activity of cells (Fields and Lancester 1993). The assay reagent, Alamar blue™, contains a reduction-oxidation (REDOX) indicator (resazurin). The metabolic activity of cells causes a chemical reduction in their medium, which leads to the production of a pink fluorescent product, resorufin (O'Brien *et al* 2000). Decreased fluorescence levels are indicative of a decrease in the synthetic rates of cells and therefore suggestive that cells have been cultured in a less favourable environment and have a lower relative viability compared to cells which yield higher fluorescence levels when incubated with Alamar blue™.

2.2.6.d.i Analysis of viability of cells within cell-seeded scaffolds

Cell-seeded scaffolds were transferred to a 24-well plate, washed with PBS and incubated with 1 mL Alamar blue™ working solution (Appendix 2.4.4) for 90 minutes in darkness within a humidified incubator (37°C, 5% CO_2). Following gentle agitation for 15 minutes, 200 μL aliquots were removed from each well and placed in a 96-well assay plate.

The fluorescence at excitation wavelength 530 nm and emission wavelength 590 nm was measured using a fluorescence plate reader (MFX Microtiter Plate Fluorimeter). As a control, scaffolds without cells were incubated for 90 minutes in 1 mL Alamar blue™ working solution and analysed as described above.

2.2.6.e 1, 9-dimethylmethylene blue (DMMB) assay for quantification of sulphated glycosaminoglycans (GAGs)

DMMB is a cationic dye, which binds to sulphate and carboxylate groups within GAGs producing a concentration dependent metachromatic change (Enobakhare *et al* 1996). The magnitude of this change can be quantified by the measurement of optical density.

2.2.6.e.i Preparation of standard solutions for assay calibration

To generate a calibration curve of GAG concentration versus optical density, a 100 μg/mL solution of chondroitin-4-sulphate was prepared (Appendix 2.4.5) and diluted with heat-treated papain solution to give standard solutions of the following concentrations: 0, 5, 10, 15, 20, 25, 30, 40, 50 and 75 μg/mL.

2.2.6.e.ii Analysis of GAGs in cartilage

Samples of papain-digested cartilage were diluted 1:100 with heat-treated papain solution. Aliquots of the diluted cartilage samples, calibration standards and heat-treated papain (20 μL) were placed in triplicate in a 96-well assay plate. DMMB solution (200 μL, Appendix 2.4.6) was added to each well and optical density measured at 540 nm using a colourimetric plate reader (MRX Microplate Reader,

Dynex Technologies (UK) Ltd). The GAG content per gram of each sample was calculated using the equation given in Appendix 3.1.

2.2.6.e.iii Analysis of GAGs in cell-seeded scaffolds

Analysis of GAG content within cell-seeded scaffolds was carried out as described in Section 2.2.6.e.ii, with the exception that cell-seeded scaffold digests were not diluted 1:100 with heat-treated papain solution.

2.2.6.f Hydroxyproline assay for quantification of total collagen content

Hydroxyproline, a major component of collagen, can be extracted from cartilage by acid hydrolysis and quantified by oxidation with N-chloro-p-toluenesulfonamide sodium salt (chloramine T). Reaction of the resulting oxidation product with p-dimethylaminobenzaldehyde (p-DAB) at 60°C leads to the generation of a coloured product, which can be measured using a colourimeter (Woessner 1961).

2.2.6.f.i Acid hydrolysis of samples

Papain-digested cartilage and cell-seeded scaffolds (250 μL) were hydrolysed by overnight incubation with equal volumes of concentrated hydrochloric acid (HCl) at 120°C. The residues were dried at 90°C, allowed to cool to room temperature and re-dissolved in 1 mL 0.25 M sodium phosphate buffer (Appendix 2.4.7). Heat-treated papain solution (1 mL) was hydrolysed with an equal volume of HCl, dried at 90°C, cooled and re-dissolved in 4 mL 0.25 M sodium phosphate buffer for use as a diluent in the assay (hydrolysed papain solution).

2.2.6.f.ii Preparation of standard solutions for assay calibration

To generate a calibration curve of hydroxyproline concentration versus optical density, a 100 μg/mL solution of hydroxyproline was prepared (Appendix 2.4.8). This solution was diluted with hydrolysed papain solution to give the following concentrations of hydroxyproline: 0, 1, 2, 4, 5, 6, 8, 10, 15, 20 and 30 μg/mL.

2.2.6.f.iii Quantification of total collagen content in cartilage

Hydrolysed cartilage samples were diluted 1:10 with hydrolysed papain solution. Aliquots of the diluted hydrolysed cartilage samples, calibration standards and hydrolysed papain solution (50 μL) were placed in triplicate in a 96-well assay plate. Chloramine T solution (50 μL; Appendix 2.4.9) was added to each well and the plate incubated at room temperature for 20 minutes. Following this incubation period 50 μL p-DAB solution (Appendix 2.4.10) was added to each well and the plate incubated at 60°C in a water bath for 30 minutes. The plate was allowed to cool to room temperature and the optical density measured at 540 nm on a colourimetric plate reader (MRX Microplate Reader). The collagen content per gram of each sample was calculated using the equation given in Appendix 3.2.

2.2.6.f.iv Quantification of total collagen content in cell-seeded scaffolds

Analysis of total collagen content within cell-seeded scaffolds was carried out as described in Section 2.2.6.f.iii, with the exception that cell-seeded scaffold digests were not diluted 1:10 in hydrolysed papain solution.

2.2.7 Histology

Histological methods allowed examination of the structural organisation of tissue. Mayer's haematoxylin was used to stain cell nuclei blue/black. Mayer's haematoxylin contains alum, a cation that binds to the anionic nuclear chromatin (Stevens and Wilson 1999). Eosin was used to stain connective tissues shades of pink/red (Stevens and Wilson 1999). Safranin O is a cationic dye that binds to negatively charged sulphate and carboxylate groups within GAG chains (Cook 1999).

2.2.7.a Processing, paraffin embedding and sectioning cartilage

Cartilage samples were fixed in 10% buffered formal saline and dehydrated by passing through an increasing series of industrial methylated spirits (IMS; 50% [*v/v*], 70% [*v/v*], 90% [*v/v*], and 100%[*v/v*]) and xylene (Histopathology Department, Queen's Medical Centre, Nottingham; (Anderson and Gordon 1999).

Processed tissue was orientated and embedded in paraffin wax. A microtome (Leica RM2165, Leica Microsystems, Milton Keynes, UK) with a stainless steel blade was

used to cut 5 μm sections. The sections were "stretched" out on a water bath at 50°C, mounted on Superfrost™ microscope slides (Scientific Laboratory Supplies, Nottingham, UK) and heated to 56°C on a hot plate.

2.2.7.b Histological analysis of cartilage

2.2.7.b.i Haematoxylin and eosin staining of cartilage

Cartilage sections were deparaffinised by heating to 56°C and rehydrated by passing through xylene, a decreasing series of IMS (100% [*v/v*], 90% [*v/v*], 70% [*v/v*] and 50%[*v/v*]) and tap water. Slides were incubated in Mayer's haematoxylin for 10 minutes at room temperature and washed in tap water for 1 minute. Sections were blued using Scott's tap water substitute for 2 minutes and washed in tap water for a further minute. Sections were then partially dehydrated through an increasing series of IMS (50% [*v/v*], 70% [*v/v*], 90% [*v/v*]) for 1 minute each and dipped in 1% alcoholic eosin (Appendix 2.5.1). Tissue sections were fully dehydrated by passing through IMS (100% [*v/v*]) and xylene prior to mounting with a distyrene plasticiser xylene mixture (DPX). Slides were viewed in bright field using an inverted microscope (Leica DM IRBE, Leica Microsystems).

2.2.7.b.ii Safranin O staining

Cartilage sections were deparaffinised by heating to 56°C and rehydrated by passing through xylene, a decreasing series of IMS (100% [*v/v*], 90% [*v/v*], 70% [*v/v*] and 50% [*v/v*]) and tap water. Sections were incubated in Mayer's haematoxylin for 10 minutes at room temperature, washed in tap water for 1 minute, dipped in 0.02% (*w/v*) aqueous fast green (Appendix 2.5.2) for 4 minutes, dipped in 1% (*v/v*) acetic acid (Appendix 2.5.3) and placed in 0.1% (*v/v*) aqueous safranin O for 10 minutes. Tissue sections were then dehydrated through an increasing series of IMS (50% [*v/v*], 70% [*v/v*], 90% [*v/v*], and 100%[*v/v*]) and xylene before mounting and viewing as described in Section 2.2.7.b.i.

2.2.7.c Processing, resin embedding and sectioning cartilage constructs

Cartilage constructs were fixed in 4% paraformaldehyde (Appendix 2.5.4) prior to embedding in Technovit 8100, a hydroxyethylmethacrylate resin. Fixed cell-seeded

scaffolds were then washed overnight in PBS, dehydrated in 100% acetone for 1 hour and infiltrated with Technovit 8100 infiltration solution (Appendix 2.5.5) for 10 hours at 4°C with agitation. Samples were agitated in 5 mL Technovit 8100 embedding solution (Appendix 2.5.6) for 5 minutes at 4°C and orientated within moulds containing 5 mL Technovit 8100 embedding solution such that sections could be taken through the transverse and sagittal planes (Figure 2.8). The moulds were sealed hermetically and stored at 4°C to allow the resin to cure. A microtome with a tungsten carbide blade was used to cut 5 μm sections, which were "stretched" out on distilled water at room temperature, mounted on Superfrost™ microscope slides and allowed to dry at room temperature.

2.2.7.d Histological analysis of cell-seeded scaffolds

2.2.7.d.i Haematoxylin and eosin staining

Resin sections were washed for 5 minutes in distilled water. Sections were incubated in Mayer's haematoxylin for 10 minutes, washed in tap water for 1 minute and the haematoxylin blued in Scott's tap water substitute for 2 minutes. Sections were then washed in tap water for 1 minute and dipped in 1% alcoholic eosin. Excess staining was eliminated by washing with 25% (*v/v*) IMS. Sections were mounted using DPX and viewed in bright field using an inverted microscope.

2.2.7.d.ii Safranin O staining

Resin sections were washed for 5 minutes in distilled water. Sections were incubated in Mayer's haematoxylin for 10 minutes at room temperature, washed in tap water for 1 minute, blued in Scott's tap water substitute for 2 minutes and tap water for 1 minute. Slides were placed in 0.02% (*w/v*) aqueous fast green for 4 minutes, dipped in 1% (*v/v*) acetic acid and placed in 0.1% (*v/v*) aqueous safranin O for 10 minutes. Excess staining was eliminated by washing with 25% (*v/v*) IMS. Sections were mounted and viewed as described in Section 2.2.7.d.i.

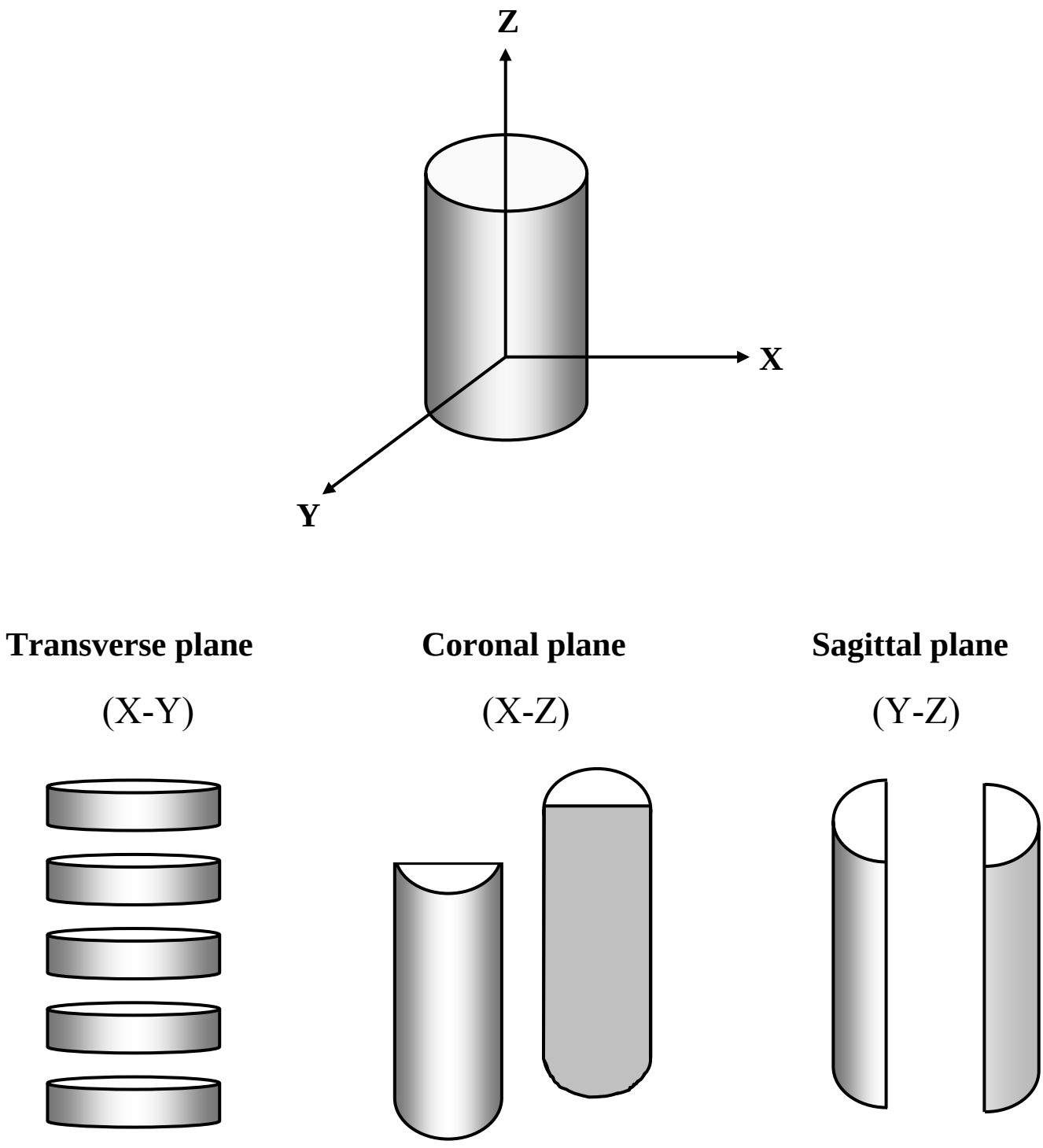

Figure 2.8 The planes of section described within this thesis.

2.2.8 Scanning electron microscopy (SEM)

By scanning an electron beam across the surface of a sample, SEM allows high-resolution images of the sample's topography to be obtained.

2.2.8.a SEM of scaffolds

Scaffolds were autoclaved at 120°C for 20 minutes, cut in half through the sagittal plane (Figure 2.8), orientated on carbon coated electron microscope stubs and sputter coated with gold for 4 minutes (Balzers Union SCD 030, Balzers, Fürstentum, Liechtenstein). The outer surface and middle region of each sample were viewed using a scanning electron microscope (Philips 505, Philips, Eindhoven, The Netherlands). Digital images were acquired using Semicaps 2000A software (version 8.2, Semicaps Pte Ltd, Singapore).

2.2.8.b SEM of cell-seeded scaffolds

Cell-seeded scaffolds were prepared for SEM using a method described by Robinson and Gray (Robinson and Gray 1999). Scaffolds were washed with PBS, fixed in 3% (*v/v*) glutaraldehyde solution (Appendix 2.6.1) at 4°C overnight, before washing in PBS and secondary fixing for 1 hour in 1% (*v/v*) osmium tetroxide solution (Appendix 2.6.2). Samples were then dehydrated through an increasing series of ethanol (25% [*v/v*], 50% [*v/v*], 70% [*v/v*], 90% [*v/v*], 95% [*v/v*] and 100% [*v/v*]) and dried using hexamethyldisilaxane (HMDS). Finally scaffolds were cut, mounted, sputter coated and viewed as described in Section 2.2.8.a.

2.2.9 Statistical analysis

For all data, the mean and standard error of the mean (SEM) were calculated. The statistical significance of results was assessed using GraphPad InStat version 3.0 (GraphPad Software Inc, San Diego, USA).

Chapter 3

Determination of the optimum conditions for seeding cells into needled felt and sparse knit scaffolds

3.1 Introduction

Scaffolds play a crucial role in tissue engineering applications, providing a matrix in which new tissue is regenerated. For successful tissue formation it is essential that the scaffold structure faciliates efficient cell seeding, supports cell attachment and promotes cell proliferation and ECM secretion (Woodfield *et al* 2002). For cartilage tissue engineering it is important that a high density of cells are distributed throughout the entire scaffold in order to promote chondrogenesis and prevent fibrous tissue formation (Freed and Vunjak-Novakovic 1998 and Li *et al* 2001). Table 3.1 summarises different seeding methods that have been used in cartilage tissue engineering studies. These include the use of spinner flasks (Freed *et al* 1994a); delivering cells into the scaffold within a vehicle, such as alginate (Marijnissen *et al* 2002) and agitating scaffolds within tissue culture plates on an orbital shaker (Brown *et al* 2000). In this thesis the method described by Brown and colleagues was used to seed cells into scaffolds. Whilst there are many reports in the literature on the need for optimising methods for seeding cells into tissue engineering scaffolds, there is little information comparing the effects of scaffold structure or cell type on the optimum seeding conditions.

Seeding method	Scaffold type	Cell type	Reference
Agitation	PGA non woven mesh	Porcine auricular chondrocytes	Brown *et al* 2000
Alginate Encapsulation	Alginate beads	Human articular chondrocytes	Gagne *et al* 2000
	PLLA non woven matrix	Bovine articular chondrocytes	Marijnisssen *et al* 2002
Perfusion	PEGT/PBT copolymer foam	Bovine articular chondrocytes	Wendt *et al* 2003
	Hyaluronan non woven mesh	Bovine articular chondrocytes	Wendt *et al* 2003
Spinner flask	PGA non woven mesh	Bovine articular chondrocytes	Freed *et al* 1994a
	PGA non woven mesh	Bovine articular chondrocytes	Vunjak-Novakovic *et al* 1998
	Hyaluronan non woven mesh	Bovine articular chondrocytes	Wendt *et al* 2003
Static	PEGT:PBT copolymer foam	Bovine articular chondrocytes	Wendt *et al* 2003
	PGA non woven mesh	Bovine articular chondrocytes	Moran *et al* 2003 Puelacher *et al* 1994

Table 3.1 Methods used for seeding cells into scaffolds for cartilage tissue engineering.

3.2 Aims and hypotheses

The first objective of this chapter was to describe the different scaffolds with respect to mass, density, the arrangement of fibres and the resistance of the scaffolds to fluid flow. The second aim was to determine the optimum rate of agitation required to allow a high density of viable BACs and OMCs to be distributed homogeneously throughout NF, SK3, SK4 and SK5 scaffolds. To establish if optimum conditions were cell type dependent, a comparison was made between BACs, OMCs and a human osteosarcoma cell line (HOS TE85). The first hypothesis was that agitation speed would influence the number, distribution and viability of cells in scaffolds. It has been reported that dynamic seeding conditions lead to higher cell densities in scaffolds than static methods (Li *et al* 2001), however it was postulated that excessive agitation may compromise cell viability. Therefore for each scaffold type there would be an optimum rate of agitation at which an appropriate number of viable cells would be evenly distributed throughout the structure. The second hypothesis was that the optimum rate of agitation would be dependent on scaffold architecture. It was proposed that more dense scaffolds would require seeding at faster agitation speeds.

3.3 Methods

3.3.1 Characterisation of needled felt and sparse knit scaffolds

3.3.1.a Scaffold design and manufacture

3.3.1.a.i Needled felt scaffolds

NF scaffolds were of the same design as PGA non-woven meshes used in various other cartilage tissue engineering studies (see Table 1.2 for details of studies using non-woven meshes). Scaffolds were manufactured from PET as described in Section 2.2.1.a.

3.3.1.a.ii Sparse knit scaffolds

SK scaffolds were designed to overcome the gas exchange and nutrient transfer limitations of other tissue engineering scaffolds.

SK scaffolds contained bundles of randomly arranged fibres separated by aligned channels and held within upper and lower knitted crusts. Three different SK scaffolds were designed (SK3, SK4 and SK5). SK scaffolds were manufactured from PET using the method given in Section 2.2.1.b.

3.3.1.b Scanning electron microscopy of scaffolds

Scaffolds were prepared for SEM and imaged as outlined in Section 2.2.8.a. Images were taken of two samples for each scaffold type. The upper surface and the middle region of each scaffold were imaged.

3.3.1.c Determination of average scaffold mass and density

The average mass of each of the scaffold types was determined by individually weighing 20 scaffolds and dividing their combined weight by the total number of scaffolds (20). Micro-callipers were used to accurately measure the diameter and thickness of each of the twenty scaffolds and the equation for the volume of a cylinder (Appendix 3.3) used to calculate the volume of each scaffold. From the mass and volume of each scaffold, the density was calculated using the equation given in Appendix 3.4. The statistical significance between the mass and density of each scaffold type was assessed using GraphPad InStat version 3.0. Results were expressed as mean ± SEM. A one way analysis of variance (ANOVA) with the Tukey-Kramer multiple comparisons post test were performed.

3.3.1.d Characterisation of scaffold resistances to fluid flow

The apparatus shown in Figure 3.1 was used to characterise the flow-resistance properties of each of the scaffolds in conjunction with the formula given in Appendix 3.5. Scaffolds were fixed within lengths of silicon tubing 10 mm in diameter such that liquid flowing through the tube must pass through the scaffold. Water was passed through the tubing at a flow rate controlled by a syringe pump and collected in a measuring cylinder. Once the height of water above the scaffold had stabilised, the time taken for a given volume of water to collect in the measuring cylinder was recorded.

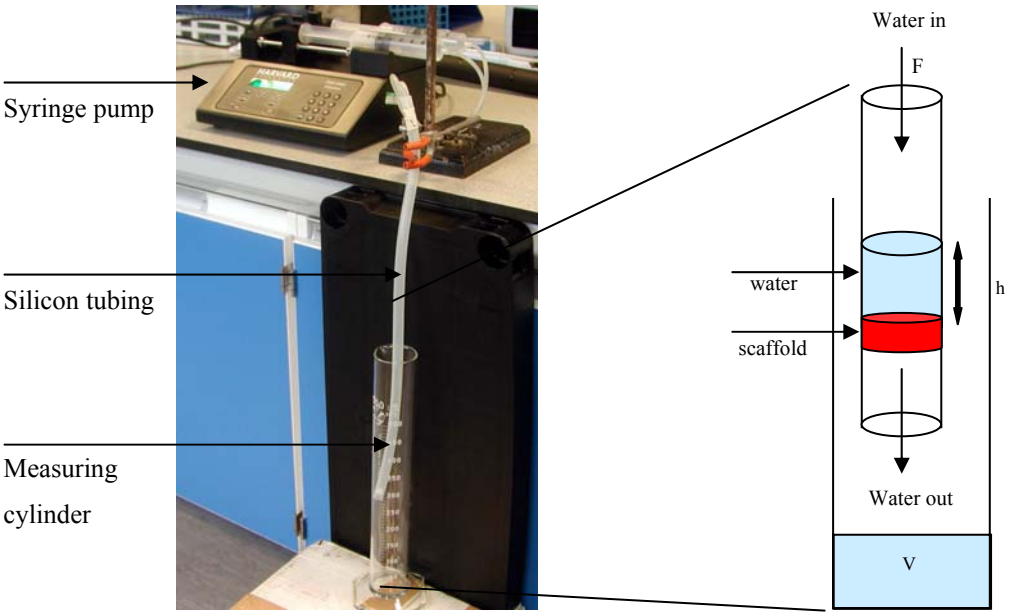

Figure 3.1 The apparatus used to characterise the resistance of each scaffold to flow where F represents the flow rate, h represents height of water above the scaffold and V represents the volume of water collected.

For each scaffold type, two scaffolds were assessed. The statistical significance of the flow resistance of each scaffold type was assessed using GraphPad InStat version 3.0. Results were expressed as mean ± SEM. An ANOVA with the Tukey-Kramer multiple comparisons post test were performed.

3.3.2 Cell culture

BACs were isolated as described in Section 2.2.3.a. Primary BACs were not expanded *in vitro* prior to use in seeding studies. OMCs were isolated and cultured as described in Sections 2.2.3.b and 2.2.4.b. OMCs were used in seeding studies between passages 4 and 10. HOS TE85 cells were obtained and cultured as described in Section 2.2.4.e and used in seeding studies between passages 81 and 95.

3.3.3 Seeding cells into scaffolds

Scaffolds were autoclaved and soaked in culture medium as described in Section 2.2.5.a. Scaffolds were seeded with BACs, OMCs or HOS TE85 cells as described in Section 2.2.5.b. Briefly, cells were re-suspended in cell culture medium to a concentration of 4×10^6 cells per mL. The cell suspension was pipetted through each scaffold (1 mL per scaffold) in a 24-well non-tissue culture treated plate and agitated at 0, 100, 200, 300 or 400 rpm for 18 hours. Scaffolds were seeded in triplicate for biochemical analysis and in duplicate for image analysis.

3.3.4 Analysis of cell viability

The Alamar blue™ assay was carried out as outlined in Section 2.2.6.d.i to assess the total relative viability of cells within each of the scaffolds following agitation for 18 hours. In brief, the cell-seeded scaffolds were transferred to a 24-well plate and washed three times with PBS. Samples were incubated with 1 mL Alamar blue™ working solution (Appendix 2.4.4) for 90 minutes in a humidified incubator (37°C, 5% CO_2). Following gentle agitation for 15 minutes, 200 µL aliquots from each sample were transferred to a 96-well assay plate. The fluorescence was measured at excitation and emission wavelengths of 530 nm and 590 nm respectively, using a fluorescence plate reader (MFX Microtiter Plate Fluorimeter).

Control scaffolds (scaffolds without cells) were incubated with Alamar blue™ working solution and analysed in the same way. The relative viability per cell for each sample was determined by dividing the total relative viability of cells within each sample by the number of cells within the scaffold (as determined using the method given in Section 3.3.5.c). The statistical significance between the total relative viability and viability per cell of scaffolds agitated at 100, 200, 300 or 400 rpm compared to those seeded statically was assessed using GraphPad InStat version 3.0. Results were expressed as mean ± SEM and a two-tailed unpaired t-test was performed in order to assess statistical significance.

3.3.5 Analysis of cell number

3.3.5.a Preparation of standard cell pellets, cell-seeded and control scaffolds

Standard cell pellets for all cell types were prepared as outlined in Section 2.2.6.a.iv. Following the Alamar blue™ assay, cell-seeded and control scaffolds were washed three times in PBS, weighed, lyophilised, re-weighed and stored at -20°C until required for analysis.

3.3.5.b Papain digestion of cell-seeded scaffolds, control scaffolds and standard cell pellets

Samples were digested with papain in order to allow dissociation of DNA from nucleoproteins (Kim *et al* 1988). The digestion was carried out as described in Section 2.2.6.b. In brief, samples were incubated in 1 mL papain solution (Appendix 2.4.1) overnight in a water bath at 60°C. Papain digests were allowed to cool to room temperature prior to analysis using the Hoechst 33258 assay.

3.3.5.c Hoechst 33258 assay for DNA quantification

The Hoechst 33258 assay was employed to quantify the number of cells within each scaffold following seeding. Standard solutions of known cell number were produced for each cell type as summarised in Section 2.2.6.c.i. The Hoechst 33258 assay was performed as described in Section 2.2.6.c.iii.

Briefly, 75 μL of each papain digested sample and standard were placed in triplicate in a 24-well assay plate. Hoechst buffer (1 mL; Appendix 2.4.2) and Hoechst 33258 working solution (1.5 mL; Appendix 2.4.3) were added to each well. Plates were incubated in darkness for 5 minutes, gently agitated and the fluorescence measured at excitation and emission wavelengths of 355 nm and 460 nm respectively, using a fluorescence plate reader. From a calibration curve of cell number versus fluorescence for each cell type, the number of cells within each scaffold was determined. Results were expressed as mean ± SEM and a two-tailed unpaired t-test was performed in order to assess statistical significance.

3.3.6 Analysis of cell distribution

Scanning electron microscopy was used to visualise the position of cells within the scaffolds. Section 2.2.8.b describes how scaffolds were prepared and imaged. In brief, cell-seeded scaffolds were washed in PBS, fixed in 3% (*v/v*) glutaraldehyde solution (Appendix 2.6.1), washed in PBS and further fixed in 1% (*v/v*) osmium tetroxide solution (Appendix 2.6.2). Samples were dehydrated by passing through increasing concentrations of ethanol and dried using hexamethyldisilaxane (HMDS). Scaffolds were cut in half through the sagittal plane and orientated on carbon coated electron microscope stubs such that the scaffold surface and centre could be seen (Figure 3.2). Samples were sputter coated with gold for 4 minutes and viewed using a Philips 505 scanning electron microscope. Digital images were obtained using Semicaps 2000A software.

3.4 Results

3.4.1 Characterisation of needled felt and sparse knit scaffolds

3.4.1.a Scaffold design

Representative scanning electron micrographs of each of the scaffolds are shown in Figure 3.3. Needled felt scaffolds contained a random entanglement of fibres with no regions of alignment (Figure 3.3 A & B). Each of the sparse knit scaffolds contained a knitted upper and lower "crust" (Figure 3.3 C, E & G).

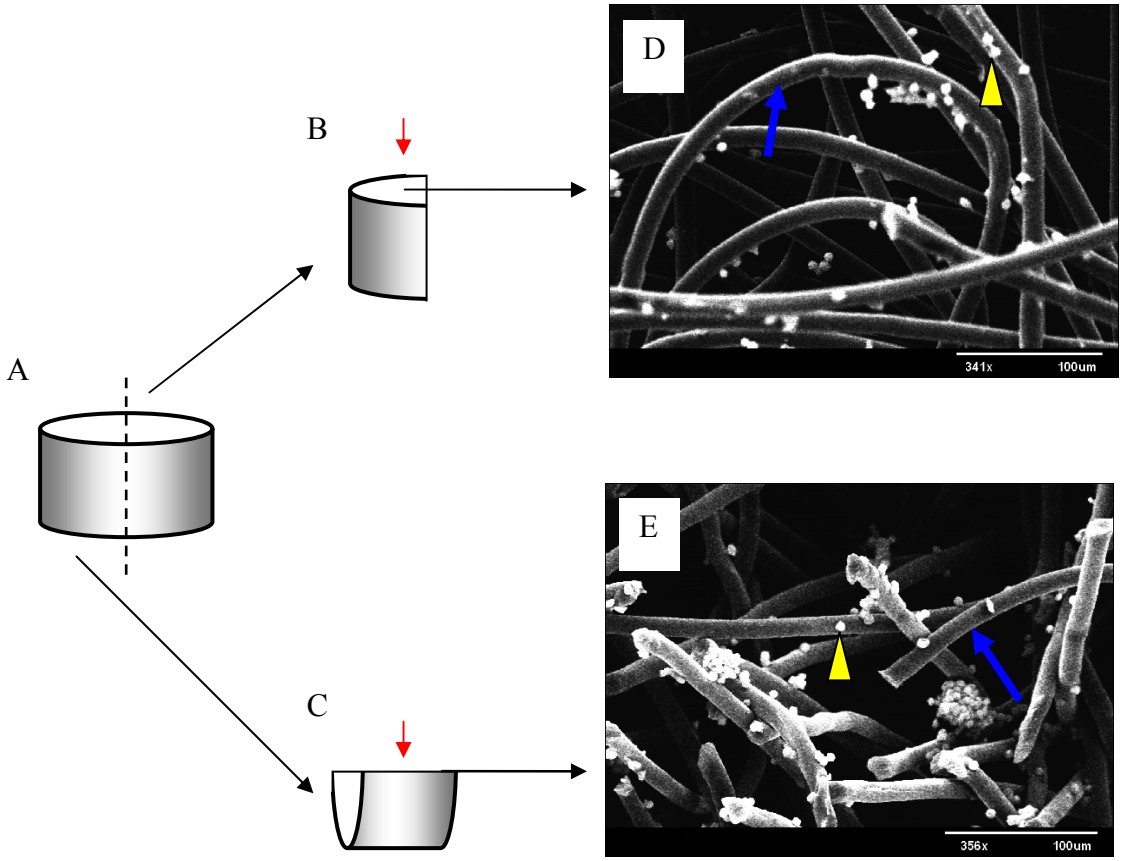

Figure 3.2 Visualisation of the distribution of cells within scaffolds using SEM following overnight seeding. Scaffolds were (A) cut through the sagittal plane and mounted on stubs such that images could be taken of (B) the upper surface and (C) centre of the scaffolds. Red arrows indicate the field of view. Blue arrows indicate the scaffold fibres and yellow arrow heads denote the presence of cells within SEM images taken of (D) the upper surface and (E) the centre of a representative scaffold.

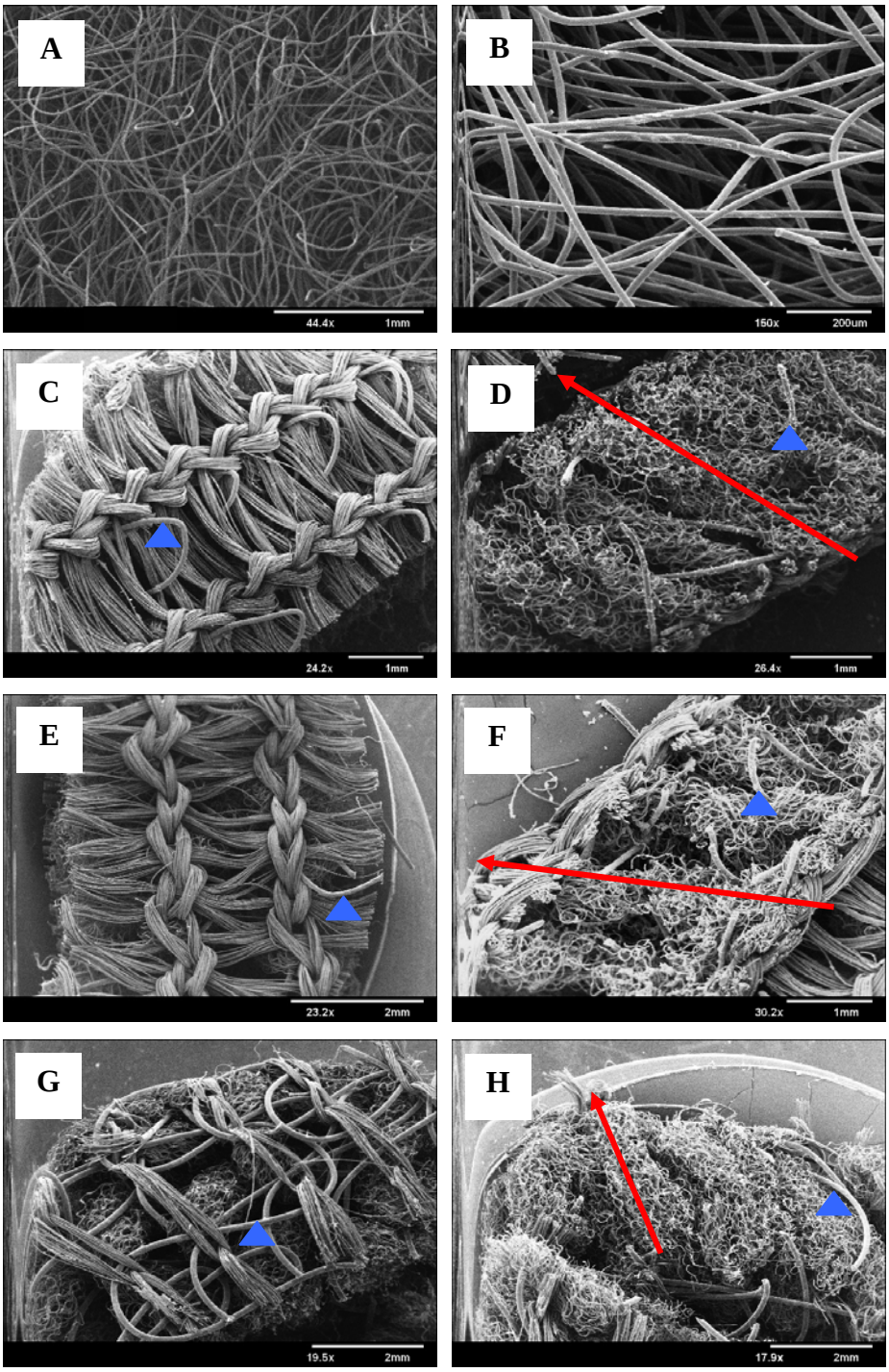

Figure 3.3 Representative scanning electron micrographs of each of the scaffold types: (A and B) needled felt, (C and D) sparse knit 3, (E and F) sparse knit 4 and (G and H) sparse knit 5. Images show the (A, C, E & G) surface and (B, D, F & H) centre of the scaffolds. Arrows (⟶) in images D, F & H indicate the orientation of aligned fibres. Thicker fibres in sparse knit scaffolds are highlighted with triangles (▲).

This knitted crust held together bundles of randomly orientated fibres which were separated by aligned channels (Figure 3.3 D, F & H). The sparse knit scaffolds also differed from the needled felt scaffold in that they contained fibres of two diameters. The larger diameter fibres within the sparse knit scaffolds played a structural role, helping keep the bundles of fibres within the knitted crusts. Sparse knit 5 scaffolds differed from sparse knits 3 and 4 since its knitted crust was of a more open structure (Figure 3.3 G). Sparse knit 3 scaffolds appeared more dense than sparse knit 4 scaffolds (Figure 3.3 D & F).

3.4.1.b Scaffold mass and density

The average mass and density of each of the scaffold types are presented in Figure 3.4 A and B. No significant difference was detected between the mass or density of NF or SK4 scaffolds.

3.4.1.c The resistance of scaffolds to fluid flow

The resistance of each of the scaffold types to the flow of liquid through them is shown in Figure 3.5. All scaffolds showed a decrease in resistance to flow with increasing flow rate. At all flow rates, NF scaffolds showed increased resistance to flow compared to the sparse knit scaffolds. At a flow rate of 50 ml per minute, the resistance of NF scaffolds to flow was significantly greater than that of the SK scaffolds. At the slower flow rates it was not possible to measure the resistance of SK4 and SK5 scaffolds to flow since a height of water could not be retained above the scaffold in the tube.

3.4.2 Assessment of optimum seeding conditions

In order to determine the optimum seeding conditions for each of the scaffold types using BACs, OMCs and HOS TE85 cells, three parameters were investigated: cell viability (Alamar Blue™ assay), seeding efficiency (Hoechst 33258 assay) and the arrangement of cells within scaffolds (SEM).

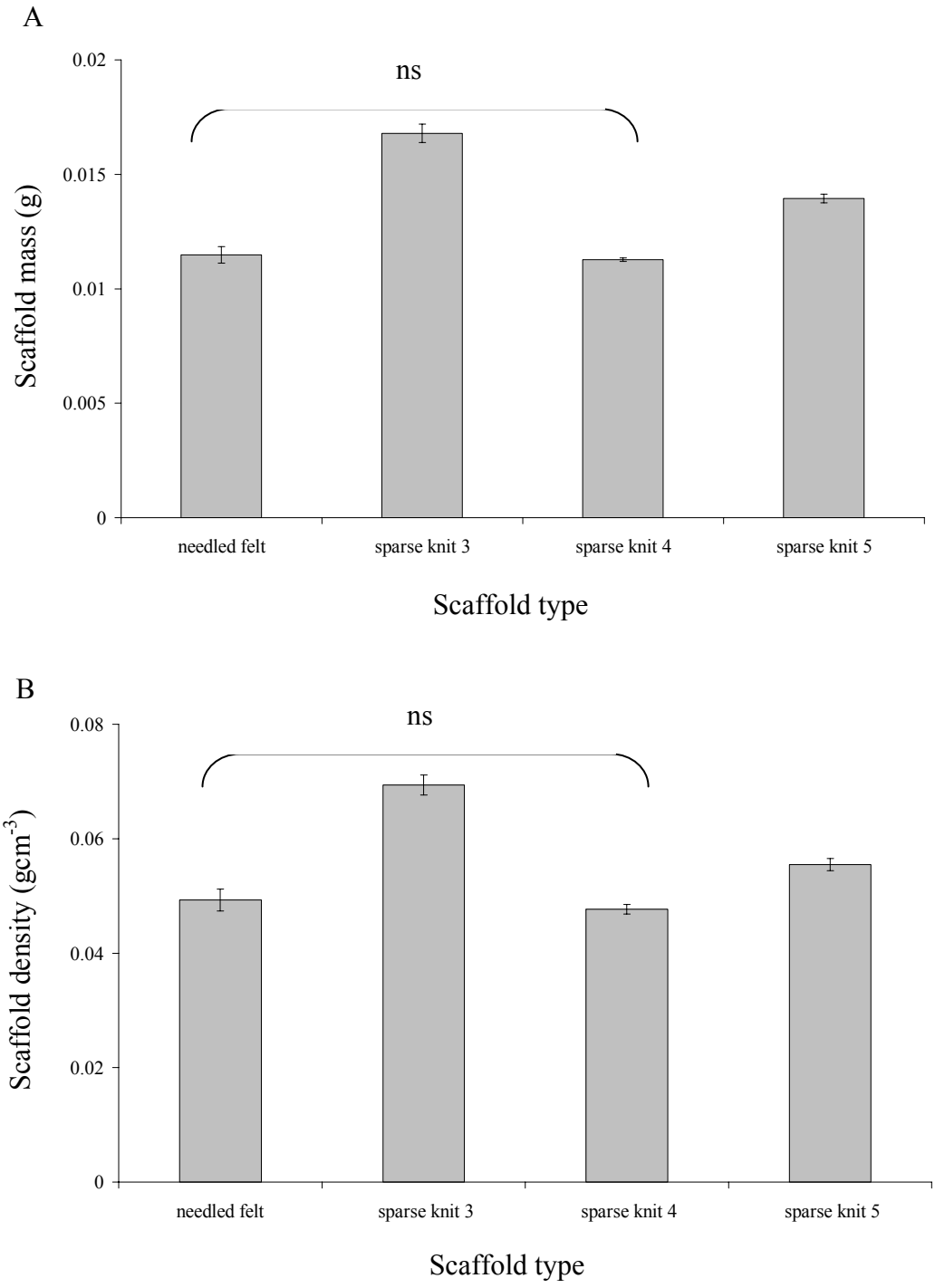

Figure 3.4 Graphs representing (A) the average mass and (B) the average density of each of the scaffold types. Results expressed as mean (n=20) ± SEM.

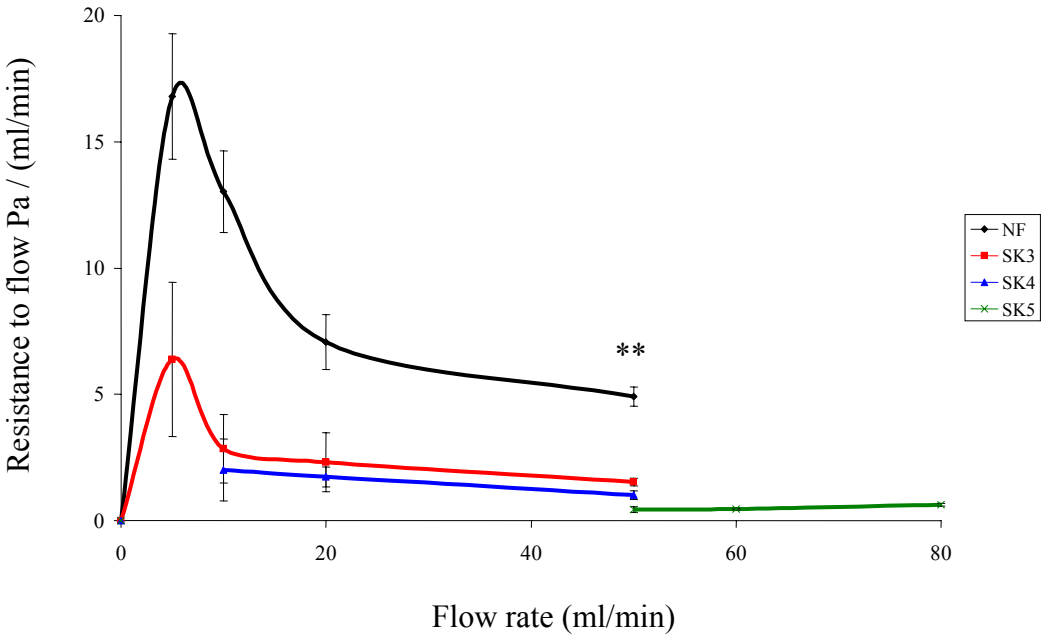

Figure 3.5 The resistance of each of the scaffolds to flow of liquid at different flow rates. Results expressed as mean (n=2) ± SEM, ** indicates $P < 0.01$.

3.4.2.a Analysis of seeding cells into NF scaffolds

3.4.2.a.i Analysis of seeding BACs into NF scaffolds

The effect of agitation speed on the number, total relative viability and relative viability per cell of BACs in NF scaffolds is presented in Figure 3.6. Seeding BACs into NF scaffolds with agitation at 200 or 300 led to significantly more cells within scaffolds, compared to scaffolds seeded statically ($P<0.001$ and $P<0.05$ respectively, Figure 3.6 A). Agitating BACs with NF scaffolds at either 100 or 400 rpm did not increase the number of cells within the scaffolds significantly compared to static seeding (Figure 3.6 A). The total relative viability of BACs in NF scaffolds was increased in scaffolds seeded with agitation at 100 rpm ($P<0.05$), 200 rpm ($P<0.001$), 300 rpm ($P<0.001$) and 400 rpm ($P<0.001$) compared to scaffolds seeded statically (Figure 3.6 B). The relative viability per cell of BACs in NF scaffolds following seeding at each of the speeds was determined by normalising the total relative viability of cells with respect to cell number (Figure 3.6 C). The normalised relative viability of BACs in NF scaffolds was significantly greater in scaffolds agitated at 400 rpm compared to scaffolds seeded under static conditions ($P<0.05$, Figure 3.6 C). No significant difference was determined between the normalised relative viabilities of BACs in NF scaffolds seeded at 100 rpm, 200 rpm or 300 rpm compared to those seeded at 0 rpm (Figure 3.6 C). Scanning electron microscopy allowed visualisation of the distribution of cells at the surface and centre of scaffolds as shown in Figure 3.2. Representative images of NF scaffolds seeded with BACs at each of the speeds are shown in Figure 3.7. NF scaffolds seeded either statically or at 100 rpm contained a small number of BACs at both the surface and in the centre (Figure 3.7 A, B, C & D). Agitation at 200 rpm led to an increased number of cells within the scaffolds, which were distributed evenly throughout the constructs (Figure 3.7 E & F). Increasing the seeding speed to 300 and 400 rpm led to a less even distribution of cells within the scaffolds, with more cells present at the centre than at the surface (Figure 3.7 G, H, I & J). The optimum speed for seeding BACs into NF scaffolds was therefore 200 rpm, since a large number of cells were evenly distributed throughout the scaffolds and the viability of cells was not significantly compromised compared to scaffolds seeded statically.

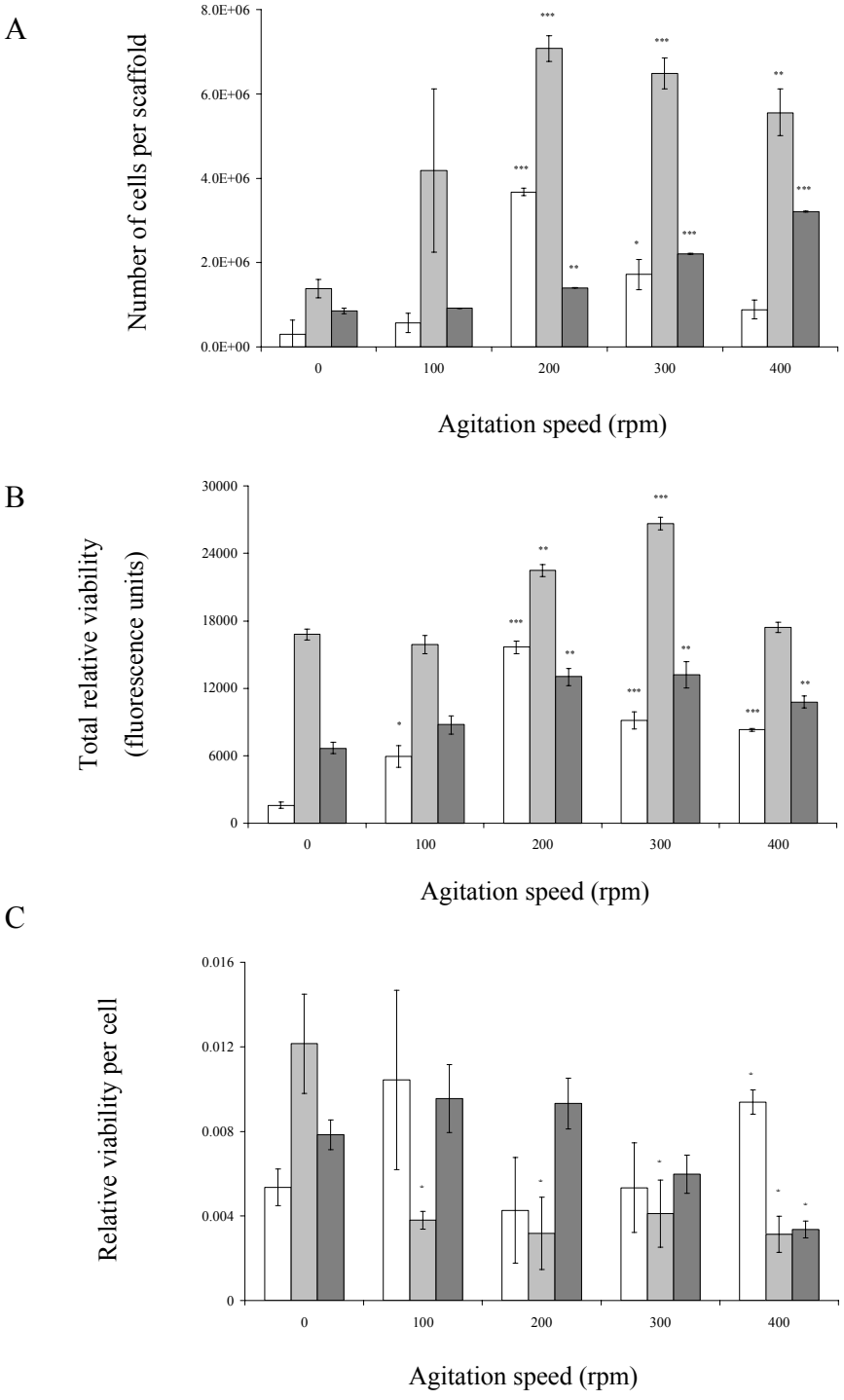

Figure 3.6 The effect of agitation speed on (A) the number, (B) the total relative viability and (C) the relative viability per cell of □ BAC ▒ OMC ■ HOS cells in NF scaffolds.

Results expressed as mean (n=3) ± SEM (* indicates $P<0.05$, ** indicates $P<0.01$ and *** indicates $P<0.001$).

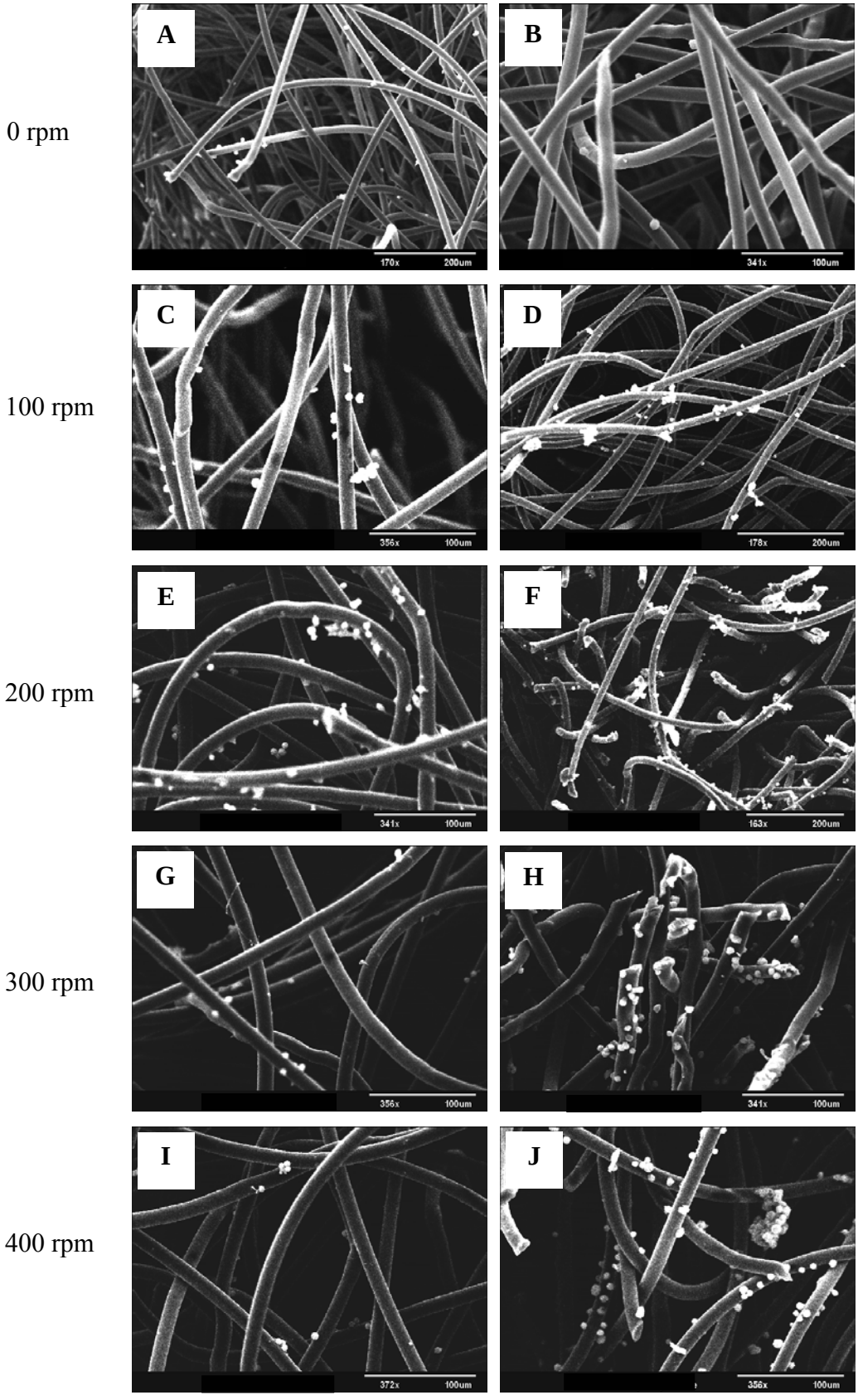

Figure 3.7 The effect of agitation speed on the arrangement of BACs at (A, C, E, G & I) surface and (B, D, F, H & J) centre of NF scaffolds.

3.4.2.a.ii Analysis of seeding OMCs into NF scaffolds

The number, total relative viability and relative viability per cell of OMCs in NF scaffolds following overnight seeding at 0, 100, 200, 300 or 400 rpm are shown in Figure 3.6. Seeding the scaffolds with agitation at 200, 300 and 400 rpm led to significant increases in the number of cells contained within the scaffolds compared to scaffolds seeded statically (Figure 3.6 A). The total relative viability was greatest for OMCs in NF scaffolds seeded at 200 and 300 rpm (Figure 3.6 B). Normalising the total relative viability with respect to cell number indicated that the viability of OMCs in NF scaffolds agitated at 100, 200, 300 and 400 rpm was compromised compared to that of OMCs which were seeded into NF scaffolds without agitation (Figure 3.6 C). Scanning electron microscopy demonstrated that the distribution of cells within the scaffolds was affected by agitation speed. Few cells were visible within scaffolds seeded either at 0 or 100 rpm (Figure 3.8 A, B, C & D). Increasing the agitation speed to 200 rpm led to more OMCs at both the surface and centre of NF scaffolds (Figure 3.8 E & F). A further increase in the number of OMCs at both the surface and centre of NF scaffolds was observed following agitation at 300 rpm (Figure 3.8 G & H). Increasing the agitation speed to 400 rpm led to an uneven distribution of cells within the scaffolds, with an increased number of cells within the central region of the scaffolds (Figure 3.8 I & J). Based on this information, agitation speeds of 200 rpm or greater were advantageous for obtaining a high density of evenly distributed OMCs within NF scaffolds, although the viability of the cells within these scaffolds was reduced compared to that of cells seeded into scaffolds without agitation.

3.4.2.a.iii Analysis of seeding HOS TE85 cells into NF scaffolds

Figure 3.6 shows the effect of agitation speed on the number, total relative viability and viability per cell of HOS TE85 cells in NF scaffolds. Agitating NF scaffolds at 200, 300 or 400 rpm led to increased numbers of cells within the scaffolds ($P<0.01$, $P<0.001$ and $P<0.001$ respectively, Figure 3.6 A). Agitating NF scaffolds with HOS TE85 cells at these speeds led to the detection of greater total relative viabilities compared to that of HOS TE85 cells in NF scaffolds seeded without agitation ($P<0.01$, Figure 3.6 B).

The relative viability per HOS TE85 cell for NF scaffolds agitated at 400 rpm was significantly lower than that of cells seeded into scaffolds without agitation ($P<0.05$, Figure 3.6 C). No significant difference was detected between the relative viability per cell of HOS TE85 cells in NF scaffolds seeded at 100, 200 or 300 rpm compared to those seeded without agitation. Representative scanning electron micrographs of NF scaffolds seeded with HOS TE85 cells at each of the speeds are shown in Figure 3.9. Few HOS TE85 cells were detected in NF scaffolds seeded at either 0 or 100 rpm (Figure 3.9 A, B, C & D). Scaffolds agitated at 200 and 300 rpm contained a greater number of cells at both the surface and centre (Figure 3.9 E, F, G & H). In NF scaffolds agitated at 400 rpm, a pellet of HOS TE85 cells was visible at the centre (Figure 3.9 J). It was therefore shown that agitating NF scaffolds with HOS TE85 cells at speeds greater than 200 rpm led to a greater number of cells within the scaffolds and that the viability of these cells was compromised when agitated at 400 rpm.

3.4.2.b Analysis of seeding cells into sparse knit 3 (SK3) scaffolds

3.4.2.b.i Analysis of seeding BACs into SK3 scaffolds

The effect of agitation speed on the number, total relative viability and viability per cell for BACs in SK3 scaffolds is presented in Figure 3.10. The number of BACs in SK3 scaffolds increased with increasing agitation speed. Significantly more cells were detected in scaffolds following overnight seeding at 200 rpm ($P<0.01$), 300 rpm ($P<0.001$) and 400 rpm ($P<0.001$) compared to scaffolds seeded without agitation (Figure 3.10 A). The total relative viability of cells within the scaffolds was increased in constructs following agitation at 100, 200, 300 and 400 rpm (Figure 3.10 B) although when these values were normalised with respect to cell number, it was clear that the viability of BACs was compromised by agitation at each of these speeds (Figure 3.10 C). Representative images of SK3 scaffolds seeded with BACs at each of the speeds are shown in Figure 3.11. Following static seeding, more cells were present at the surface of SK3 scaffolds than in the middle (Figure 3.11 A & B).

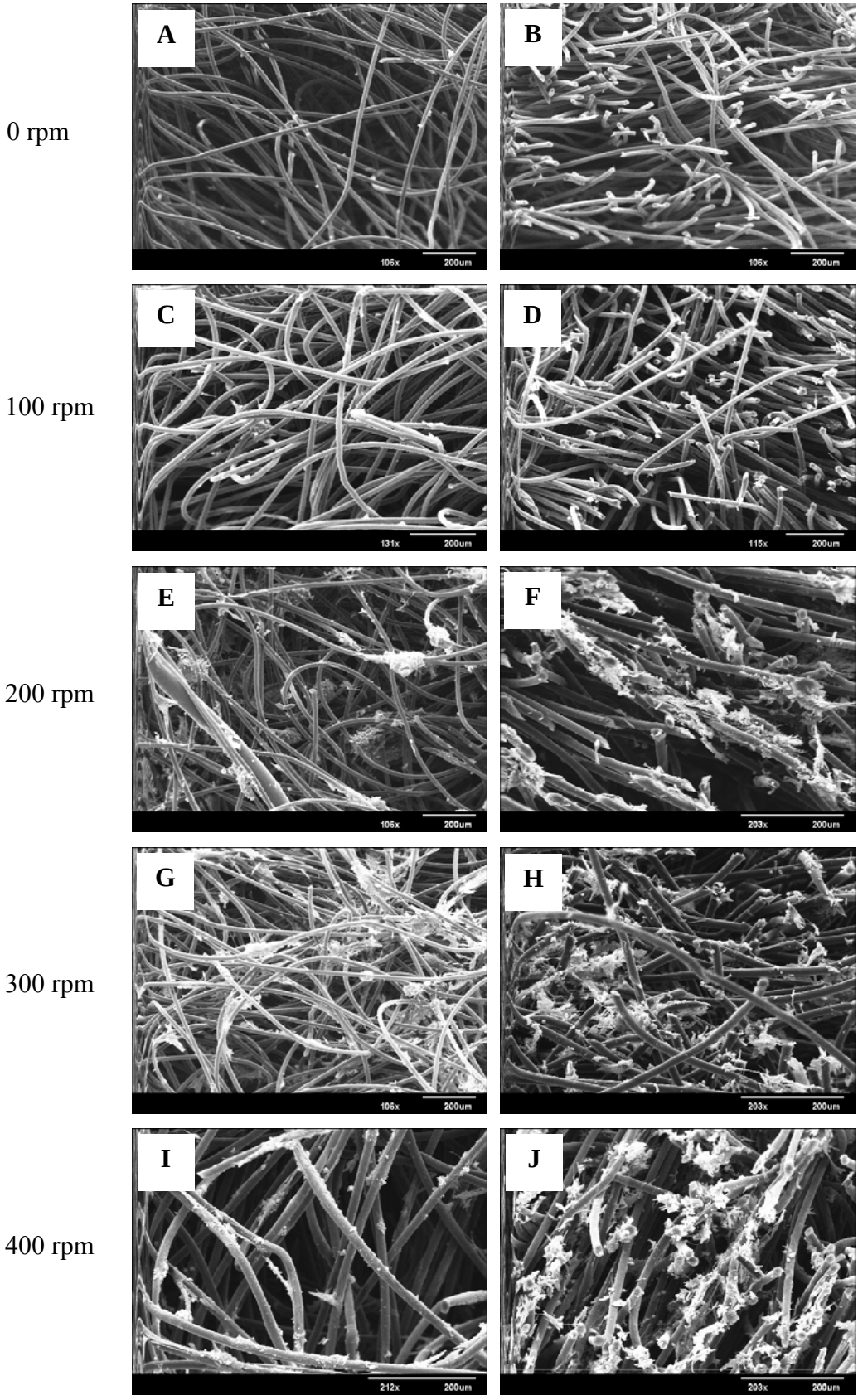

Figure 3.8 The effect of agitation speed on the arrangement of OMCs at (A, C, E, G & I) surface and (B, D, F, H & J) centre of NF scaffolds.

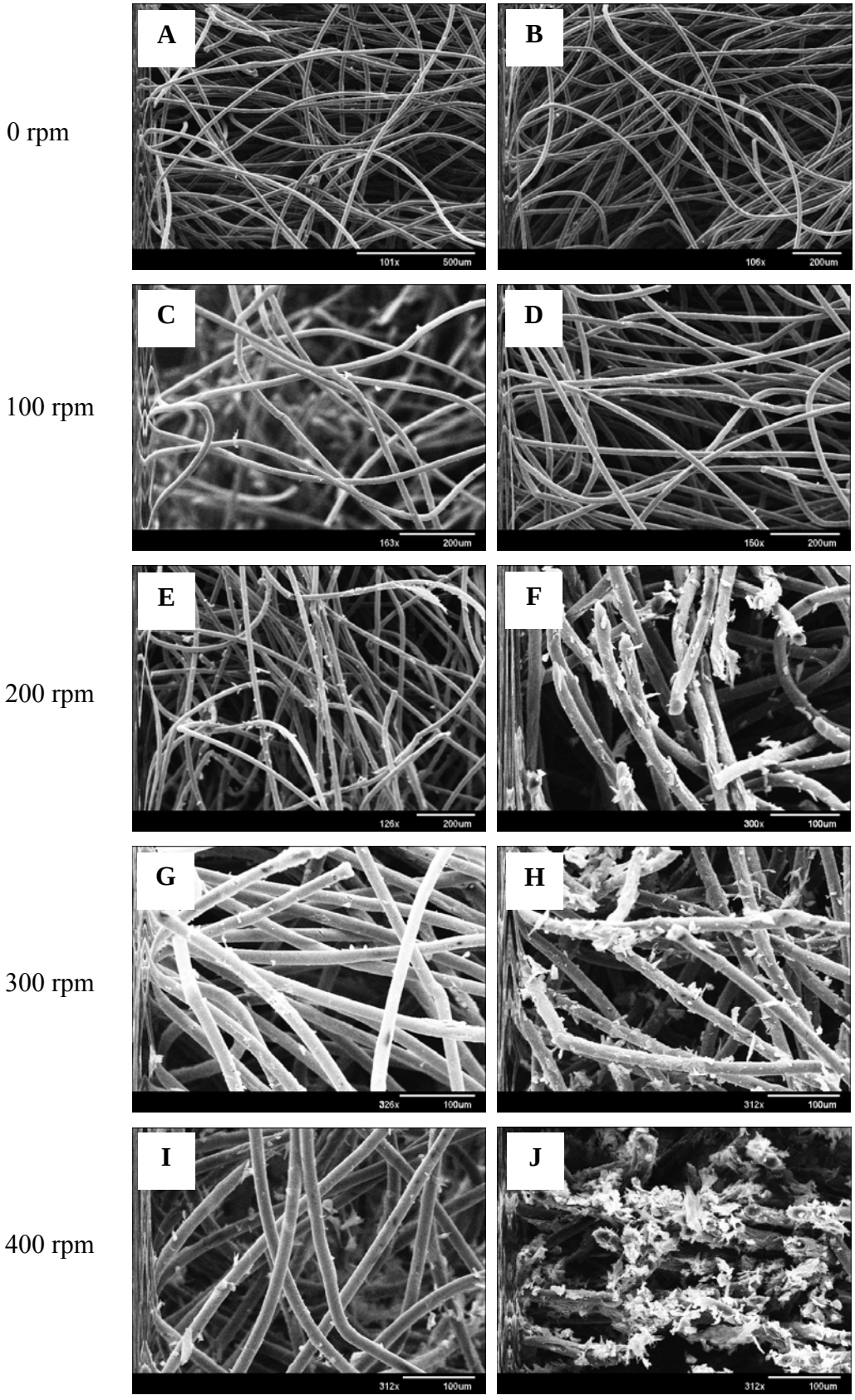

Figure 3.9 The effect of agitation speed on the arrangement of HOS TE85 cells at (A, C, E, G & I) surface and (B, D, F, H & J) centre of NF scaffolds.

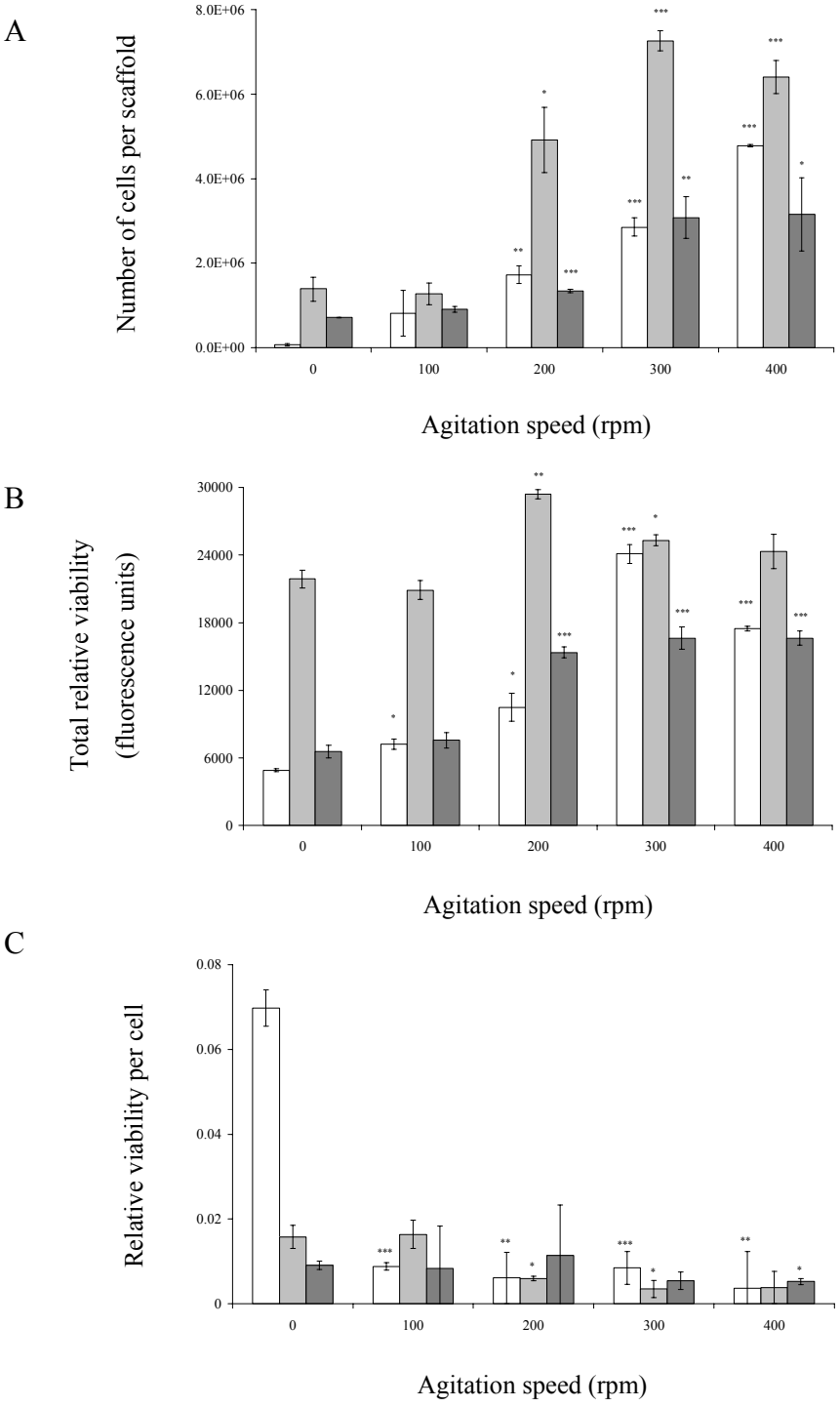

Figure 3.10 The effect of agitation speed on (A) the number, (B) the total relative viability and (C) the relative viability per cell of □ BAC, ▒ OMC and ■ HOS cells in SK3 scaffolds.

Results expressed as mean (n=3) ± SEM (* indicates $P<0.05$, ** indicates $P<0.01$ and *** indicates $P<0.001$).

Overnight agitation at 100 rpm led to more cells in the centre of SK3 scaffolds compared to at the surface (Figure 3.11 C & D). SK3 scaffolds agitated with BACs overnight at 200, 300 or 400 rpm contained a more even distribution of cells although more cells were visible in the scaffolds seeded at 300 or 400 rpm compared to those seeded at 200 rpm (Figure 3.11 E, F, G & H). This data shows that agitating SK3 scaffolds with BACs at speeds greater than 200 rpm leads to more cells evenly distributed throughout the scaffold, although the viability of the cells is compromised.

3.4.2.b.ii Analysis of seeding OMCs into SK3 scaffolds

Figure 3.10 shows the effect of agitation speed on the number and viability of OMCs in SK3 scaffolds. Seeding SK3 scaffolds with OMCs at speeds of 200 rpm ($P<0.05$), 300 rpm ($P<0.001$) or 400 rpm ($P<0.001$) led to a significant increase in the number of cells, compared to seeding them statically (Figure 3.10 A). The total relative viability of OMCs in SK3 scaffolds seeded at 200 rpm and 300 rpm was significantly greater than that of OMCs in these scaffolds seeded statically ($P<0.01$ and $P<0.05$ respectively, Figure 3.10 B). Normalising the relative viability with respect to cell number indicated that agitation of SK3 scaffolds with OMCs at 200 and 300 rpm led to a reduction in cell viability, compared to that of OMCs in SK3 scaffolds seeded without agitation ($P<0.05$, Figure 3.10 C). SEM revealed few OMCs either at the surface or in the centre of SK3 scaffolds seeded in static plates (Figure 3.12 A & B). Agitation of SK3 scaffolds with OMCs at 100, 200, 300 or 400 rpm led to more evenly distributed cells (Figure 3.12 C, D, E, F, G, H, I & J). It was also observed that OMCs at the surface of SK3 scaffolds agitated at 400 rpm were flattened, whilst those in the centre were rounded (Figure 3.12 I & J). This information shows that agitation speeds greater than 200 rpm are required to increase the number of OMCs within SK3 scaffolds and to ensure that the cells are distributed throughout the constructs, although agitation at 200 and 300 rpm was detrimental to cell viability

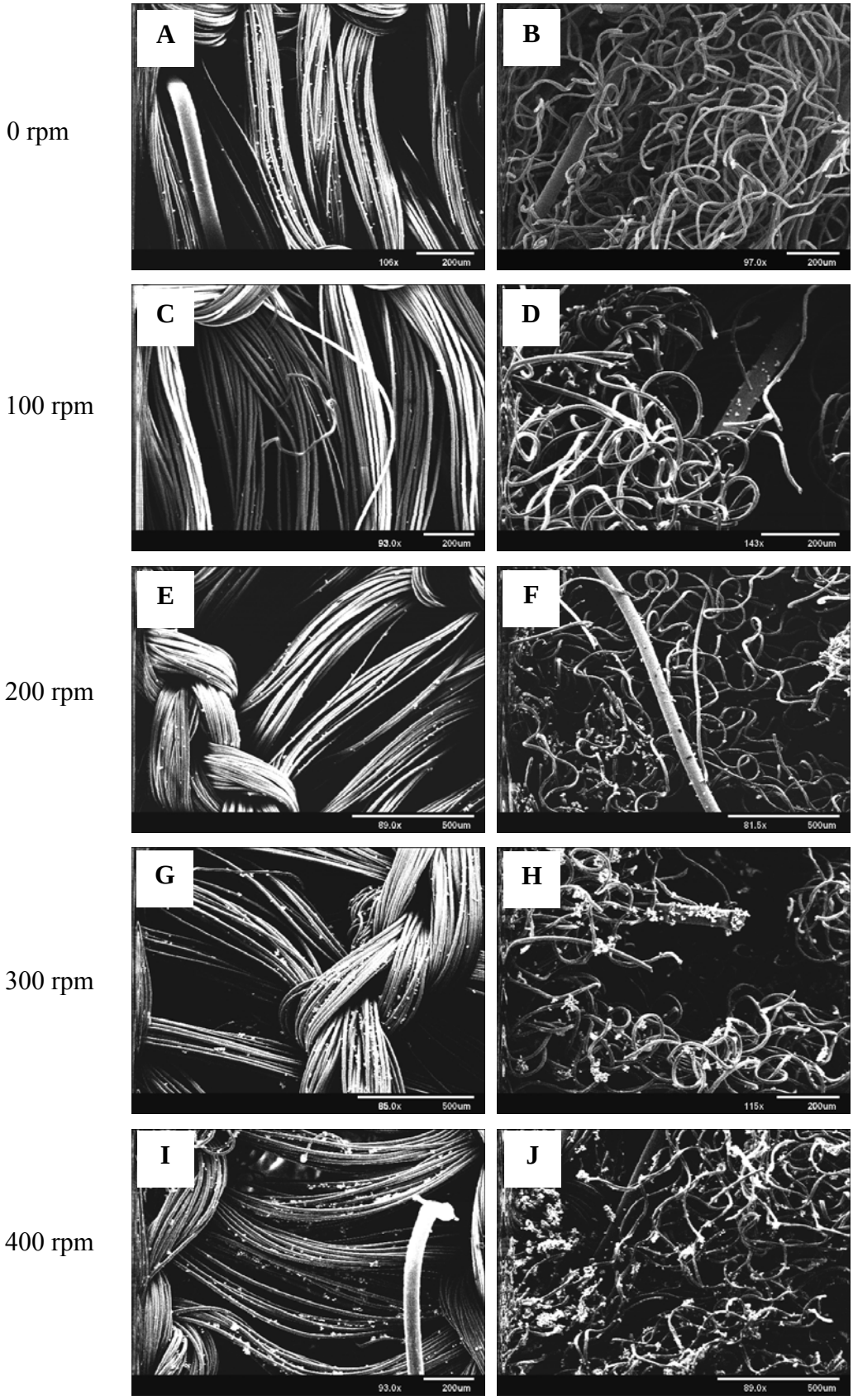

Figure 3.11 The effect of agitation speed on the arrangement of BACs at (A, C, E, G & I) surface and (B, D, F, H & J) centre of SK3 scaffolds.

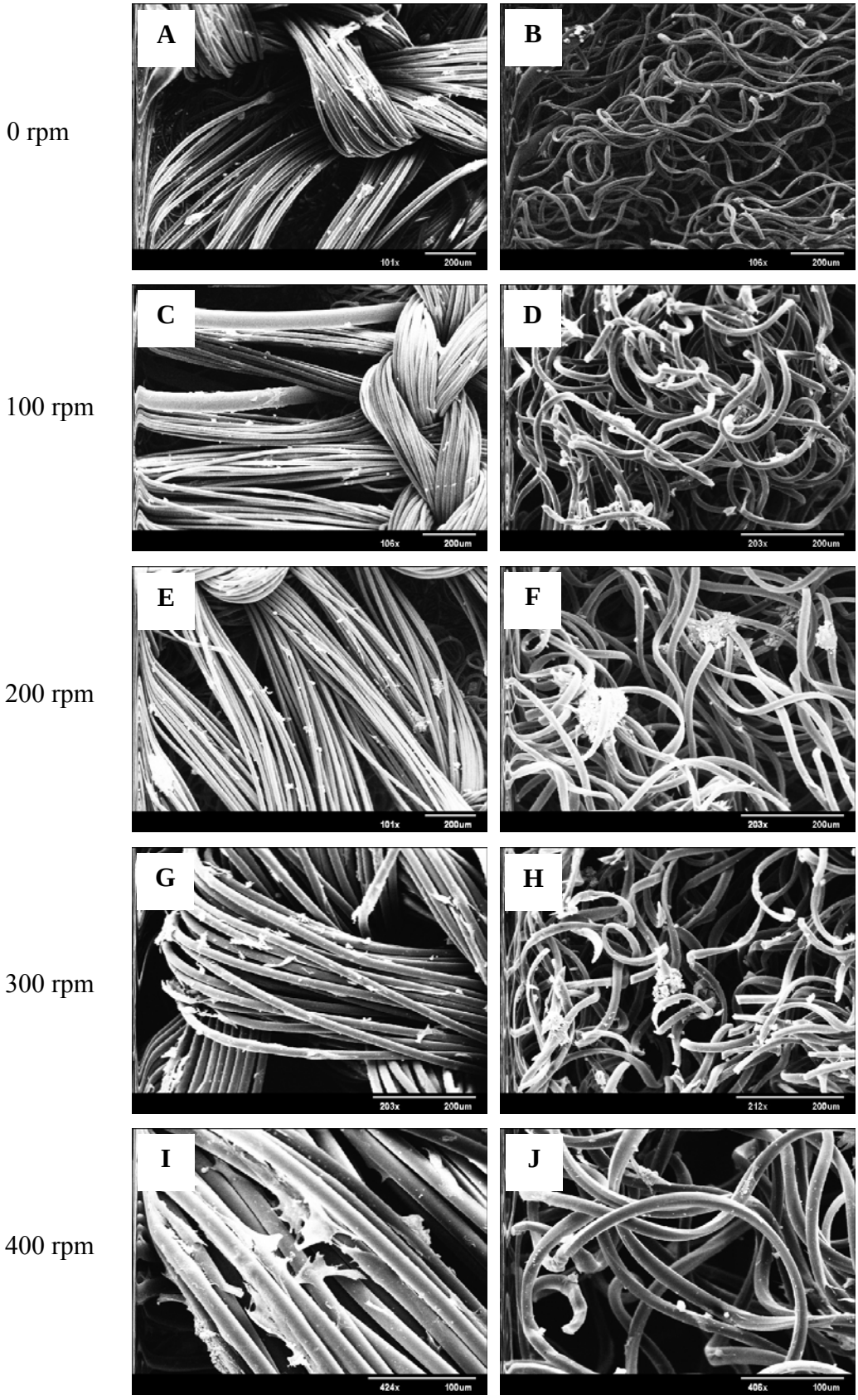

Figure 3.12 The effect of agitation speed on the arrangement of OMCs at (A, C, E, G & I) surface and (B, D, F, H & J) centre of SK3 scaffolds.

3.4.2.b.iii Analysis of seeding HOS TE85 cells into SK3 scaffolds

The number and relative viability of HOS TE85 cells seeded into SK3 scaffolds at different agitation speeds are presented in Figure 3.10. Agitating SK3 scaffolds with HOS TE85 cells at 200, 300 or 400 rpm led to a significant increase in the number of cells retained within the scaffolds compared to those seeded without agitation ($P<0.001$, $P<0.01$ and $P<0.05$ respectively, Figure 3.10 A). The total relative viability of HOS TE85 cells in these scaffolds was also significantly greater than that of scaffolds seeded at 0 rpm ($P<0.001$, Figure 3.10 B). The viability per HOS TE85 cell in SK3 scaffolds was determined by normalising the total relative viability with respect to cell number. It was shown that the viability of HOS TE85 cells in SK3 scaffolds was only compromised following agitation at 400 rpm (Figure 3.10 C). Representative scanning electron micrographs of HOS TE85 cells in SK3 scaffolds are shown in Figure 3.13. Few HOS TE85 cells were visible in SK3 scaffolds which were seeded either without agitation or at 100 rpm (Figure 3.13 A, B, C & D). In SK3 scaffolds agitated at 200, 300 or 400 rpm more cells were visible (Figure 3.13 E, F, G, H, I & J). HOS TE85 cells were distributed more evenly throughout SK3 scaffolds agitated at 300 rpm (Figure 3.13 G & H). In summary, seeding SK3 scaffolds with HOS TE85 cells at agitation speeds of 200 and 300 rpm led to increased numbers of cells retained within the scaffolds without causing a significant reduction in cell viability.

3.4.2.c Analysis of seeding cells in sparse knit 4 (SK4) scaffolds

3.4.2.c.i Analysis of seeding BACs into SK4 scaffolds

The effect of agitation speed on the number and relative viability of BACs within SK4 scaffolds is shown in Figure 3.14. SK4 scaffolds seeded with BACs at agitation at each of the speeds contained more cells than scaffolds seeded without agitation (Figure 3.14 A). Greater total relative cell viability was detected for BACs cells in these scaffolds (Figure 3.14 B). Normalising the total relative viability with respect to cell number indicated that agitation at each of these speeds led to compromised cell viability (Figure 3.14 C).

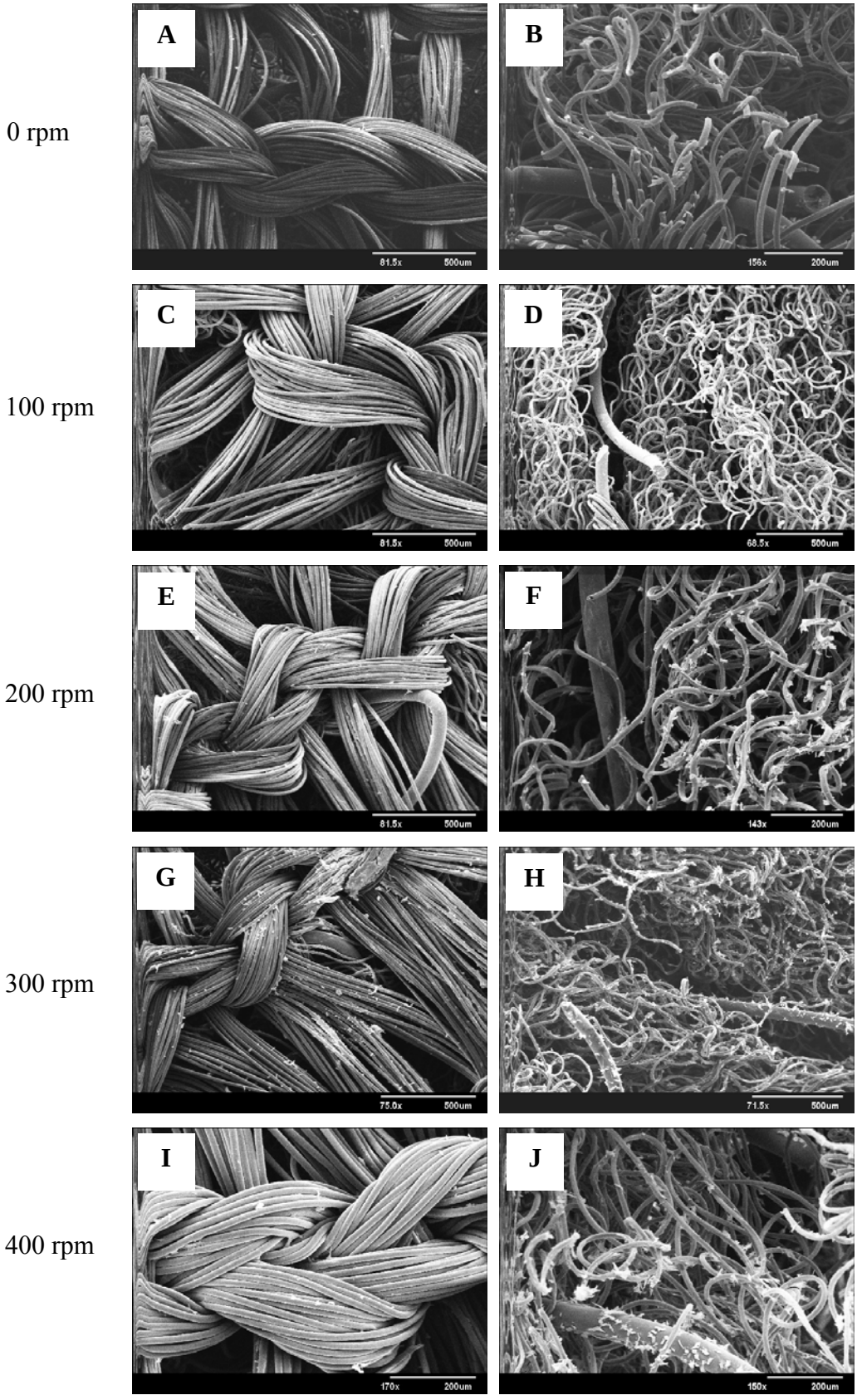

Figure 3.13 The effect of agitation speed on the arrangement of HOS TE85cells at (A, C, E, G & I) surface and (B, D, F, H & J) centre of SK3 scaffolds.

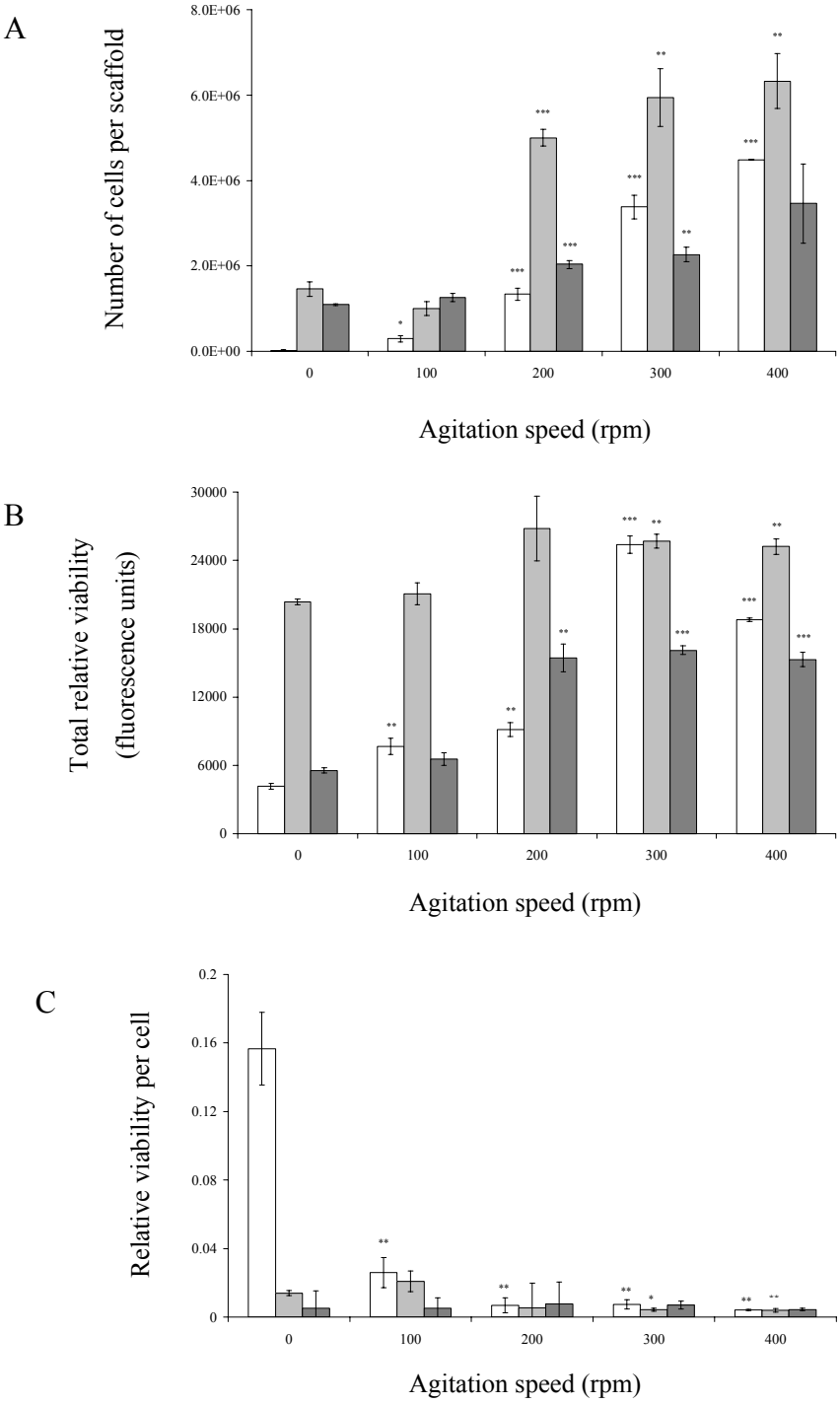

Figure 3.14 The effect of agitation speed on (A) the number, (B) the total relative viability and (C) the relative viability per cell of □BAC, ▒ OMC and ▒ HOS cells in SK4 scaffolds.

Results expressed as mean (n=3) ± SEM (* indicates $P<0.05$, ** indicates $P<0.01$ and *** indicates $P<0.001$).

More BACs were visible at the surface of SK4 scaffolds than in the centre following static seeding (Figure 3.15 A & B). Few cells were visible in scaffolds agitated at 100 or 200 rpm (Figure 3.15 C, D, E & F). A greater number of BACs were detected in SK4 scaffolds agitated at 300 and 400 rpm and it was observed that these cells were present both at the surface and in the centre of scaffolds (Figure 3.15 G, H, I & J). This data shows that whilst the number and distribution of BACs within SK4 scaffolds can be improved by seeding them at agitation speeds of 300 or 400 rpm, the viability of these cells may be compromised.

3.4.2.c.ii Analysis of seeding OMCs into SK4 scaffolds

Figure 3.14 shows graphs presenting the effect of seeding speed on the number and relative viability of OMCs within SK4 scaffolds. Agitating SK4 scaffolds with OMCs at 200 rpm ($P<0.001$), 300 rpm ($P<0.01$) or 400 rpm ($P<0.01$) led to significant increases in the number of cells retained within the scaffolds, compared to scaffolds seeded statically (Figure 3.14 A). The total relative viability of OMCs in these scaffolds was significantly increased at 300 and 400 rpm ($P<0.01$, Figure 3.14 B). Assessment of the relative viability of each OMC within the scaffolds showed that whilst the viability of the cells was not compromised by agitation at 100 or 200 rpm, it was reduced in cells agitated at 300 and 400 rpm (Figure 3.14 C). SK4 scaffolds seeded with OMCs at 0 or 100 rpm contained more cells at the surface than in the centre (Figure 3.16 A, B, C & D). Scaffolds agitated at 200, 300 and 400 rpm contained a higher density of evenly distributed cells than scaffolds seeded at 0 and 100 rpm (Figure 3.16 E, F, G, H, I & J). It was therefore shown that agitation at speeds greater than 200 rpm led to more OMCs within SK4 scaffolds although at 300 and 400 rpm the viability of these cells was compromised.

3.4.2.c.iii Analysis of seeding HOS TE85 cells into SK4 scaffolds

The effect of agitation speed on the number and viability of HOS TE85 cells seeded into SK4 scaffolds is presented in Figure 3.14. Seeding the scaffolds with agitation at 200, 300 and 400 rpm led to an increase in the number of cells retained within the scaffolds compared to SK4 scaffolds seeded statically or at 100 rpm (Figure 3.14 A).

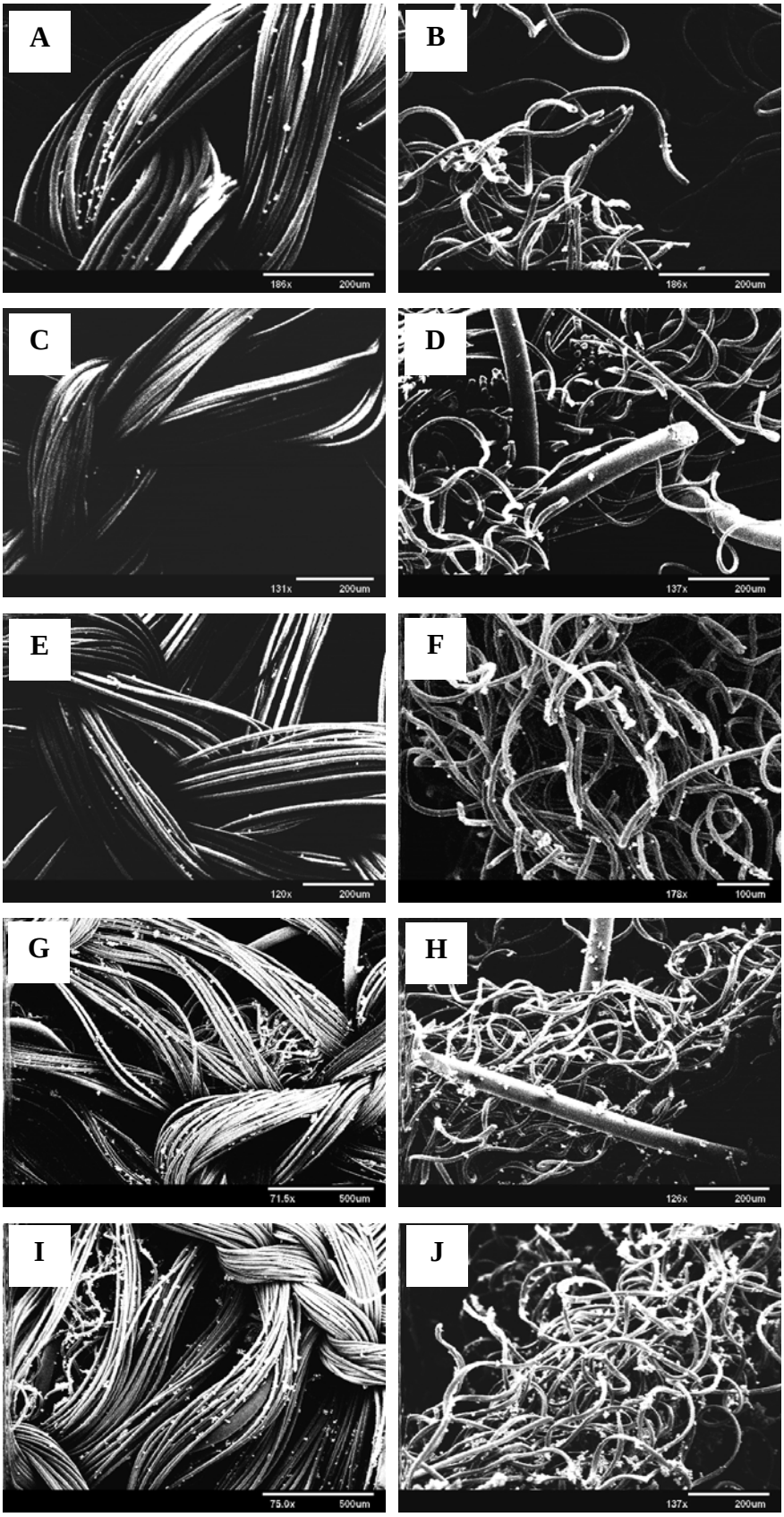

Figure 3.15 The effect of agitation speed on the arrangement of BACs at (A, C, E, G & I) surface and (B, D, F, H & J) centre of SK4 scaffolds.

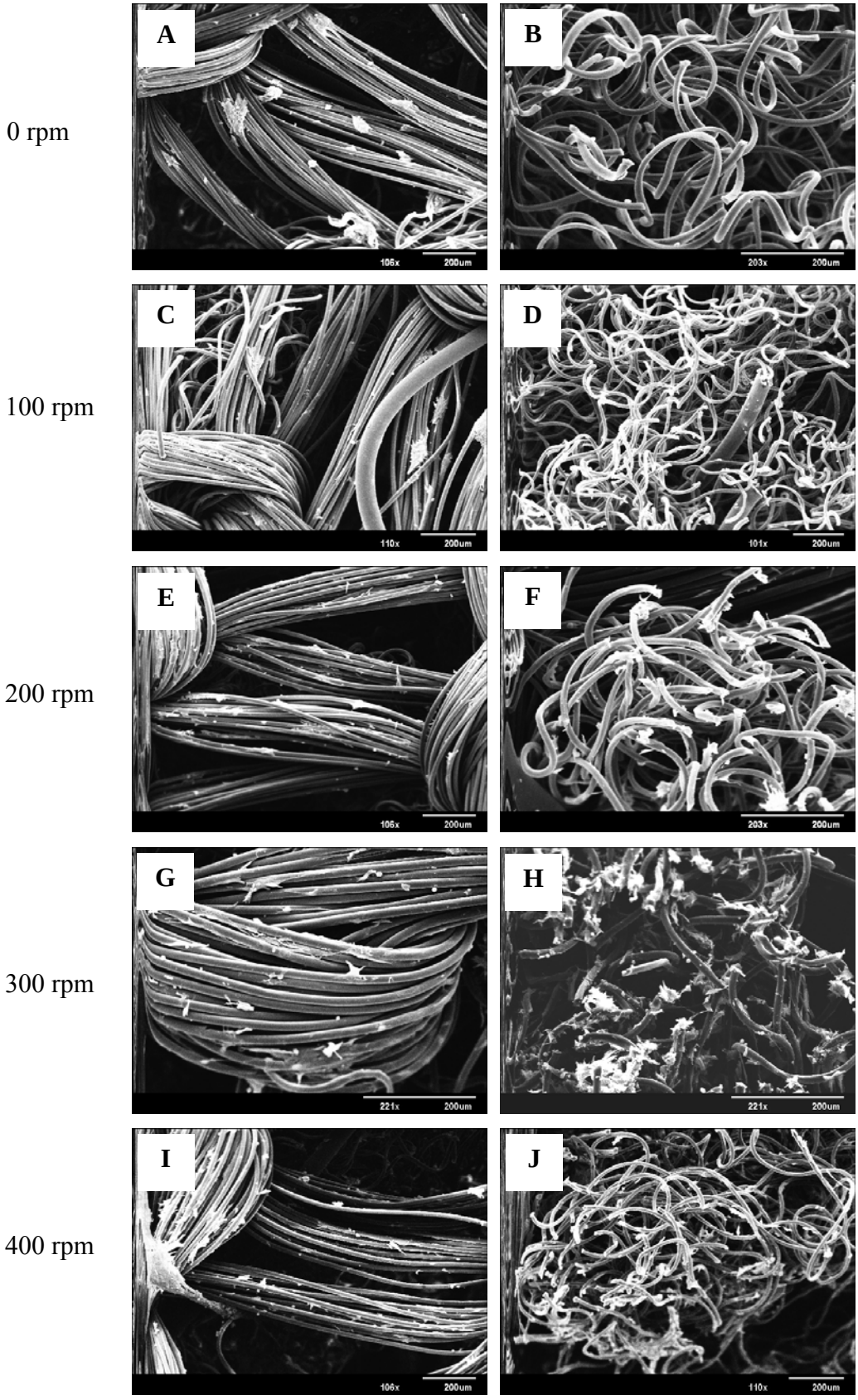

Figure 3.16 The effect of agitation speed on the arrangement of OMCs at (A, C, E, G & I) surface and (B, D, F, H & J) centre of SK4 scaffolds.

The increased number of HOS TE85 cells within SK4 scaffolds was significant following agitation at 200 and 300 rpm ($P<0.001$ and $P<0.01$ respectively). The total relative viability of HOS TE85 cells in SK4 scaffolds was also greater for cells in scaffolds seeded at 200, 300 and 400 rpm compared to those seeded either without agitation or with agitation at 100 rpm (Figure 3.14 B). The relative viability per cell, as determined by normalising the total relative viability with respect to cell number, for HOS TE85 cells seeded into SK4 scaffolds is shown in Figure 3.14 C. No significant difference was detected between the relative viabilities of HOS TE85 cells seeded into SK4 scaffolds at each of the speeds. Using SEM, few cells were visible either at the surface or in the centre of scaffolds seeded at 0 or 100 rpm (Figure 3.17 A, B, C & D). In scaffolds seeded at 200 rpm, more HOS TE85 cells were visible at the centre of scaffolds than at the surface (Figure 3.17 E & F). Agitating SK4 scaffolds with HOS TE85 cells overnight at 300 and 400 rpm led to a more even distribution of cells within the scaffolds (Figure 3.17 G, H, I & J). The data presented shows that agitating SK4 scaffolds with HOS TE85 cells at 200, 300 and 400 rpm led to an increase in the number of cells retained within the scaffolds, without compromising the viability of the cells. The distribution of HOS TE85 cells within these scaffolds was more even at 300 and 400 rpm compared to the other speeds.

3.4.2.d Analysis of seeding cells into sparse knit 5 (SK5) scaffolds

SK5 scaffolds were introduced to the project in the final year, when it had been decided to use OMCs in preference to BACs for cartilage formation studies to ensure consistency in the cell type being used by all partners in this project. For this reason, seeding optimisation studies on SK5 scaffolds were only performed using OMCs and HOS TE85 cells.

3.4.2.d.i Analysis of seeding OMCs into SK5 scaffolds

Figure 3.18 shows the effect of agitation speed on the number, total relative viability and viability per cell of OMCs seeded into SK5 scaffolds. Increased cell numbers were detected in scaffolds seeded at 200 and 300 rpm compared to those scaffolds seeded at 0, 100 or 400 rpm (Figure 3.18 A).

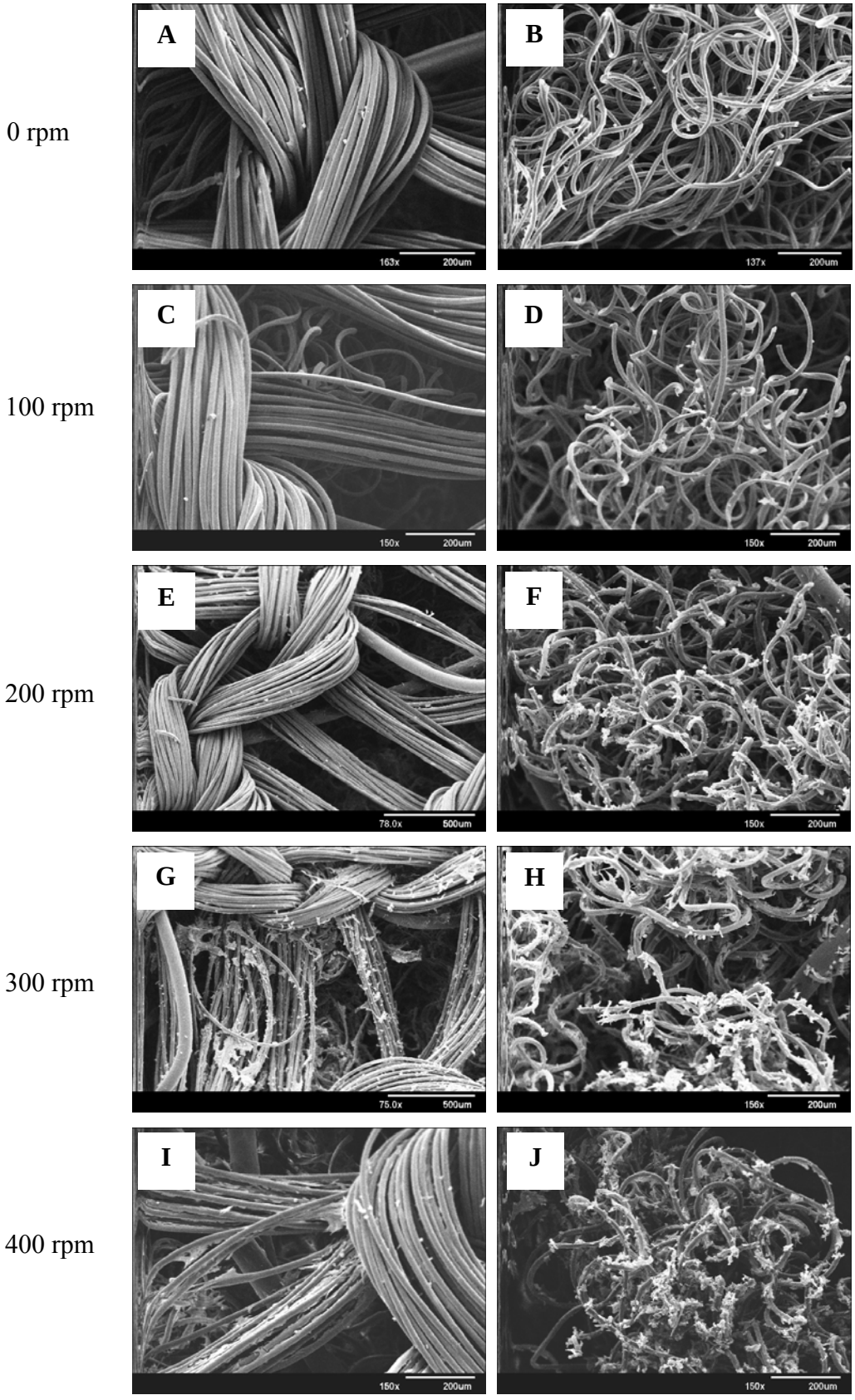

Figure 3.17 The effect of agitation speed on the arrangement of HOS TE85 cells at (A, C, E, G & I) surface and (B, D, F, H & J) centre of SK4 scaffolds.

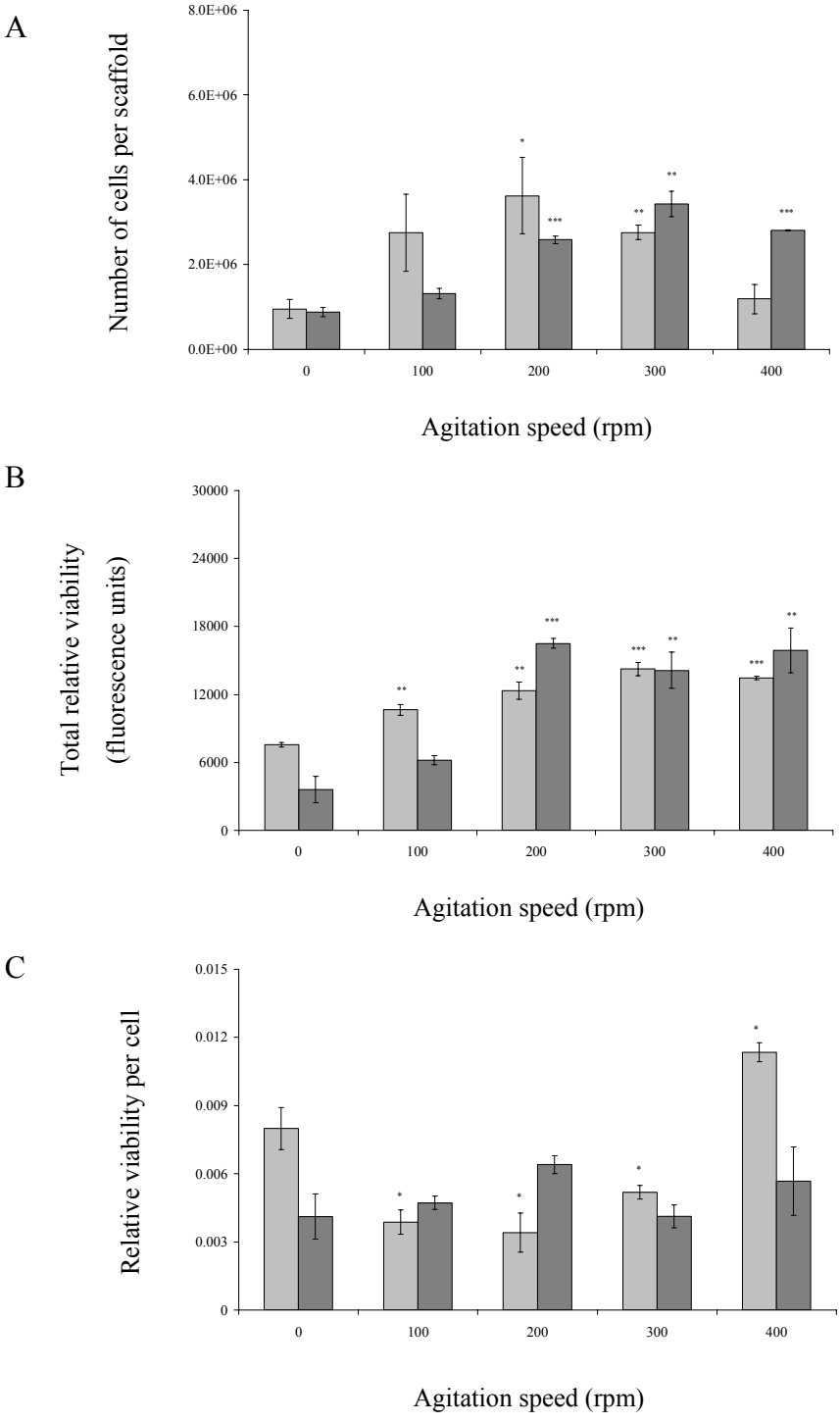

Figure 3.18 The effect of agitation speed on (A) the number, (B) the total relative viability and (C) the relative viability per cell of □ OMC and ■ HOS cells in SK5 scaffolds.

Results expressed as mean (n=3) ± SEM (* indicates $P<0.05$, ** indicates $P<0.01$ and *** indicates $P<0.001$).

The total relative viability of OMCs in SK5 scaffolds agitated at each of the speeds was greater than that of those cells seeded into SK5 scaffolds without agitation (Figure 3.18 B). The relative viability of each cell was compromised in those scaffolds agitated at 100, 200 and 300 rpm whilst that of cells in scaffolds seeded at 400 rpm was greater compared to the cells in scaffolds seeded without agitation (Figure 3.18 C). Representative scanning electron micrographs of SK5 scaffolds seeded with OMCs are presented in Figure 3.19. Few cells were visible in scaffolds seeded without agitation (Figure 3.19 A & B). Following agitation at 100, 200 and 300 rpm, more OMCs were visible within SK5 scaffolds (Figure 3.19 C, D, E, F, G & H). SK5 scaffolds agitated with OMCs at 400 rpm were similar in appearance to those seeded without agitation with few cells visible within the scaffolds (Figure 3.19 I & J). Therefore, seeding OMCs into SK5 scaffolds at either 200 or 300 rpm led to increased numbers of cells within the scaffolds, although the viability was reduced compared to that of cells in scaffolds seeded statically.

3.4.2.d.ii Analysis of seeding HOS TE85 cells into SK5 scaffolds

The effect of agitation speed on the number and relative viability of HOS TE85 cells in SK5 scaffolds is shown in Figure 3.18. Agitating SK5 scaffolds with HOS TE85 cells at 200, 300 and 400 rpm led to greater numbers of cells within the scaffolds compared to seeding without agitation or seeding at 100 rpm (Figure 3.18 A). This was also reflected in the increase in total relative viability of HOS TE85 cells seeded into these scaffolds (Figure 3.18 B). The relative viability of each HOS TE85 cell did not appear to be affected by agitation as shown by no significant differences between the relative viabilities of cells seeded into SK5 scaffolds at each of the speeds (Figure 3.18 C). SK5 scaffolds seeded with HOS TE85 cells either without agitation or with agitation at 100 rpm did not appear to contain many cells (Figure 3.20 A, B, C & D). SEM revealed more HOS TE85 cells within SK5 scaffolds seeded with agitation at 200 and 300 rpm and that these cells were distributed evenly throughout the scaffold (Figure 3.20 E, F, G & H). SK5 scaffolds seeded with HOS TE85 cells at 400 rpm contained evenly distributed cells (Figure 3.20 I & J).

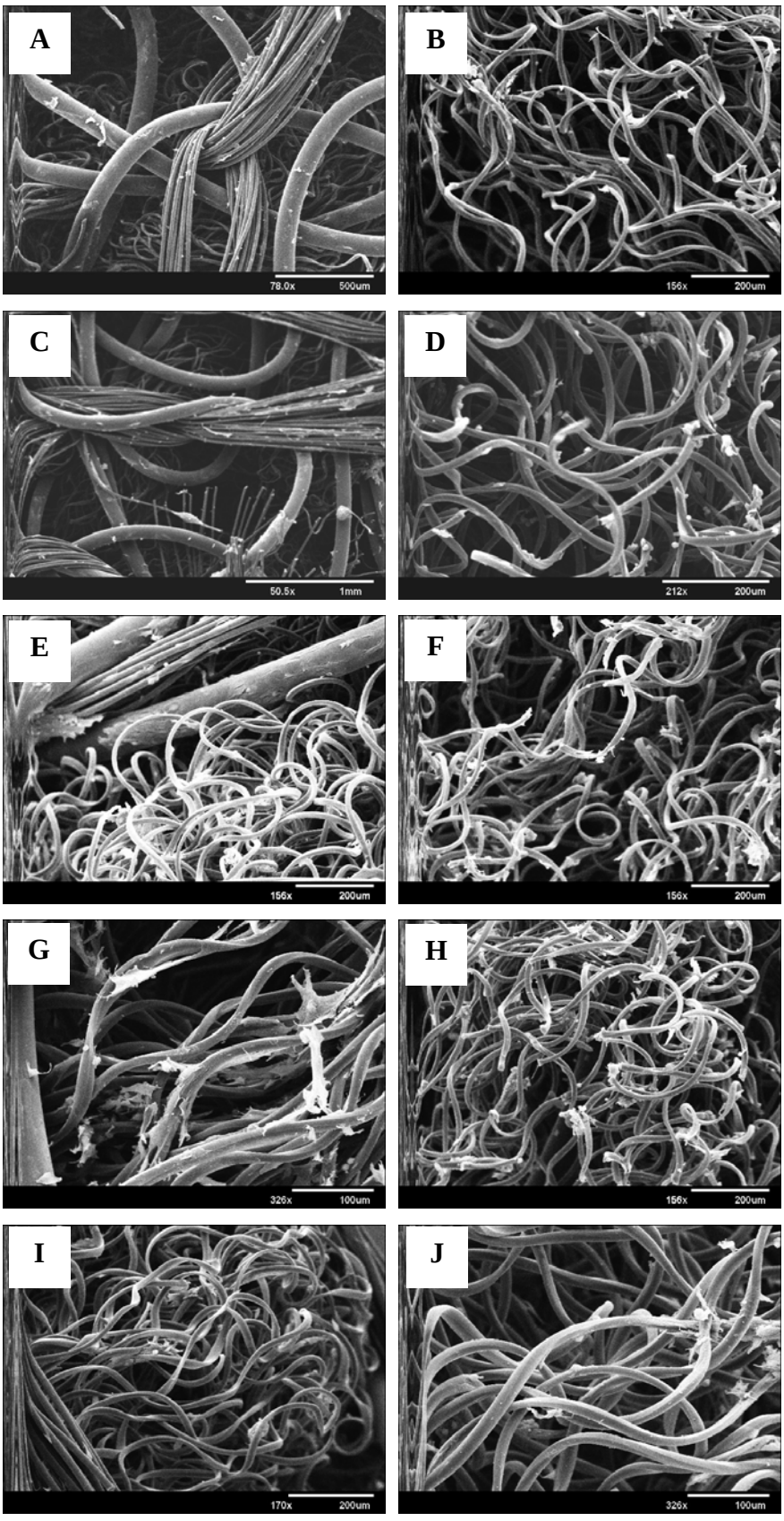

Figure 3.19 The effect of agitation speed on the arrangement of OMCs at (A, C, E, G & I) surface and (B, D, F, H & J) centre of SK5 scaffolds.

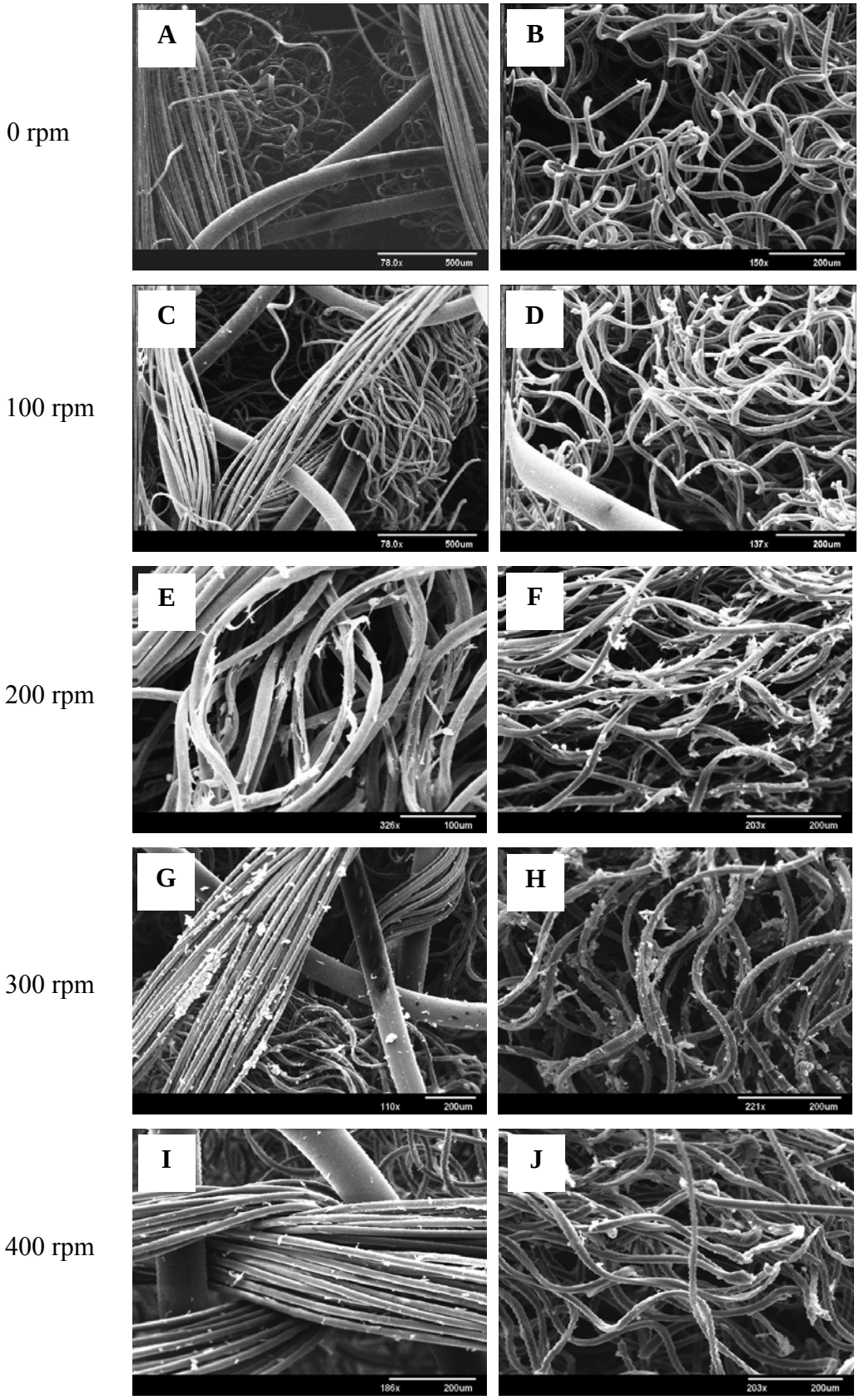

Figure 3.20 The effect of agitation speed on the arrangement of HOS TE85 cells at (A, C, E, G & I) surface and (B, D, F, H & J) centre of SK5 scaffolds.

Agitating SK5 scaffolds with HOS TE85 cells at 200, 300 and 400 rpm therefore allowed a greater number of cells to be seeded evenly into the scaffolds, without compromising cell viability.

3.5 Discussion

Scaffolds are used in tissue engineering systems to provide cells with a three dimensional support upon which they may attach, proliferate and secrete ECM components (Sharma and Elisseeff 2004). One of the essential features of a tissue engineering scaffold is that it must contain pores so that nutrients can be supplied to the growing tissue (Vunjak-Novakovic 2003). It is evident from Table 1.2 that various scaffolds have been used in cartilage engineering studies and that these scaffolds have differed in terms of the material from which they have been manufactured and their structure. Many previous cartilage tissue engineering studies have used scaffolds containing a random distribution of fibres. Promising results have been observed in studies using these scaffolds with different cell sources and culture systems (Martin *et al* 1998 and Vunjak-Novakovic *et al* 1999). One limitation of these scaffolds is that the ultimate size of the cartilage construct is limited by the availability of nutrients during culture. It is well accepted that in larger constructs the formation of tissue at the scaffold periphery impedes the flow of nutrients from the culture environment into the centre of the scaffold and so cell viability is lost and the centre of the growing tissue become necrotic (Freed *et al* 1999). One of the hypotheses of this thesis was that scaffolds containing both random and anisotropic porosity would be beneficial for viable tissue regeneration *in vitro* since the presence of wider aligned channels within the scaffold would facilitate the flow of nutrient-containing medium into the construct throughout the culture period.

The first section of this chapter was concerned with characterising these novel scaffolds with respect to mass, density, the arrangement of fibres and the resistance of the scaffolds to fluid flow. Three different SK scaffolds were designed and manufactured by Smith & Nephew.

These scaffolds all contained bundles of randomly arranged fibres separated by aligned channels to facilitate nutrient transfer. NF scaffolds, containing randomly arranged fibres, were used in the studies presented in this thesis as a control scaffold. The resistance of each of the scaffolds to the flow of liquid was assessed and at each of the flow rates it was determined that the resistance of the SK scaffolds was lower than that of the NF scaffolds, indicating that the presence of aligned channels within the sparse knit scaffolds did improve their flow properties. It was also found that SK4 scaffolds were similar to NF scaffolds with respect to mass and density. In comparison, SK3 and SK5 scaffolds were more dense than NF scaffolds. In addition, the crusts on SK3 and SK4 scaffolds were more densely knitted than that of SK5 scaffolds.

The density with which cells are initially seeded into scaffolds and their arrangement within the scaffolds are important parameters in tissue engineering. These factors affect cell proliferation, differentiation and migration, and ultimately the quality of the engineered tissue (Li *et al* 2001). The aim of the second section of this chapter was therefore to determine the optimum agitation speed for seeding BACs, OMCs and HOS TE85 cells into NF, SK3, SK4 and SK5 scaffolds. The effect of agitation speed on the number, relative viability and distribution of cells within the scaffolds was determined. Since it is important that a high density of evenly distributed cells are initially seeded into scaffolds for *in vitro* cartilage regeneration, the optimum agitation speed for each cell and scaffold type was selected based on the number and distribution of cells (Vunjak-Novakovic *et al* 1998). For all scaffold and cell types, seeding with agitation increased the number of cells within the scaffolds. This is in agreement with previous studies that have reported improved seeding using dynamic seeding methods (Li *et al* 2001). In the studies presented in this chapter it was found that agitation speed influenced the number, distribution and viability of the cells seeded into the scaffolds. Following overnight agitation at 200 rpm, a large number of BACs and OMCs were distributed evenly throughout NF scaffolds. In contrast, for HOS TE85 cells it was necessary to agitate NF scaffolds at 300 rpm in order to ensure a high number of cells were retained within the scaffold.

It was determined that for seeding each of the three cell types into SK3 scaffolds, overnight agitation at 300 rpm led to both an increase in cell number and a more homogeneous distribution of cells. Whilst a reduction in relative viability was detected for BACs and OMCs seeded into SK3 scaffolds with agitation, this effect was not observed in HOS TE85 cells. For all cell types, agitation at 300 rpm also led to an increase in the number of cells contained within SK4 scaffolds. Following overnight agitation at this speed the cells were evenly distributed within the scaffolds. As for SK3 scaffolds, a reduction in the relative viability of BACs and OMCs, but not HOS TE85 cells, was detected following agitation at 300 rpm. Overnight agitation at 200 rpm allowed an increased number of OMCs to be seeded into SK5 scaffolds compared to the other agitation speeds, although it was observed that the number of OMCs detected within these scaffolds was lower than the number detected within each of the other scaffold types. As for NF scaffolds, it was found that overnight seeding at 300 rpm allowed a large number of HOS TE85 cells to be seeded homogeneously into SK5 scaffolds. A reduction in the relative viability of OMCs was detected following agitation at 100, 200 and 300 rpm, compared to that of OMCs seeded into SK5 scaffolds without agitation. As for the other sparse knit scaffolds, the viability of HOS TE85 cells seeded into SK5 scaffolds with agitation was not compromised.

Following overnight seeding at 200, 300 and 400 rpm, the number of OMCs in NF, SK3 and SK4 scaffolds was found to be greater than the 4×10^6 cells initially seeded into the scaffolds. This suggests that the proliferation rate of OMCs under these conditions was greater than that of the other two cell lines. It is well documented that chondrocytes within articular cartilage have a low proliferative rate (Buckwalter and Mankin 1998b). The cells within meniscal fibrocartilage display phenotypic traits of both chondrocytes and fibroblasts and are generally known as fibrochondrocytes (Huckle *et al* 2003). It is probable, therefore, that OMCs have a greater capacity for proliferation than BACs and that the increased number of OMCs within scaffolds following overnight incubation is due to cell proliferation.

In addition, it was noted that the relative viability of HOS TE85 cells seeded into SK scaffolds was not compromised by agitation. This indicates that this osteosarcoma cell line is more resilient to agitation than the two primary chondrocyte cell lines.

The first hypothesis proposed was that agitation speed would influence the number, distribution and viability of cells in scaffolds. For all scaffolds, seeding with agitation led to an increased number of cells contained within the scaffolds compared to static seeding. This study therefore supports previous work that has shown improved seeding of cells into scaffolds using dynamic rather than static methods (Li *et al* 2001). In dynamic seeding, cells are transported into scaffolds by convection as a result of an increase in the relative velocity between the cells and the scaffold (Vunjak-Novakovic *et al* 1996). It has been postulated that high seeding densities could enhance *in vitro* formation of tissues by mimicking phases of cell condensation and differentiation that occur during embryonic development (Gurdon 1988 and Tachetti *et al* 1992). Indeed, enhanced biochemical composition and structural stability have been observed in engineered cartilage that resulted from constructs with high initial cell loading (Vunjak-Novakovic *et al* 1998).

In addition to high seeding densities, uniform spatial distributions of cells within scaffolds are necessary for functional tissue formation (Vunjak-Novakovic *et al* 1998). Galban and colleagues have proposed that non-uniform seeding may lead to spatial variations in cell and nutrient concentration within scaffolds and hence impede cartilage formation by limiting mass transport (Galban and Locke 1999). The speed with which the scaffolds were agitated was shown to affect the distribution of cells within each of the scaffolds. For NF scaffolds, increasing the speed of agitation from 0 to 200 rpm led to a more even distribution of cells within the scaffolds, however further increasing the speed to 400 rpm led to an increased number of cells at the centre of scaffolds and few at the surface. This is in agreement with reports from Li and colleagues that enhanced cell seeding does not necessarily coincide with improved uniformity (Li *et al* 2001).

It was found for BACs and OMCs that the relative viability per cell was affected by agitation, for example seeding OMCs into NF scaffolds with agitation at 100, 200, 300 and 400 rpm led to a reduction in relative viability in comparison to that of OMCs seeded into NF scaffolds without agitation. Although there are several reports in the literature on the effect of different seeding conditions on the number and distribution of cells in tissue engineering scaffolds, few authors mention the effect of the seeding conditions on cell viability.

The second hypothesis was that the optimum rate of agitation would be dependent on scaffold architecture. The scaffold is important for providing a structure to which cells can attach and for supporting tissue formation (Vunjak-Novakovic *et al* 1998). Scaffold structures used in cartilage tissue engineering studies include non-woven fibre meshes (Freed *et al* 1994a and Puelacher *et al* 1994) and porous foam scaffolds (Wendt *et al* 2003). Wendt and colleagues have reported similar optimum seeding conditions for both non-woven and porous foam scaffolds with different pore structures (Wendt *et al* 2003). The scaffolds used by Wendt and co-workers had "open" upper and lower scaffold surfaces and so differed from the SK3 and SK4 scaffolds used in our study which had dense upper and lower "crusts". It was proposed that the presence of more dense upper and lower "crusts" may impede the penetration of cells into the scaffolds; hence these scaffolds would require seeding at faster agitation speeds than those scaffolds with more open structures (NF and SK5). In this study, the optimum agitation speed for seeding BACs and OMCs into SK3 and SK4 scaffolds was determined to be 300 rpm, whilst the optimum agitation speed for NF and SK5 scaffolds was 200 rpm, thus confirming this hypothesis. In contrast, for HOS TE85 cells, no difference in optimum agitation speed was determined for the scaffolds with more open structures compared to those with the more dense upper and lower crusts. It is unknown why there are variations in optimum agitation speed for different cell types, however it is postulated that it may be due to differences in cell size and density. In order to ascertain whether cell density influences cell seeding, the density of each cell type could be compared using centrifugation. It is also possible that the different cell types interact differently with the scaffold materials and the fibres.

This study demonstrated that different seeding conditions were required to ensure a high density of homogeneously distributed cells were seeded into each of the scaffold types for BACS, OMCs and HOS TE85 cells, therefore highlighting the need for seeding optimisation studies prior to commencing tissue engineering studies as both scaffold architecture and cell type may influence the optimum seeding conditions.

3.6 Conclusions

The work presented within this chapter describes a novel scaffold structure which has enhanced flow properties compared to a more traditional fibrous tissue engineering scaffold. The effect of agitation speed on the number, viability and distribution of BACs, OMCs and HOS TE85 cells within NF and SK scaffolds was determined. The optimum agitation speed for seeding each of the cell types into the different scaffolds was determined and is summarised in Table 3.2. The optimum seeding conditions varied with both scaffold architecture and cell type. In terms of scaffold architecture, faster agitation speeds were required to ensure a high density of cells were able to penetrate the more densely knitted scaffolds. With respect to cell type, for identical scaffolds, faster agitation speeds were required for HOS TE85 cells than chondrocytes. The work presented in this chapter highlights the importance of performing studies of this nature prior to commencing tissue engineering work in order to determine the optimum parameters for seeding particular cell lines into scaffold structures.

Scaffold Type	Scaffold description	Scaffold density	Optimum seeding speed (BACs)	Optimum seeding speed (OMCs)	Optimum seeding speed (HOS)
Needled felt 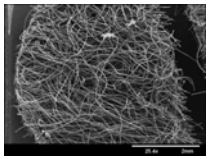	Open scaffold structure with randomly orientated fibres.	0.049 g cm^{-3}	200 rpm	200 rpm	300 rpm
Sparse knit 3 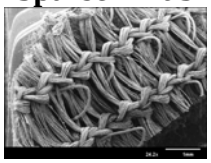	Bundles of randomly arranged fibres separated by aligned channels and held together by densely knitted upper and lower "crust".	0.069 g cm^{-3}	300 rpm	300 rpm	300 rpm
Sparse knit 4 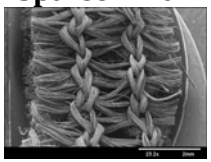	As sparse knit 3.	0.047 g cm^{-3}	300 rpm	300 rpm	300 rpm
Sparse knit 5 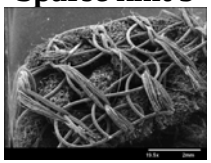	As sparse knit 3, except upper and lower "crust" less dense.	0.083 g cm^{-3}	N/A	200 rpm	300 rpm

Table 3.2 Summary of scaffold properties and optimum seeding conditions.

Chapter 4

Comparison of the roles of scaffold architecture and bioreactor systems on initial cartilage formation *in vitro*

4.1 Introduction and aims

As previously described, there have been numerous attempts to engineer cartilage *in vitro* over the past decade. One of the key challenges in cartilage tissue engineering is that of producing tissue constructs of clinically useful sizes. Freed and co-workers have reported that to overcome this challenge there is a need to ensure that an appropriate supply of nutrients is available to the entire construct throughout the *in vitro* culture period (Freed *et al* 1998 and Obradovic *et al* 2000). Pei and colleagues have proposed that optimisation of parameters such as scaffold material, scaffold structure and culture system is necessary in order to enhance *in vitro* cartilage regeneration and allow formation of larger constructs with an appropriate structure and composition (Pei *et al* 2002). This is in agreement with Freed and Vunjak-Novakovic, who suggested that two environmental factors play an important role in *in vitro* tissue regeneration: (1) scaffold structure and (2) the culture system (Freed and Vunjak-Novakovic 1998). There have been several attempts to improve the supply of nutrients to growing tissues *in vitro* based on modifications to both the culture systems used and the scaffold architecture (Malda *et al* 2005). These include studies by Bhardwaj and colleagues and Woodfield and co-workers who investigated the use of scaffolds with different structures for tissue engineering cartilage (Bhardwaj *et al* 2001 and Woodfield *et al* 2002).

The aim of this chapter was to compare different scaffold architectures and culture systems for their suitability for tissue engineering cartilage. The hypotheses proposed within this thesis were that scaffolds combining random and anisotropic porosity and a novel flow-perfusion bioreactor would be advantageous for *in vitro* cartilage formation. In this chapter, needled felt and each of the sparse knit scaffolds were compared for *in vitro* cartilage tissue formation over a four week period. In addition, the novel flow-perfusion bioreactor was compared with a commercially available culture system, the RCCS™, and static 6-well tissue culture plates.

4.2 Methods

4.2.1 Preparation of scaffolds

Scaffolds were manufactured and prepared for cell-seeding as described in Sections 2.2.1 and 2.2.5.a.

4.2.2 Cell culture

OMCs were isolated from ovine meniscal cartilage and cultured as outlined in Sections 2.2.3.b and 2.2.4.b.

4.2.3 Culture of cell-seeded scaffolds

Scaffolds were seeded with OMCs as described in Section 2.2.5.b under the conditions optimised in Chapter 3. For NF and SK5 scaffolds an agitation speed of 200 rpm was used and for SK3 and SK4 scaffolds the agitation speed was 300 rpm (Table 3.2). Following overnight seeding, scaffolds were transferred to either static 6-well plates (Section 2.2.5.c), RCCS™ vessels (Section 2.2.5.d), or the flow-perfusion bioreactor (Section 2.2.5.e). All cultures were maintained for four weeks. For both static and RCCS™ cultures, medium was replenished at a rate of 50% three times per week. Medium was supplied to the flow-through bioreactor at a rate of 0.15 mL per minute. For each culture condition, five scaffolds of each type were cultured, three of which were used for biochemical analysis and two for histology.

The experiments were repeated twice such that for each scaffold type and culture environment, six samples were analysed for their biochemical content and four for their histological appearance.

4.2.4 Analysis of constructs

Following the four-week culture period, scaffolds were removed from their respective culture environments and washed three times in sterile PBS.

4.2.4.a Biochemical analyses and assessment of increase in construct weight

Scaffolds for biochemical analysis were transferred to pre-weighed Eppendorf tubes and re-weighed in order to calculate the wet weight of the constructs. Scaffolds were lyophilised and re-weighed so that a "dry weight" for each construct could be obtained. The percentage increase in construct weight was determined using the equation given in Appendix 3.6. Samples were digested using papain, as outlined in Section 2.2.6.b. Following overnight incubation, samples were allowed to cool and aliquots taken for DNA, GAG and collagen assays.

4.2.4.a.i Assessment of cell number

The total cell number for each construct was determined using the Hoechst 33258 assay. The assay was performed as in Section 2.2.6.c. The number of cells within each construct was determined and normalised with respect to the mass of the constructs (Appendix 3.7).

4.2.4.a.ii Assessment of GAG content

The DMMB assay was used to quantify the GAG content of each construct according to the procedure outlined in Section 2.2.6.e. The GAG content for each sample was calculated using the equation given in Appendix 3.1.

4.2.4.a.iii Assessment of total collagen content

The total collagen content of each sample was assessed using the hydroxyproline assay (Section 2.2.6.f) and calculated using the equation given in Appendix 3.2.

4.2.4.b Histological analysis

Prior to histological examination, samples were fixed in 4% paraformaldehyde at 4°C (Appendix 2.5.4).

4.2.4.b.i Resin embedding constructs

Constructs were processed, embedded in Technovit 8100 resin and sectioned as described in Section 2.2.7.c.

4.2.4.b.ii Safranin O staining

Sections were stained with safranin O as outlined in Section 2.2.7.d.ii. Following staining, sections were mounted and imaged using an inverted microscope (Leica DM IRBE, Leica Microsystems).

4.2.5 Statistical analysis

The statistical significance of results was assessed using GraphPad InStat version 3.0 (GraphPad Software Inc, San Diego, USA). Results were expressed as mean ± SEM. An ANOVA and the Tukey-Kramer Multiple Comparisons post-test were performed. Results were considered significant when $P<0.05$ (*), very significant when $P<0.01$ (**) and extremely significant when $P<0.001$ (***).

4.3 Results

4.3.1 Increase in construct weight

The increase in construct weights with culture time was determined as outlined in Section 4.2.4.a. Figures 4.1 and 4.2 show the increase in construct weight for each of the scaffold types following 4-week static, RCCS™ or flow perfusion culture. The two graphs show the same data expressed using different parameters for the x axis in order to clearly show the statistical significance of the results. All scaffolds cultured in either static 6-well plates or the RCCS™ showed greater increases in dry weight than those cultured in the flow perfusion system (Figure 4.1). For NF and SK4 scaffolds, the increase in weight of constructs cultured within the RCCS™ was greater than that of constructs cultured statically (Figure 4.1).

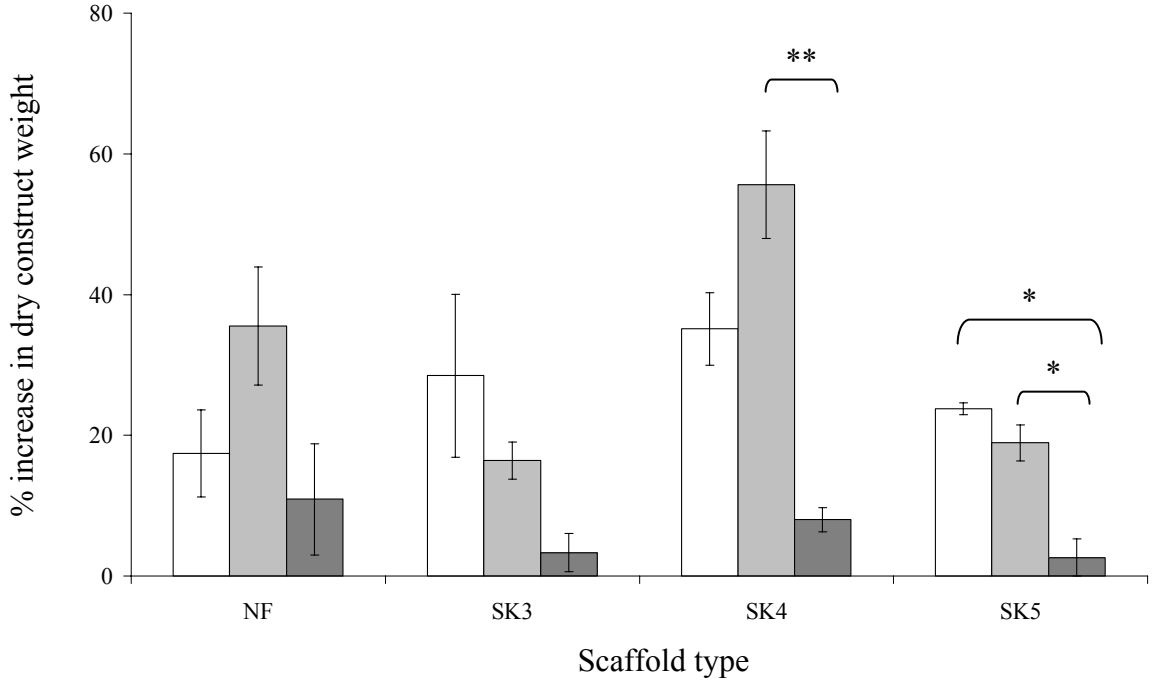

Figure 4.1 Comparison of the % increase in construct weight for each of the scaffold types following 4-week □ static, ▒ RCCS™ or ■ flow perfusion culture. Results expressed as mean (n=3) ± SEM (* indicates $P<0.05$, ** indicates $P<0.01$).

Following 4 week static and flow perfusion culture, no significant differences between the increases in construct weight for each of the scaffold types was detected (Figure 4.2). SK4 scaffolds cultured within the RCCS™, however, showed a greater increase in weight than either SK3 or SK5 scaffolds ($P<0.05$, Figure 4.2).

4.3.2 Cell content

The number of cells per gram of dry construct following 4-week culture was measured as described in Section 4.2.4.a.i. Figures 4.3 and 4.4 show a comparison of the cell content in NF, SK3, SK4 and SK5 scaffolds following culture in each of the systems. Over the four week culture period the number of cells within all scaffolds increased. For NF, SK3 and SK4 scaffolds, no statistically significant difference in the cell content of the scaffolds was detected for each of the culture systems. For SK5 scaffolds, the number of cells in scaffolds cultured statically was significantly greater than the number in constructs cultured in either RCCS™ or flow perfusion systems ($P<0.05$ and $P<0.001$ respectively, Figure 4.3). In addition, more cells were detected in SK5 scaffolds following RCCS™ culture than following culture in the flow perfusion system ($P<0.001$, Figure 4.3). Following 4-week static culture, NF scaffolds contained more cells per gram construct than SK5 scaffolds ($P<0.001$, Figure 4.4). Comparing each of the scaffold types following RCCS™ culture, the cell content of NF scaffolds was greater than that of SK3 and SK5 scaffolds ($P<0.05$ and $P<0.001$ respectively, Figure 4.4). In addition SK4 scaffolds cultured within the RCCS™ contained more cells per gram than SK5 scaffolds ($P<0.05$, Figure 4.4). NF scaffolds cultured within the flow perfusion bioreactor contained a greater number of cells per gram than each of the other scaffold types ($P<0.001$, Figure 4.4). Of the sparse knit scaffolds cultured within the flow perfusion system, SK4 scaffolds contained a greater concentration of cells than either SK3 or SK5 scaffolds ($P<0.001$, Figure 4.4) and SK3 scaffolds contained an increased number of cells compared to SK5 scaffolds ($P<0.001$, Figure 4.4).

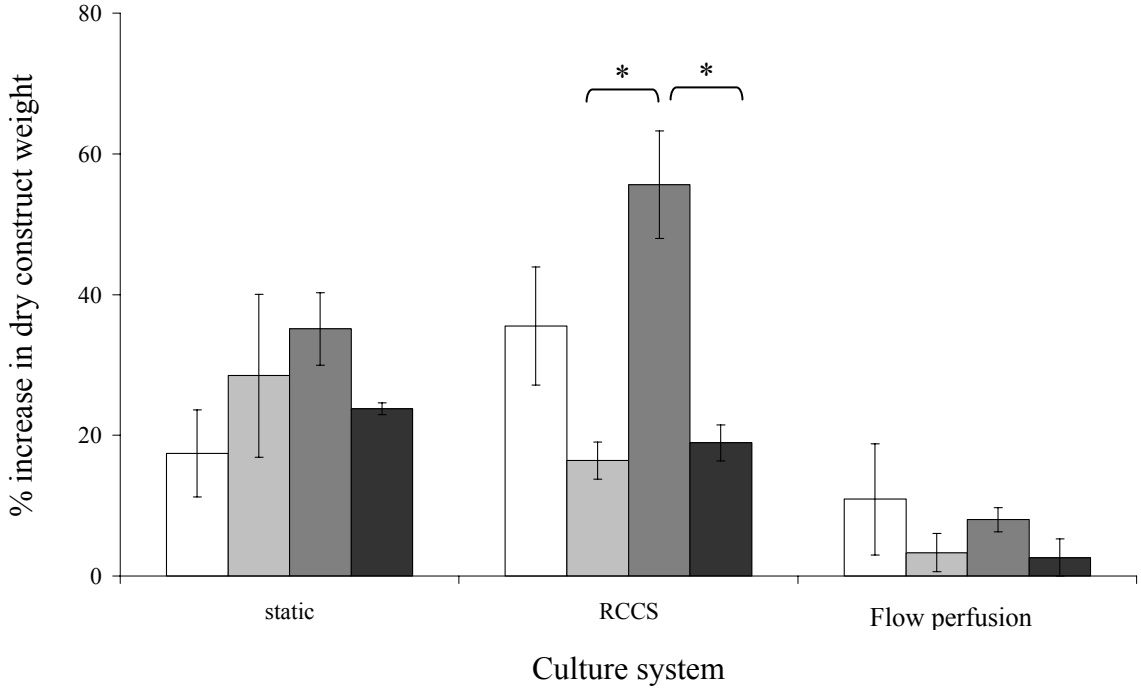

Figure 4.2 Comparison of the % increase in construct weight of □NF, □ SK3, ■ SK4 and ■ SK5 constructs following 4-week culture in each of the culture systems. Results expressed as mean (n=6) ± SEM (* indicates $P<0.05$).

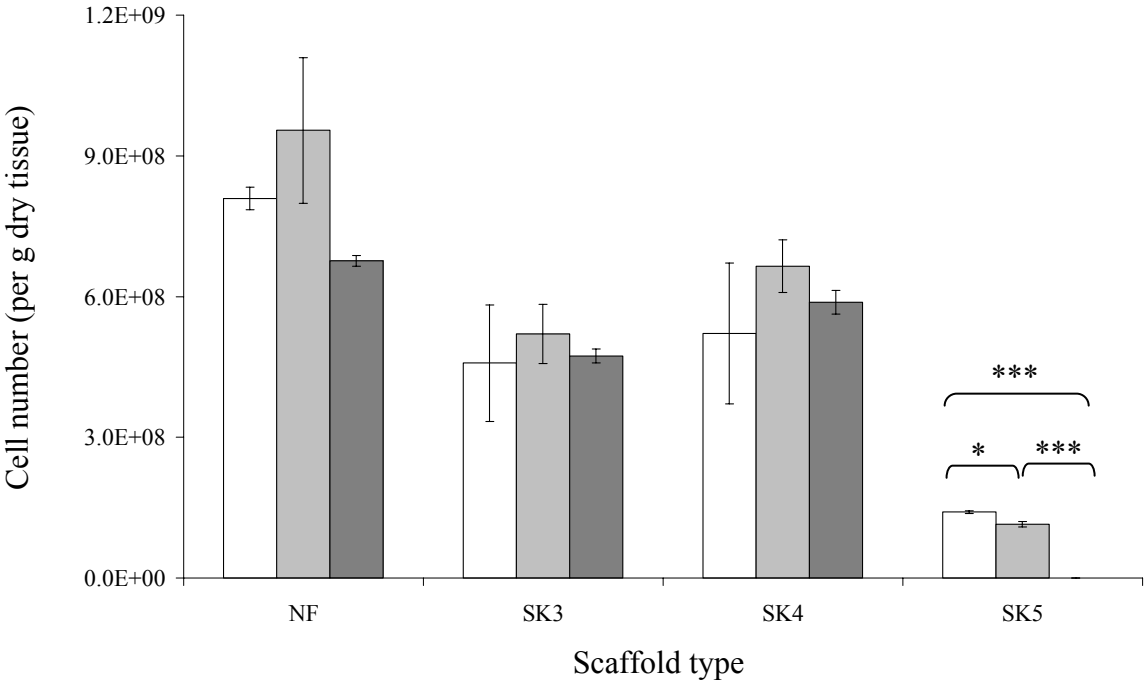

Figure 4.3 Comparison of the cell number (per gram dry construct weight) in each of the scaffold types following 4-week □ static, ▒ RCCS™ or ■ flow perfusion culture. Results expressed as mean (n=6) ± SEM (* indicates $P<0.05$, *** indicates $P<0.001$).

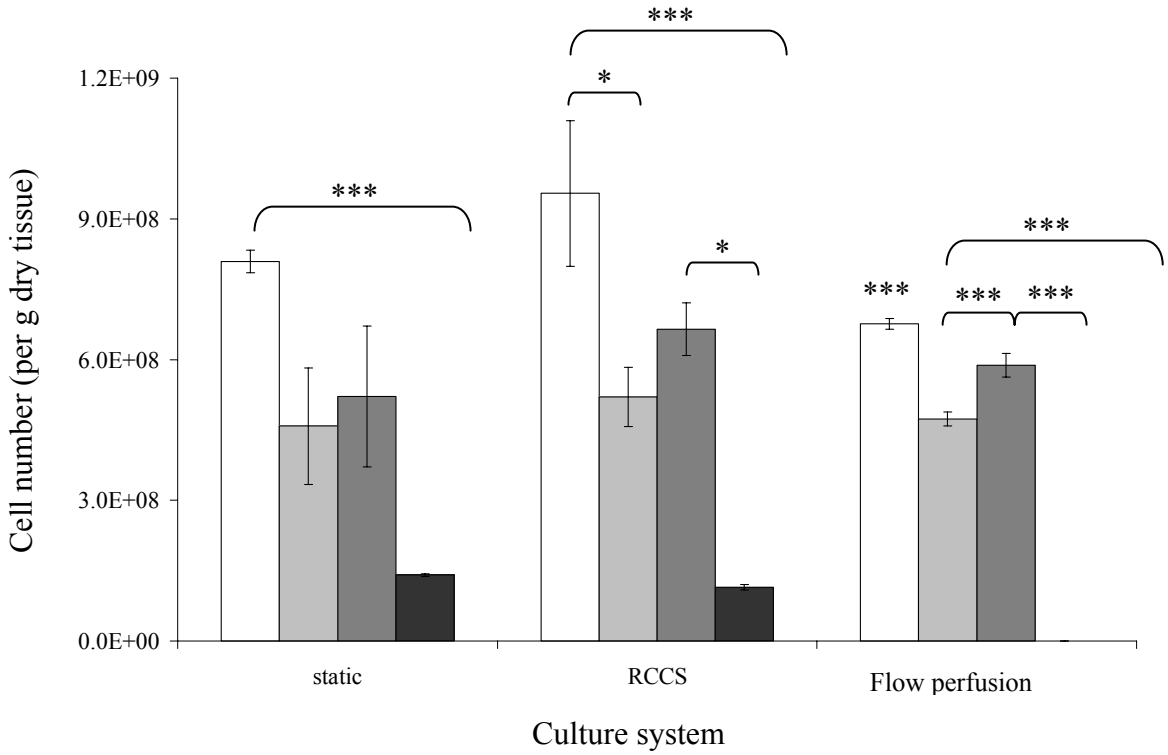

Figure 4.4 Comparison of the cell number (per g dry construct weight) of □ NF, ▒ SK3, ▒ SK4 and ■ SK5 constructs following 4-week culture in each of the culture systems. Results expressed as mean (n=6) ± SEM (* indicates $P<0.05$, *** indicates $P<0.001$).

4.3.3 GAG content

The GAG content of each of the constructs was assessed using the DMMB assay as described in Section 4.2.4.a.ii. Figures 4.5 and 4.6 show the GAG content of NF, SK3, SK4 and SK5 scaffolds as a percentage of the dry construct weight following 4-week culture in each of the systems. NF constructs contained a greater concentration of GAGs following culture in the RCCS™, compared to either static or flow perfusion culture ($P<0.001$, Figure 4.5). Similarly, following RCCS™ culture SK3 constructs had a greater GAG content compared to static and flow perfusion culture ($P<0.001$, Figure 4.5). In addition, the GAG content of SK3 scaffolds was significantly increased following static culture compared to flow perfusion culture ($P<0.01$, Figure 4.5). GAGs accounted for a greater proportion of SK4 scaffolds following RCCS™ and static culture compared to flow perfusion culture ($P<0.001$, Figure 4.5). SK4 scaffolds cultured within the RCCS™ also contained a higher concentration of GAGs than those cultured statically ($P<0.001$, Figure 4.5). Both static and RCCS™ culture led to higher concentrations of GAGs within SK5 scaffolds, as compared to flow perfusion culture ($P<0.05$, Figure 4.5). There was no statistically significant difference between the GAG content of each scaffold type following 4-week static or flow perfusion culture. NF scaffolds contained a greater concentration of GAGs than SK3 and SK5 scaffolds following RCCS™ culture ($P<0.05$ and $P<0.001$ respectively, Figure 4.6). RCCS™ culture led to a greater concentration of GAGs in SK3 and SK4 scaffolds, compared to SK5 scaffolds ($P<0.01$ and $P<0.001$ respectively, Figure 4.6).

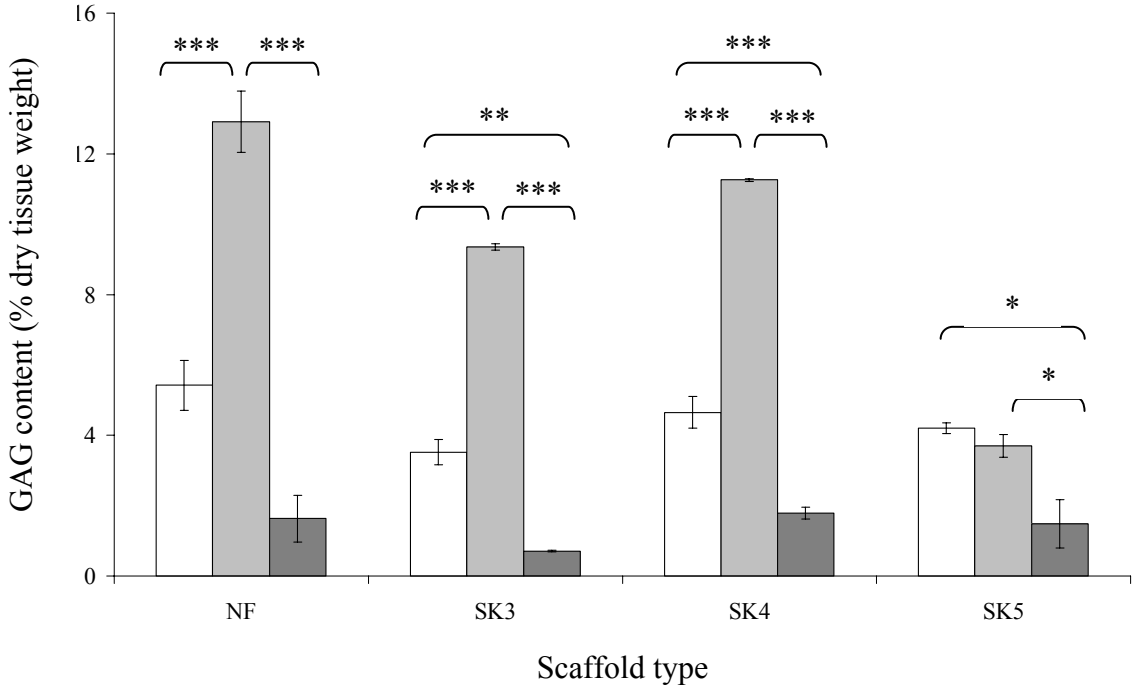

Figure 4.5 Comparison of the GAG composition (% dry tissue weight) of each scaffold type following 4 week □ static, ▒ RCCS™ or ▓ flow perfusion culture. Results expressed as mean (n=6) ± SEM (* indicates $P<0.05$, ** indicates $P<0.01$, *** indicates $P<0.001$).

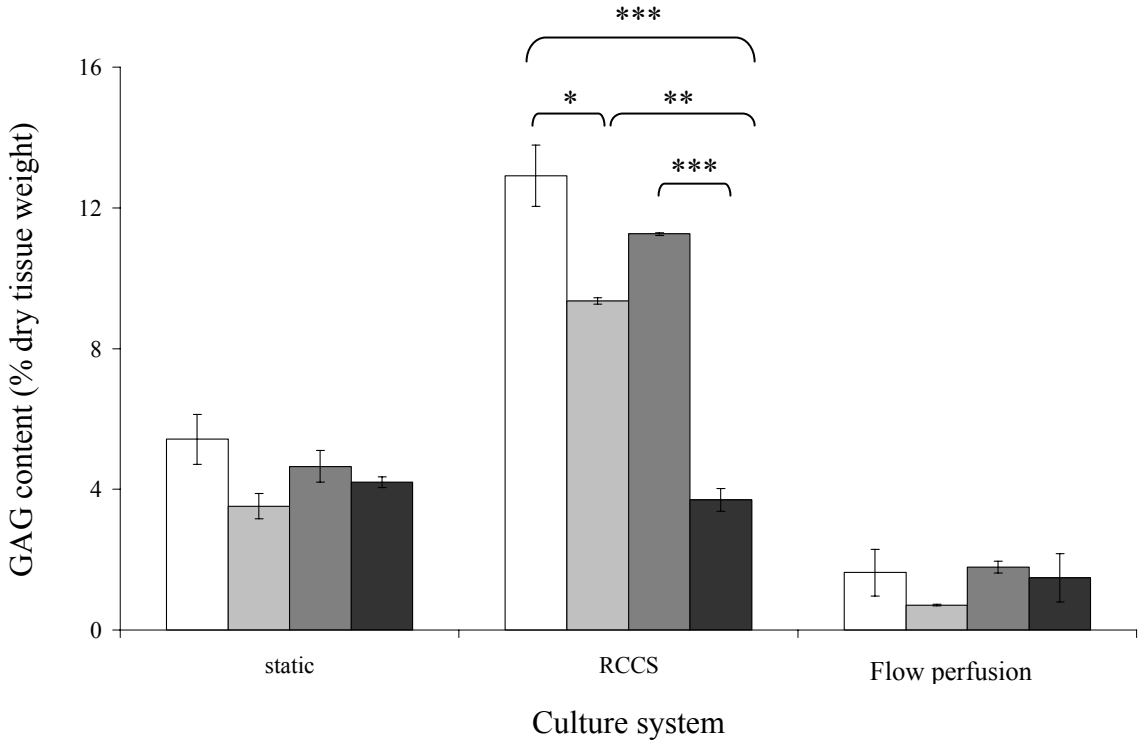

Figure 4.6 Comparison of the GAG composition (% dry tissue weight) of □ NF, ▒ SK3, ▒ SK4 and ■ SK5 constructs following 4-week culture in each of the culture systems. Results expressed as mean (n=6) ± SEM (* indicates $P<0.05$, ** indicates $P<0.01$, *** indicates $P<0.001$).

4.3.4 Total collagen content

The hydroxyproline assay was used to determine the total collagen content of constructs as outlined in Section 4.2.4.a.iii. Figures 4.7 and 4.8 show the collagen content as a percentage of the construct dry weight for NF, SK3, SK4 and SK5 scaffolds following 4-week culture in each of the systems. Following RCCS™ culture, the collagen content of NF constructs was greater compared to static and flow perfusion culture ($P<0.01$ and $P<0.001$ respectively, Figure 4.7). There was no significant difference between the different culture systems with respect to the collagen content of SK3 scaffolds following 4 weeks culture. The collagen content of SK4 scaffolds was greater following RCCS™ culture compared to both static and flow perfusion culture ($P<0.05$, Figure 4.7). Static culture led to a higher collagen content in SK5 scaffolds than either RCCS™ or flow perfusion culture ($P<0.01$, Figure 4.7). NF scaffolds contained a significantly greater amount of collagen than SK3 scaffolds following static culture ($P<0.01$, Figure 4.8). There was no significant difference between the collagen content of the other scaffold types following static culture. Although on average the collagen content of NF and SK4 scaffolds was greater than other scaffolds following 4-week RCCS™ culture, no significance was detected between these scaffolds and SK3 or SK5 scaffolds. Following 4-week flow perfusion culture, NF scaffolds contained a higher concentration of collagen than SK5 scaffolds ($P<0.05$, Figure 4.8). No significant difference was detected between the collagen contents of the other scaffolds following flow perfusion culture.

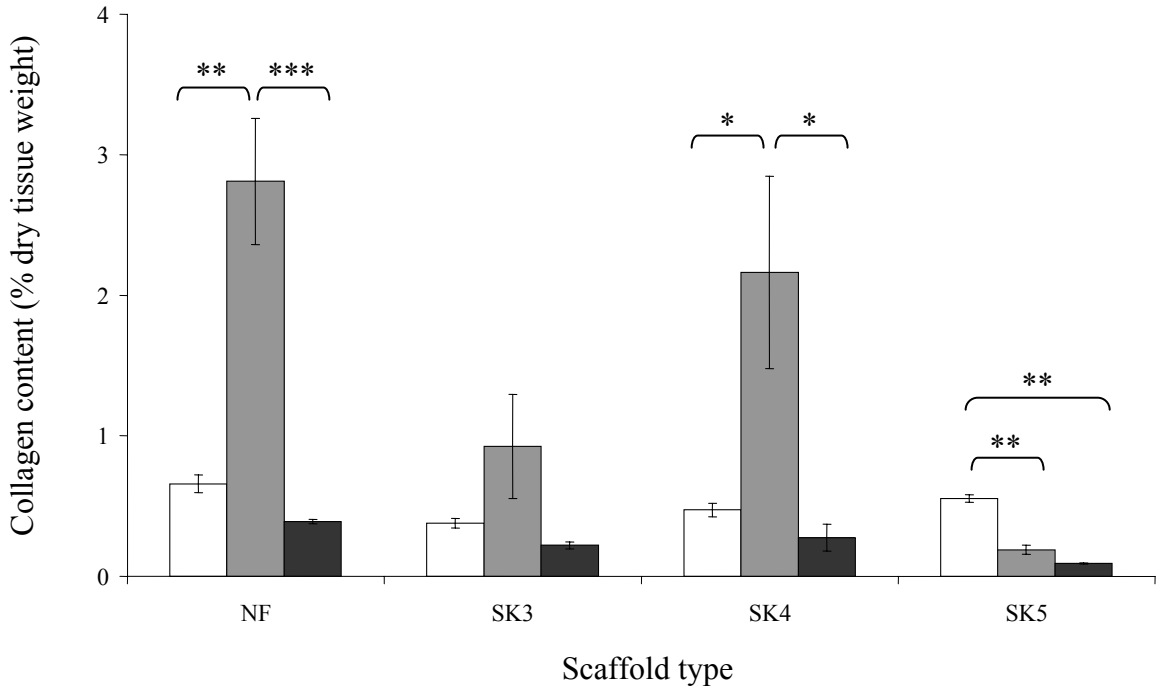

Figure 4.7 Comparison of the collagen composition (% dry tissue weight) of each scaffold type following 4 week □ static, ▒ RCCS™ or ■ flow perfusion culture. Results expressed as mean (n=6) ± SEM (* indicates $P<0.005$, ** indicates $P<0.01$).

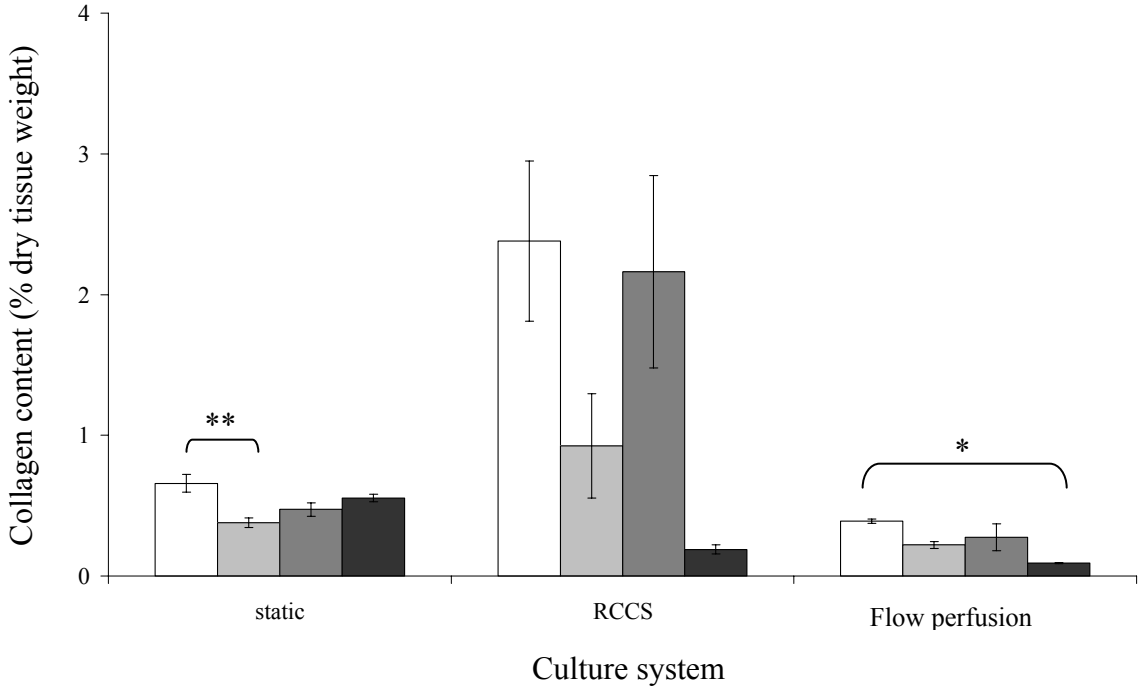

Figure 4.8 Comparison of the collagen composition (% dry tissue weight) of □ NF, ▒ SK3, ▒ SK4 and ■ SK5 constructs following 4-week culture in each of the culture systems. Results expressed as mean (n=6) ± SEM (* indicates $P<0.05$, ** indicates $P<0.01$).

4.3.5 Safranin O staining

Following 4-week culture, scaffolds were fixed, embedded, sectioned and stained with safranin O as described in Section 4.2.4.b. For all scaffolds and culture environments, cells within the scaffolds stained positively with safranin O. Figure 4.9 shows representative images of NF scaffolds following 4-week static, RCCS™ and flow perfusion culture. NF scaffolds cultured under static conditions contained cells both at the surface and in the centre (Figure 4.9 A & B). More intense safranin O staining was visible at the outer edge of the scaffolds. NF scaffolds cultured within the RCCS™ were similar in appearance to those cultured in static plates (Figure 4.9 C & D). Cells were present throughout the scaffolds with more intense staining visible at the outer edges. Figure 4.9 E & F shows representative sections through NF scaffolds that were cultured in the flow perfusion bioreactor. Fewer cells were present in these scaffolds compared to those cultured either in static plates or the RCCS™.

Figure 4.10 shows sections taken from SK3 scaffolds following static, RCCS™ or flow perfusion culture for 4 weeks. Following static culture, cells were present throughout the knitted surface of SK3 scaffolds (Figure 4.10 A). In the central region of scaffolds, cells were restricted to the bundles of fibres and the aligned channels could be seen between the fibres (Figure 4.10 B). At the surface of constructs cultured in the RCCS™ more cells appeared to be present than in those cultured in static plates (Figure 4.10 C). The central region of constructs cultured in the RCCS™ was similar to that of those cultured statically, with cells present within the bundles of fibres and aligned channels visible between the bundles (Figure 4.10 D). SK3 scaffolds cultured within the flow perfusion system contained few cells (Figure 4.10 E & F). More cells were present within the knitted crusts than in the centre of constructs.

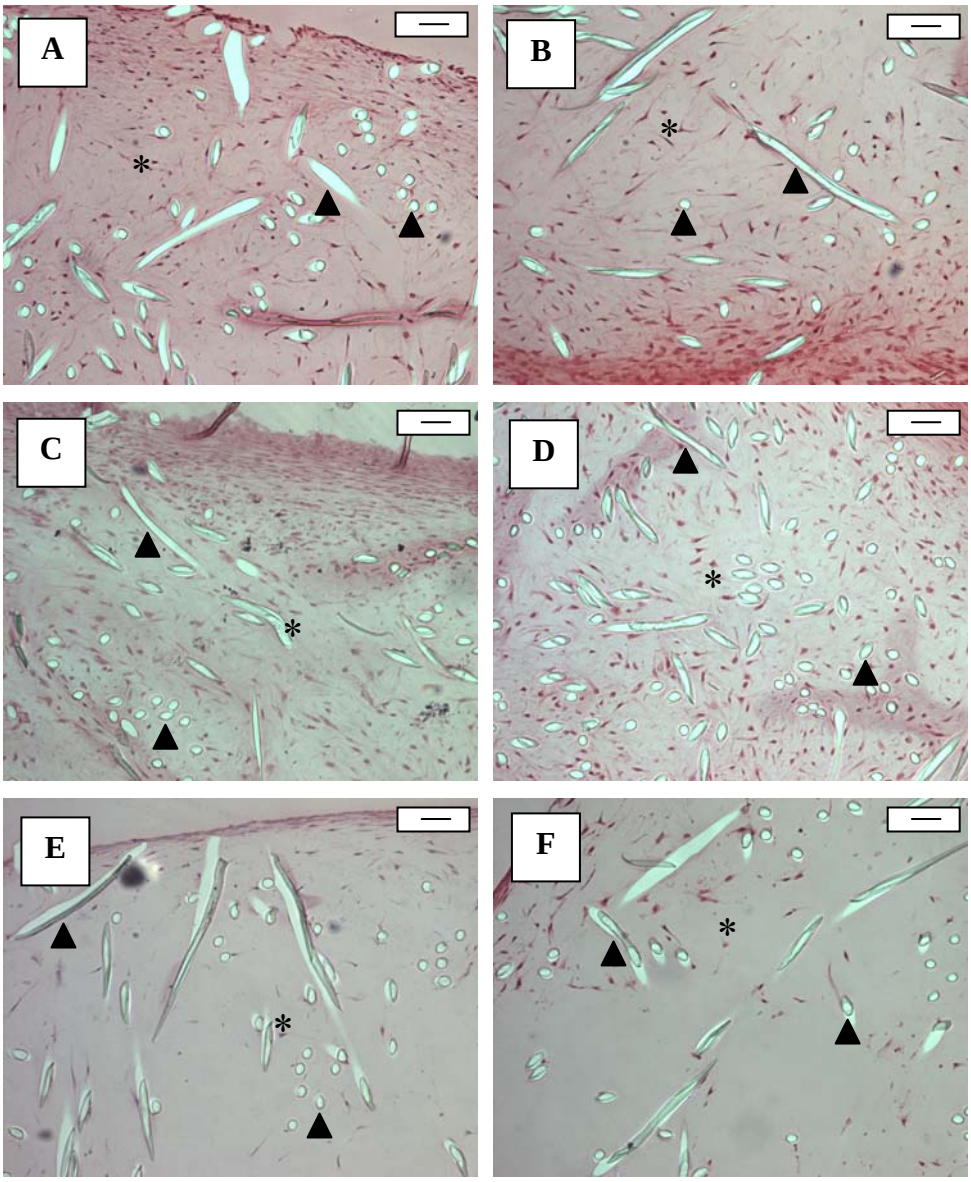

Figure 4.9 Representative images showing haematoxylin and safranin O staining of NF constructs following 4-week (A & B) static, (C & D) RCCS™ and (E & F) flow perfusion culture. Images show (A, C & E) top surface and (B, D & F) centre of constructs. Scale bars represent 50 μm. Asterisks (*) highlight the appearance of cells and arrow heads (◄) highlight polymer fibres within images.

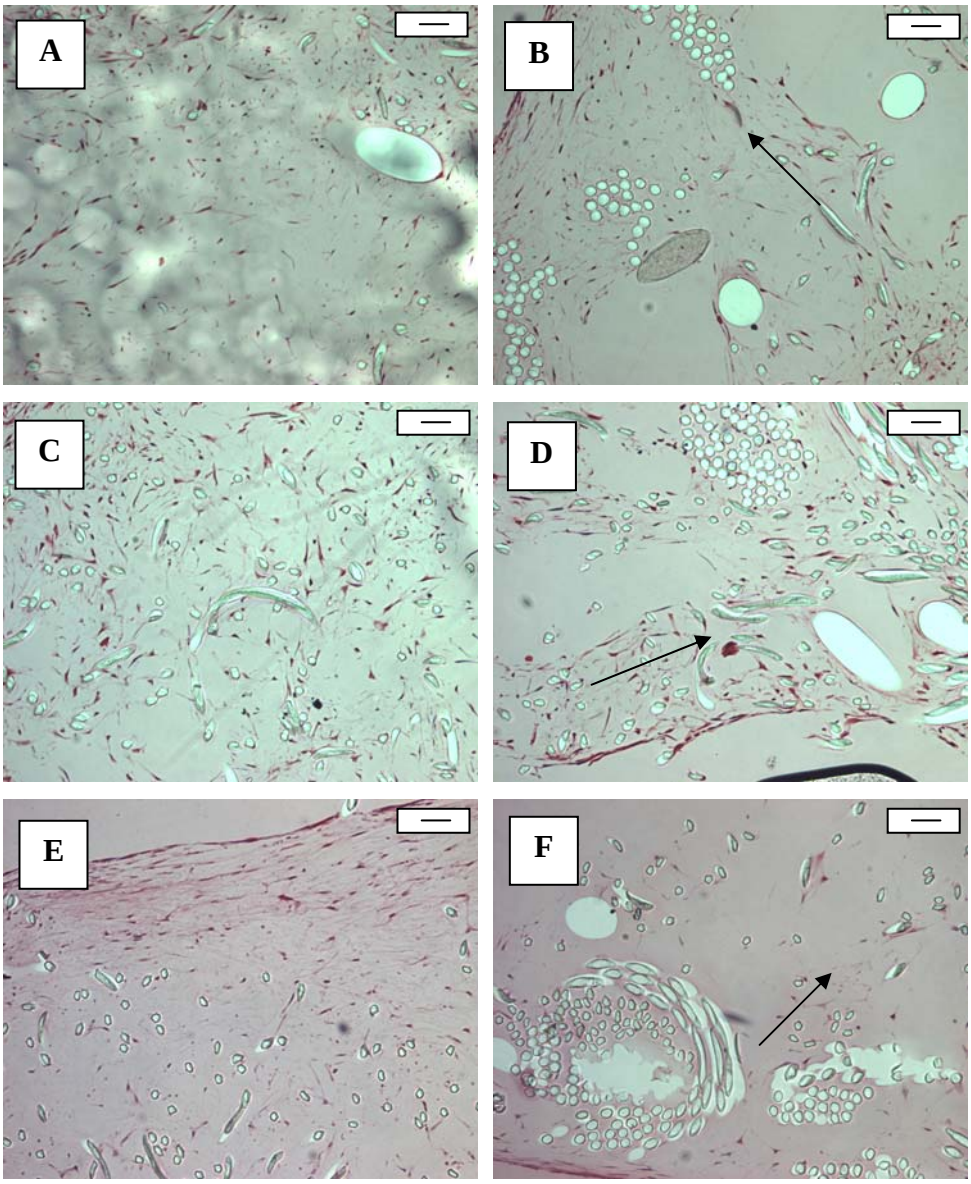

Figure 4.10 Representative images showing haematoxylin and safranin O staining of SK3 constructs following 4-week (A & B) static, (C & D) RCCS™ and (E & F) flow perfusion culture. Images show (A, C & E) top surface and (B, D & F) centre of constructs. Scale bars represent 50 μm. The orientation of aligned fibres within the constructs is highlighted with arrows (⟶).

Representative images of SK4 scaffolds following 4-week static, RCCS™ or flow perfusion culture are shown in Figure 4.11. Following static culture, constructs contained a homogeneous distribution of cells (Figure 4.11 A & B). The presence of aligned channels between the bundles of fibres was difficult to detect within the centre of these samples (Figure 4.11 B) indicative that matrix formation may have occurred within the channels. Sections taken from SK4 scaffolds cultured within the RCCS™ for 4 weeks were similar in appearance to those cultured statically (Figure 4.11 C & D). Cells within these constructs were evenly distributed throughout both the knitted crust and the scaffold centre, with the aligned channels not clearly visible. SK4 scaffolds cultured within the flow-perfusion bioreactor contained few cells which were present predominantly at the outer edge of the construct (Figure 4.11 E & F).

Representative sections through SK5 scaffolds following 4-week static, RCCS™ or flow perfusion culture are shown in Figure 4.12. Following culture in each of the three systems, SK5 scaffolds contained few cells and a thin layer of safranin O staining was visible at the outer edge of constructs. SK5 scaffolds cultured within the RCCS™ appeared to contain more cells than those constructs cultured statically or in the flow perfusion system (Figure 4.12 C & D). To allow comparison of the histological appearance of all samples Figure 4.13 shows representative sections from the centre of constructs from each scaffold type and culture system. Constructs cultured within the flow perfusion bioreactor contained fewer cells than scaffolds cultured either in static 6-well plates or the RCCS™, regardless of scaffold type (Figure 4.13 C, F, I & L).

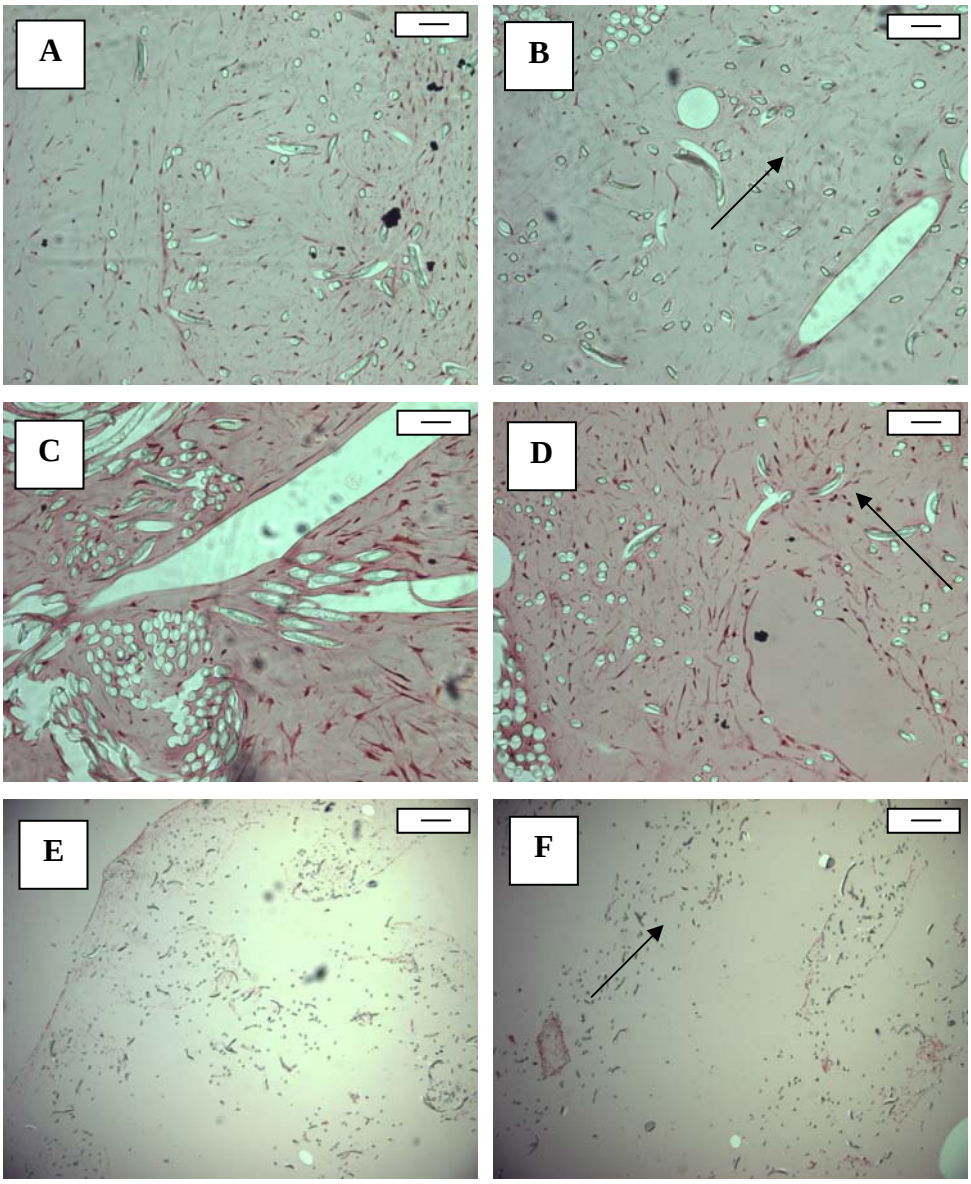

Figure 4.11 Representative images showing haematoxylin and safranin O staining of SK4 constructs following 4-week (A & B) static, (C & D) RCCS™ and (E & F) flow perfusion bioreactor culture. Images show (A, C & E) top surface and (B, D & F) centre of constructs. Scale bars represent 50 μm for images A, B, C & D and 100 μm for images E & F. The orientation of aligned fibres within the constructs is highlighted with arrows (⟶).

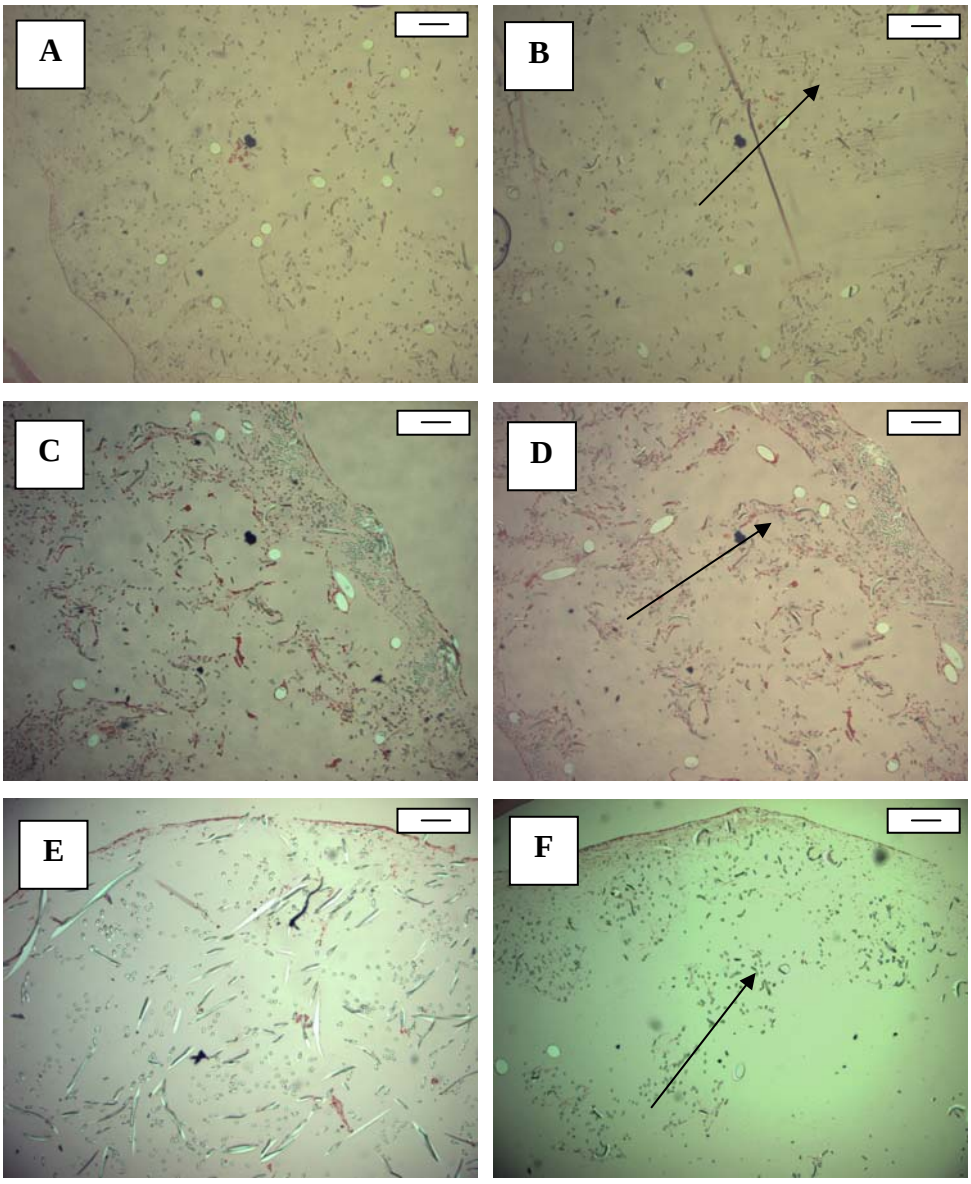

Figure 4.12 Representative images showing haematoxylin and safranin O staining of SK5 constructs following 4-week (A & B) static, (C & D) RCCS™ and (E & F) flow perfusion bioreactor culture. Images show (A, C & E) top surface and (B, D & F) centre of constructs. Scale bars represent 100 μm. The orientation of aligned fibres within the constructs is highlighted with arrows (⟶).

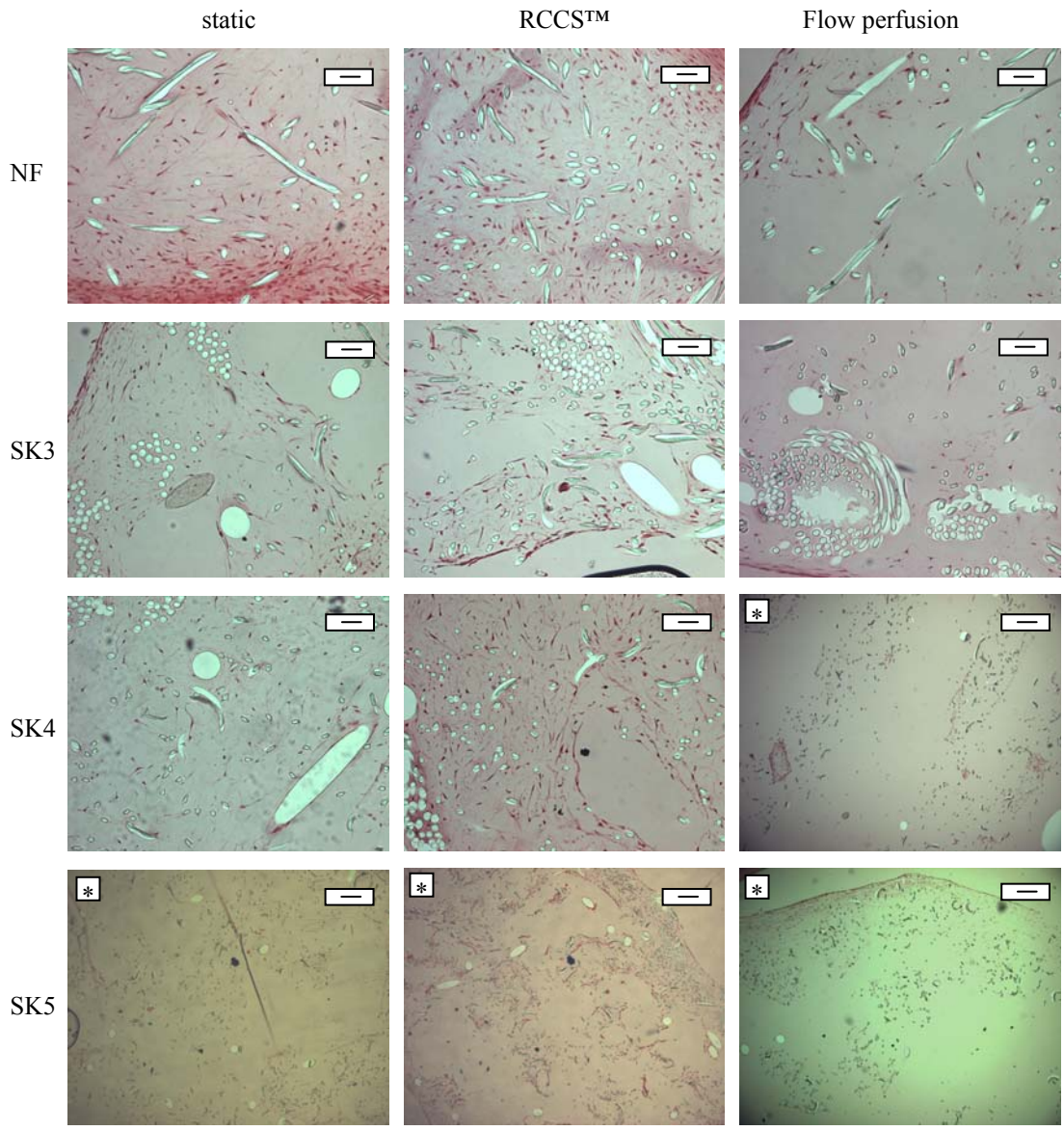

Figure 4.13 Representative images showing haematoxylin and safranin O staining of sections taken through the centre of each of the scaffold types following 4 week static, RCCS™ and flow perfusion culture. Images show NF, SK3, SK4 scaffolds and SK5 scaffolds. In all images the scale bar represents 50 μm except those marked with *, where the scale bar represents 100 μm.

4.4 Discussion

The aim of this chapter was to compare different scaffold architectures and culture systems for their suitability for engineering tissues *in vitro*. It was postulated that scaffolds combining random and anisotropic porosity and a novel flow perfusion bioreactor system would be advantageous for regenerating tissues of a clinically relevant size. To test these hypotheses, each of the different scaffolds were cultured in either static 6-well tissue culture plates, the RCCS™ or the flow perfusion system for 4 weeks with OMCs and the resulting cartilage compared between scaffold and culture systems.

Following 4 week culture, NF scaffolds cultured within the RCCS™ and SK4 scaffolds cultured either in static plates or the RCCS™ all showed an increase in weight of more than 30%. For all culture systems, NF scaffolds contained a greater number of cells following 4 week culture than the other scaffolds. SK4 scaffolds that were cultured in the RCCS™ contained more cells than SK5 scaffolds cultured in the same way. For all scaffold types, constructs cultured within the RCCS™ had a higher GAG content compared to those cultured within static 6-well plates and those cultured within the flow perfusion system. In the same way, the GAG content of constructs cultured statically was greater than that of those cultured within the flow perfusion system. It is possible that GAGs were produced by cells in scaffolds cultured within the flow perfusion system but during the flow of medium through the scaffold the GAG was washed away before an extracellular matrix could form. GAGs formed a greater component of all samples compared to collagen at this stage of culture. During embryonic limb development, the limb first forms from a proteoglycan matrix which is later strengthened by the formation of collagen fibrils and eventually remodelled into bone and cartilage. It is therefore likely that the 4-week old constructs were immature and further culture would allow the formation of a collagen meshwork and later maturation into cartilage. NF and SK4 scaffolds contained more collagen following 4-week RCCS™ culture than following either static or flow-perfusion culture.

Histological examination of the constructs revealed that fewer cells were present in scaffolds cultured within the flow perfusion bioreactor compared to either those cultured in either static plates or the RCCS™. It was also observed that SK5 scaffolds contained few cells regardless of the environment in which they were cultured.

There have been many attempts to regenerate functional tissues *in vitro* using tissue engineering strategies based on using scaffolds and bioreactors (Vunjak-Novakovic 2003). Scaffolds play a vital role in tissue engineering strategies since they provide a three-dimensional matrix to which attached cells proliferate and excrete extracellular matrix components (Hutmacher 2000, Agrawal and Ray 2001 and Sharma and Elisseeff 2004). Vunjak-Novakovic has reported that it vital that these scaffolds contain pores to allow the supply of nutrients to the tissue and that the structure of the scaffold controls the mass transfer of nutrients and metabolites to growing tissues (Vunjak-Novakovic 2003). The first hypothesis proposed in this thesis was that scaffolds containing both random and anisotropic porosity would be advantageous for *in vitro* tissue regeneration since they would facilitate the supply of fresh nutrients to the growing tissue and the removal of excretion products. It has previously been reported that fibrous scaffolds are more suitable for cartilage tissue engineering than either porous scaffolds (Sittinger *et al* 1996) or agarose gels (Vunjak-Novakovic *et al* 1999). In this study it was found that of the three novel scaffolds which contained both random and anisotropic porosity, two of them (SK3 and SK4) supported cartilage formation whilst the third (SK5) did not. A potential explanation for the limited tissue formation with SK5 scaffolds may be that the scaffold was not sufficiently dense to retain proteins within the structure and allow tissue to form. GAGs, for example, may have been produced by the cells and secreted into the culture medium. The control scaffolds (NF scaffolds) also supported *in vitro* cartilage formation. SK5 scaffolds contained fewer cells than the other scaffold types; however their respective GAG and collagen compositions were similar, except following RCCS™ culture.

As reported in Chapter 3, SK5 scaffolds showed less resistance to flow than the other scaffold types. It is possible that the lower number of cells in SK5 scaffolds was the result of cells being washed out of the scaffolds during medium replenishment. SK3 scaffolds had a similar cell and GAG content to NF and SK4 scaffolds, although it was found that following RCCS™ culture, SK3 scaffolds contained less collagen. It was shown in Chapter 3 that SK3 scaffolds were more dense than NF and SK4 scaffolds (which were of a similar density). This suggests that scaffold density may be important for supporting extracellular matrix protein secretion in certain culture environments. Based on the GAG and total collagen composition of the different constructs, SK4 scaffolds appeared to be the most suitable, of the three novel scaffolds, for cartilage regeneration.

It has been reported that *in vitro* culture conditions strongly influence cartilage formation (van der Kraan *et al* 2002). Bioreactors offer several advantages over static culture systems including providing growing constructs with uniform mixing of nutrients and facilitating the maintenance of these nutrient levels (Temenoff and Mikos 2000a). Examples of bioreactor systems used for *in vitro* cartilage engineering include the spinner flask, rotating wall bioreactors (for example the RCCS™) and perfusion systems (Freed and Vunjak-Novakovic 1997, Freed *et al* 1998 and Sittinger *et al* 1994). It is believed that the composition and morphology of tissue engineered constructs is enhanced following dynamic culture (Vunjak-Novakovic 2003). Studies by Sittinger and colleagues have reported good cartilage formation in constructs following 2 and 7 week culture in flow perfusion systems (Sittinger *et al* 1994 and Bujia *et al* 1995). In contrast, a recent study by Mizuno and co-workers showed limited cartilage formation by articular chondrocytes following culture in a flow perfusion system (Mizuno *et al* 2001). The second hypothesis proposed in this thesis was that a novel flow perfusion bioreactor would enhance the quality of engineered cartilage by facilitating mass transfer of nutrients and metabolites. In the studies described in this chapter a novel flow perfusion bioreactor that was designed and built by Smith & Nephew was compared with RCCS™ and static culture for *in vitro* cartilage formation.

With respect to the GAG and collagen content of constructs it appeared in these studies that the flow perfusion system did not support *in vitro* cartilage formation. Cartilage-like tissue formation was observed in NF and SK4 scaffolds that were cultured in the RCCS™, a system that has previously been shown to support cartilage formation (Freed *et al* 1998). It has been observed that rotating wall bioreactors have led to the production of cartilage with composition and mechanical properties more similar to that of native cartilage compared to constructs generated using mixed or static flasks (Vunjak-Novakovic *et al* 1999 and Martin *et al* 2000). These observations have led to the proposition that hydrodynamic culture conditions facilitate the formation of functional cartilage (van der Kraan *et al* 2002). It is generally accepted that cartilage generation in static cultures is restricted by the limited supply of nutrients since mass transport is reliant on simple diffusion (Vunjak-Novakovic 2003).

4.5 Conclusions

From the studies presented in this chapter it has been shown that of the different scaffolds, NF and SK4 scaffolds showed improved initial cartilage formation, with respect to GAG and collagen production following 4-week culture and the best performing bioreactor was the RCCS™. To further test the hypothesis that scaffolds with random and anisotropic porosity facilitate *in vitro* cartilage formation, NF and SK4 scaffolds were cultured for 8 weeks in either static plates or the RCCS™. The results of these studies are presented in Chapter 5 of this thesis.

Chapter 5

Further assessment of the role of scaffold architecture on cartilage formation *in vitro*

5.1 Introduction and aims

As described in Chapter 4, scaffolds are an integral part of any tissue engineering strategy, acting as structural templates which modulate and coordinate tissue formation (Freed and Vunjak-Novakovic 1998). One of the important features of a tissue engineering scaffold is its porous network. This network must allow cell migration, proliferation and synthesis of ECM components (Woodfield *et al* 2002). In addition, the porosity must be sufficient to permit high seeding densities and minimise diffusional constraints during *in vitro* cultivation (Freed *et al* 1999). It has previously been shown that it is necessary for the pores within the scaffolds to be interconnected to facilitate nutrient transfer to, and waste removal from, cells throughout scaffold (Lu *et al* 2001 and Woodfield *et al* 2002). One of the current challenges of tissue engineering is that of satisfying the mass transfer requirements of the growing construct throughout its culture since it is known that cell proliferation increases mass transfer requirements whilst accumulation of ECM within the scaffold decreases its porosity (Freed and Vunjak-Novakovic 1998). In addition to construct density and the nutrient requirements of cells within the scaffold, the mass transport requirements of a tissue engineering construct will depend on the dimensions of the construct. Tissue engineering studies to date have concentrated on cylindrical scaffolds 3-10 mm in diameter and 1-5 mm thick, with volumes in the range 0.007-0.39 cm^3 (Vunjak-Novakovic *et al* 1998).

It has been proposed that a cartilage defect may be so large as to be equivalent to a cylinder 2.5 cm in diameter and 2.5 cm thick, occupying a volume of 12.3 cm^3 (Kladny *et al* 1999, Anderson *et al* 2002 and Woodfield *et al* 2002). Figure 5.1 shows the discrepancy between the size of current tissue engineering scaffolds and the potential size of a cartilage defect. There is therefore a need to used advanced scaffold designs which take into account the actual size of tissue defects and the nutrient requirements of a tissue engineered construct of those dimensions (Woodfield *et al* 2002). One of the hypotheses of this thesis was that scaffolds combining random and anisotropic porosity would facilitate *in vitro* tissue regeneration by improving the supply of nutrients to the growing tissue. Having shown in Chapters 3 and 4 that a high density of cells could be seeded into these scaffolds and that they supported *in vitro* cartilage formation, the aim of this chapter was to assess cartilage formation and cell viability in these scaffolds following 8-week culture.

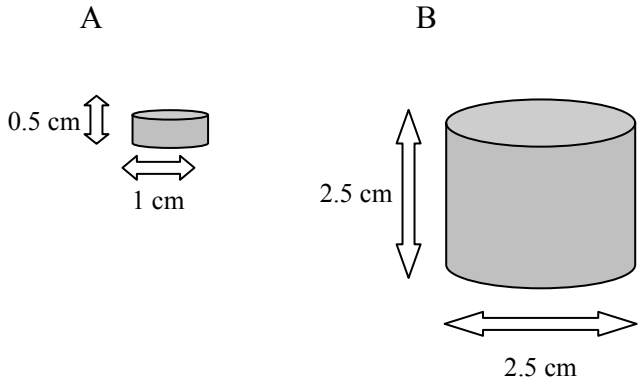

Figure 5.1 A schematic representation of the difference in size between (A) current tissue engineering scaffolds (0.39 cm^3) and (B) a cartilage defect (12.3 cm^3).

5.2 Methods

5.2.1 Preparation of scaffolds

Scaffolds were manufactured and prepared for cell-seeding as described in Sections 2.2.1 and 2.2.5.a.

5.2.2 Cell culture

OMCs were isolated from ovine meniscal cartilage and cultured as outlined in Sections 2.2.3.b and 2.2.4.b.

5.2.3 Culture of cell-seeded scaffolds

Scaffolds were seeded with OMCs as described in Section 2.2.5.b under the conditions optimised in Chapter 3. NF scaffolds were seeded with agitation at 200 rpm and SK4 scaffolds were seeded with agitation at 300 rpm (Table 3.2). Following overnight seeding, scaffolds were transferred to either static 6-well plates (Section 2.2.5.c) or RCCS™ vessels (Section 2.2.5.d). All cultures were maintained for eight weeks. For both static and RCCS™ cultures, medium was replenished at a rate of 50% three times per week. For each culture condition, seven scaffolds of each type were cultured, three of which were used for biochemical analysis, two for histology and two for Live/Dead™ staining. The experiments were repeated twice such that for each scaffold type and culture environment, six samples were used in biochemical assays, four were stained with Live/Dead™ stain and examined using confocal microscopy and four were embedded in resin and stained with safranin O.

5.2.4 Analyses of constructs

Following the eight-week culture period, scaffolds were removed from their respective culture environments and washed three times in sterile PBS.

5.2.4.a Analysis of viability

Prior to biochemical analysis, the total relative viability of scaffolds was determined using the Alamar blue™ assay, as described in Section 2.2.6.d.i. Briefly, scaffolds were incubated for 90 minutes with Alamar blue™ working solution (Appendix 2.4.4) after which time 200 μL aliquots were removed and the fluorescence measured at excitation and emission wavelengths of 530 nm and 590 nm, respectively. Scaffolds which were not cultured with cells were also incubated with Alamar blue™ working solution and the resulting fluorescence used as a control. The relative viability per cell for OMCs within the constructs was determined by normalising the total relative viability with respect to the number of cells within the scaffolds.

5.2.4.b Biochemical analyses and assessment of increase in construct weight

Following analysis for total relative viability, scaffolds were washed three times with PBS. Scaffolds were transferred to pre-weighed Eppendorf tubes and re-weighed in order to allow calculation of the construct wet weight. Scaffolds were lyophilised and re-weighed so that a "dry weight" for each construct could be obtained. The percentage increase in construct weight was determined using the equation given in Appendix 3.6. Samples were digested using papain, as outlined in Section 2.2.6.b. Following overnight incubation, samples were allowed to cool and aliquots taken for DNA, GAG and collagen assays.

5.2.4.b.i Assessment of cell number

The total cell number for each construct was determined using the Hoechst 33258 assay. The assay was performed as in Section 2.2.6.c. The number of cells within each construct was determined and normalised with respect to the mass of the constructs (Appendix 3.7).

5.2.4.b.ii Assessment of GAG content

The DMMB assay was used to quantify the GAG content of each construct according to the procedure outlined in Section 2.2.6.e. The GAG content for each sample was calculated using the equation given in Appendix 3.1.

5.2.4.b.iii Assessment of total collagen content

The total collagen content of each sample was assessed using the hydroxyproline assay (Section 2.2.6.f) and calculated using the equation given in Appendix 3.2.

5.2.4.c Histological analysis

Prior to histological examination, samples were fixed in 4% paraformaldehyde at 4°C (Appendix 2.5.4).

5.2.4.c.i Resin embedding constructs

Constructs were processed, embedded in Technovit 8100 resin and sectioned as described in Section 2.2.7.c.

5.2.4.c.ii Safranin O staining

Sections were stained with safranin O as outlined in Section 2.2.7.d.ii. Following staining, sections were mounted and imaged using an inverted microscope.

5.2.4.d Live/Dead™staining and confocal microscopy

Prior to staining with Live/Dead™ stain, scaffolds were washed three times with Dulbecco's PBS (DPBS). Scaffolds were incubated with Live/Dead™ working solution (Appendix 2.7.1) for 30 minutes. Following the incubation period, scaffolds were cut through the sagittal plane (Figure 2.8) and mounted on glass microscope slides with DABCO mountant (Appendix 2.7.2) such that images could be obtained from both the surface and centre of constructs. The Live/Dead™ assay works on the principle that live cells have ubiquitous intracellular esterase activity which allows enzymatic conversion of calcein AM to calcein. The second component of the stain, ethidium homodimer, is able to penetrate the compromised membranes of non-viable cells and upon binding to nucleic acids its fluorescence is enhanced, allowing the presence of dead (red) cells to be detected. Viable and non viable cells can therefore be distinguished on the basis of colour with live cells appearing green and dead cells appearing red.

Scaffolds were imaged using a laser scanning confocal microscope (Leica TCS4D system with a Leica DMRBE upright fluorescence microscope and an argon krypton laser) by Dr Susan Anderson and Mr Ian Ward (School of Biomedical Sciences, University of Nottingham). The green fluorescence of calcein was excited using the 488 nm laser line and the red fluorescence of ethidium homodimer was excited with the 568 nm laser line.

5.2.5 Analyses of native ovine cartilage

To allow comparison between the tissue-engineered cartilage and native cartilage, samples of ovine articular and meniscal cartilage were analysed with respect to biochemical composition and histological appearance.

5.2.5.a Isolation and preparation of ovine cartilage

5.2.5.a.i Isolation and preparation of ovine meniscal cartilage

Ovine meniscal cartilage was isolated as described in Section 2.2.2.b. Tissue was prepared for biochemical analysis as outlined in Section 2.2.6.a.i. Samples of ovine meniscal cartilage were reserved for histological evaluation and prepared as described in Section 2.2.7.a.

5.2.5.a.ii Isolation and preparation of ovine articular cartilage

Ovine articular cartilage was isolated using the method described in Section 2.2.2.c. Samples of tissue were taken for biochemical and histological assessment and prepared as described in Sections 2.2.6.a.ii and 2.2.7.a.

5.2.5.b Biochemical analyses of ovine cartilage

Samples of ovine meniscal and articular cartilage were digested with papain in preparation for biochemical analysis as outlined in Section 2.2.6.b. Samples of both articular and meniscal cartilage were taken from 6 different animals.

5.2.5.b.i Assessment of number of cells in cartilage samples

The Hoechst 33258 assay was used to determine the DNA content of cartilage samples and carried out using the method given in Section 2.2.6.c.

The DNA content of samples was related to number of cells using a standard curve of cell number versus fluorescence for the appropriate cell type. The number of cells per gram dry sample weight was determined using the equation given in Appendix 3.7. The statistical significance between the cellularity of the samples was assessed using GraphPad InStat version 3.0 (GraphPad Software Inc, San Diego, USA). Results were expressed as mean ± SEM. An unpaired, two-tail t-test was performed and since the standard deviations of the two samples were not equal a Welch correction was applied.

5.2.5.b.ii Determination of the GAG content of cartilage samples

The GAG content of samples of each of the cartilage types was determined using the DMMB assay (Section 2.2.6.e). Statistical analysis of the results was carried out as described in Section 5.2.5.b.i.

5.2.5.b.iii Quantification of the total collagen content of cartilage samples

The total collagen content of ovine meniscal and articular cartilage samples was quantified using the hydroxyproline assay (Section 2.2.6.f). Statistical analysis of the results was carried out as described in Section 5.2.5.b.i.

5.2.5.c Histological assessment of ovine cartilage samples

Ovine meniscal and articular cartilage samples were embedded in paraffin, sectioned and stained as described in Sections 2.2.7.a and 2.2.7.b.

5.2.6 Statistical analysis

The statistical significance of results was assessed using GraphPad InStat version 3.0 (GraphPad Software Inc, San Diego, USA). Results were expressed as mean ± SEM. An ANOVA and the Tukey-Kramer Multiple Comparisons post-test were performed. Results were considered significant when $P<0.05$ (*), very significant when $P<0.01$ (**) and extremely significant when $P<0.001$ (***).

5.3 Results

5.3.1 Increase in construct weight

The increase in the weight of the constructs was determined as outlined in Section 5.2.4.b. Figure 5.2 shows the percentage increase in construct weight following 8-week culture for both NF and SK4 scaffolds cultured in either static 6-well plates or the RCCS™. The weight of all scaffolds increased over the eight week period compared to the weight of the respective constructs after 4-week culture (Table 5.1). The percentage increase in construct weights was similar for both scaffold types under the different culture conditions; both scaffold types showing approximately a 40% increase in weight following static culture and a 68% increase following RCCS™ culture. For SK4 scaffolds, the increase in weight for constructs cultured within the RCCS™ was significantly greater than that of those cultured statically ($P<0.001$, Figure 5.2).

5.3.2 Cell content

The number of cells per gram of dry construct weight was determined as described in Section 5.2.4.b.i. A graph representing the number of cells in NF and SK4 scaffolds following 8-week static and RCCS™ culture is given in Figure 5.3. NF scaffolds contained a similar number of cells relative to the construct weights following both static and RCCS™ culture. SK4 scaffolds were also composed of a similar number of cells regardless of their culture environment. The cellularity of NF scaffolds cultured in the RCCS™ for 8 weeks was found to be significantly greater than that of SK4 scaffolds following 8-week RCCS™ culture ($P<0.01$, Figure 5.3). The overall cellularity of the constructs was lower than the respective constructs following 4-week culture, although the decreases were not significant (Table 5.1). The cell content of ovine articular and meniscal cartilage is shown in Figure 5.4. It was found that articular cartilage contained more cells than meniscal cartilage ($P<0.05$, Figure 5.4). While the cellularity of NF constructs was similar to that of native articular cartilage, the cellularity of SK4 constructs was more similar to that of native meniscal cartilage (Table 5.2).

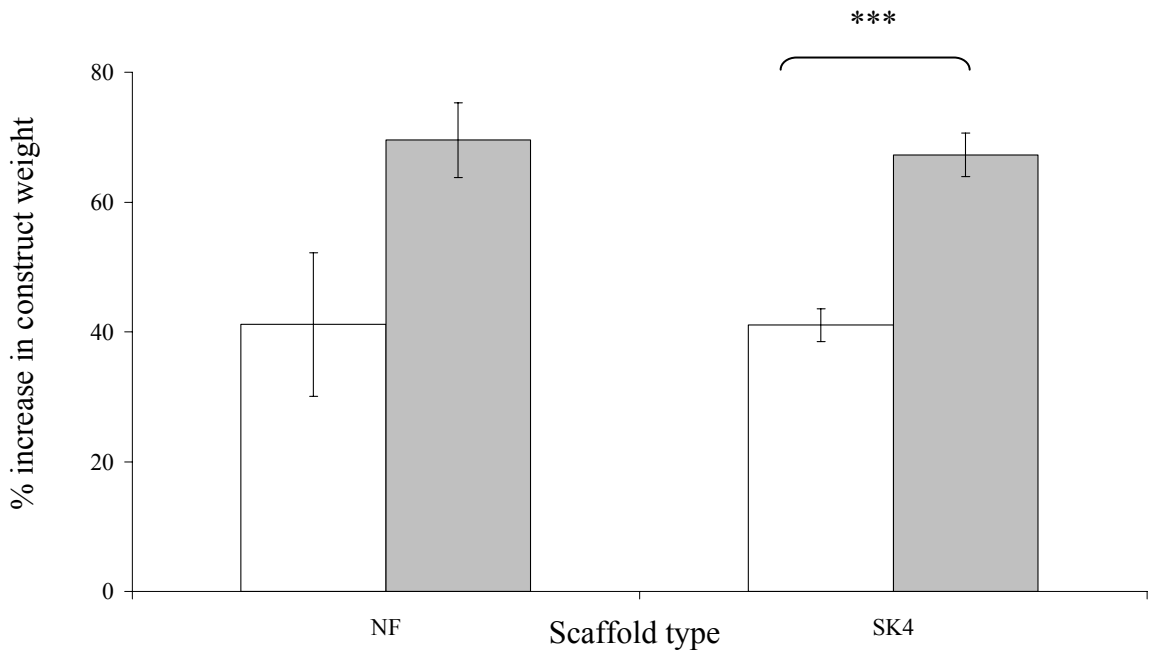

Figure 5.2 Comparison of the % increase in the weight of NF and SK4 scaffolds following 8-week □ static or ▨ RCCS™ culture. Results expressed as mean (n=6) ± SEM (*** indicates P<0.001).

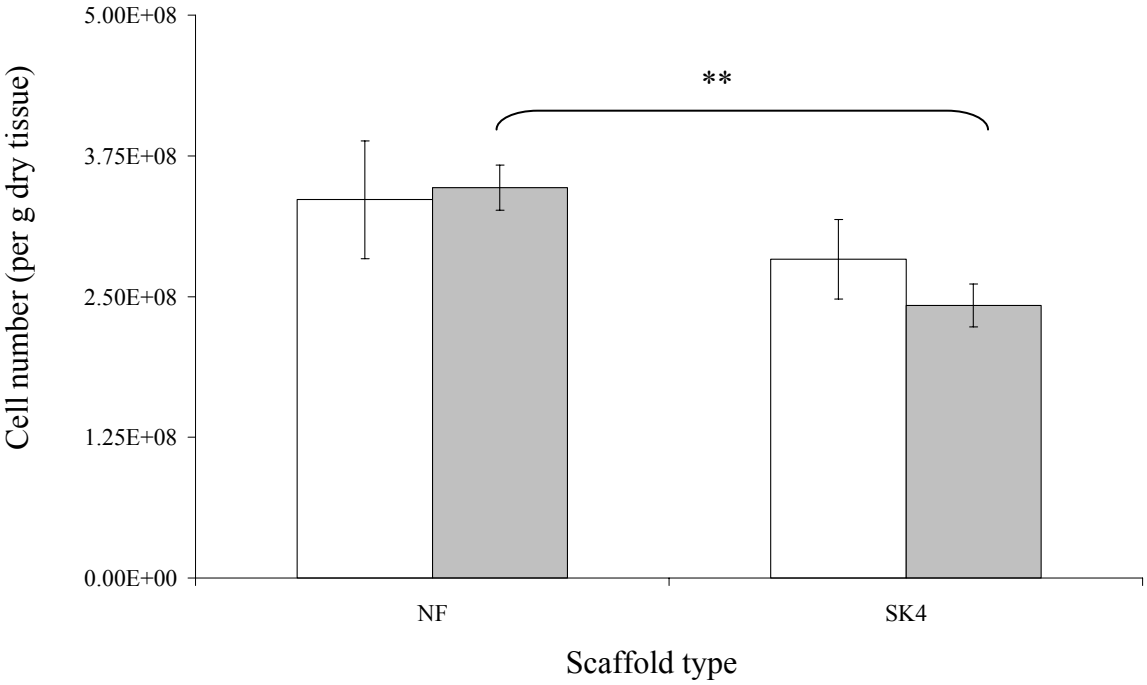

Figure 5.3 Comparison of the number of cells (per gram construct weight) in NF and SK4 scaffolds following 8-week ☐ static or ▩ RCCS™ culture. Results expressed as mean (n=6) ± SEM (** indicates P<0.01).

Scaffold type / Culture environment	**% increase in weight** n=6 ± SEM		**Cell number (per g dry construct)** n=6 ± SEM		**GAG content (% dry construct)** n=6 ± SEM		**Collagen content (% dry construct)** n=6 ± SEM	
	4 week	8 week	4 week	8 week	4 week	8 week	4 week	8 week
NF static	17.4 % ± 6.2 %	41.1 % ± 11.0 %	$8.9 \times 10^8 \pm 2.4 \times 10^7$	$3.4 \times 10^8 \pm 5.2 \times 10^7$	5.4 % ± 0.7 %	12.3 % * ± 1.3 %	0.6 % ± 0.1 %	5.6 % * ± 1.0 %
NF RCCS™	35.5 % ± 8.4 %	69.5 % * ± 5.7 %	$9.5 \times 10^8 \pm 1.6 \times 10^8$	$3.5 \times 10^8 \pm 2.0 \times 10^7$	12.9 % ± 0.9 %	12.5 % ± 0.6 %	2.8 % ± 0.4 %	10.7 % *** ± 0.3 %
SK4 static	35.1 % ± 5.2 %	41.1 % ± 2.5 %	$5.2 \times 10^8 \pm 1.5 \times 10^8$	$2.8 \times 10^8 \pm 3.6 \times 10^7$	4.7 % ± 0.4 %	11.8 % *** ± 0.7 %	0.5 % ± 0.1 %	4.0 % *** ± 0.3 %
SK4 RCCS™	55.7 % ± 7.7 %	67.3 % ± 3.4 %	$6.7 \times 10^8 \pm 5.7 \times 10^7$	$2.4 \times 10^8 \pm 1.9 \times 10^7$	11.3 % ± 0.1 %	10.1 % ± 1.5 %	2.2 % ± 0.7 %	8.1 % *** ± 0.3 %

Table 5.1 Comparison of the increase in weight and biochemical composition of constructs following 4- and 8-week culture. Asterisks indicate significant differences between 4 and 8 week data (* $P<0.05$, ** $P<0.01$ and *** $P<0.001$).

Tissue component	Ovine meniscal cartilage	Ovine articular cartilage	NF static construct	NF RCCS construct	SK4 static construct	SK4 RCCS construct
Cell number (per g dry weight) ± SEM	$2.3 \times 10^8 \pm 1.1 \times 10^7$	$3.5 \times 10^8 \pm 5.6 \times 10^7$	3.4×10^8 ** $\pm 5.2 \times 10^7$	3.5×10^8 *** $\pm 2.0 \times 10^7$	2.8×10^8 * $\pm 3.6 \times 10^7$	$2.4 \times 10^8 \pm 1.9 \times 10^7$
GAG content (% dry weight) ± SEM	5.9 % ± 0.5 %	12.6 % ± 2.3 %	12.3 % *** ± 1.3 %	12.5 % *** ± 0.6 %	11.8 % *** ± 0.7 %	10.1 % ** ± 1.5 %
Collagen content (% dry weight) ± SEM	17.0 % ± 0.9 %	9.1 % ± 2.3 %	5.6 % *** ± 1.0 %	10.7 % *** ± 0.3 %	4.0 % ***, ▲ ± 0.3 %	8.1 % *** ± 0.3 %

Table 5.2 Comparison of the biochemical composition of native ovine meniscal and articular cartilages with that of the 8-week tissue engineered constructs. Asterisks indicate significant differences between construct components and that of native tissue (* for differences compared to meniscal cartilage and ▲ for differences compared to articular cartilage; * (▲) $P<0.05$, ** $P<0.01$ and *** $P<0.001$).

5.3.3 GAG content

The GAG content of constructs was assessed using the method given in Section 5.2.4.b.ii and is shown in Figure 5.5. The GAG content of all constructs was similar, regardless of scaffold type or culture environment. Whilst the GAG content of scaffolds cultured in the RCCS™ for 4 or 8 weeks was not significantly different, a significant increase was seen in the GAG contents of NF and SK4 scaffolds cultured statically ($P<0.05$ and $P<0.001$ respectively, Table 5.1). Figure 5.6 shows the GAG content of samples of ovine articular and meniscal cartilage. No significant difference was detected between the GAG content of each of the constructs and that of native ovine articular cartilage, whereas the difference between that of each of the constructs and native ovine meniscal cartilage was considered very significant ($P<0.01$ for SK4 RCCS™ and $P<0.001$ for all other constructs, Table 5.2).

5.3.4 Total collagen content

The total collagen content of NF and SK4 scaffolds following 8-week static and RCCS™ culture was determined as outlined in Section 5.2.4.b.iii. Figure 5.7 shows a graphical representation of this data. For both NF and SK4 constructs, the collagen content of scaffolds cultured within the RCCS™ was significantly greater than that of those scaffolds cultured within static 6-well plates ($P<0.01$ and $P<0.001$ for NF and SK4 scaffolds respectively, Figure 5.7). In addition, the collagen content of NF scaffolds cultured within the RCCS™ was significantly greater than the collagen content of SK4 scaffolds cultured in the same way ($P<0.01$, Figure 5.7). For all scaffold type and culture system combinations the collagen content significantly increased between constructs cultured for 4 weeks and those cultured for 8 weeks ($P<0.05$ for SK4 RCCS™ and $P<0.001$ for all other constructs, Table 5.1). The collagen content of native ovine articular and meniscal cartilage was determined and is shown in Figure 5.8. The collagen content of all constructs was significantly lower than that of native ovine meniscal cartilage ($P<0.001$, Table 5.2) and with the exception of SK4 scaffolds which were cultured statically, there was no significant difference between the total collagen content of each of the constructs and native ovine articular cartilage (Table 5.2).

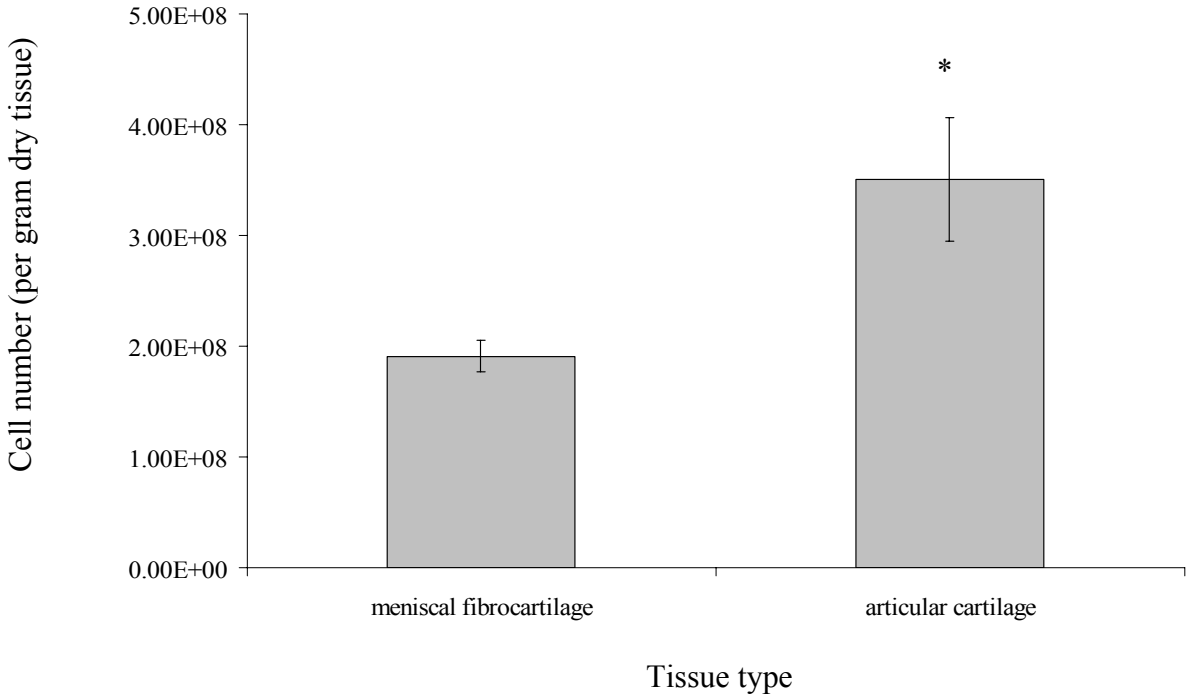

Figure 5.4 The cell content of ovine meniscal and articular cartilage samples. Results expressed as mean (n=6) ± SEM (* indicates $P<0.05$).

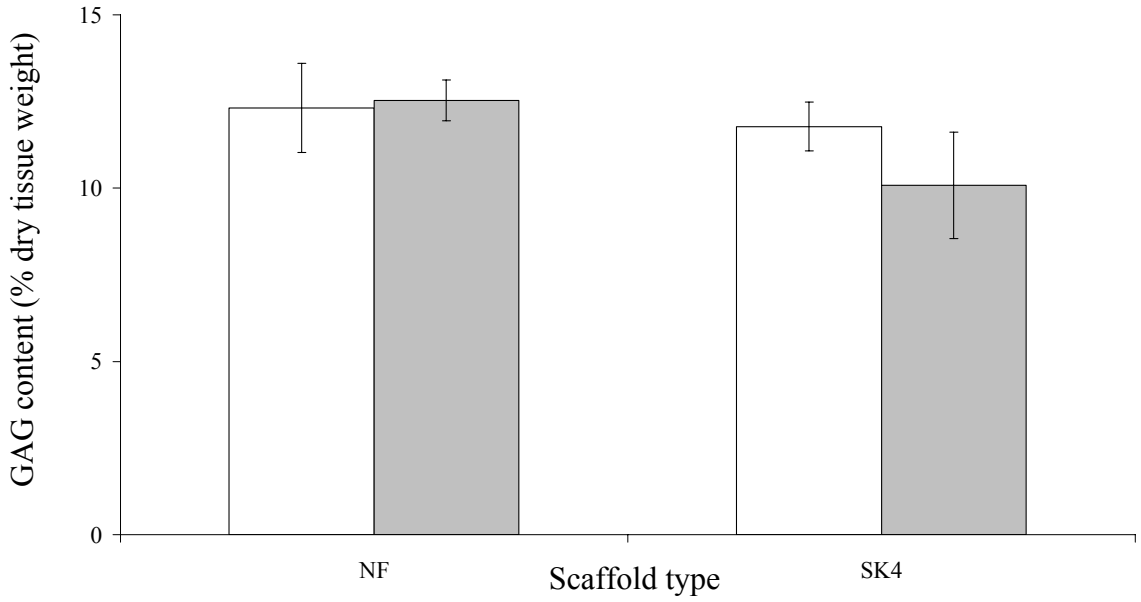

Figure 5.5 Comparison of the GAG content of NF and SK4 scaffolds following 8-week ☐ static or ▩ RCCS™ culture. Results expressed as mean (n=6) ± SEM.

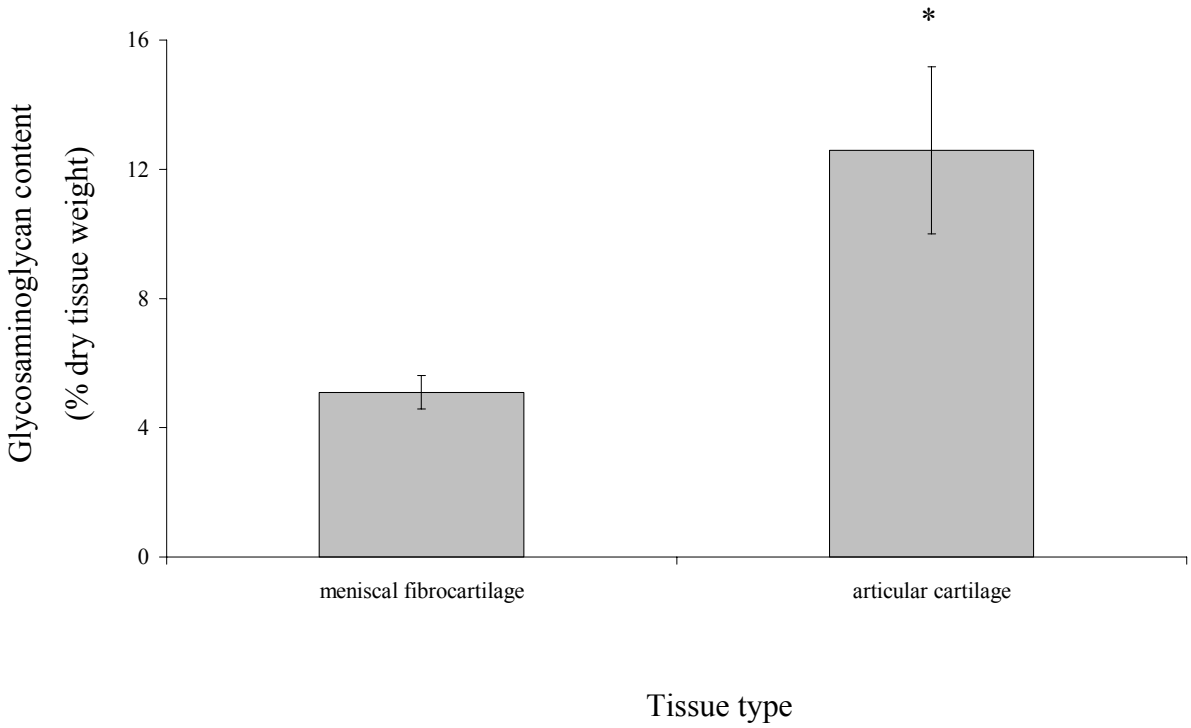

Figure 5.6 The glycosaminoglycan content of ovine meniscal and articular cartilage samples. Results expressed as mean (n=6) ± SEM (* indicates $P<0.05$).

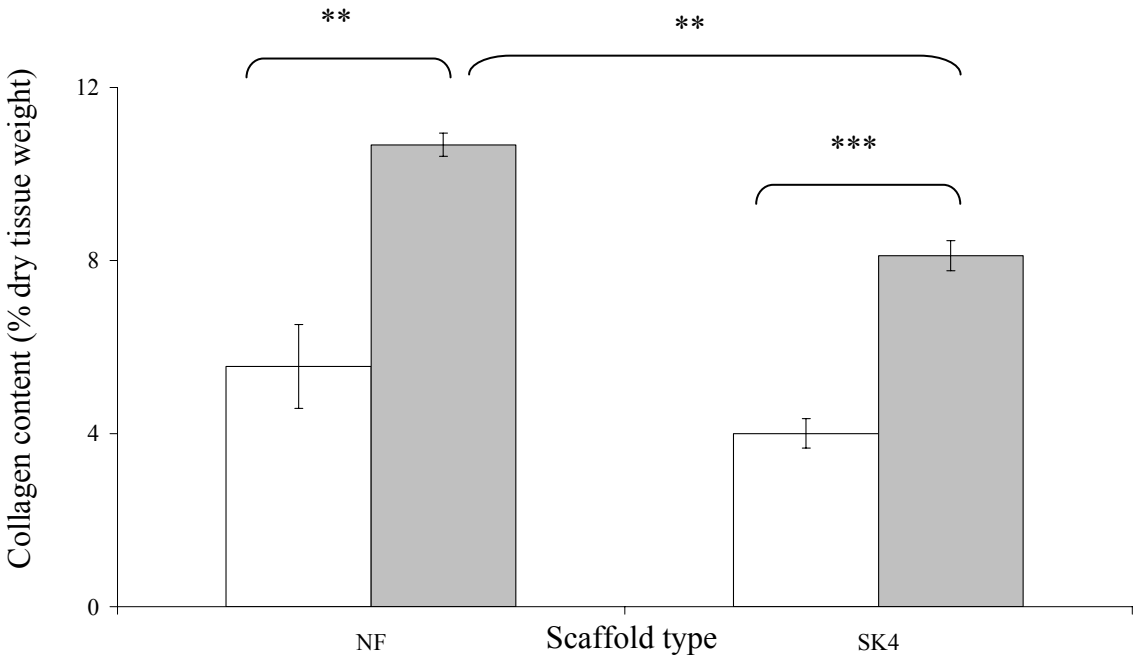

Figure 5.7 Comparison of the collagen content of NF and SK4 scaffolds following 8-week □ static or ▩ RCCS™ culture. Results expressed as mean (n=6) ± SEM (** indicates P<0.01, *** indicates P<0.001).

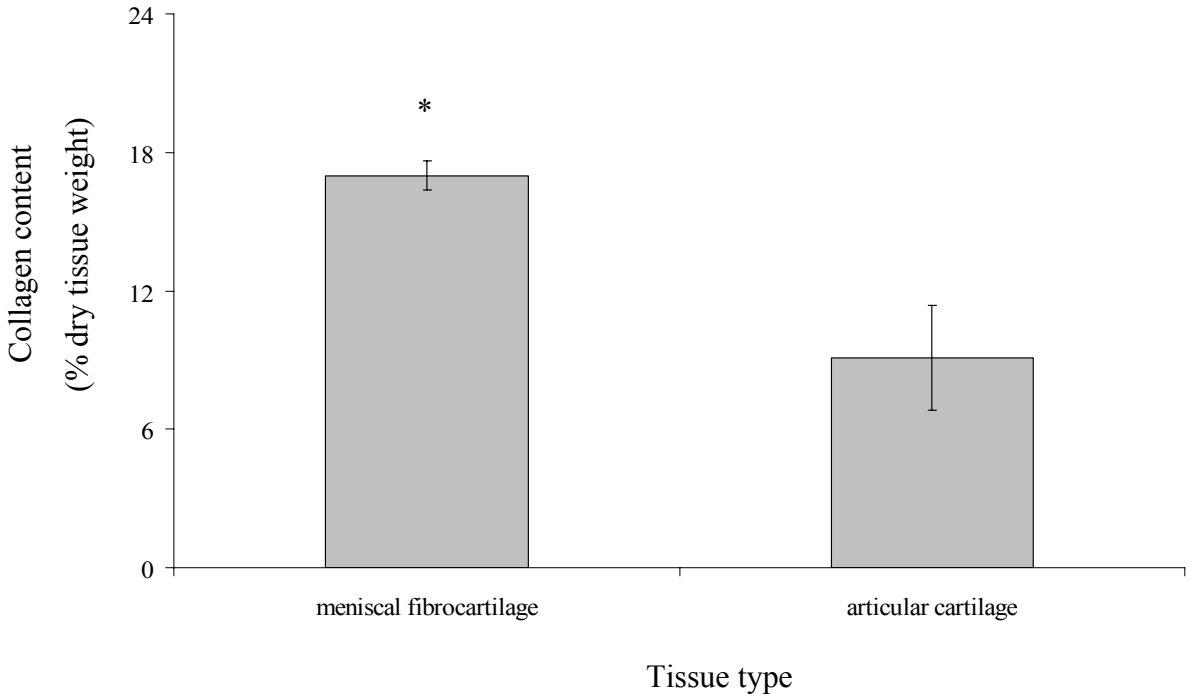

Figure 5.8 The collagen content of ovine meniscal and articular cartilage samples. Results expressed as mean (n=6) ± SEM (* indicates $P<0.05$).

5.3.5 Safranin O staining

Samples of each of the constructs were fixed in 4% paraformaldehyde, embedded in Technovit 8100 resin and sectioned as described in Section 5.2.4.c. Sections taken through the surface and central regions of the scaffolds were stained with safranin O as outlined in Section 5.2.4.c.ii. Representative images of sections taken from each of the different constructs are shown in Figures 5.9, 5.10 and 5.11. More cells were visible in NF scaffolds following 8 week RCCS™ culture than static culture (Figure 5.9). In general, more cells appeared to be present at the surface of statically cultured NF scaffolds than in the centre (Figure 5.9 C & D). More cells were also visible in SK4 scaffolds following 8-week RCCS™ culture, compared to static culture (Figure 5.10). Cells in SK4 scaffolds cultured within the RCCS™ appeared to be evenly distributed throughout the constructs (Figure 5.10 A & B). The cells within the central region of these constructs were present not only within the bundles of fibres but also the aligned channels, suggesting that matrix had filled the spaces between the spacer fibres (Figure 5.10 B). Statically cultured SK4 scaffolds also contained evenly distributed cells (Figure 5.10 C & D) and cells present within both the spacer fibres and aligned channels (Figure 5.10 D). Figure 5.11 shows a summary of representative sections from all constructs. NF and SK4 scaffolds cultured within the RCCS™ for 8 weeks were similar in appearance with more intense safranin O staining than respective scaffolds cultured within static 6-well plates (Figure 5.11). The histological appearance of native cartilage samples are shown in Figure 5.12. Within both cartilage types, chondrocytes (visible by positive haematoxylin staining) were contained within lacunae (highlighted with arrows in Figure 5.12). The fibrous nature of meniscal cartilage is visible (Figure 5.12 A & B). Less intense safranin O staining was observed in meniscal samples as a result of the lower GAG content of this tissue (Figure 5.12 B & D). The stratified structure of articular cartilage was clearly visible with fewer cells present at the subchondral region of the tissue and chondrocytes arranged in columns in the central region (Figure 5.12 C). The difference in more intense staining in sections of native tissue compared tissue engineered constructs may be due to the greater permeability of the tissue to stain compared to the resin in which the constructs were embedded.

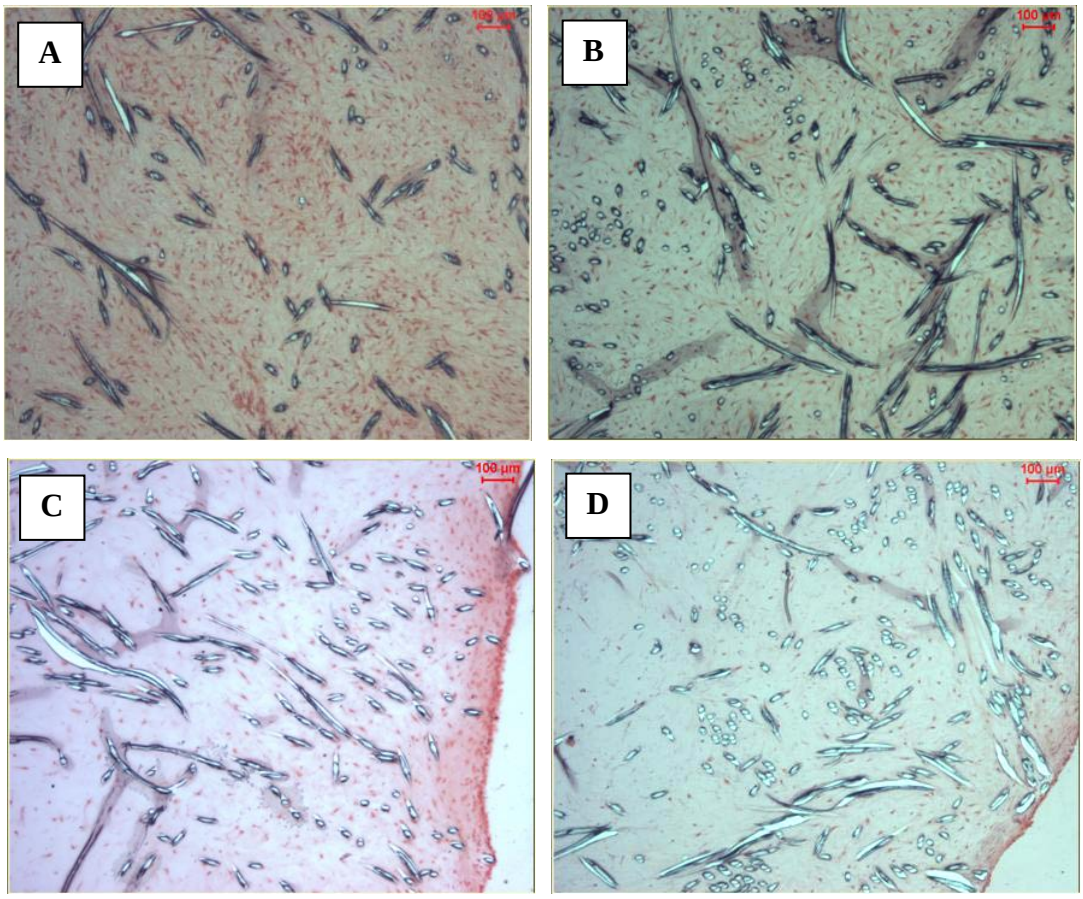

Figure 5.9 Representative images of haematoxylin and safranin O stained sections through NF scaffolds following 8 week (A and B) RCCS™ and (C and D) static culture. Images show (A and C) sections taken through the surface and (B and D) the centre of constructs. Scale bars represent 100 µm.

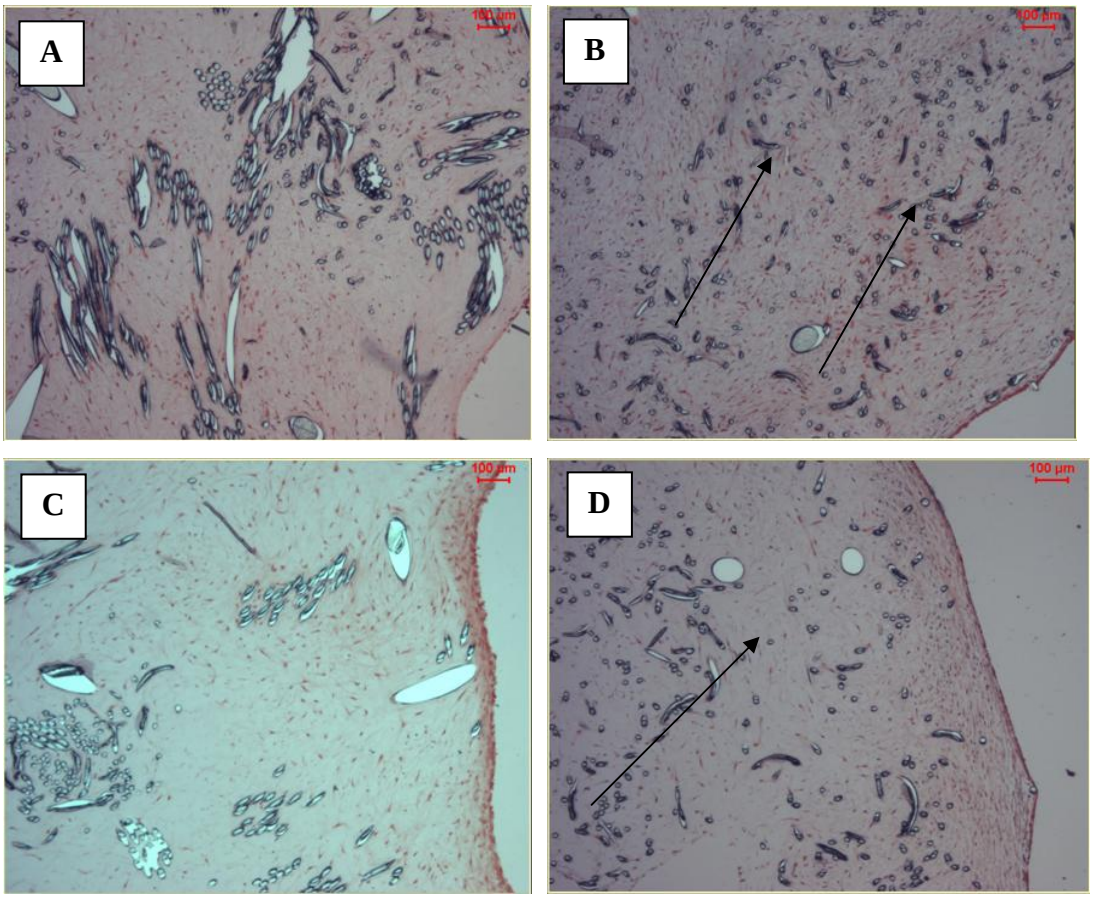

Figure 5.10 Representative images of haematoxylin and safranin O stained sections through SK4 scaffolds following 8 week (A and B) RCCS™ and (C and D) static culture. Images show (A and C) sections taken through the surface and (B and D) the centre of constructs. Scale bars represent 100 µm. Arrows indicate the aligned bundles of fibres.

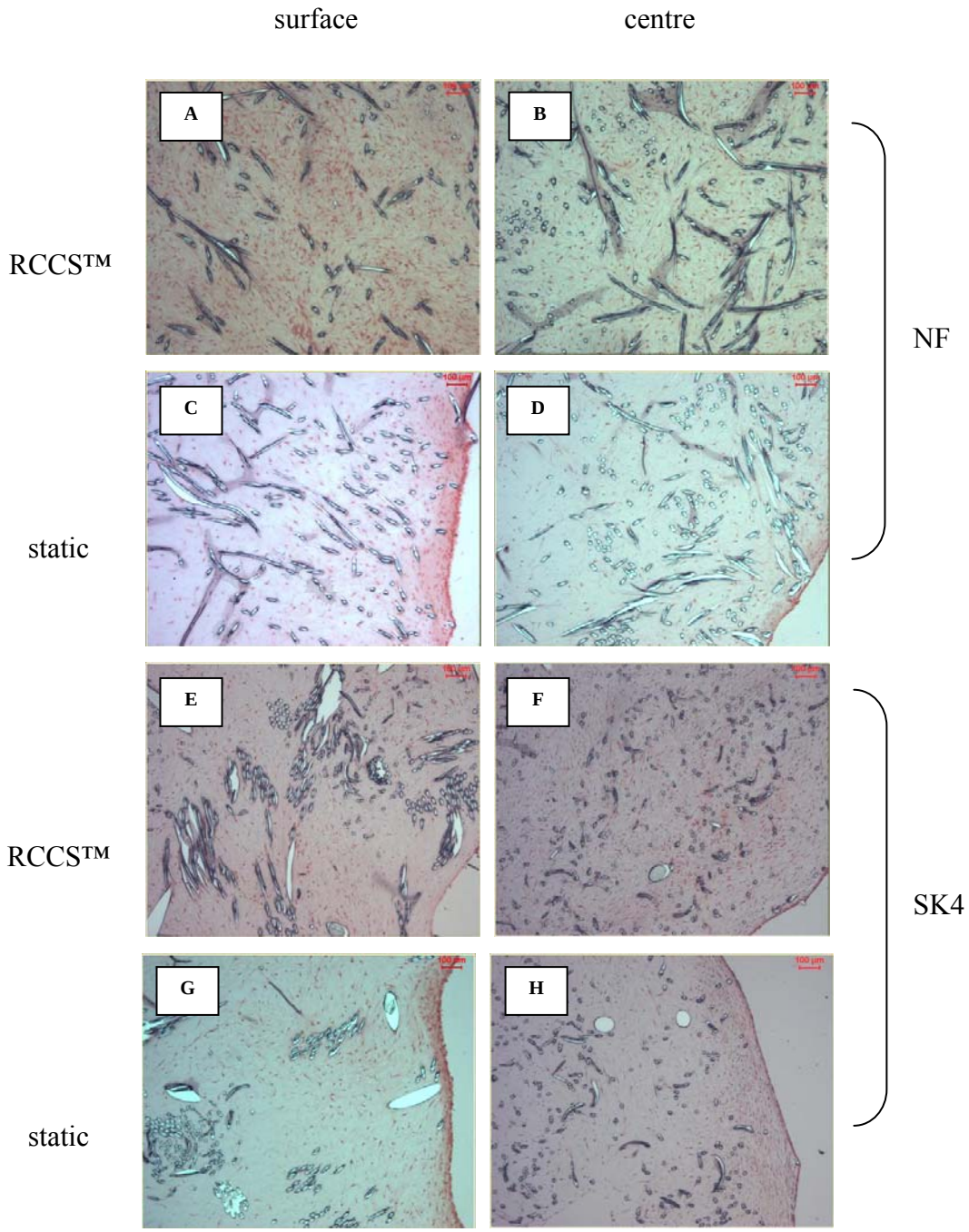

Figure 5.11 Representative images of haematoxylin and safranin O stained sections through all constructs following 8 week culture. Images A, B, C & D taken from NF scaffolds and images E, F, G & H taken from SK4 scaffolds. Sections taken through (A, C, E & G) the surface and (B, D, F & H) the centre of constructs. Scaffolds were cultured in either (A, B, E & F) the RCCS™ or (C, D, G & H) static 6 well plates. Scale bars represent 100 μm.

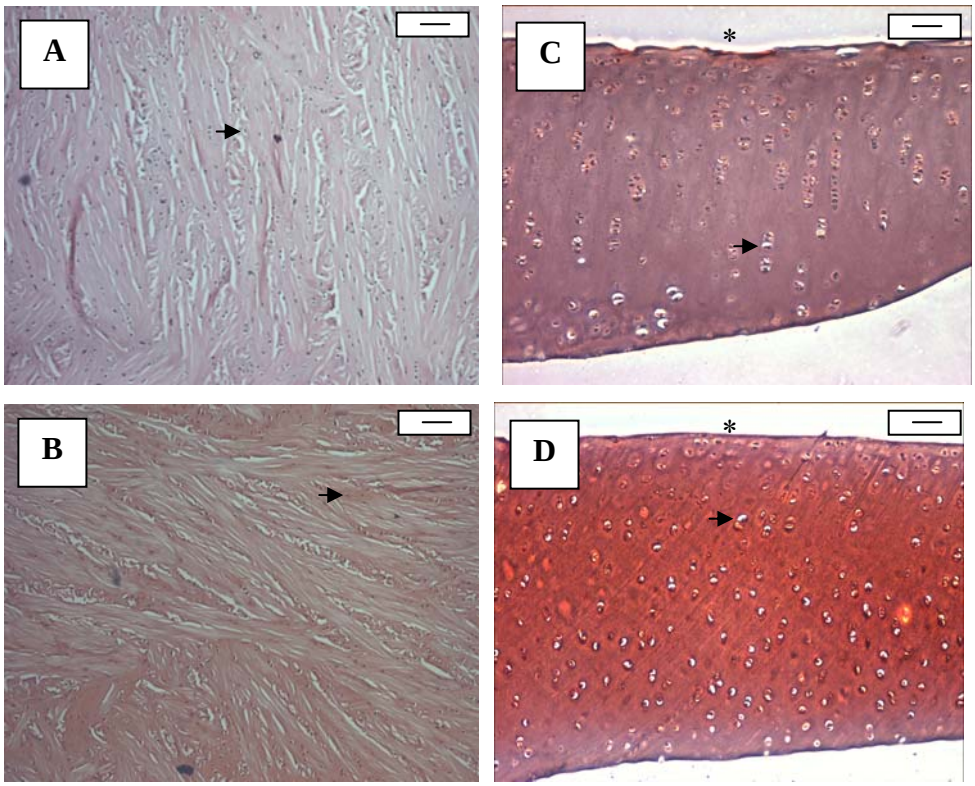

Figure 5.12 Representative images showing (A and B) meniscal and (C and D) articular cartilage samples following (A and C) haematoxylin and eosin and (B and D) safranin O staining. Asterisks (*) on articular cartilage samples indicate the articular surface of the tissue. Arrows (➔) on images highlight the presence of cells within lacunae. Scale bar represents 50 μm on images A and B and 200 μm on images C and D.

5.3.6 Relative cell viability

The total relative viability of cells within the constructs was determined using the Alamar blue assay, as outlined in Section 5.2.4.a. The total relative viability of cells within NF and SK4 scaffolds following 8-week static and RCCS™ culture is shown in Figure 5.13 A. The total relative viability of the constructs was not significantly different between the different scaffold types or culture environments. The relative viability per cell of OMCs within the different constructs was determined by normalising the total relative viability with respect to the number of cells within the scaffolds. Figure 5.13 B presents the viability per cell of OMCs within NF and SK4 scaffolds following 8-week culture in either static 6-well plates or the RCCS™. For both scaffold types, the relative viability per cell was greater for OMCs cultured in static conditions ($P<0.05$).

5.3.7 Live/Dead™ staining

In order to assess the distribution of viable and non viable cells within the different constructs following 8-week culture, scaffolds were stained with Live/Dead™ stain using the method described in Section 5.2.4.d. Representative images of each of the different constructs are shown in Figures 5.14, 5.15 and 5.16. NF scaffolds contained a mixed population of viable and non viable cells, as indicated by the presence of both red and green cells within constructs (Figure 5.14). In general, NF scaffolds cultured within the RCCS™ for 8 weeks contained more non viable cells at the surface than in the centre (Figure 5.14 A & B). The distribution of viable and non-viable cells at the surface of NF scaffolds was similar for constructs cultured in each of the systems (Figure 5.14 A & C). NF scaffolds cultured within static 6-well plates for 8 weeks contained a higher number of non viable cells at the centre than those cultured within the RCCS™ (Figure 5.14 B & D). SK4 scaffolds also contained a mixed population of live and dead cells (Figure 5.15). Fewer cells were detected in the centre of SK4 scaffolds cultured in the RCCS™ for 8 weeks, compared to at the surface of these constructs (Figure 5.15 A & B). SK4 scaffolds cultured within static plates for 8 weeks contained an even distribution of cells (Figure 5.15 C & D).

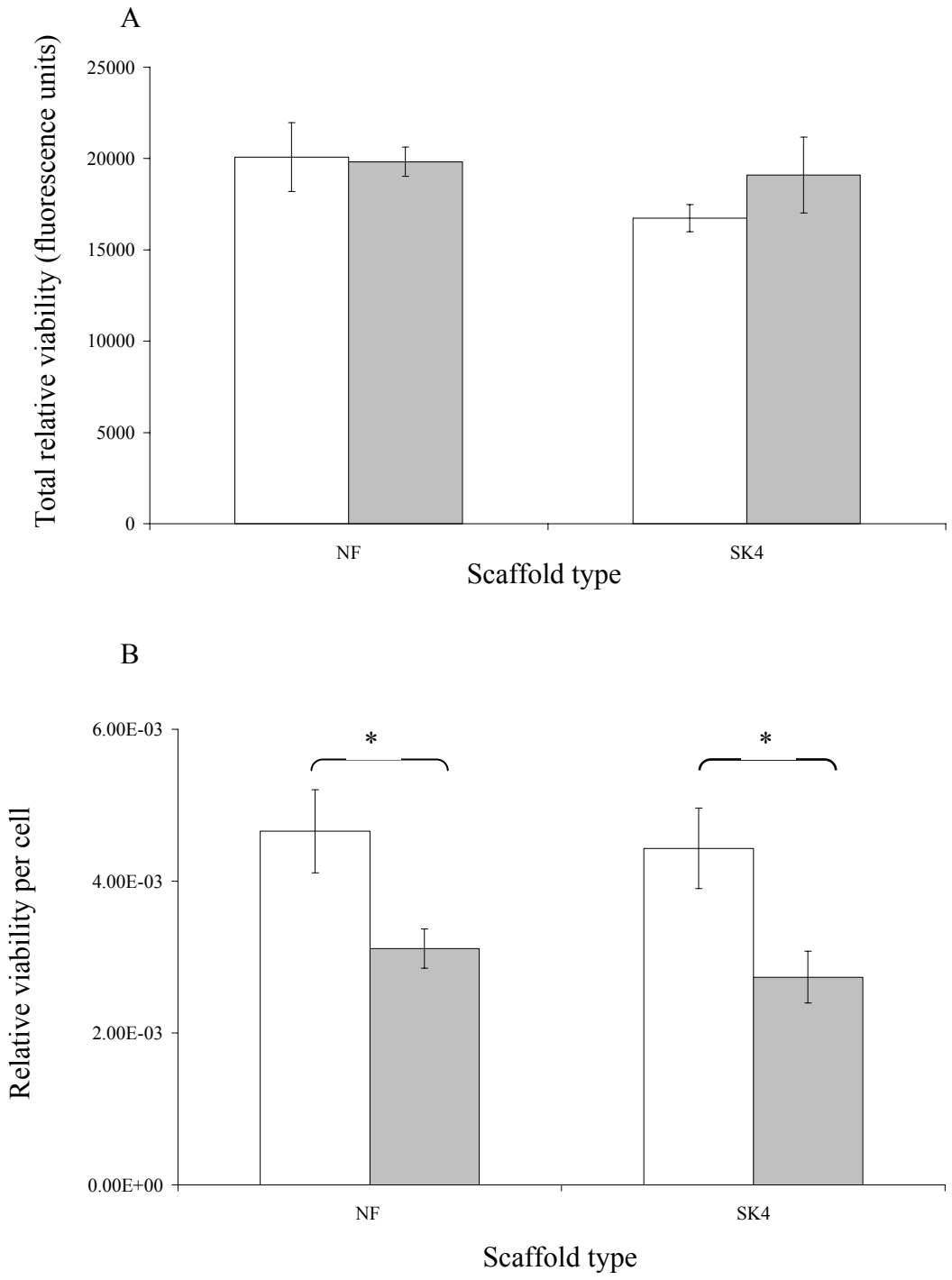

Figure 5.13 Comparison of (A) the total relative viability and (B) the relative viability per cell of OMCs in NF and SK4 scaffolds following 8-week □ static or ▩ RCCS™ culture. Results expressed as mean (n=6) ± SEM (* indicates $P<0.05$).

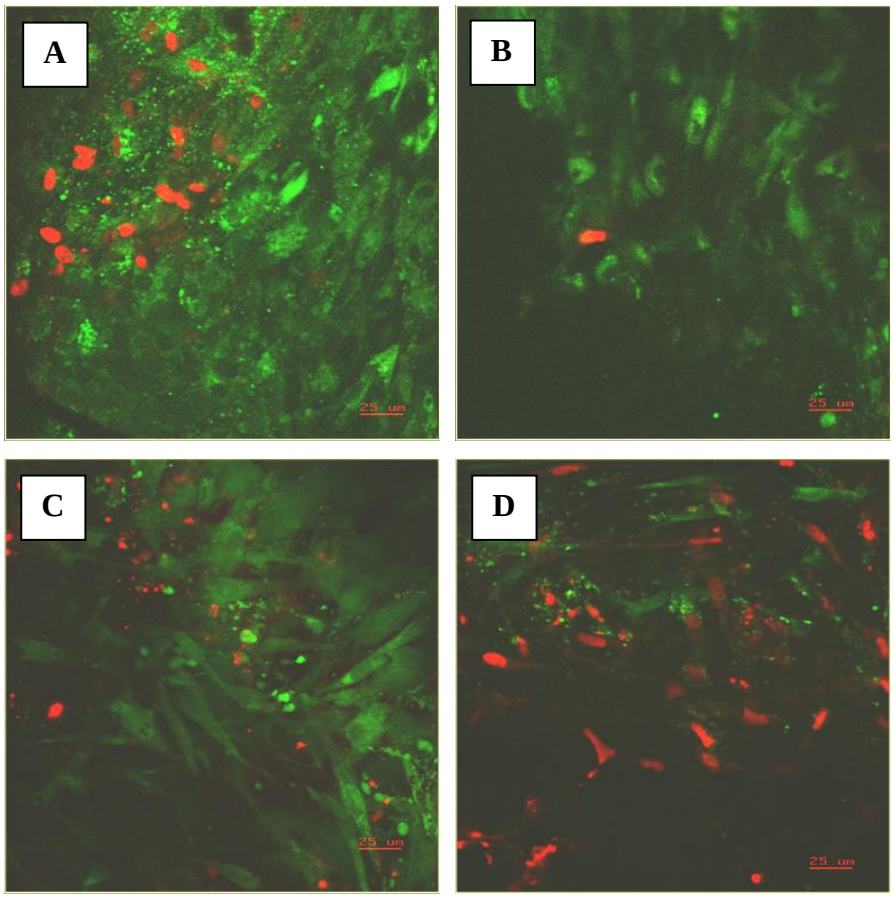

Figure 5.14 Representative images of NF scaffolds stained with Live/Dead™ stain following 8 week (A and B) RCCS™ and (C and D) static culture. Images show (A and C) images taken of the surface and (B and D) the centre of constructs. Scale bars represent 25 μm.

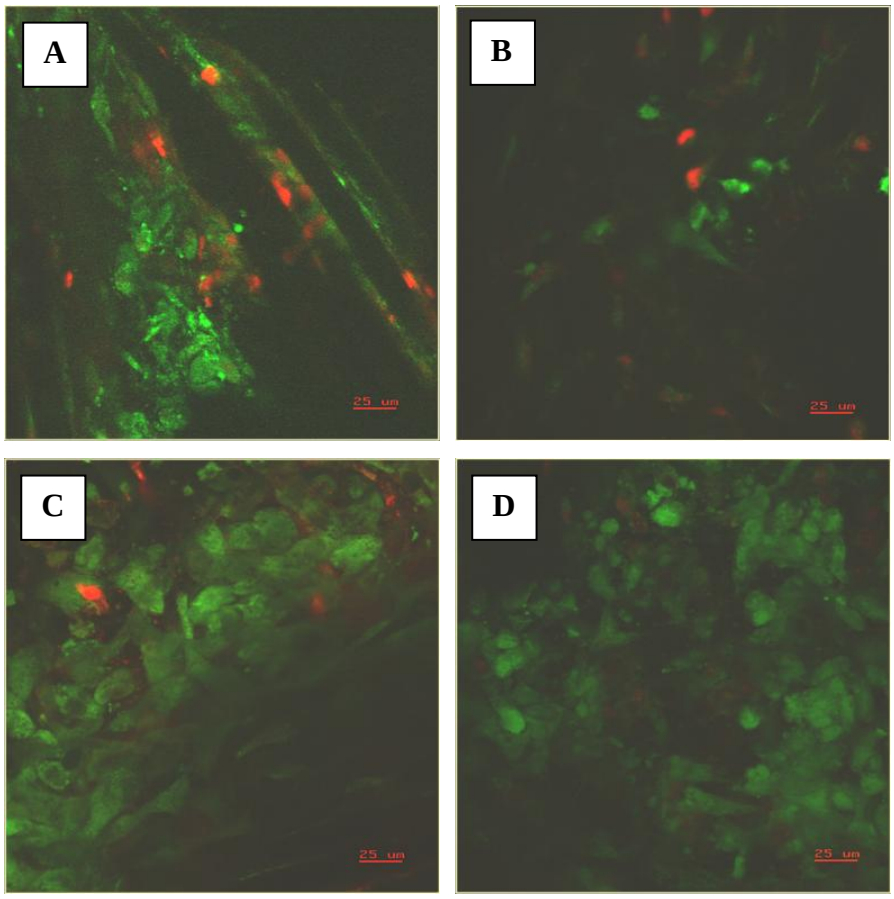

Figure 5.15 Representative images of SK4 scaffolds stained with Live/Dead™ stain following 8 week (A and B) RCCS™ and (C and D) static culture. Images show (A and C) images taken of the surface and (B and D) the centre of constructs. Scale bars represent 25 μm.

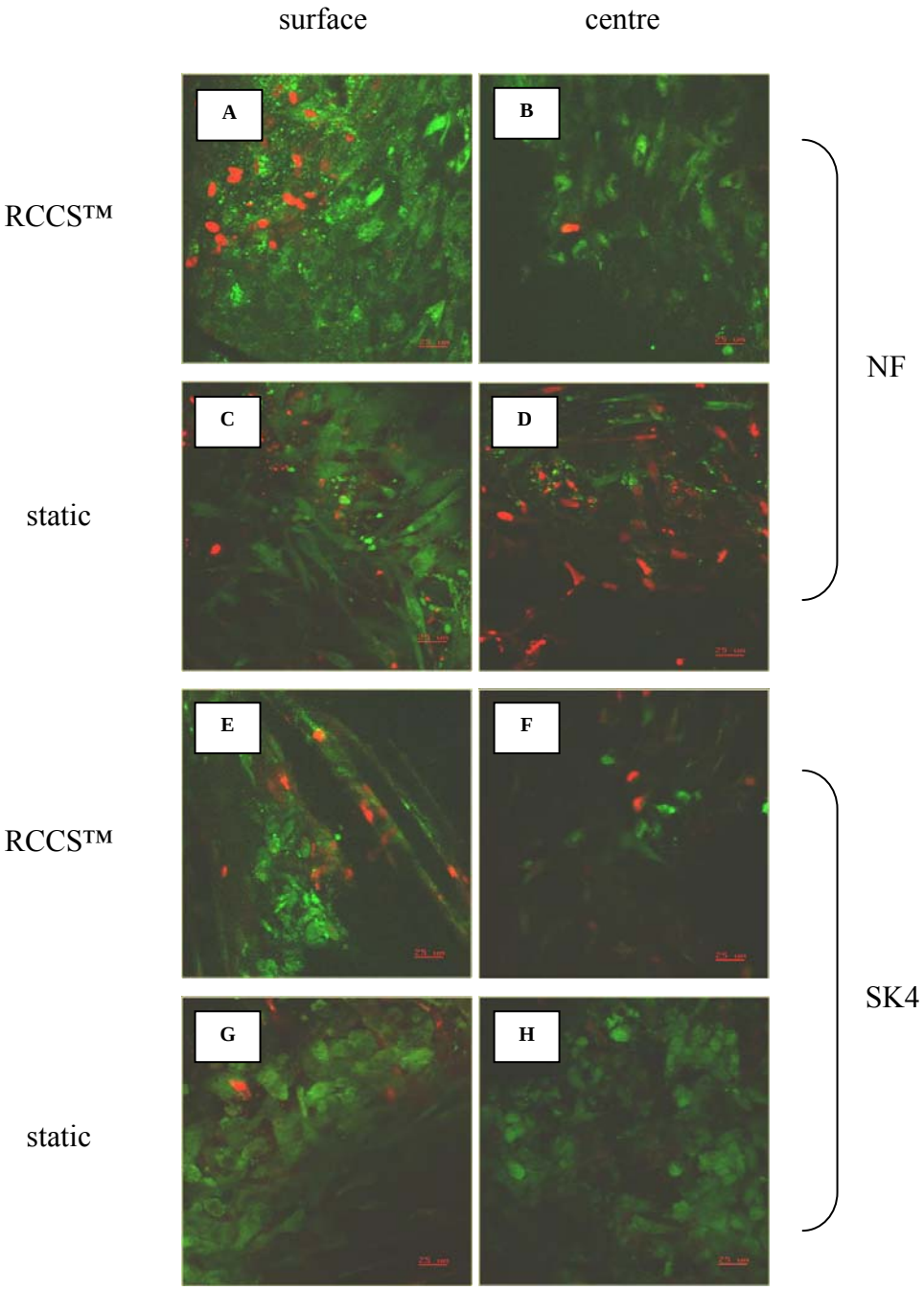

Figure 5.16 Representative images of scaffolds stained with Live/Dead™ stain following 8 week culture. Images A, B, C & D taken from NF scaffolds and images E, F, G & H taken from SK4 scaffolds. Sections taken through (A, C, E & G) the surface and (B, D, F & H) the centre of constructs. Scaffolds were cultured in either (A, B, E & F) the RCCS™ or (C, D, G & H) static 6 well plates. Micron bars represent 25 μm.

More viable cells were present at both the surface and centre of SK4 scaffolds following static culture, as compared to SK4 scaffolds cultured within the RCCS™ for 8 weeks (Figure 5.15). Figure 5.16 shows all the images from Figures 5.14 and 5.15 to allow comparison between the scaffold types. NF and SK4 scaffolds that were cultured within the RCCS™ for 8 weeks were similar in appearance with mixed populations of viable and non-viable cells throughout the constructs and generally more cells present at the surface than in the centre (Figure 5.16 A, B, E & F). More viable cells were present at the centre of SK4 scaffolds than NF scaffolds following 8-week static culture (Figure 5.16 D & H).

5.4 Discussion

The main aim of this thesis was to investigate whether scaffolds combining random and anisotropic porosity were advantageous for tissue engineering. The hypothesis was that these scaffolds would facilitate *in vitro* tissue regeneration by improving the supply of nutrients to the growing tissue. The aim of this chapter was to test this hypothesis by comparing the cartilage formed in these scaffolds following eight week culture in either static plates or RCCS™ culture with that formed in a random fibrous scaffold.

The increase in construct weight was shown to be affected by the culture environment but not scaffold architecture, with statically cultured constructs showing an increase of approximately 40% and those cultured in the RCCS™ showing an approximate increase of 68%. The cellularity of the constructs was assessed and found to differ slightly between scaffold types, with NF scaffolds containing more cells than SK4 scaffolds. With the exception of SK4 scaffolds which were cultured within the RCCS™ there was no significant difference between the cellularities of the constructs and that of native ovine articular cartilage. The biochemical composition of constructs was assessed with respect to total GAG and collagen content.

The GAG content of all constructs was similar, regardless of scaffold type or culture environment and was not found to differ significantly from that of native ovine articular cartilage. All constructs were, however, composed of a significantly greater proportion of GAGs than native meniscal tissue. It was also observed that the GAG content of statically cultured NF and SK4 scaffolds was found to increase significantly from week 4 to week 8. Positive safranin O staining, indicative of the presence of sulphated GAGs, was observed in all constructs, although it appeared more intense in RCCS™ cultured constructs. The total collagen content varied between NF and SK4 scaffolds cultured for 8 weeks in each of the culture systems. In general, scaffolds cultured within the RCCS™ contained more collagen than those cultured in static plates following 8-week culture. In addition, NF scaffolds contained more collagen than SK4 scaffolds following 8-week RCCS™ culture. The collagen content of all constructs increased significantly between weeks 4 and 8 and was found to be similar to that of native ovine articular cartilage following 8-week RCCS™ culture.

The viability of cells within the scaffolds was assessed using the Alamar blue™ and Live/Dead™ viability/cytotoxicity assays. The Alamar blue™ assay results indicated that the relative viability of OMCs in both NF and SK4 scaffolds was greater following static culture, suggesting that the dynamic culture system caused a decrease in cell viability, although this decrease in viability was not sufficient to prevent tissue formation by the cells. The Live/Dead™ assay allows visual distinction between viable and non viable cells. The distribution of live and dead cells was found to be similar for both scaffold types following 8-week RCCS™ culture. The greatest observed difference was in the viability of cells at the centre of constructs cultured for 8 weeks in static plates. Whilst both live and dead cells were present at the centre of NF scaffolds, a higher number of cells, of which the majority were viable, were present at the centre of SK4 scaffolds.

One of the current challenges of tissue engineering is that of satisfying the mass transfer requirements of the growing construct throughout its culture (Freed and Vunjak-Novakovic 1998).

Woodfield and co-workers have previously emphasised the importance of using advanced scaffold designs which take into account the mass transport requirements of tissue engineered constructs the size of tissue defects (Woodfield *et al* 2002 and Malda *et al* 2004). It was hypothesised that scaffolds with a novel architecture combining random and anisotropic porosity would be advantageous for tissue engineering since the presence of wider aligned channels within the porous network would facilitate the mass transport of nutrients to and removal of waste products from the growing tissue. The results presented in this chapter demonstrated that cartilaginous tissue with a similar biochemical composition was generated in SK4 and NF scaffolds following 8-week culture in the RCCS™. As shown in Table 1.2, non woven fibrous scaffolds have been used in many tissue engineering studies. Scaffolds with the same architecture as the NF scaffolds used in the studies presented in this thesis have supported attachment of different cell types, for example bovine articular chondrocytes and embryonic chick bone marrow stromal cells, and subsequent extracellular matrix production (Freed *et al* 1993b and Martin *et al* 1998). Rotating wall bioreactors such as the RCCS™ have been found to be highly efficacious for *in vitro* cartilage engineering. In a study by Pei and colleagues, constructs cultured within the RCCS™ were thicker and contained more evenly distributed GAGs than constructs cultured in static plates (Pei *et al* 2002). The findings of this study that 8-week RCCS™ culture supported chondrogenesis in NF scaffolds is therefore in agreement with those reported from other studies. It was found that the tissue formed in SK4 scaffolds following 8-week RCCS™ was similar to that formed in NF scaffolds cultured under the same conditions, indicating that the novel scaffold architecture did not have a detrimental effect on *in vitro* tissue formation. The supply of nutrients to cells within a tissue engineering scaffold *in vitro* is controlled largely by diffusion (Freed and Vunjak-Novakovic 1998). In dynamic culture systems, such as the RCCS™, fluid motion within the system increases the mass transfer of nutrients to cells. The mass transfer of nutrients within static culture systems is, in contrast, limited (Freed *et al* 1994b).

This phenomenon has been used to explain why tissue engineered constructs obtained from static culture systems have generally been found to be inhomogeneous and contain lower quantities of ECM components than constructs obtained from dynamic culture systems (Freed *et al* 1994b and Pei *et al* 2002). In this study the viability of cells at the centre of scaffolds was assessed using Live/Dead™ staining. NF and SK4 scaffolds cultured within the RCCS™ contained similar distributions of viable and non-viable cells.

Following static culture, a large number of non-viable cells were present at the centre of NF scaffolds. This may be due to the limited supply of nutrients to the cells at the centre of these scaffolds. At the centre of SK4 scaffolds cultured within static plates, however, the majority of cells were found to be viable. This suggests that the presence of wider channels within the porous structure facilitated the supply of nutrients to the growing tissue in a non-ideal culture environment. The novel scaffold architecture combining random and anisotropic porosity therefore appears to be beneficial for *in vitro* tissue regeneration in culture systems usually less favourable with respect to nutrient mass transfer.

5.5 Conclusions

The work presented in this chapter shows that both the NF and SK4 scaffolds supported cartilage formation and that this tissue formation was facilitated by the commercially available RCCS™. It was also shown that in a less optimum culture environment where the supply of nutrients is a limiting factor for tissue regeneration, the novel scaffold architecture combining random and anisotropic porosity was advantageous.

Chapter 6
General Discussion and Conclusions

One of the challenges of engineering tissues *in vitro* is that of producing constructs of a clinically relevant size. A common phenomenon in tissue engineering studies is the formation of a capsule of tissue at the periphery of the construct, which restricts the supply of nutrients to the centre of the growing tissue, causing cell and tissue death (Freed *et al* 1999). There is therefore a need to improve the transfer of nutrients to the entire construct throughout the *in vitro* culture period (Obradovic *et al* 2000). Previous attempts to improve the supply of nutrients to growing tissues *in vitro* have been based on modifications to scaffold architecture and culture environment (Bhardwaj *et al* 2001, Woodfield *et al* 2002 and Malda *et al* 2005). Scaffolds are an integral part of any tissue engineering system, providing cells with a structural template which modulates and coordinates tissue formation (Freed and Vunjak-Novakovic 1998). Porosity is a particularly important feature of a tissue engineering scaffold, since it influences the number of cells that can initially be seeded into the scaffold and the transfer of nutrients to, and waste from, cells during culture (Freed *et al* 1999, Lu *et al* 2001 and Woodfield *et al* 2002). The aims of the work presented in this thesis were to evaluate novel scaffolds, which combined random and anisotropic porosity, and a novel flow perfusion bioreactor for their suitability engineering tissues *in vitro*. The first hypothesis was that the presence of wider aligned channels within a random porous network would be advantageous for *in vitro* tissue formation since the transfer of nutrients to cells throughout the construct would be enhanced. The second hypothesis was that the continuous flow of medium within the flow perfusion bioreactor would improve the transfer of nutrients to cells within constructs and hence facilitate *in vitro* tissue formation. Cartilage was selected as an example tissue on which to perform the studies since the phenomenon of capsule formation at the periphery of scaffolds has been reported in previous cartilage tissue engineering studies (Freed *et al* 1999).

Prior to commencing tissue engineering studies, the scaffolds were characterised and the conditions required for seeding cells into the scaffolds evaluated. It was found that the sparse knit scaffolds (which contained both random and anisotropic porosity) showed less resistance to fluid flow than the needled felt scaffolds. For all scaffold types it was determined that seeding with agitation led to a greater number of cells within the scaffolds compared to static seeding. This is in agreement with reports in the literature that improved cell seeding was observed in scaffolds seeded dynamically, compared to scaffolds seeded statically (Li *et al* 2001). The selection of an optimum agitation speed for each scaffold and cell type was more complex than initially anticipated since in addition to allowing more cells to be seeded into the scaffolds, agitation led to a reduction in cell viability. This reduction in cell viability did not, however, prevent cell proliferation or tissue formation in the later tissue formation studies using OMCs. The Alamar blue™ assay detects changes in the synthetic rates of cells and therefore reduction in the fluorescence levels in a particular culture system would suggest that it is cytotoxic. This may explain the apparent discrepancy between the good performance of sparse knit 4 scaffolds and the reduced viability of cells in these scaffolds. Optimum seeding speeds were selected based on cell number and distribution since it has been proposed that it is essential that a large number of cells are homogeneously seeded into scaffolds in order to ensure functional tissue formation *in vitro* (Vunjak-Novakovic *et al* 1998). It was found that scaffold architecture influenced the optimum seeding conditions as higher agitation speeds were required for seeding BACs and OMCs into the sparse knit scaffolds with more densely knitted upper and lower crusts (SK3 and SK4) than for scaffolds which had more open structures (NF and SK5). It was also determined that the optimum conditions required for seeding the osteosarcoma cell line into NF and SK5 scaffolds were different to those required for the two chondrocyte cell types. This study therefore highlighted the need for seeding optimisation studies prior to commencing tissue engineering studies since both scaffold architecture and cell type may affect cell seeding.

Initial studies investigated cartilage formation by OMCs in each of the scaffold types following four week static, RCCS™ or flow perfusion culture.

Cartilage formation was assessed using biochemical assays for GAG and collagen production and safranin O staining for GAGs. For all scaffold types, lower levels of GAGs were detected in constructs cultured within the flow perfusion system compared to those cultured either in static tissue culture plates or the RCCS™. This finding was in agreement with that of Mizuno and colleagues who detected reduced GAG production in scaffolds cultured within a flow perfusion culture system compared to that in scaffolds cultured in static plates (Mizuno *et al* 2001). Higher levels of GAGs and collagens were present in NF, SK3 and SK4 scaffolds cultured within the RCCS™ compared to those scaffolds cultured in static 6-well plates. This work is supported by the findings of Vunjak-Novakovic and colleagues, who have reported the advantages of microgravity bioreactor systems for cartilage tissue engineering (Vunjak-Novakovic *et al* 1999 and Pei *et al* 2002). Whilst the GAG levels of NF, SK3 and SK4 scaffolds were similar following RCCS™ culture, it was observed that the collagen level of the SK3 scaffolds was reduced compared to that of the NF and SK4 scaffolds. NF and SK4 scaffolds, which were of a similar density, were less dense than SK3 scaffolds. This suggests that scaffold density may influence the production of ECM components by cells. Lower levels of GAGs and collagens were detected in SK5 scaffolds cultured within the RCCS™ compared to the other scaffolds. Although these scaffolds showed the least resistance to fluid flow, they were the most difficult to seed with cells, as indicated by the lower numbers of OMCs seeded into the scaffolds compared to NF, SK3 and SK4 scaffolds at each of the agitation speeds. The poor cartilage formation observed in SK5 scaffolds cultured within the RCCS™ may be the result of the low cell seeding since it is has been reported that for *in vitro* cartilage formation, a high density of cells within tissue engineering scaffolds is necessary (Vunjak-Novakovic 2003).

Further cartilage formation studies were carried out on NF and SK4 scaffolds by culturing them with OMCs in either static plates or the RCCS™ for eight weeks. For all constructs, an increase in weight, decrease in cellularity and increase in collagen content was detected between samples cultured for 4 and 8 weeks. In addition the GAG content of NF and SK4 scaffolds cultured in static 6-well plates increased from weeks 4 to 8.

The GAG and collagen content of NF and SK4 scaffolds following 8-week RCCS™ culture was similar to that reported by Freed and colleagues who cultured BACs in PGA non woven scaffolds in rotating wall bioreactors (Freed *et al* 1994a, Vunjak-Novakovic *et al* 1999 and Pei *et al* 2002). In both NF and SK4 scaffolds cultured within the RCCS™ the distribution of live and dead cells at the centre of 8-week constructs was similar, with mixed populations of live and dead cells visible. Following static culture, however, a difference was detected between the number and viability of cells at the centre of each of the scaffold types. Within NF scaffolds, fewer cells were visible at the centre of the scaffolds and of these, a large number were non viable. In contrast, more cells were observed at the centre of SK4 scaffolds and the majority of these cells were viable. It was therefore concluded that the wider aligned channels within the sparse knit scaffold were advantageous in a culture system where the transfer of nutrients was dependent on diffusion. As previously mentioned, one of the key challenges in tissue engineering is that of producing tissue constructs of clinically useful sizes. Evaluation of SK4 scaffolds of clinically relevant sizes should be considered for future work.

In the studies presented in this thesis, it was determined that the biochemical composition of the NF and SK4 constructs following 8-week RCCS™ culture was similar to that determined experimentally for native ovine articular cartilage. Huckle and co-workers have previously proposed that meniscal fibrochondrocytes may be used for engineering articular cartilage, although there was some controversy as to whether the cartilage engineered in their study was truly hyaline (Huckle *et al* 2003). Meniscal fibrochondrocytes are advantageous for cartilage tissue engineering since their proliferative capacity is greater than that of articular chondrocytes which facilitates *in vitro* expansion of the cells and allows a sufficient number of cells to be obtained for *in vitro* tissue formation. A disadvantage of using these cells, however, is that they have a natural propensity to produce a fibrous matrix which contains type I collagen, in contrast to hyaline cartilage which contains a large amount of type II collagen and very little type I collagen.

There is some evidence in this thesis to suggest that meniscal fibrochondrocytes may be used to generate articular cartilage *in vitro* since the biochemical composition of the engineered tissue was more similar to that of articular cartilage, although further studies to assess the collagen and GAG types present in the tissue would be required to allow a more conclusive comparison between the engineered cartilage and native articular cartilage.

It has recently been reported that a population of chondroprogenitor cells reside within the superficial zone of cartilage (Douthwaite *et al* 2004). These cells have been shown to regenerate cartilaginous tissue in pellet cultures, within cartilage defects and when injected intravenously *in ovo* (Thomson *et al* 2004). It has also been shown that these cells can undergo more population doublings than chondrocytes isolated from full thickness articular cartilage and still retain their ability to form articular cartilage (Bishop 2003). These cells are therefore advantageous for articular cartilage engineering since they have the natural ability to form hyaline cartilage and they can be expanded *in vitro* in order to obtain a sufficient number of cells from a small biopsy of tissue. Future studies could investigate the formation of cartilage in SK4 scaffolds by these cells.

The histological sections of the cartilage engineered in these studies differed from those of the native articular cartilage and meniscal fibrocartilage. The cells within the engineered tissue were not contained within lacunae and the engineered tissue lacked the organisation of the native tissues, for example the superficial, transitional, middle and calcified zones of native articular cartilage were not visible. Future cartilage studies could investigate the ability for the tissue to mature further. These studies could include investigation of the use of culture systems that provide the growing tissue with mechanical stimuli, for example the dynamic culture system used by Chowdhury and colleagues (Chowdhury *et al* 2003).

In conclusion, novel tissue engineering scaffolds containing both random and anisotopic porosity (sparse knit scaffolds) were characterised and assessed for their suitability for *in vitro* cartilage formation.

It was found that sparse knit scaffolds had improved flow properties compared to random fibrous scaffolds (needled felt scaffolds). Similar cartilage formation was observed in sparse knit 4 and needled felt scaffolds, following both 4 and 8 week culture. In addition, the commercially available RCCS™ was found to be optimal for *in vitro* cartilage formation compared to either static plates or the novel flow perfusion bioreactor. In 8-week static cultures, a greater number of viable cells were detected at the centre of sparse knit 4 scaffolds than needled felt scaffolds, indicating that the novel scaffolds were advantageous in culture systems where nutrient supply was dependent on diffusion alone.

References

Agrawal CM and Ray RB. Biodegradable polymeric scaffolds for musculoskeletal tissue engineering. *Journal of Biomedical Materials Research*, 55, 141-150 (2001).

Aigner J, Tegeler J, Hutzler P, Campoccia D, Pavesio A, Hammer C, Kastenbauer E and Naumann A. Cartilage tissue engineering with novel nonwoven structured biomaterial based on hyaluronic acid benzyl ester. *Journal of Biomedical Materials Research*, 42, 172-181 (1998).

Alberts B, Johnson A, Lewis J, Raff M, Roberts K and Walter P. *Molecular Biology of the Cell*. Garland Science, New York (2002).

Allemann F, Mizuno S, Eid K, Yates KE, Zaleske D and Glowacki J. Effects of hyaluronan on engineered articular cartilage extracellular matrix gene expression in 3-dimensional collagen scaffolds. *Journal of Biomedical Materials Research*, 55, 13-19 (2001).

Almarza AJ and Athanasiou KA. Design characteristics for the tissue engineering of cartilaginous tissues. *Annals of Biomedical Engineering*, 32(1), 2-17 (2004).

Altman RD, Kates J, Chun LE, Dean DD and Eyre D. Preliminary observations of chondral abrasion in a canine model. *Annals of the Rheumatic Diseases*, 51, 1056-1062 (1992).

Amiel D, Coutts RD, Abel M Stewart W, Harwood F and Akeson WH. Rib perichondral grafts for the repair of full-thickness articular-cartilage defects: a morphological and biochemical study in rabbits. *Journal of Bone and Joint Surgery*, 67(A), 911-920 (1985).

Anderson AF, Mandelbaum BR, Erggelet C, Micheli LJ, Fu F, Moseley JB and Browne JE. A controlled study of autologous chondrocyte implantation versus marrow stimulation techniques for full-thickness articular cartilage lesions of the femur. *Transcripts of the American Academy of Orthopaedic Surgeons*, 29, 607 (2002).

Anderson G and Gordon KC. Tissue processing, microtomy and paraffin sections. In: *Theory and Practice of Histological Techniques*. Editors: Bancroft JD and Stevens A. Churchill Livingston, 47-67 (1999).

Archer CW, McDowell J, Bayliss MT, Stephens MD and Bentley G. Phenotypic modulation in subpopulations of human articular chondrocytes *in vitro*. *Journal of Cell Science,* 97, 361-371, (1990).

Archer CW, Morrison H and Pitsillides A. The development of diarthrodial joints and articular cartilage. *Journal of Anatomy,* 184, 447-456 (1994).

Arthritis Research Campaign, Arthritis the big picture, available at http://www.arc.org.uk/about_arth/bigpic.htm (2002).

Aston JE and Bentley G. Repair of articular surfaces by allografts of articular and growth-plate cartilage. *Journal of Bone and Joint Surgery*, 68B, 29-35 (1986).

Behrens F, Shepard N and Mitchell N. Metabolic recovery of articular cartilage after intra-articular injections of glucocorticoid. *Journal of Bone and Joint Surgery*, 58A, 1157-1160 (1976).

Benjamin M and Ralphs JR. Biology of fibrocartilage cells. *International Review of Cytology*, 233, 1-45 (2004).

Bentley G and Greer RB. Homotransplantation of isolated epiphyseal and articular cartilage chondrocytes into the joint surfaces of rabbits. *Nature*, 230, 385-388 (1971).

Bentley G and Minas T. Science, Medicine and the future - Treating joint damage in young people. *British Medical Journal*, 320, 1585-1588 (2000).

Bhardwaj T, Pilliar RM, Grynpas MD and Kandel RA. Effect of material geometry on cartilagenous tissue formation *in vitro*. *Journal of Biomedical Materials Research*, 57, 190–199 (2001).

Bishop J. Oral presentation at Smith & Nephew Student Research Day, York (2003).

Brittberg M, Lindahl A, Nilsson A, Ohlsson C, Isaksson O and Peterson L. Treatment of deep cartilage defects in the knee with autologous chondrocyte transplantation. *New England Journal of Medicine*, 331 (14), 889-895 (1994).

Brittberg M. Autologous chondrocyte transplantation. *Clinical Orthopaedics and Related Research*, 367S, S147-S155 (1999).

Brown AN, Kim BS, Alsberg E and Mooney DJ. Combining chondrocytes and smooth muscle cells to engineer hybrid soft tissue constructs. *Tissue Engineering,* **6**(4), 297-305 (2000).

Brun P, Abatangelo G, Radice M, Zacchi V, Guidolin D, Gordini DD and Cortivo R. Chondrocyte aggregation and reorganisation into three-dimensional scaffolds. *Journal of Biomedical Materials Research*, 46, 337-346 (1999).

Bryant SJ and Anseth KS. The effects of scaffold thickness on tissue engineered cartilage in photocrosslinked poly(ethylene oxide) hydrogels. *Biomaterials*, 22, 619-626 (2001).

Buckwalter JA, Woo SL, Goldberg VM, Hadley EC, Booth F, Oegema TR and Eyre D. Current Concepts Review: soft tissue aging and musculoskeltal function. *Journal of Bone and Joint Surgery*, 75A(10), 1533-1548 (1993).

Buckwalter J and Lohmander S. Current concepts review: operative treatment of osteoarthrosis. *Journal of Bone and Joint Surgery*, 76A(9), 1405-1418 (1994).

Buckwalter JA and Mankin HJ. Articular cartilage part I: tissue design and chondrocyte-matrix interactions. *Journal of Bone and Joint Surgery*, 79A (4), 600-611 (1997a).

Buckwalter JA and Mankin HJ. Articular cartilage part II: degeneration and osteoarthritis, repair, regeneration and transplantation. *Journal of Bone and Joint Surgery*, 79A (4), 612-632 (1997b).

Buckwalter JA and Mankin HJ. Articular cartilage repair and transplantation. *Arthritis and Rheumatology*, 41 (8), 1331-1342 (1998a).

Buckwalter JA and Mankin HJ. Articular cartilage: tissue design and chondrocyte-matrix interactions. *AAOS Institution Course Lecture*, 47, 477-486 (1998b).

Bujia J, Sittinger M, Minuth WW, Hammer C, Burmester G and Kastenbauer E. Engineering of cartilage tissue using biroesorbable fleeces and perfusion culture. *Acta Oto-laryngologica*, 115, 307-310 (1995).

Burg KJL, Holder Jr WD, Culberson CR, Beiler RJ, Greene KG, Loebsack AB, Roland WD, Eiselt P, Mooney DJ and Halberstadt CR. Comparative study of seeding methods for three-dimensional polymeric scaffolds. *Journal of Biomedical Materials Research*, 51, 629-649 (2000).

Buschmann MD, Gluzband YA, Grodzinsky AJ, Kimura JH and Hunziker EB. Chondrocytes in agarose culture synthesize a mechanically functional extracellular matrix. *Journal of Orthopaedic Research,* 10, 745-752 (1992).

Byers PD. The effect of high femoral osteotomy on osteoarthritis of the hip. An anatomical study of six hips. *Journal of Bone and Joint Surgery*, 56B, 279-290 (1974).

Campbell CJ. The healing of cartilage defects. *Clinical Orthopaedics*, 64, 45-63 (1969).

Caplan AI, Elyaderani M, Mochizuki Y, Wakitani S and Goldberg VM. Principles of cartilage repair and regeneration. *Clinical Orthopaedics and Related Research*, 342, 254-272 (1997).

Carver SE and Heath CA. Increasing extracellular matrix production in regenerating cartilage with intermittent physiological pressure. *Biotechnology Bioengineering*, 62, 166-174 (1999).

Caterson EJ, Nesti LJ, Li WJ, Danielson KG, Albert TJ, Vaccaro AR and Tuan RS. Three-dimensional cartilage formation by bone marrow-derived cells seeded in polyloctide/alginate amalgam. *Journal of Biomedical Materials Research*, 57, 394-403 (2001).

Cesarone CF, Bolognesi C and Santi L. Improved microfluorometric DNA determination in biological material using Hoechst 33258. *Analytical Biochemistry,* 100, 188-197 (1979).

Chang CH, Liu HC, Lin CC, Chou CH and Lin FH. Gelatin-chondroitin-hyaluronan tri-copolymer scaffold for cartilage tissue engineering. *Biomaterials*, 24, 4853-4858 (2003).

Chapekar MS. Tissue engineering: challenges and opportunities. *Journal of Biomedical Materials Research*, 53 (6), 617-620 (2000).

Chen FS, Frenkel SR and Di Cesare PE. Repair of articular cartilage defects: Part II treatment options. *The American Journal of Orthopaedics*, 28, 88-96 (1999).

Chen G, Ushida T and Tateishi T. Scaffold design for tissue engineering. *Macromolecular Bioscience*, 2, 67-77 (2002).

Chesterman PJ and Smith AU. Homotransplantation of articular cartilage and isolated chondrocytes. An experimental study in rabbits. *Journal of Bone and Joint Surgery*, 50B, 184-197 (1968).

Chowdhury TT, Bader DL, Shelton JC and Lee DA. Temporal regulation of chondrocyte metabolism in agarose constructs subjected to dynamic compression. *Archives in Biochemistry and Biophysics*, 417(1), 105-111 (2003).

Cima LG and Langer R. Engineering human tissue. *Chemical Engineering Progress*, 89(6), 46-54 (1993).

Collier S and Ghosh P. Effects of transforming growth factor-beta on proteoglycan synthesis by cell and explant cultures derived from the knee-joint meniscus. *Osteoarthritis Cartilage,* 3(2), 127-138 (1995).

Convery FR, Akeson WH and Meyers MH. The repair of large osteochondral defects. An experimental study in horses. *Clinical Orthopaedics*, 81, 253-262 (1972).

Cook HC. Carbohydrates. In: *Theory and Practice of Histological Techniques*. Editors: Bancroft JD and Stevens A. Churchill Livingston, 173-211 (1999).

Cuevas P, Burgos J and Baird A. Basic fibroblast growth factor (FGF) promotes cartilage repair *in vivo*. *Biochemical and Biophysical Research Communications*, 156, 611-618 (1988).

Czitrom AA, Keating S and Gross AE. The viability of articular cartilage in fresh osteochondral allografts after clinical transplantation. *Journal of Bone and Joint Surgery*, 72A, 574-581 (1990).

Deasy B, Qu-Peterson Z and Huard J. Multipotentiality of muscle-derived stem cells, *Transcripts of the Orthopaedic Research Society*, 27, 658 (2002).

Douthwaite GP, Bishop JC, Redman SN, Khan IM, Rooney P, Evans DJR, Haughton L, Bayram Z, Boyer S, Thomson B, Wolfe MS and Archer CW. The surface of articular cartilage contains a progenitor cell population. *Journal of Cell Science*, 117(6), 889-897 (2004).

Drury PL and Shipley M. Rheumatology and bone disease. In: *Clinical Medicine*. Editors: Kumar P and Clark M. W B Saunders, London, 447-448 (1998).

Dunkelman NS, Zimber MP, LeBaron RG, Pavelec R, Kwan M and Purchio AF. Cartilage production by rabbit articular chondrocytes on polyglycolic acid scaffolds in a closed bioreactor system. *Biotechnology Bioengineering*, 46, 299-305 (1995).

Elford PR, Graeber M, Ohtsu H, Aeberhard M, Legendre B, Wishart WL and MacKenzie AR. Method of regenerating articular cartilage. United States Patent number 5,368,051 (1994).

Elisseeff J, McIntosh W, Fu K, Blunk BT and Langer R. Controlled release of IGF-I and TGF-β1 in a photopolymerizing hydrogel for cartilage tissue engineering. *Jounral of Orthopaedic Research*, 19(6), 1098-1104 (2001).

Enobakhare BO, Bader DL and Lee DA. Quantification of sulfated glycosaminoglycans in chondrocyte/alginate cultures, by use of 1,9-dimethylmethylene blue. *Analytical Biochemistry*, 243(1), 189-191 (1996).

Erikson G, Franklin D, Gimble J and Guilak F. Adipose tissue-derived stem cells display a chondrogenic phenotype in culture. T*ranscripts of the Orthopaedic Research Society*, 26, 198 (2001).

Farndale RW, Buttle DJ and Barrett AJ. Improved quantitation and discrimination of sulfated glycosaminoglycans by use of dimethylmethylene blue. *Biochimica Et Biophysica Acta*, 883(2), 173-177 (1986).

Fields RD and Lancaster MV. Dual-attribute continuous monitoring of cell-proliferation cytotoxicity. *American Biotechnology Laboratory,* 11(4), 48-78 (1993).

Fragonas E, Valente M, Pozzi-Mucelli M, Toffanin R, Rizzo R, Silvestri F and Vittur F. Articular cartilage repair in rabbits by using suspensions of allogenic chondrocytes in alginate. *Biomaterials*, 21, 795-801 (2000).

Freed LE and Vunjak-Novakovic G. Cultivation of cell-polymer cartilage implants in bioreactors. *Journal of Cellular Biochemistry*, 51, 257-264 (1993).

Freed LE and Vunjak-Novakovic G. Cultivation of cell-polymer tissue constructs in simulated microgravity. *Biotechnology and Bioengineering*, 46, 306-313 (1995).

Freed LE and Vunjak-Novakovic G. Microgravity tissue engineering. *In vitro Cell Development Biology - Animal*, 33, 381-385 (1997).

Freed LE and Vunjak-Novakovic G. Culture of organised cell communities. *Advanced Drug Delivery Reviews*, 33, 15-30 (1998).

Freed LE, Marquis JC, Nohria A, Mikos AG, Emmanuel J and Langer R. Neocartilage formation *in vivo* and *in vitro* using cells cultured on synthetic biodegradable polymers. *Journal of Biomedical Materials Research*, 27, 11-23, (1993).

Freed LE, Vunjak-Novakovic G, Biron RJ, Eagles DB, Lesnoy DC, Barlow SK and Langer R. Biodegradable polymer scaffolds for tissue engineering. *Bio/Technology*, 12, 689-693 (1994a).

Freed LE, Marquis JC, Vunjak G, Emmaual J and Langer R. Composition of cell-polymer cartilage implants. *Biotechnology and Bioengineering,* 43, 605-614 (1994b).

Freed LE, Vunjak-Novakovic G, Marquis JC and Langer R. Kinetics of chondrocyte growth in cell-polymer implants. *Biotechnology and Bioengineering,* 43, 597-604 (1994c).

Freed LE, Langer R, Martin I, Pellis G and Vunjak-Novakovic. Tissue engineering of cartilage in space. *Proceedings of the New York Academy of Sciences USA*, 94, 13885-13890 (1997).

Freed LE, Hollander AP, Martin I, Barry JR, Langer R and Vunjak-Novakovic G. Chondrogenesis in a cell-polymer-bioreactor system. *Experimental Cell Research*, 240, 58-65 (1998).

Freed LE, Martin I and Vunjak-Novakovic G. Frontiers in tissue engineering: *in vitro* modulation of chondrogenesis. *Clinical Orthopaedics and Related Research*, 367S, S46-S58 (1999).

Freyman T M, Yannas IV and Gibson LJ. Cellular materials as porous scaffolds for tissue engineering. *Progress in Materials Science*, 46, 273-282 (2001).

Friedman MJ, Berasi CC, Fox JM, Del Pizzo W, Snyder SJ and Ferkel RD. Preliminary results with abrasion arthoplasty in the osteoarthritic knee. *Clinical Orthopaedics*, 182, 200-205 (1984).

Fujisato T, Sajiki T, Liu Q and Ikada Y. Effect of basic fibroblast growth factor on cartilage regeneration in chondrocyte seeded collagen sponge scaffolds. *Biomaterials*, 17, 155-162 (1996).

Furukawa T, Eyre DR, Koide S and Glimcher MJ. Biochemical studies on repair cartilage resurfacing experimental defects in the rabbit knee. *Journal of Bone and Joint Surgery*, 62A, 79-89 (1980).

Gagne TA, Chappell-Afonso K, Johnson JL, McPherson JM, Oldham CA, Tubo RA, Vaccaro C and Vasios GW Enhanced proliferation and differentiation of human articular chondrocytes when seeded at low cell densities in alginate *in vitro*. *Journal of Orthopaedic Research*, 18(6), 882-890 (2000).

Galban CJ and Locke BR. Effects of spatial variation of cells and nutrient and product concentrations coupled with product inhibition on cell growth in a polymer scaffold. *Biotechnology Bioengineering*, 64, 633-643 (1999).

Gillogly SD, Voigt M and Blackburn T. Treatment of articular cartilage defects of the knee with autologous chondrocyte implantation. *The Journal of Orthopaedic and Sports Physical Therapy*, 28, 241-251 (1998).

Goldberg VM and Caplan AI. Biologic resurfacing of articular surfaces. *American Academy Orthopaedic Surgeons Inst Course Lect*, 48, 623-627 (1999).

Gooch KJ, Blunk T, Courter DL, Sieminski AL, Bursac PM, Vunjak-Novakovic G and Freed LE. IGF-1 and mechanical environment interact to modulate engineered cartilage development. *Biochemical and Biophysical Research Communications,* 286, 909-915 (2001).

Grad S, Kupcsik L, Gorna K, Gogolewski S and Alini M. The use of biodegradable polyurethane scaffolds for cartilage tissue engineering: potential and limitations. *Biomaterials*, 24, 5163-5171 (2003).

Grande DA, Halberstadt C, Naughton G, Schwartz R and Manji R. Evaluation of matrix scaffolds for tissue engineering of articular cartilage grafts. *Journal of Biomedical Materials Research*, 34, 211-220 (1997).

Grande DA, Breitbart AS, Mason J, Paulino C, Laser J and Schwartz R. Cartilage tissue engineering: current limitations and solutions. *Clinical Orthopaedics and Related Research*, 367S, S176-S185 (1999).

Grigolo B, Lisignoli G, Piacentini A, Fiorini M, Gobbi P, Mazzotti G, Duca M, Pavesio A and Facchini A. Evidence for redifferentiation of human chondrocytes grown on a hyaluronan-based biomaterial (HYAFF™ 11): molecular, immunohistochemical and ultrastructural analysis. *Biomaterials,* 23, 1187-1195 (2002).

Gugala Z and Gogolewski S. *In vitro* growth and activity of primary chondrocytes on a resorbable polylactide three-dimensional scaffold. Journal *of Biomedical Materials Research*, 49, 183-191 (2000).

Guilak F and Mow VC. The mechanical environment of the chondrocyte: a biphasic finite element model of cell-matrix interactions in articular cartilage. *Journal of Biomechanics*, 33, 1663-1673 (2000).

Gurdon JB. A community effect in animal development. *Nature* 336, 772-774 (1988).

Hangody L, Kish G and Karpati Z. Mosaicplasty for the treatment of articular cartilage defects: application in clinical practice. *Orthopaedics*, 21, 751-756 (1998).

Hardingham TE. The role of link-protein in the structure of cartilage proteoglycan aggregates. *The Biochemical Journal*, 177, 237-247 (1979).

Hasler EM, Herzog W, Wu JZ, Muller W and Wyss U. Articular cartilage biomechanics: Theoretical models, material properties, and biosynthetic response. *Critical Reviews in Biomedical Engineering*, 27, 415-488 (1999).

Hayashi T, Abe E and Jasin HE. Fibronectin synthesis in superficial and deep layers of normal articular cartilage. *Arthritis and Rheumatism*, 39, 567-573 (1996).

Hayes AJ, MacPherson S, Morrison H, Douthwaite GP and Archer CW. The development of articular cartilage: evidence for an appositional growth mechanism. *Anatomy and Embryology*, 203, 469-479 (2001).

Heath CA and Magari SR. Mini-review: Mechanical factors affecting cartilage regeneration *in vitro. Biotechnology and Bioengineering*, 50, 430-437 (1996).

Hedbom E and Heinegard D. Binding of fibromodulin and decorin to separate sites on fibrillar collagens. *Journal of Biological Chemistry*, 268, 27307-27312 (1993).

Herndon CW and Chase SW. Experimental studies in the transplantation of whole joints. *Journal of Bone and Joint Surgery*, 34A, 564-578 (1952).

Homminga G, van der Linden T, Terwindt-Rouwenhorst E and Drukker J. Repair of articular defects by perichondral grafts: experiments in the rabbit. *Acta Orthopaedica Scandinavica*, 60(3), 326-329 (1989).

Homminga GN, Bulstra SK, Bouwmeester PSM and van der Linden T. Perichondral grafting for cartilage lesions of the knee. *Journal of Bone and Joint Surgery*, 72(B), 1003-1007 (1990).

Hou Q, DeBank PA and Shakesheff KM. Injectable scaffolds for tissue regeneration. *Journal of Materials Chemistry*, 14, 1915-1923 (2004).

Huckle J, Dootson G, Medcalf N, McTaggart S, Wright E, Carter A, Schreiber R, Kirby B, Dunkelman N, Stevenson S, Riley S, Davisson T and Ratcliffe A. Differentiated chondrocytes for cartilage tissue engineering. In: *Tissue engineering of cartilage and bone (Novartis Foundation Symposium)*. Editors: Bock G and Goode J. John Wiley & Sons Ltd, Chichester, 249, 103-117 (2003).

Hunziker EB. Biologic repair of articular cartilage: defect models in experimental animals and matrix requirements. *Clinical Orthopaedics and Related Research*, 367S, S135-S146 (1999a).

Hunziker EB. Articular cartilage repair: are the intrinsic biological constraints undermining this process insuperable. *Osteoarthritis Cartilage*, 7, 15-28 (1999b).

Hutmacher DW. Scaffolds in tissue engineering bone and cartilage. *Biomaterials*, 21, 2529-2543 (2000).

Ishaug-Riley SL, Okun LE, Prado G, Applegate MA and Ratcliffe A. Human articular chondrocyte adhesion and proliferation on synthetic biodegradable polymer films. *Biomaterials*, 20, 2245-2256 (1999).

Isogai N, Asamura S, Higashi T, Ikada Y, Morita S, Hillyer J, Jacquet R and Landis WJ. Tissue engineering of an auricular cartilage model utilising cultured chondrocyte-poly($_{L}$-lactide-ε-caprolactone) scaffolds. *Tissue Engineering*, 10(5/6), 673-687 (2004).

Iwata H. Pharmacologic and clinical aspects of intraarticular injection of hyaluronate. *Clinical Orthopaedics*, 289, 285-291 (1993).

Jackson DW and Simon TM. Tissue engineering principles in orthopaedic surgery. *Clinical Orthopaedics*, 367S, S31-S45 (1999).

Jakob M, Démarteau O, Schäfer D, Hintermann B, Dick W, Heberer M and Martin I. Specific growth factors during the expansion and redifferentiation of adult human articular chondrocytes enhance chondrogenesis and cartilaginous tissue formation *in vitro*. *Journal of Cellular Biochemistry*, 81, 368-377 (2001).

Johnson LL. Arthroscopic abrasion arthroplasty. Historical and pathological perspective: Present status. *Arthroscopy*, 2, 54-69 (1986).

Kafienah W, Jakob M, Démarteau O ,Frazer A, Barker MD, Martin I and Hollander AP. Three-dimensional tissue engineering of hyaline cartilage: comparison of adult nasal and articular chondrocytes. *Tissue Engineering*, 8(5), 817-526 (2002).

Kellner K, Schulz MB, Göpferich A and Blunk T. Insulin in tissue engineering of cartilage: a potential model system for growth factor application. *Journal of Drug Targeting*, 9, 439-448 (2001).

Kim YJ, Sah RLY, Doong JYH and Grodzinsky AJ. Fluorometric assay of DNA in cartilage explants using Hoechst 33258. *Analytical Biochemistry*, 174(1), 168-176 (1988).

Kladny B, Martus P, Schiwy-Bochat K, Weseloh G and Swoboda B. Measurement of cartilage thickness in the human knee joint by magnetic resonance imaging using a three-dimensional gradient echo sequence. *International Orthopaedics*, 23, 264-267 (1999).

Kreder HJ, Moran M, Keeley FW and Salter RB. Biologic resurfacing of a major joint defect with cryopreserved allogeneic periosteum under the influence of continuous passive motion in a rabbit model. *Clinical Orthopaedics*, 300, 288-296 (1994).

Kreklau B, Sittinger M, Mensing MB, Voigt C, Berger G, Burmester GR, Rahmanzadeh R and Gross U. Tissue engineering of biphasic joint cartilage transplants. *Biomaterials*, 20, 1743-1749 (1999).

Kuo CK and Ma PX. Ionically crosslinked alginate hydrogels as scaffolds for tissue engineering: part 1, structure, gelation rate and mechanical properties. *Biomaterials*, 22, 511-521 (2001).

Langer R and Vacanti JP. Tissue engineering. *Science*, 260, 920-926 (1993).

Langer R. Tissue engineering. *Molecular Therapy*, 1(1), 12-15 (2000).

LeBaron RG and Athanasiou KA. *Ex-vivo* synthesis of articular cartilage. *Biomaterials*, 21, 2575-2587 (2000).

Lee CR Breinan HA, Nehrer S and Spector M. Articular cartilage chondrocytes in Type I and Type II collagen-GAG matrices exhibit contractile behaviour *in vitro*. *Tissue Engineering*, 6(5), 555-565 (2000).

LGC. Biomaterials State of the Art Report, available at http://www.biomaterials-partnership.org.uk (2002).

Li Y, Ma T, Kniss DA, Lasky LC and Yang ST. Effects of filtration seeding on cell density, spatial distribution, and proliferation in nonwoven fibrous matrices. *Biotechnology Progress*, 17(5), 935-944 (2001).

Lindenhayen K, Perka C, Spitzer RS, Heilmann HH, Pommerening K, Mennicke J and Sittinger M. Retention of hyaluronic acid in alginate beads: Aspects for *in vitro* cartilage engineering. *Journal of Biomedical Materials Research*, 44, 149-155 (1999).

Loeser RF. Integrin-mediated attachment of articular chondrocytes to extracellular matrix proteins. *Arthiritis and Rheumatism*, 36(8), 1103-1110 (1993).

Lohmander LS. Tissue engineering of cartilage: do we need it, can we do it, is it good and can we prove it? In: *Tissue Engineering of Cartilage and Bone (Novartis Foundation Symposium)*. Editors : Bock G and Goode J. John Wiley & Sons Ltd, Chichester, 249, 2-16 (2003).

Lu L, Zhu X, Valenzuela RG, Currier BL and Yaszemski MJ. Biodegradable polymer scaffolds for cartilage tissue engineering. *Clinical Orthopaedics and Related Research*, 391S, S251-S270 (2001).

Malda J, Woodfield TBF, van der Vloodt F, Kooy FK, Marten DE, Tramper J, van Blitterswijk CA and Riesle J. The effect of PEGT/PBT scaffold architecture on oxygen gradients in tissue engineered cartilaginous constructs. *Biomaterials*, 25 5773-5780 (2004).

Malda J, Woodfield TBF, van der Vloodt F, Wilson C, Martens DE, Tramper J, van Blitterswijk CA and Riesle J. The effect of PEGT/PBT scaffold architecture on the compostion of tissue engineered cartilage. *Biomaterials*, 26, 63-72 (2005).

Mandl EW, van der Veen SW, Verhaar JAN and van Osch GJVM. Serum-free medium supplemented with high-concentration FGF-2 for cell expansion culture of human ear chondrocytes promotes redifferentiation capacity. *Tissue Engineering*, 8(4), 573-580 (2002).

Mankin H. The reaction of articular cartilage to injury and osteoarthritis. *New England Journal of Medicine*, 291, 1285-1292 (1974).

Mankin HJ. The response of articular cartilage to mechanical injury. *Journal of Bone and Joint Surgery*, 64A, 460-466 (1982).

Marijnissen WJCM, van Osch GJVM, Aigner J, Verwoerd-Verhoef HL and Verhaar JAN. Tissue-engineered cartilage using serially passaged articular chondrocytes. Chondrocytes in alginate, combined *in vivo* with a synthetic (E210) or biological biodegradable carrier (DBM). *Biomaterials*, 21, 571-580 (2000).

Marijnissen W, van Osch G, Aigner J, van der Veen SW, Hollander AP, Verwoerd-Verhoef HL and Verhaar JAN. Alginate as a chondrocyte-delivery substance in combination with a non-woven scaffold for cartilage tissue engineering. *Biomaterials,* 23(6), 1511-1517 (2002).

Marler JJ, Upton J, Langer R and Vacanti JP. Transplantation of cells in matrices for tissue regeneration. *Advanced Drug Delivery Reviews*, 33, 165-182 (1998).

Martin I, Padera RF, Langer R, Vunjak-Novakovic G and Freed LE. *In vitro* differentiation of chick embryo bone marrow stromal cells in cartilaginous and bone-like tissues. *Journal of Orthopaedic Reseacrh*, 16, 181-189 (1998).

Martin I, Vunjak-Novakovic G, Yang J, Langer R and Freed LE. Mammalian chondrocytes expanded in the presence of fibroblast growth factor 2 maintain the ability to differentiate and regenerate three-dimensional cartilaginous tissue. *Experimental Cell Research,* 253, 681-688 (1999).

Martin I, Obradovic B, Treppo S, Grodzinsky AJ, Langer R, Freed LE and Vunjak-Novakovic G. Modulation of the mechanical properties of tissue engineered cartilage. *Biorheology*, 37, 141-147 (2000).

Martin I, Suetterlin R, Baschong W, Heberer M, Vunjak-Novakovic G and Freed LE. Enhanced cartilage tissue engineering by sequential exposure of chondrocytes to FGF-2 during 2D expansion and BMP-2 during 3D cultivation. *Journal of Cellular Biochemistry*, 83(1), 121-128 (2001).

Masuda K, Sah RL, Hejna MJ and Thonar EJMA. A novel two-step method for the formation of tissue-engineered cartilage by mature bovine chondroyctes: the alginate-recovered-chondrocyte (ARC) method. *Journal of Orthopaedic Reserach*, 21, 139-148 (2003).

McDevitt CA and Webber RJ. The ultrastructure and biochemistry of meniscal cartilage. *Clinical Orthopaedics*, 252, 8-18 (1990).

Middleton JC and Tipton AJ. Synthetic biodegradable polymer as orthopaedic devices. *Biomaterials*, 21, 2335-2346 (2000).

Miralles G, Baudoin R, Dumas D, Baptiste D, Hubert P, Stoltz JF, Dellacherie E, Mainard D, Netter P and Payan E. Sodium alginate sponges with or without sodium hyaluronate: *in vitro* engineering of cartilage. *Journal of Biomedical Materials Research*, 57, 268-278 (2001).

Mitchell N and Shepard N. The resurfacing of adult articular cartilage by multiple perforations through the subchondral bone. *Journal of Bone and Joint Surgery*, 58A, 230-233 (1976).

Mizuno S, Allemann F and Glowacki J. Effects of medium perfusion on matrix production by bovine chondrocytes in three-dimensional collagen sponges. *Journal of Biomedical Materials Research*, 56A, 368-375 (2001).

Mooney V and Ferguson A. The influence of immobilisation and motion on the formation of fibrocartilage in the repair granuloma after joint resection in the rabbit. *Journal of Bone and Joint Surgery*, 48A, 1145-1155 (1966).

Moran CG and Tourret LJ. Clincal review: recent advances in orthopaedics. *British Medical Journal*, 322, 902-905 (2001).

Moran JM, Pazzano D and Bonassar LJ. Characterisation of polylactic acid - polyglycolic acid composites for cartilage tissue engineering. *Tissue Engineering*, 9(1), 63-70 (2003).

Mow VC, Fithian DC and Kelly MA. Chapter 1 Fundamentals of articular cartilage and meniscus biomechanics. In: *Articular Cartilage and Knee Joint Function: Basic Science and Arthroscopy*. Editor: Ewing JW. Raven Press, New York, 1-18 (1990).

Mueller SM, Shortkroff S, Schneider TO, Breinan HA, Yannas IV and Spector M. Meniscus cells seeded into type I and type II collagen-GAG matrices *in vitro*. *Biomaterials*, 20, 701-709 (1999).

Nakano T, Dodd CM and Scott PG. Glycosaminoglycans and proteoglycans from different zones of the porcine knee meniscus. *Journal of Orthopaedic Research*, 15, 213-220 (1997).

Nehrer S, Breinan HA, Ramappa A, Hsu HP, Minas T, Shortkroff S, Sledge CB, Yanas IV and Spector M. Chondrocyte seeded collagen matrices implanted in chondral defect in a canine model. *Biomaterials*, 19, 2313-2328 (1998).

Newman AP. Articular cartilage repair. *American Journal of Sports Medicine*, 26 (2), 309-324 (1998).

Nicoll S, Wedrychowska A and Bhatnagar R. Induction of a chondrocyte-like phenotype in human dermal fibroblasts by high density micromass culture in a functionally hypoxic environment: regulation by protein kinase C *Transcripts of the Orthopaedic Research Society*, 23, 36 (1998).

O'Brien J, Wilson I, Orton T and Pognan F. Investigation of the alamar blue (resazurin) fluorescent dye for the assessment of mammalian cell cytotoxicity. *European Journal Of Biochemistry*, 267(17), 5421-5426 (2000).

O'Driscoll SW. The healing and regeneration of articular cartilage. *Journal of Bone and Joint Surgery*, 80A (12), 1795-1812 (1998).

Obradovic B, Meldon JH, Freed LE and Vunjak-Novakovic G. Glycosaminoglycan deposition in engineered cartilage: experiments and mathematical model. *AIChE J,* 46, 1860-1871 (2000).

Olah EH and Kostenszky KS. Effect of prednisolone on the glycosaminoglycan components of the regenerating articular cartilage. Acta Biologica Hungarica, 27, 129-134 (1976).

Outerbridge HK, Outerbridge AR and Outerbridge RE. The use of a lateral patellar autologous graft for the repair of a large osteochondral defect in the knee. *Journal of Bone and Joint Surgery*, 77A, 65-72 (1995).

Pei M, Solchaga LA, Seidel J, Zeng L, Vunjak-Novakovic G, Caplan I and Freed LE. Bioreactors mediate the effectiveness of tissue engineering scaffolds. *FASEB Journal,* 16, 1691-1694 (2002).

Peretti GM, Randolph MA, Villa MT, Buragas MS and Yaremchuk MJ. Cell-based tissue-engineered allogeneic implant for cartilage repair. *Tissue Engineering*, 6 (5), 567-576 (2000).

Petersen W and Tillmann B. Collagenous fibril texture of the human knee joint menisci. *Anatomy and Embryology (Berl.)*, 197, 317-324 (1998).

Pittenger M, Mackay A, Beck S, Jaiswal R, Douglas R, Mosca J, Moorman M, Simonetti D and Marshak C. Multilineage potential of adult human mesenchymal stem cells. *Science*, 284, 143-147 (1999).

Pridie KH. A method for resurfacing osteoarthritic knee joints. *Journal of Bone and Joint Surgery*, 41B, 618-619 (1959).

Puelacher WC, Kim SW, Vacanti JP, Schloo B, Mooney D and Vacanti CA. Tissue-engineered growth of cartilage: the effect of varying the concentration of chondrocytes seeded onto synthetic polymer matrices. *International Journal of Oral and Maxillofacial Surgery*, 23, 49-53 (1994).

Redman SN, Douthwaite GP, Thomson BM and Archer CW. The cellular responses of articular cartilage to sharp and blunt trauma. *Osteoarthritis and Cartilage*, 12(2) 106-116 (2004).

Robinson G and Gray T. Electron microscopy 2: practical procedures. In: *Theory and Practice of Histological Techniques*. Editors: Bancroft J and Stevens A. Churchill Livingston, 585-625 (1996).

Roche S, Ronzière MC, Herbage D and Freyria AM. Native and DPPA cross-linked collagen sponges seeded with fetal bovine epiphyseal chondrocytes used for cartilage tissue engineering. *Biomaterials,* 22, 9-18 (2001).

Rubak JM, Poussa M and Ritsila V. Chondrogenesis in repair of articular cartilage defects by free periosteal grafts in rabbits. *Acta Orthopaedica Scandinavica*, 53, 181-186 (1982).

Rudert M, Hirschmann F, Schulze M and Wirth CJ. Bioartificial cartilage. *Cells Tissues Organs*, 167, 95-105 (2000).

Salter RB, Gross A and Hall JH. Hydrocortisone arthropathy – an experimental investigation. *Canadian Med Assn J*, 97, 374-377 (1967).

Salter RB, Simmonds DF, Malcolm BW, Rumble EJ, MacMichael D and Clements ND. The biological effect of continuous passive motion on the healing of full-thickness defects in articular cartilage: an experimental investigation in the rabbit. *Journal of Bone and Joint Surgery*, 62A(8), 1232-1251 (1980).

Salter RB, Hamilton HW, Wedge JH, Tile M, Torode IP, O'Driscoll SW, Murnaghan JJ, and Saringer JH. Clinical application of basic research on continuous passive motion for disorders and injuires of synovial joints: a preliminary report of a feasibility study. *Journal of Orthopaedic Research*, 1, 325-342 (1984).

Saris DBF, Mukjerjee N, Berglund LJ, Schultz FM, An KN and O'Driscoll SW. Dynamic pressure transmission through agarose gels. *Tissue Engineering*, 6(5), 531-537 (2000).

Sato K and Urist MR. Bone morphogenetic protein-induced cartilage development in tissue culture. *Clinical Orthopaedics*, 183, 180-187 (1984).

Sato T, Chen G, Ushida T, Ishii T, Ochiai N and Tateishi T. Tissue-engineered cartilage by *in vivo* culturing of chondrocytes in PLGA-collagen hybrid sponge. *Materials Science and Engineering C*, 17, 83-89 (2001).

Sawtell RM, Downes S and Kayser MV. An *in vitro* investigation of the PEMA/THFMA system using chondrocyte culture. *Journal of Materials Science: Materials in Medicine*, 6, 676-679 (1995).

Schaefer D, Martin I, Shastri P, Padera RF, Langer R, Freed LE and Vunkjak-Novakovic G. *In vitro* generation of osteochondral composites. *Biomaterials*, 21, 2599-2606 (2000).

Schatten WE, Bergenstal DM, Kramer WM, Swarm RL and Siegel S. Biological survival and growth of cartilage grafts. *Plastic Reconstruction Surgery*, 22, 11-28 (1958).

Scott PG, Nakano T and Dodd CM. Isolation and characterisation of small proteoglycans from different zones of the porcine knee meniscus. *Biochimica et Biophysica Acta*, 1336, 254-262 (1997).

Serafini-Fracassini A and Smith JW, *The Structure and Biochemistry of Cartilage.* Churchill Livingston, London (1974).

Shapiro F, Koide S and Glimcher MJ. Cell origin and differentiation in the repair of full-thickness defects of articular cartilage. *Journal of Bone and Joint Surgery*, 75A, 532-553 (1993).

Sharma B and Elisseeff JH. Engineering structurally organised cartilage and bone tissues. *Annals of Biomedical Engineering*, 32(1), 148-159 (2004).

Shortkroff S, Barone L, Hsu HP, Wrenn C, Gagne T, Chi T, Breinan H, Minas T, Sledge CB, Tubo R and Spector M. Healing of chondral and osteochondral defects in a canine model: the role of cultured chondrocytes in regeneration of articular cartilage. *Biomaterials*, 17, 147-154 (1996).

Sittinger M, Bujia J, Minuth WW, Hammer C and Burmester GR. Engineering of cartilage tissue using bioresorbable polymer carriers in perfusion culture. *Biomaterials*, 15, 451-456 (1994).

Sittinger M, Reitzel D, Douner M, Hierlemann H, Hammer C, Kastenbauer E, Planck H, Burmester GR and Bujia J. Resorbable polyesters in cartilage engineering: affinity and biocompatibility of polymer fibre structures to chondrocytes. *Journal of Biomedical Materials Research (Applied Biomaterials)*, 33, 57-63 (1996).

Skoog T, Ohlsén L and Sohn SA. Perichondral potential for cartilaginous regeneration. *Scandinavian Journal of Plastic and Reconstructive Surgery*, 6, 123-125 (1972).

Smith MM and Ghosh P. The synthesis of hyaluronic acid by human synovial fibroblasts is influenced by the nature of the hyaluronate in the extracellular environment. *Rheumatology International*, 7, 113-122 (1987).

Sommarin Y, Larsson T and Heinegård D. Chondrocyte-matrix interactions: attachment to proteins isolated from cartilage. *Experimental Cell Research*, 184, 181-192 (1989).

Stevens A and Wilson I. The haematoxylins and eosin. In: *Theory and Practice of Histological Techniques*. Editors: Bancroft JD and Stevens A. Churchill Livingston, 99-112 (1999).

Suh JKF and Matthew HWT. Application of chitosan-based polysaccharide biomaterials in cartilage tissue engineering : a review. *Biomaterials*, 21, 2589-2598 (2000).

Sullins KE, McIllwraith CW, Powers BE and Norrdin RW. Evaluation of periosteal grafts in articular cartilage repair in horses. *Veterinary Surgery*, 14, 66-67 (1985).

Sweigart MA and Athanasiou KA. Toward tissue engineering of the knee meniscus. *Tissue Engineering*, 7(2), 111-129 (2001).

Sweigart MA, AufderHeide AC and Athanasiou KA. Chapter 1: Fibrochondrocytes and their use in tissue engineering of the meniscus. In: *Topics in Tissue Engineering*. Editors: Ashammakhi N and Ferretti P. E-book available at: http://www.tissue-engineering-oc.com/ebook_topics_in_t_e/, 1-19 (2003).

Tachetti C, Tavella S, Dozin B, Quarto R, Robino G and Cancedda R. Cell condensation in chondrogenic differentiation. *Experimental Cell Research*, 200, 26-33 (1992).

Tavella S, Bellese G, Castagnola P, Martin I, Piccini D, Doliana R, Colombatti A, Cancedda R and Tacchetti C. Regulated expression of fibronectin, laminin and related integrin receptors during the early chondrocyte differentiation. *Journal of Cell Science*, 110, 2261-2270 (1997).

Tay AG, Farhadi J, Suetterlin R, Pierer G, Hebereer M and Martin I. Cell yield, proliferation and postexpansion differentiation capacity of human ear, nasal and rib chondrocytes. *Tissue Engineering*, 10(5/6), 762-770 (2004).

Temenoff J S and Mikos AG. Review: tissue engineering for regeneration of articular cartilage. *Biomaterials*, 21, 431-440 (2000a).

Temenoff JS and Mikos AG. Injectable biodegradable materials for orthopaedic tissue engineering. *Biomaterials*, 21, 2405-2412 (2000b).

Thomson BM, Smith MF, Archer CW and Douthwaite GP. Tissue Implant. United States Patent Application US 2004/0033212 A1 (2004).

Thornton AJ, Alsberg E, Albertelli M and Mooney DJ. Shape-defining scaffolds for minimally invasive tissue engineering. *Transplantation*, 77(12), 1798-1803 (2004).

Tsai CL, Liu TK, Fu SL, Perng JH and Lin AC. Preliminary study of cartilage repair with autologous periosteum and fibrin adhesive system. *Journal of the Formosan Medical Association*,91, S239-S245 (1992).

Uchio Y, Ochi M, Matsusaki M, Kurioka H and Katsube K. Human chondrocyte proliferation and matrix synthesis cultured in Atelocollagen® gel. *Journal of Biomedical Materials Research*, 50(2), 138-143 (2000).

Vacanti CA, Kim WS, Schloo B, Upton J and Vacanti JP. Joint resurfacing with cartilage grown *in situ* from cell-polymer structures. *The American Journal of Sports Medicine*, 22(4), 485-488 (1994).

Vachon A, McIlwraith CW, Trotter GW, Norrdin RW and Powers BE. Neochondrogenesis in free intra-articular, periosteal and perichondral autografts in horses. *American Journal of Veterinary Research*, 50(10), 1787-1794 (1989).

van Beuningen HM, van der Kraan PM, Arntz OJ and van den Berg WB. Stimulation of osteophyte formation and cartilage proteoglycan synthesis by intra-articularly injected TGF-β. *Orthopaedic Trans*, 17, 714-715 (1993-1994).

van der Kraan PM, Buma P, van Kuppevelt T and van den Berg WB. Interaction of chondrocytes, extracellular matrix and growth factors: relevance for articular cartilage tissue engineering. *Osteoarthritis Cartilage*, 10, 631-637 (2002).

van Kampen GPJ and van de Stadt RJ. Cartilage and chondrocyte responses to mechanical loading *in vitro.* In: *Joint loading, biology and health of articular structures*. Butterworth, Kent, 112-125 (1987).

van Susante JLC, Pieper J, Buma P, van Kuppevelt TH, van Beuningen H, van der Kraan PM, Veerkamp JH, van den Berg WB and Veth RPH. Linkage of chondroitin-sulfate to type I collagen scaffolds stimulates the bioactivity of seeded chondrocytes *in vitro*. *Biomaterials*, 22, 2359-2369 (2001).

Von der Mark K, Mollenhauer J, Pfaffle M and van Menxel M. Role of anchorin CII in the interaction of chondrocytes with extracellular collagen. In: *Articular Cartilage Biochemistry*. Editors: Kuettner K, Schleyerbach R and Hascall VC. Raven Press, New York (1986).

Vunjak-Novakovic G, Freed LE, Biron RJ and Langer R. Effects of mixing on the composition and morphology of tissue engineered cartilage. *AICHE J*, 42, 850-860 (1996).

Vunjak-Novakovic G, Obradovic B, Martin I, Bursac PM, Langer R and Freed LE. Dynamic cell seeding of polymer scaffolds for cartilage tissue engineering. *Biotechnology Progress*, 14, 193-202 (1998).

Vunjak-Novakovic G, Martin I, Obradovic B, Treppo S, Grodzinsky AJ, Langer R and Freed LE. Bioreactor cultivation conditions modulate the composition and mechanical properties of tissue engineered cartilage. *Journal of Orthopaedic Research*, 17, 130-138 (1999).

Vunjak-Novakovic G. The fundamentals of tissue engineering: scaffolds and bioreactors. In: *Tissue Engineering of Cartilage and Bone (Novartis Foundation Symposium)*. Editors: Bock G and Goode J. John Wiley & Sons Ltd, Chichester, 249, 34-51 (2003).

Wakitani S, Goto T, Pineda SJ, Young RG, Mansour JM, Caplan AI and Goldberg VM. Mesenchymal cell-based repair of large, full thickness defects of articular cartilage. *Journal of Bone and Joint Surgery*, 76A (4), 579-592 (1994).

Waldman SD, Grynpas MD, Pilliar RM and Kandel RA. The use of specific chondrocyte populations to modulate the properties of tissue-engineered cartilage. *Journal of Orthopaedic Research*, 21, 132-138 (2003).

Ward AC, Dowthwaite GP and Pitsillides AA. Hyaluronan in joint cavitation. *Biochemical Society Transactions*, 27, 128-135 (1999).

Watson M S, Whitaker M J, Howdle S M and Shakesheff K M. Incorporation of proteins into polymer materials by a novel supercritical fluid processing method. *Advanced Materials*, 14, 1802-1804 (2002).

Webber RJ, Zitaglio T and Hough AJ. *In vitro* cell proliferation and proteoglycan synthesis of rabbit meniscal fibrochondrocytes as a function of age and sex. *Arthritis and Rheumatism*, 29(8), 1010-1016 (1986).

Wendt D, Marsano A, Jakob M, Heberer M and Martin I. Oscillating perfusion of cell suspensions through three-dimensional scaffolds enhances cell seeding efficiency and uniformity. *Biotechnology Bioengineering*, 84, 205-214 (2003).

Whitaker MJ, Quirk RA, Howdle SM and Shakesheff KM. Growth factor release from tissue engineering scaffolds. *Journal of Pharmacy and Pharmacology*, 53, 1427-1437 (2001).

Wirth CJ and Rudert M. Techniques of cartilage growth enhancement: a review of the literature. *Arthroscopy*, 12, 300-308 (1996).

Woessner JF. The determination of hydroxyproline in tissue and protein samples containing small proportions of this imino acid. *Archives of Biochemistry and Biophysics,* 93, 440-447 (1961).

Woo SL, Matthews JV, Akeson WH, Amiel D and Convery FR. Connective tissue response to immobility. Correlative study of biomechanical and biochemical measurements of normal and immobilised rabbit knees. *Arthritis Rheumatism*, 18(3), 257-264 (1975).

Woodfield TBF, Bezemer JM, Pieper JS, van Blitterswijk CA and Riesle J. Scaffolds for tissue engineering of cartilage. *Critical Reviews in Eukaryotic Gene Expression*, 12, 207–35 (2002).

Wyre RM and Downes S. An *in vitro* investigation of the PEMA/THFMA polymer system as a biomaterial for cartilage repair. *Biomaterials*, 21, 335-343 (2000).

Yang X B, Green D W, Roach H I, Clarke N M P, Anderson H C, Howdle S M, Shakesheff K M, and Oreffo R O C. Novel osteoinductive biomimetic scaffolds stimulate human osteoprogenitor activity - Implications for skeletal repair. *Connective Tissue Research,* 44, 312-317 (2003).

Appendix 1

Materials

Material	Supplier
1,4 diazobicyclo-2-2-2-octane (DABCO)	Sigma-Aldrich D2522
1, 9 dimethylemethylene blue (DMMB)	Sigma-Aldrich 34, 108-8
Acetone	Fisher Chemicals A/0520/17
Alamar Blue™ solution	Serotec BUF012B
Antibiotic Antimycotic solution	Sigma-Aldrich A5955
Ascorbic acid-2-phosphate	Sigma-Aldrich A8960
BisBenzimide (Hoechst no. 33258)	Sigma-Aldrich B2883
Chondroitin-4-sulphate	Sigma-Aldrich C8529
cis-4-hydroxy-L-proline	Sigma-Aldrich H1637
Citric acid	Sigma-Aldrich C7129
Collagenase (Worthington's type II)	Lorne Laboratories LS004176
Concentrated hydrochloric acid (HCl)	Fisher Chemicals H/1200/PB17

Cysteine hydrochloride	Sigma-Aldrich C1276
Dimethylsulphoxide (DMSO)	Sigma-Aldrich D8418
Di-sodium hydrogen phosphate dodecahydrate	Fluka 71663
Distyrene plasticiser xylene mountant (DPX)	Nustain AE020
Dulbecco's Modified Eagle's Medium (DMEM)	Sigma-Aldrich D6429
Dulbecco's phosphate buffered saline (DPBS)	Sigma-Aldrich D8537
Eosin (yellowish)	Nustain AD046
Ethanol	Fisher Chemicals E/0650DF/15
Ethylenediaminetetracetic acid (EDTA)	Sigma-Aldrich ED2SS
Fast Green	Nustain AD060
Foetal calf serum (FCS)	Sigma-Aldrich F7524
Formal saline (10% buffered)	Nustain AF010
Formic acid	VWR International 101157H
Gentamicin solution (10 mg/mL)	Invitrogen Ltd 15710-049
Glacial acetic acid	Sigma-Aldrich A6283

Glutaraldehyde solution (50%)	TAAB G006
Glycerol	Sigma-Aldrich G7893
Hank's balanced salt solution (HBSS) (without phenol red)	Sigma-Aldrich H1387
4-(2-hydroxyethyl)-1-piperazineethanesulfonic acid (HEPES)	Sigma-Aldrich H3375
Hexamethyldisilaxane (HMDS)	Sigma-Aldrich H4875
Industrial methylated spirits (IMS)	Fisher Chemicals M/4450/17
L-glutamine solution (200 mM in dH_2O)	Sigma-Aldrich G7513
L-proline	Sigma-Aldrich P8449
Live/Dead™ viability/cytotoxicity assay kit	Molecular Probes L3224
Mayer's haematoxylin	Nustain AS040
N-chloro-p-toluenesulfonamide (Chloramine T)	Sigma-Aldrich C9887
Non essential amino acid solution (NEAA)	Sigma-Aldrich M7145
Osmium tetroxide solution (2% *w/v*)	TAAB O006
Papain	Sigma-Aldrich P4762
Paraformaldehyde	Sigma-Aldrich P6148

p-dimethylaminobenzaldehyde (p-DAB)	Sigma-Aldrich D8904
Perchloric acid (60%)	VWR International 101752U
Phosphate buffered saline (PBS)	Oxoid Products BR0014
Pronase E	VWR International 1074330005
Propan-2-ol	Fisher Chemicals P/7490/17
Safranin O	Nustain AS106
Saline sodium citrate solution (SSC; 20% *v/v*)	Sigma-Aldrich S6639
Scott's tap water substitute	Nustain AE077
Sodium acetate	Sigma-Aldrich S5636
Sodium bicarbonate	Sigma-Aldrich S6014
Sodium chloride	Sigma-Aldrich S9888
Sodium dihydrogen phosphate dihydrate	Fluka 71502
Sodium formate	Fisher Chemicals S/4082/53
Sodium hydroxide (1 M solution)	Fisher Chemicals J/7620/17
Sodium hydroxide (pellets)	Fisher Chemicals S/4880/53

Sodium phosphate dibasic	Sigma-Aldrich S0876
Sodium phosphate monobasic	Sigma-Aldrich S8282
Technovit 8100 resin kit	TAAB T220
Toluene	Fisher chemicals T/2200/17
Trizma base	Sigma-Aldrich T6066
Trypan blue	Sigma-Aldrich T8154
Trypsin solution (25 g/L in 0.9% NaCl)	Sigma-Aldrich T4549
Xylene	Fisher Chemicals X/0200/17

Appendix 2

Solutions

2.1 Isolation of cartilage

2.1.1 Phosphate buffered saline (PBS)

PBS	1 tablet
Distilled H_2O	100 mL

PBS tablets were dissolved in distilled water and autoclaved for 20 minutes at 120°C.

2.1.2 Gentamicin PBS solution

PBS	100 mL
Gentamicin solution (10 mg/mL)	0.5 mL

Gentamicin PBS solution was stored at 4°C until required.

2.2 Isolation of chondrocytes

2.2.1 Cartilage digestion medium

FCS	50 mL
NEAA	10 mL
L-glutamine solution (200 mM)	10 mL
Gentamicin solution (10 mg/mL)	5 mL
HEPES	10 g
DMEM	1 L

All supplements were passed through a 0.2 μm filter into the DMEM. Cartilage digestion medium was stored at 4°C.

2.2.2 Pronase digestion medium

Pronase E	0.1 g
Cartilage digestion medium	100 mL

Pronase E was passed through a 0.2 μm filter into the cartilage digestion medium. Pronase digestion medium was prepared immediately before use. Cartilage was digested using 10 mL of pronase digestion medium per g of tissue.

2.2.3 Collagenase digestion medium

Collagenase (Type II)	0.2 g
Cartilage digestion medium	100 mL

Collagenase was passed through a 0.2 μm filter into the cartilage digestion medium. Collagenase digestion medium was prepared immediately before use. Cartilage was digested using 10 mL of collagenase digestion medium per g of tissue.

2.3 Cell culture

2.3.1 Chondrocyte medium

FCS	100 mL
NEAA	10 mL
L-glutamine	10 mL
Antibiotic antimycotic solution	10 mL
Ascorbic acid-2-phosphate	0.18 g
L-proline	0.046 g
DMEM	1 L

All supplements were passed through a 0.2 μm filter into the DMEM. Antibiotic antimycotic solution was composed of 10 000 units/mL penicillin G, 100 mg/mL streptomycin sulphate and 25μg/mL amphotericin B. Chondrocyte medium was stored at 4°C.

2.3.2 Trypsin EDTA in PBS

EDTA solution (0.02% *w/v* in dH_2O)	10 mL
Trypsin solution (25 g/L in 0.9% NaCl)	100 mL
PBS	to 1 L

EDTA and trypsin solutions were passed through a 0.2 μm filter into PBS. Trypsin EDTA in PBS was stored at -20°C.

2.3.3 Freezing medium

DMSO	2 mL
FCS	18 mL

Freezing medium was passed through a 0.2 μm filter and stored at -20°C.

2.3.4 HOS TE85 medium

FCS	100 mL
NEAA	10 mL
L-glutamine	10 mL
Anitbiotic antimycotic solution	5 mL
Ascorbic acid-2-phosphate	0.15 g
DMEM	1 L

All supplements were passed through a 0.2 μm filter into the DMEM. HOS TE85 medium was stored at 4°C.

2.4 Biochemical analysis

2.4.1 Papain solution

2.4.1.a *Papain buffer*

Sodium phosphate (dibasic)	1.42 g (0.1 M)
Cysteine hydrochloride	0.079 g (0.005 M)
EDTA	0.186 g (0.005 M)
Distilled H_2O	200 mL

The pH of papain buffer was adjusted to 6.5 when necessary using 1 M HCl or NaOH as appropriate. Papain buffer was stored at 4°C for up to 3 months.

2.4.1.b *Papain solution*

Papain	0.1056 g
Papain buffer	100 mL

Papain solution was prepared immediately before use.

2.4.2 Hoechst buffer

Sodium chloride	5.844 g (0.1 M)
EDTA	3.802 g (0.01 M)
Trizma base	1.211 g (0.01 M)
Distilled H_2O	1 L

The pH of Hoechst buffer was adjusted to 7.0 when necessary using 1 M HCl or NaOH as appropriate. Hoechst buffer was stored at 4°C for up to 6 months.

2.4.3 Hoechst 33258 working solution

2.4.3.a ***SSC solution (1% v/v)***

SSC solution (20% (*v/v*) in dH_2O)	1 mL
Distilled H_2O	to 20 mL

1% (*v/v*) SSC solution was prepared immediately before use.

2.4.3.b ***Hoechst 33258 stock solution***

BisBenzimide (Hoechst 33258)	0.01 g
1% (*v/v*) SSC solution	10 mL

Hoechst 33258 stock solution was stored at -20°C for up to 1 year.

2.4.3.c ***Hoechst 33258 working solution***

Hoechst 33258 stock solution	100 µL
Hoechst buffer	to 200 mL

Hoechst 33258 solution was prepared immediately before use.

2.4.4 Alamar blue™ working solution

2.4.4.a ***HBSS solution***

HBSS	9.8 g
Sodium bicarbonate	0.35 g
Distilled H_2O	to 1 L

HBSS solution was passed through a 0.2 µm filter and stored at 4°C.

2.4.4.b Alamar blue™ working solution

Alamar blue™	2 mL
HBSS	to 20 mL

Alamar blue™ working solution was prepared immediately before use.

2.4.5 Chondroitin-4-sulphate working solution (100μg/mL)

2.4.5.a Chondroitin-4-sulphate stock solution (1 mg/mL)

Chondroitin-4-sulphate	0.01 g
Distilled H_2O	10 mL

Chondrotin-4-sulphate stock solution was prepared immediately before use.

2.4.5.b Chondroitin-4-sulphate working solution (100μg/mL)

Chondroitin-4-sulphate stock solution	1 mL
Heat-treated papain solution	to 10 mL

Chondroitin-4-sulphate working solution was stored at -20°C for up to 1 year.

2.4.6 DMMB solution

Sodium formate	2 g (0.03 M)
DMMB	0.016 g (0.046 mM)
Ethanol (100%)	5 mL
Formic acid	2 mL
Distilled H_2O	to 1 L

DMMB was stored at room temperature in a foil-wrapped brown bottle for up to 3 months.

2.4.7 Sodium phosphate buffer (0.25 M)

Sodium phosphate (dibasic)	35.5 g (0.25 M)
Distilled H_2O	to 1 L

The pH of 0.25 M sodium phosphate buffer was adjusted to 6.5 when necessary using 1 M HCl or NaOH as appropriate. The buffer was stored at 4°C for up to 3 months.

2.4.8 Hydroxyproline working solution (100μg/mL)

2.4.8.a Hydroxyproline stock solution (1 mg/mL)

cis-4-hydroxy-L-proline	0.01 g
Distilled H_2O	10 mL

Hydrxyproline stock solution was prepared immediately before use.

2.4.8.b Hydroxyproline working solution (100 μg/mL)

Hydroxyproline stock solution	1 mL
Hydrolysed papain solution	to 10 mL

Hydroxyproline solution was stored at -20°C for up to 1 year.

2.4.9 Chloramine T solution

2.4.9.a Chloramine stock solution

2.4.9.a.i Chloramine stock solution a

Sodium acetate	120 g
Citric acid	50 g
Distilled H_2O	650 mL

2.4.9.a.ii *Chloramine stock solution b*

Sodium hydroxide	34 g
Distilled H_2O	250 mL

2.4.9.a.iii *Chloramine stock solution*

Chloramine stock solution a	650 mL
Chloramine stock solution b	250 mL
Glacial acetic acid	12 mL
Toluene	500 µL
Distilled H_2O	to 1 L

Chloramine stock solution was stored at 4°C for up to 3 months.

2.4.9.b ***Chloramine working solution***

Propan-2-ol	150 mL
Chloramine stock solution	500 mL
Distilled H_2O	to 750 mL

The pH of chloramine working solution was adjusted to 6.0 when necessary using 1 M HCl or NaOH as appropriate. The solution was stored at 4°C for up to 3 months.

2.4.9.c ***Chloramine T solution***

Chloramine T	0.3525 g (0.07 M)
Propan-2-ol	2.5 mL
Chloramine working solution	20 mL

Chloramine T solution was prepared immediately before use.

2.4.10 p-DAB solution

p-DAB	3.75 g (1.16 M)
Perchloric acid (60%)	6.5 mL
Propan-2-ol	15 mL

p-DAB solution was prepared immediately before use.

2.5 Histology

2.5.1 Alcoholic eosin solution (1% *w/v*)

Eosin	1 g
IMS (25% *v/v* in dH_2O)	100 mL

Alcoholic eosin solution was stored in a foil-wrapped bottle at room temperature.

2.5.2 Aqueous fast green solution (0.02% *w/v*)

Fast green	0.02 g
Distilled H_2O	100 mL

Aqueous fast green solution was stored in a foil-wrapped bottle at room temperature.

2.5.3 Acetic acid solution (*1% v/v*)

Glacial acetic acid	1 mL
Distilled H_2O	to 100 mL

Acetic acid solution was stored at room temperature.

2.5.4 Paraformaldehyde solution (4% *v/v*)

2.5.4.a ***Phosphate buffer (0.2 M)***

Sodium dihydrogen phosphate dihydrate	13.8 g (0.1 M)
Di-sodium hydrogen phosphate dodecahydrate	35.85 g (0.1 M)
Distilled H_2O	to 1 L

The pH of 0.2 M phosphate buffer was adjusted to 7.4 when necessary using 1 M HCl of NaOH as appropriate.

2.5.4.b ***Paraformaldehyde (10% w/v)***

Sodium hydroxide (1 M)	20 mL
Paraformaldehyde	10 g
Distilled H_2O	to 100 mL

2.5.4.c ***Paraformaldehyde (4% v/v)***

10% (w/v) paraformaldehyde	80 mL
0.2 M phosphate buffer	100 mL
Distilled H_2O	to 200 mL

4% (*v/v*) paraformaldehyde solution was stored at -20°C for up to 1 year.

2.5.5 Technovit 8100 infiltration solution

Technovit 8100 hardener I	0.6 g
Technovit 8100 liquid	to 100 mL

Technovit 8100 infiltration solution was stored at 4 °C for up to 1 month.

2.5.6 Technovit 8100 embedding solution

Technovit 8100 hardener II	0.5 mL
Technovit 8100 infiltration solution	to 50 mL

Technovit 8100 embedding solution was prepared immediately before use.

2.6 Scanning electron microscopy

2.6.1 Glutaraldehyde solution (3% *v/v*)

2.6.1.a Sodium phosphate buffer (0.1 M)

Sodium phosphate (monobasic)	2.76 g (0.023 M)
Sodium phosphate (dibasic)	2.84 g (0.02 M)
Distilled H_2O	to 1 L

The pH of 0.1 M sodium phosphate buffer was adjusted to 7.2 when necessary using 1 M HCl or NaOH as appropriate. The buffer was stored at room temperature until required.

2.6.1.b Glutaraldehyde solution (3% v/v)

0.1 M sodium phosphate buffer	18.8 mL
Glutaraldehyde solution (50% (*v/v*) in dH_2O)	1.2 mL

The 3% (*v/v*) glutaraldehyde solution was stored at 4°C.

2.6.2 Osmium tetroxide solution (1% *v/v*)

2.6.2.a Sodium phosphate buffer (0.05 M)

0.1 M sodium phosphate buffer	50 mL
Distilled H_2O	50 mL

The 0.05 M sodium phosphate buffer was stored at room temperature until required.

2.6.2.b ***Osmium tetroxide solution (1% v/v)***

0.05 M sodium phosphate buffer	5 mL
Osmium tetroxide solution (2% (*w/v*) in dH_2O)	5 mL

The 1% (*v/v*) osmium tetroxide solution was prepared immediately before use.

2.7 Confocal microscopy

2.7.1 Live/Dead™ working solution

The Live/Dead™ viability/cytotoxicity assay kit reagents were thawed and allowed to reach room temperature.

2.7.1.a ***Ethidium homodimer solution***

Ethidium homodimer-1 (2 mM)	20 μL
Dulbecco's PBS (DPBS)	10 mL

The solution was thoroughly mixed.

2.7.1.b ***Live/Dead™ working solution***

Ethidium homodimer solution	10 mL
Calcein AM solution (4 mM)	5 μL

Live/Dead™ working solution was prepared immediately before use and kept protected from light.

2.7.2 DABCO mountant

2.7.2.a ***DABCO in PBS***

1,4 diazobicyclo-2-2-2-octane (DABCO)	20 mg
PBS	10 mL

The pH of DABCO in PBS was adjusted to 8.6 when necessary using 1 M HCl or NaOH as appropriate. The buffer was stored at 4°C until required.

2.7.2.b DABCO mountant

glycerol	9 mL
DABCO in PBS	1 mL

DABCO mountant was stored at 4°C for up to 3 months.

Appendix 3

Equations

3.1 Quantification of GAG content

$$\text{GAG content (\%)} = \frac{[\text{chondroitin-4-sulphate}]\ (\mu g/mL) \times \text{dilution factor} \times \text{papain volume}\ (\mu L)}{10^6 \times \text{dry tissue weight (g)}} \times 100\%$$

Where:

[Chondroitin-4-sulphate]	- concentration of chondroitin-4-sulphate in sample calculated from the calibration curve
Dilution factor	- amount the digested sample was diluted by
Papain volume	- volume of the original papain digest that was used
10^6	- correction factor to take into account the different units
Dry tissue weight	- mass of lyophilised sample that was digested

3.2 Quantification of collagen content

$$\text{collagen content (\%)} = \frac{[\text{hydroxyproline}]\ (\mu g/ml) \times \text{DF} \times \text{proportion hydrolysed}}{10^6 \times \text{dry tissue weight} \times 0.143} \times 100\%$$

Where:

[Hydroxyproline]	- concentration of hydroxyproline in sample calculated from the calibration curve
DF	- amount the digested sample was diluted by
Proportion hydrolysed	- proportion of the original papain digest that was hydrolysed
10^6	- correction factor to take into account the different units
Dry tissue weight	- mass of lyophilised sample that was digested

0.143 - correction factor to take into account that 14.3% of collagen is hydroxyproline

3.3 Calculation of the volume of a cylinder

$$\text{volume } (m^3) = \pi \times r^2\ (m^2) \times h\ (m)$$

Where:

$\pi = 3.14217$

r = radius of the circle (1/2 the diameter)

h = height (or thickness) of the cylinder

3.4 Calculation of density

$$\text{density } (g\ m^{-3}) = \frac{\text{mass (g)}}{\text{volume } (m^3)}$$

3.5 Characterisation of scaffold resistance to flow

$$R = \frac{P \times g \times h}{F}$$

Where:

R = scaffold resistance to flow

P = pressure of air (1000 mbar)

F = flow rate

g = force due to gravity (9.81Pa)

h = height of water above scaffold

3.6 Assessment of increase in construct weight

$$\text{weight increase (\%)} = \frac{\text{scaffold weight after culture (g) - scaffold weight before culture (g)}}{\text{scaffold weight before culture}} \times 100\%$$

3.7 Normalisation of cell number with respect to dry sample weight

$$\text{number of cells per gram dry tissue weight} = \frac{\text{total number of cells in sample}}{\text{dry weight of sample (g)}}$$